New Approaches for the Treatment of Triple Negative Breast Cancer

Andrew Sulaiman

A thesis submitted to the Faculty of Graduate and Postdoctoral Studies in partial fulfillment of the requirements for the degree of Doctor of Philosophy in Biochemistry

Department of Biochemistry, Microbiology and Immunology

Faculty of Medicine

University of Ottawa

Abstract

Triple-negative breast cancer (TNBC) is the most refractory subtype of breast cancer to current treatments and accounts disproportionately for the majority of breast cancer-related deaths. Research has not yet identified specific therapies for TNBC and chemotherapy remains the conventional therapy in the clinic. While conventional chemotherapy regimens have demonstrated success at reducing bulk tumor burden, they have been shown to enrich cancer stem cells (CSCs). CSCs promote chemoresistance, metastasis, heterogeneous tumor regeneration and disease relapse. Owing to tumor plasticity and the conversion between CSC and non-CSC subpopulations development of a strategy capable of inhibiting both non-CSC and CSC subpopulations is crucial for TNBC therapy. In this compilation of my main research projects, several new approaches for the treatment of TNBC were identified which target not only the bulk tumor population but also the CSC populations residing within the tumor:

1. Co-suppression of Wnt, HDAC, and ESR1 using clinically relevant low-dose inhibitors effectively repressed both bulk and CSC subpopulations and converted CSCs to non-CSCs in TNBC cells.

2. Co-inhibition of mTORC1, HDAC, and ESR1 was capable of reducing both bulk and CSC subpopulations as well as the conversion of fractionated non-CSC to CSCs in in a human TNBC xenograft model and hampered tumorigenesis following treatment.

3. Inhibition of Wnt and YAP retarded tumor growth of TNBC cells in either epithelial or mesenchymal states, and both $CD44^{high}/CD24^{low}$ and ALDH+ CSC subpopulations were diminished in a human xenograft model reducing tumorigenicity following treatment.

Acknowledgments

I would like to thank Dr. Lisheng Wang for his guidance, support and encouragement throughout the entirety of my graduate studies. When I arrived at Dr. Wang's lab for my MSc, he was the ideal mentor. He was thorough and informative; however, he was also laid back, supportive and encouraging. Dr. Wang pushed me to work hard, aim high and he is the driving force behind the accomplishments throughout my graduate studies. He always encouraged me to develop my own ideas on project and granted me independence and responsibility in the lab which proved to be invaluable. Personally, I could not envision myself working with any other supervisor and his tutelage greatly assisted my development as a researcher and passion for science.

I would also like to thank my Thesis Advisory Committee members Dr. Christina Addison and Dr. Tommy Alain. Their feedback, guidance and insight into my research as it was developing helped shape my research into what it is.

I would like to thank all of the colleagues I have worked together with over the last four years. The conversations and insights helped quicken long days and made coming in on the weekends a bit better. In particular, I would like to thank Dr. Li Li and Dr. Deyong Jia, for their help getting me established in the lab, listening to my ideas and giving me great feedback and career advice. I would also like to thank my undergraduate students whom I had the privilege to mentor and supervise during my PhD. These students contributed greatly to my research, taught me how to lead a research group and seeing them develop into young scientists was its own reward.

Most importantly, I would like to thank my family: my father Raymond, my mother Tara, my two brothers Steven and Brandon and my cat Ari who supported me unconditionally and encouraged me to reach me goals. A special thank you to Sarah McGarry who has been with me from the beginning of this journey and has been my rock during graduate school. Without the support, and encouragement from all of you, I would not be where I am today. Thank you all for everything.

Authorizations

First Author Publications:

Chapter 1:

1. **Andrew Sulaiman**, Zemin Yao and Lisheng Wang. Re-evaluating the role of epithelial-mesenchymal-transition in cancer progression. *Journal of Biomedical Research*, 2017; 31(0): 1–10

2. **Andrew Sulaiman** and Lisheng Wang. Bridging the divide: preclinical research discrepancies between triple-negative breast cancer cell lines and patient tumors. *Oncotarget*, 2017; 8(68): 113269–113281 Published under a Creative Commons Attribution (CC BY 3.0) License: https://creativecommons.org/licenses/by/3.0/

Chapter 2:

3. **Andrew Sulaiman**, Brandon Sulaiman, Lara Khouri, Sarah McGarry, Carolyn Nessim, Angel Arnaout, Sean Xuguang Li, Christina Addison, Jim Dimitroulakos, and Lisheng Wang. Both bulk and CSC subpopulations in TNBC are susceptible to Wnt, HDAC and ERα co-inhibition. *FEBS Letters*, 2017;590(24):4606-4616.

Chapter 3:

4. **Andrew Sulaiman**, Sarah McGarry, Sara El-Sahli, Ka Mien Lam, Jason Chambers, Shelby Kaczmarek, Li Li, Christina Addison, Jim Dimitroulakos, Angel Arnaout, Carolyn Nessim, Zemin Yao, Guang Ji, Haiyan Song, Suresh Gadde, Xuguang Li, Lisheng Wang. Co-inhibition of mTORC1, HDAC and ESR1α Regards the Growth of Triple Negative Breast Cancer and Suppresses Cancer Stem Cells. Cell Death and Disease 2018; 9(8): 815 doi: 10.1038/s41419-018-0811-7). Published under a Creative Commons Attribution (CC BY) License: https://creativecommons.org/licenses/by/4.0/deed.ast

Chapter 4:

5. **Andrew Sulaiman**, Sarah McGarry, Li Li, Deyong Jia, Sarah Ooi, Christina Addison, Jim Dimitroulakos, Angel Arnaout, Carolyn Nessim, Zemin Yao, Guang Ji, Haiyan Song, Suresh Gadde, Xuguang Li, Lisheng Wang. Dual inhibition of Wnt and YAP signaling retards the growth of both mesenchymal and epithelial TNBC. *Molecular Oncology*, 2018; 12(4):423-440. Published under a Creative Commons Attribution (CC BY) License: https://creativecommons.org/licenses/by/4.0/deed.ast

Chapter 5:

6. **Andrew Sulaiman**, Sarah McGarry, Sara El-Sahli, Li Li, Jason Chambers, Alexandra Phan, Marceline Côté, Greg O. Cron, Tommy Alain, Yevgeniya Le, Seung-Hwan Lee, Sheng Liu, Daniel Figeys, Suresh Gadde and Lisheng Wang. Co-Targeting Bulk Tumor and CSCs in Clinically Translatable TNBC Patient-Derived Xenografts via Combination Nanotherapy. *Molecular Cancer Therapeutics* (2018, Submitted)

Table of Contents

List of Figures

Chapter 1

Chapter 2

Chapter 3

Chapter 4

Chapter 5

List of Tables

List of Abbreviations

4E-BP1	4E (eIF4E)-binding protein 1
ALDH	aldehyde dehydrogenase
CD24	cluster of differentiation 24
CD44	hyaluronic acid receptor
CSC	cancer stem cell
CTNNB1	Catenin Beta 1
DEAB	N,N-diethylaminobenzaldehyde
DLS	Dynamic Light Scattering
DMEM	Dulbecco's Modified Eagle Medium
E/M	Epithelial/Mesenchymal
EMT	epithelial to mesenchymal transition
EPR	Enhanced permeability and retention effect
ER	Estrogen Receptor
ERBB2/HER2	human epidermal growth factor receptor type 2
ESR1	estrogen receptor alpha
FACS	fluorescence-activated cell sorter
FBS	Fetal Bovine Serum
FDA	Food and Drug Administration
HAT	Histone Acetyltransferase
HDAC	histone deacetylase
HDAC	Histone Deacetylase
HMG-CoA	3-hydroxy-3-methyl-glutaryl-coenzyme A
Hybrid E/M	Hybrid Epithelial/Mesenchymal
IL-6	Interleukin 6
IL-8	Interleukin 8
IVIS	in vivo imaging system
MET	mesenchymal to epithelial transition

MRI	magnetic resonance imaging
mTORC1	mammalian target of rapamycin complex 1
MTT	3-(4,5-Dimethylthiazol-2-Yl)-2,5-Diphenyltetrazolium Bromide
NCS	Newborn Calf Serum
NF-kB	kappa-light-chain-enhancer of activated B cells
NOD-SCID	Non-obese Diabetic/Severe combined immunodeficiency
NP	Nanoparticle
NSG	NOD-SCID gamma
PDX	patientderived xenograft
PGR	progesterone receptor
P-NPs	Paclitaxel encapsulated Nanoparticles
PP2A	protein phosphatase 2
PR	Progesterone Receptor
PV-NPs	Verteporfin and Paclitaxel encapsulated Nanoparticles
Rap	Rapamycin
S6K1	Ribosomal protein S6 kinase beta-1
S6RP	S6 ribosomal protein
shRNA	short hairpin RNA
siRNA	short interfering RNA
Tam	tamoxifen
TCGA	The Cancer Genome Atlas
TGF-β	Transforming growth factor beta
TNBC	triple negative breast cancer
TNF-α	Tumor necrosis factor alpha
VBT	Valproic Acid, BC21 and Tamoxifen
V-NPs	Verteporfin encapsulated Nanoparticles
VPA	valproic acid
VRT	Valproic Acid, Rapamycin and Tamoxifen

WNT	Wingless/Integrated
YAP	Yes-associated protein

Chapter 1: Introduction/Background

1.1 Breast Cancer

Cancer remains an epidemic throughout the world. According to Statistics Canada, in 2016, cancer was the number one leading cause of death, exceeding both heart disease and cerebrovascular disease (Appendix 3, Statistics Canada, 2016). Currently, one in two Canadians are projected to develop cancer within their lifetime with one in four Canadians expected to die from cancer (Canadian Cancer Statistics, 2018).

A study by GLOBOCAN demonstrated that worldwide there was an estimated 14.1 million new cancer cases and 8.2 million cancer deaths in 2012 (Ferlay *et al.*, 2015). When GLOBOCAN repeated their study in 2018, it was found that the numbers increased to 18.1 million new cancer cases and 9.6 million cancer deaths throughout the world (Bray *et al.*, 2018).

Breast Cancer is the most frequently diagnosed and a leading cause of cancer-related deaths amongst women throughout the world (Bray *et al.*, 2018). In 2018, it was demonstrated that there were 2,088,849 new breast cancer cases and 626,679 breast cancer mortalities in that year alone (Bray *et al.*, 2018). With such numbers, it is no surprise that breast cancer accounts for 1 in 4 cancer cases amongst the female population worldwide (Bray *et al.*, 2018).

1.2 Breast Cancer Classifications

Within normal breast tissues, there exists lobules and ducts. Lobules are glands which are responsible for milk production. These glands are connected to the nipple via ducts which facilitate milk transportation. Approximately 80% of breast cancers are invasive ductal carcinoma and ~10% of breast cancers are invasive lobular carcinomas. The remaining 10% are comprised of: micropapillary (invasive ductal carcinoma which grow as high density masses surrounded by clear spaces), inflammatory (invasive ductal carcinoma which is capable of eliciting an immune

response and is characterized as being highly aggressive), medullary (undifferentiated cells with a syncytial growth pattern and an absence of glandular components), tubular (invasive ductal carcinoma with well differentiated tumor cells growing in small round tubules of epithelial cells), and mucinous (invasive ductal carcinoma surrounded by mucin) (Dieci *et al.*, 2014; Vincent-Salomon *et al.*, 2007) breast cancers.

1.3 Breast Cancer Sub-Types

Breast cancer can be further classified via the presence/absence of the estrogen receptor (ER), progesterone receptor (PR) and the human epidermal growth factor receptor-2 (HER-2) protein. The ER (α and β) are stimulated by oestrogens; but can also act independently in the absence of oestrogens (Thomas and Gustafsson, 2011). Once activated, the ER can affect gene transcription (directly and indirectly), impacting proliferation, anti-apoptosis and cell cycle regulation (Frasor *et al.*, 2003). The function of PR (α versus β) are convoluted. Progesterone acts as a potent mitogen, mediates mammary gland stem cell self-renewal and stimulates proliferation of breast cancer through PR signalling (Daniel *et al.*, 2011; Joshi *et al.*, 2010). PR is a target gene of ER transcription (and is positively correlated with ER expression) and there is a large overlap between ER and PR regulated genes (Daniel *et al.*, 2011).

HER-2 is a type I transmembrane growth factor receptor in the same family as the epithelial growth factor receptor (HER-1). Upon activation, HER-2 will dimerize and promote a phosphorylation cascade, activating a wide variety of signal pathways such as: MAPK, STAT, P13K/Akt and NF-kβ which will in turn promote proliferation, disease progression and metastasis (Hou *et al.*, 2003; Moasser, 2007; Roy and Perez, 2009). The majority of breast cancer patients are positive for ER (56%), PR (49%) and negative for HER-2 (84.4%)(Inwald *et al.*, 2015). Based

on the presence/absence of these markers, breast cancers can be divided into the following sub-types.

Luminal A breast cancer is defined as possessing ER and PR whilst being negative for HER-2 (Inic *et al.*, 2014). Luminal B breast cancer is positive for ER and may be positive or negative for PR. Additionally, Luminal B breast cancer may be positive or negative for HER-2 (Inic *et al.*, 2014) and proliferates at a greater rate (high Ki-67 levels) compared to Luminal A. There has been evidence supporting the existence of a Luminal C breast cancer sub-type (Sørlie *et al.*, 2001). This proposed sub-type possesses ER expression; however, its gene expression displays similarities with HER-2/basal breast cancers despite not possessing HER-2 (Sørlie *et al.*, 2001). HER-2 positive breast cancer is negative for ER and PR but is positive for HER-2 (Prat and Perou, 2011).

Triple negative breast cancer (TNBC) is described as being negative for ER, PR and HER-2. It is typically referred to as basal-like and is characterized by its gene signature (cytokeratins 5, 6, and 17 gene expression), aggressiveness and risk of recurrence. Importantly, around 71% of TNBC are basal-like with the remaining resembling Luminal A, ER+, PR+/- and HER-2- sub-types (Badve *et al.*, 2011; Prat *et al.*, 2013). Reasons for these differences include tumor heterogeneity, the location from which the sample was attained and even potential misdiagnosis.

An additional classification amongst breast cancer is via claudin-low status. Claudin-low status is determined via the lack of expression of tight-junctions, and diminished epithelial and adhesional gene expression (low E-cadherin, claudin-3, claudin-4 and claudin-7 gene expression) (Dias *et al.*, 2017). As claudin-low tumors are mainly found within TNBC samples, this has been used to sub-divide TNBC (Perou, 2011). A phenotype claudin-low TNBC exhibits is increased stemness, and metastatic potential via epithelial to mesenchymal transition (Dias *et al.*, 2017).

1.4 Prognosis

Prognosis of those with breast cancer varies widely due to patient heterogeneity, tumor grade, disease stage and sub-type of breast cancer. A report by Zuo *et al* demonstrated that for patients with stage 1, 2, 3 or 4 breast cancer, the 5 year overall survival rate was 96.5%, 91.6%, 74.8% and 40.7% respectively (Zuo *et al.*, 2017). When grouped by sub-type, Shen *et al* reported that for women over 50 years of age, the 5 year disease free survival for Luminal A breast cancer was 95.7%, for Luminal B patients it was 92.4% (HER-2 negative), for Luminal B patients with HER-2 expression it was 94.8%, for HER-2 positive patients it was 82% and for TNBC patients it was 53.3% (Shen *et al.*, 2016).

Additionally, it was found that the frequency for distant metastasis amongst the breast cancer sub-types was 81.1% for TNBC, 66.7% for HER-2 positive, 52.2% for Luminal A, 50.0% for Luminal B (HER-2 negative), and 33.3% for Luminal B (HER-2 positive) (Shen *et al.*, 2016). In TNBC patients who have suffered a metastasis, the overall 12 month survival rate was 37% if the cancer metastasized to the bone, 29% if metastasize to a solid organ or 19% if it metastasized to multiple sites (Morante *et al.*, 2018). These results highlight the poor clinical outcomes associated with TNBC in comparison to the other breast cancer subtypes due to the aggressiveness, high risk of recurrence and capacity to metastasize.

1.5 Breast Cancer Treatment

TNBC accounts for ~15% of all breast cancers but is associated with a disproportionately worsened prognosis in comparison with other subtypes. One of the associated reasons behind this divergent prognosis is the treatment options available for TNBC. For all breast cancer sub-types, surgery is the primary option for invasive carcinomas. The surgical options include breast

conservation surgery (Lumpectomy), partial or complete mastectomy. Following surgery, radiotherapy may be recommended. Following breast conservation surgery, whole breast radiotherapy is commonly prescribed. For patients who have undergone a mastectomy, radiation to the chest wall or regional lymph nodes is recommended if the tumor was greater than 5 cm in size or if an aggressive phenotype was demonstrated (Zhang *et al.*, 2012).

Following surgery in addition to or instead of radiotherapy, endocrine or chemotherapy may be recommended. For ER+ breast cancers, the selective estrogen receptor mimic (SERM), tamoxifen can bind to and inhibit ER function, preventing breast cancer growth (Dutertre *et al*, 2000). These effects are magnified in premenopausal women through ovarian function ablation via oophorectomy or treatment with Gonadotrophin-releasing hormone analogues (to prevent estradiol production) (Prowell *et al*, 2004). For post-menopausal women, aromatase inhibitors (such as Anastrozole) would be recommended to prevent estradiol production from non-ovarian sources.

HER-2 positive breast cancers are treated with monoclonal antibodies such as Herceptin, which specifically bind to the HER-2 receptor (Smith *et al.*, 2007). Upon the binding of Herceptin, HER-2+ breast cancers undergo cell cycle arrest and apoptosis is promoted. Herceptin can be used in conjunction with non-anthracycline chemotherapies such as docetaxel/carboplatin/trastuzumab to increase efficacy (Nabholtz *et al*, 2001).

For TNBC patients, there is no specific treatment regimen to combat this disease. As such, non-specific chemotherapeutics in the anthracyclin family (such as doxorubicin), the taxane family (such as paclitaxel) and/or other chemotherapeutic agents (such as cyclophosphamide, and/or 5-flurouracil) are prescribed (Isakoff, 2010).

1.6 Cancer Stem Cells

There has been a strong body of evidence linking the growth and progression of breast cancers to a small subset of cells within the tumors known as cancer stem cells (CSCs)(Economopoulou *et al.*, 2012; Gong *et al.*, 2010; Reuben *et al.*, 2011). CSCs have the ability to differentiate, self-renew and give rise to new tumors of origin *in vivo*. They also exhibit stem cell-like properties, such as asymmetric division and quiescence. The CSC theory hypothesizes that within the tumor, there exists a cellular hierarchy with CSCs at the apex. Through their differentiation and self-renewing capabilities, CSCs generate both non-CSC (bulk) and CSC populations which drive chemotherapeutic resistance, tumor progression, metastasis and disease relapse.

A well-known study reported by Al Hajj *et al* demonstrated that the $CD44^{+}/CD24^{-}$ subpopulation fractionated from breast cancer patients exhibited a greater than 100-fold increase in tumorigenicity (ability to form tumors) compared to unsorted cells. This landmark study, characterized the $CD44^{+}/CD24^{-}$ CSC population in breast cancer and highlighted the existence of tumorigenic CSCs (Al-Hajj *et al.*, 2003).

ALDH (Aldehyde Dehydrogenase) is frequently used as a marker of hematopoietic stem cells (Kastan *et al.*, 1990). ALDH is comprised of 19 isomers and functions in ester hydrolysis and oxidizing aldehydes to carboxylic acids. This enzyme plays an important function in cellular detoxification after exposure to chemotherapeutic agents (eg. cyclophosphamide) providing apoptotic resistance (Marcato *et al.*, 2011). It has been found that CSCs can be identified by high ALDH expression in a wide variety of cancers including breast cancer (Ma and Allan, 2011). In

breast cancer, fractionated $ALDH^+$ cells are capable of forming tumors with as little as 500 cells (Ginestier *et al.*, 2007).

While other breast cancer CSC markers exist (such as CD133, EpCAM, CD90, etc) the above markers are the most characterized and are frequently used in the field.

1.7 CSCs and Metastasis

The following review, for which I am the first author, was published in the Journal of Biomedical Research and will discuss $CD44^+/CD24^-$, $ALDH^+$ CSCs, their phenotypic states and how they mediate metastasis in breast cancer via epithelial to mesenchymal transition (EMT) and *vice-versa*. It will also introduce the hybrid EMT concept as a model for metastasis.

Andrew Sulaiman, Zemin Yao and Lisheng Wang. Re-evaluating the role of epithelial-mesenchymal-transition in cancer progression. *Journal of Biomedical Research*, 2017; 31(0): 1–10

AS wrote the manuscript and created the figures. LW and ZY provided feedback, critiques and edited the article.

Abstract

Epithelial-mesenchymal transition (EMT) and mesenchymal-epithelial transition (MET) are essential for embryonic development and also important in cancer progression. In a conventional model, epithelial-like cancer cells transit to mesenchymal-like tumor cells with great motility via EMT transcription factors; these mesenchymal-like cells migrate through the circulation system, relocate to a suitable site and then convert back to an epithelial-like phenotype to regenerate the tumor. However, recent findings challenge this conventional model and support the existence of a stable hybrid epithelial/mesenchymal (E/M) tumor population. Hybrid E/M tumor cells exhibit both epithelial and mesenchymal properties, possess great metastatic and tumorigenic capacity and are associated with poorer patient prognosis. The hybrid E/M model and associated regulatory networks represent a conceptual change regarding tumor metastasis and organ colonization. It may lead to the development of novel treatment strategies to ultimately stop cancer progression and improve disease-free survival.

Introduction

Metastasis is a process through which cancer cells dissociate from the primary tumor site, invade the surrounding tissue, hijack the circulation as a means of transport, and ultimately reconstitute the tumor at a secondary site. This process constitutes over 90% of cancer-associated deaths despite significant advances in cancer treatment (Gupta and Massague, 2006). Epithelial-mesenchymal transition (EMT) is critical during embryo development and organogenesis. Aberrant activation of EMT is thought to promote tumor dissociation, migration, and cancer stem cell enrichment in multiple forms of cancer (Friedl and Wolf, 2003; Garg, 2013; Steinestel *et al.*, 2014; Tan *et al.*, 2014). These mesenchymal-like tumor cells migrate from the tumor front, through the basement membrane and into circulation where they are referred to as circulating tumor cells

(CTCs) (Cristofanilli *et al.*, 2005). A small number of CTCs display cancer stem cell (CSC) features such as immune evasion, invasiveness, tumorigenicity, and resistance to different treatments (Yang *et al.*, 2015). Once the CSCs reach a suitable secondary tumor site, they undergo a reverse process, mesenchymal-epithelial transition (MET), halting migration and allowing reconstitution of tumor at the secondary site (Figure 1.0A) (Gunasinghe *et al.*, 2012; Yao *et al.*, 2011).

This classic and simplified view of metastasis, during past several decades, has geared research towards targeting the migrating mesenchymal cancer cells (Creighton *et al.*, 2010; Davis *et al.*, 2014; Huang *et al.*, 2013; Sokol *et al.*, 2005; Tojo *et al.*, 2005; Vazquez-Martin *et al.*, 2010). However, controversy has surrounded this model (Chui, 2013; Fischer *et al.*, 2015; Iwanami *et al.*, 2014; Tarin *et al.*, 2005; Zheng *et al.*, 2015) which does not take into consideration of cellular plasticity, the tumorigenicity of epithelial cells, the full extent of tumor niches involved in EMT induction, the possibility of co-migration of both epithelial and mesenchymal cells, and hybrid epithelial-mesenchymal (E/M) tumor cells (Figure 1.0B). By addressing these deficiencies, a new model may lead to novel strategies to treat cancer metastasis and progression.

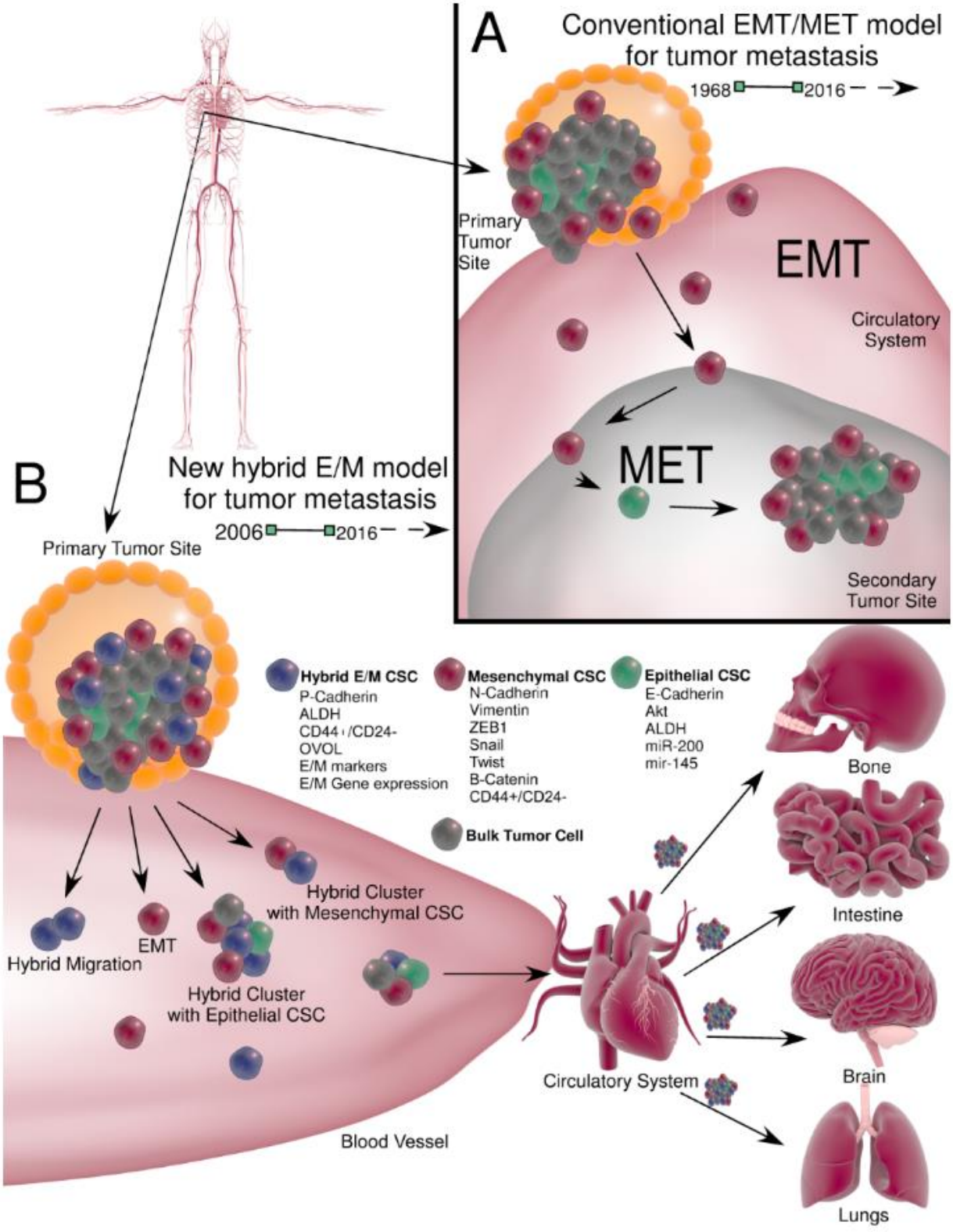
A
Conventional EMT/MET model for tumor metastasis
1968
2016
Primary Tumor Site
EMT
Circulatory System
MET
Secondary Tumor Site
B
New hybrid E/M model for tumor metastasis
2006
2016
Primary Tumor Site
Hybrid E/M CSC
P-Cadherin
ALDH
CD44+/CD24-
OVOL
E/M markers
E/M Gene expression
Mesenchymal CSC
N-Cadherin
Vimentin
ZEB1
Snail
Twist
B-Catenin
CD44+/CD24-
Epithelial CSC
E-Cadherin
Akt
ALDH
miR-200
mir-145
Bulk Tumor Cell
Hybrid Cluster with Mesenchymal CSC
EMT
Hybrid Migration
Hybrid Cluster with Epithelial CSC
Blood Vessel
Circulatory System
Bone
Intestine
Brain
Lungs

Figure 1.0: A schematic diagram of Hybrid E/M and classical EMT/MET CSCs. (A) The classic EMT/MET model of metastasis which was coined in 1976(Hay, 1968). Mesenchymal CSCs are transformed from epithelial state through an EMT process. They then migrate outside the primary tumor, pass through the basement membrane and enter circulation. When mesenchymal CSCs reach a suitable secondary site prior to development of a new tumor, they undergo MET to regain an epithelial CSC phenotype for tumor development. **(B)** The hybrid E/M CSCs begun gaining traction from 2006 onwards(Lee *et al.,* 2006). These hybrid CSCs migrate from the primary tumor alone or in clusters together with epithelial or mesenchymal tumor CSCs by crossing the basement membrane to enter circulation system and then relocate to a suitable secondary tumor site. The secondary tumor may develop from the hybrid E/M CSCs, epithelial tumor CSCs present in the cluster or mesenchymal CSCs that undergo MET.

A General Overview of Classical EMT/MET and Their Regulators

The classical EMT process in cancer encompasses the gradual remodeling of epithelial-like tumor cells towards a mesenchymal-like phenotype. Mesenchymal traits include the repression of epithelial markers, enrichment of mesenchymal markers, enrichment of the $CD44^{high}/CD24^{low}$ CSC population, absence of cellular polarity due to the re-arrangement of actin cytoskeleton and re-distribution of adhesion molecules, individualistic migration, and resistance to apoptosis (do Nascimento Gonçalves *et al.*, 2016; Kong *et al.*, 2016; Lamouille *et al.*, 2014; Ma *et al.*, 2015a; Ma *et al.*, 2016; Moreno-Bueno *et al.*, 2008). Epithelial traits on the other hand, are opposite to the mesenchymal traits and exhibit some additional features such as enriched ALDH+ CSC subpopulation and collective migration (Das *et al.*, 2015; Liu *et al.*, 2014; Yauch *et al.*, 2005).

In literature, EMT is commonly characterized by decreased E-cadherin expression. E-cadherin binds to neighbouring cadherins through its extracellular domain, mediating cell-cell adhesion, preventing tumor cell migration and *in vivo* dissemination/invasiveness (Frixen *et al.*, 1991; Vleminckx *et al.*, 1991). The intracellular domain of E-cadherin binds to β-Catenin (an effector of Wnt signalling), preventing the nuclear translocation of β-catenin and β-catenin/T-cell

factor (TCF)-mediated transactivation, impeding Wnt signalling and acquisition of mesenchymal traits (Li and Mattingly, 2008; Orsulic *et al.*, 1999). In addition to E-cadherin repression, the mesenchymal markers vimentin and N-cadherin are upregulated and EMT transcription factors (EMT-TF), such as SNAIL, SLUG, ZEB and TWIST are also upregulated. These transcription factors inhibit the epithelial phenotypes of the tumor cells while promoting acquisition of the mesenchymal phenotype through a plethora of incompletely defined mechanisms, including microRNA networks (Zhang *et al.*, 2010), protein stabilization (Diaz *et al.*, 2014), gene expression (Minafra *et al.*, 2014), epigenetic/chromatin modification (Kiesslich *et al.*, 2013) and long non-coding RNA regulation (Xu *et al.*, 2016b). SNAIL and SLUG both inhibit E-cadherin expression, promoting β-catenin nuclear translocation and subsequent Wnt pathway upregulation (Bolós *et al.*, 2003; Cano *et al.*, 2000). In addition, they promote the formation of the β-catenin–TCF4 transcription complex which binds to the *TGF-β3* gene promoter and promoting its expression which in turn further stimulates Wnt signalling through *LEF1* gene expression, ultimately enhancing acquisition of mesenchymal traits (Medici *et al.*, 2008; Nishita *et al.*, 2000). TGF-β signalling also stimulates zinc finger E-box-binding homeobox 1 and 2 (ZEB1 and ZEB2) which bind to phosphorylated receptor-activated Smads (Gregory *et al.*, 2011) and various transcription factors as well as histone acetyltransferases such as p300 and p/CAF, leading to epigenetic modification of gene expression (Postigo *et al.*, 2003). Similarly, TWIST affects a large number of transcriptional processes, overrides oncogene-induces senescence and represses E-cadherin while promoting N-cadherin expression (Montserrat *et al.*, 2011; Vesuna *et al.*, 2008). TWIST is notably activated through hypoxia-inducible factor 1α under intratumoral hypoxic conditions (Yang *et al.*, 2008), a trait associated with chemotherapy resistance (Song *et al.*, 2006). These

EMT-TFs may work together through overlapping and distinct molecular mechanisms to regulate a complex network in tumor cells to control epithelial *versus* mesenchymal plasticity.

In addition, various biological processes such as inflammation within the tumor microenvironment mediate EMT. When breast epithelial cells, adjacent to the tumor, were exposed to inflammatory cytokines tumor necrosis factor-α (TNFα) and interleukin-1β (IL-1β) for 2-3 weeks, ZEB1 and SNAIL (two major EMT transcription factors) were significantly upregulated (Leibovich-Rivkin *et al.*, 2013). The exposed breast epithelial cells then displayed upregulated matrix metalloproteinases (MMPs, capable of degrading the basement membrane to facilitate tumor cell migration) (Bernhard *et al.*, 1994; Pei and Weiss, 1996) and increased migratory/invasive capabilities, suggesting that tumor microenvironment influences plasticity and tumor cell dissemination by promoting EMT (Leibovich-Rivkin *et al.*, 2013).

More recently, mesenchymal stem cells (MSC) from human adipose tissue have been shown to produce soluble factors after exposure to interferon-γ (IFN-γ) or TNF-α to enhance the malignancy of the MCF-7 breast cancer cells and shift the cells towards a mesenchymal phenotype with the increased migration capacity, enhanced vimentin expression and decreased E-cadherin expression (Trivanović *et al.*, 2016).

It has been found that bacteria can influence the tumor microenvironment and promote EMT. When gastric cancer cells were exposed to *H. pylori*-infected MSC supernatant enriched with IL-6 (interleukin-6), IL-8 and platelet-derived growth factor-β cytokines, a mesenchymal phenotype was induced, characterized by increased migration, N-cadherin and vimentin expression while decreased E-cadherin expression (Zhang *et al.*, 2016).

Paracrine/autocrine signalling within the tumor in response to chemotherapy has also been associated with EMT promotion. IL-6, IL-8 and monocyte chemoattractant protein-1 (MCP-1) cytokines along with NF-κB/IκBa and STAT3 (Signal transducer and activator of transcription 3) were found to be upregulated in triple negative breast cancer cells after exposure to commonly prescribed chemotherapeutics, leading to upregulation of stem cell-associated gene and protein expression, enrichment of $CD44^{high}/CD24^{low}$ cancer stem-like cells, and enhanced tumorigenicity in nude mice (Jia *et al.*, 2016).

Together, identification of signalling pathways and factors capable of regulating EMT has been the focus of considerable research during the past several decades in hopes that through prevention of EMT-mediated migration, tumor metastasis would have been halted (Creighton *et al.*, 2010; Davis *et al.*, 2014; Huang *et al.*, 2013; Sokol *et al.*, 2005; Tojo *et al.*, 2005; Vazquez-Martin *et al.*, 2010).

From Classical EMT/MET to the Hybrid EMT/MET Model

There is a plethora of literature in regards to EMT, tumor dissemination and migration through the surrounding tissue into the bloodstream and other organs. However, proof of MET at a metastatic site from a re-localized mesenchymal CTC has not yet been proved, challenging the classical EMT/MET theory regarding mesenchymal to epithelial conversion in the secondary tumor site (Bastid, 2012). Additional arguments against classical EMT theory in metastasis and clinical applicability are the methodologies used and data generated from transgenic mice (Terao *et al.*, 2011), xenograft implantation (Yoshida *et al.*, 2014), and *in vitro* petri dish work (Yoshida *et al.*, 2014). These experimental results are seemingly incompatible with pathological observations obtained from patients' tissues (Ledford, 2011). Some tumors even exhibit opposite characteristics based on EMT/MET markers. For instance, in prostate cancer, secondary tumors

with highly metastatic potential were found to possess a glandular appearance indicative of epithelial morphology (Rubin *et al.*, 2000). A similar phenotype is displayed in ovarian cancer which possesses elevated E-cadherin expression and an epithelial phenotype yet is highly metastatic (Christiansen and Rajasekaran, 2006; Park *et al.*, 2016; Scotton *et al.*, 2001; Yang *et al.*, 2016).

To tackle the clinical applicability of EMT, lineage tracing is required. Recent reports addressed this issue by generating a mesenchymal promoter (vimentin or fibroblast specific protein-1)-induced Cre-mediated fluorescent marker in breast and lung cancer (Fischer *et al.*, 2015). The cells would irreversibly gain fluorescence *in vivo* upon induction of a mesenchymal phenotype through EMT. The mice spawned breast adenocarcinoma, which predominantly exhibited an epithelial phenotype based on E-cadherin expression and lacked of vimentin and fluorescence expression. Lung metastasis developed spontaneously in the mouse models, which exhibited no change in fluorescence, indicating the same epithelial phenotype within the secondary tumor (confirmed via E-cadherin upregulation and vimentin repression), demonstrating that tumor cells did not activate the mesenchymal-specific promoter or undergo EMT during metastasis (Fischer *et al.*, 2015).

Additionally, another study developed a genetically engineered mouse model to delete SNAIL or TWIST through Cre-mediation in pancreatic ductal adenocarcinoma (PDAC) (Zheng *et al.*, 2015). Significantly, this deletion supressed ZEB2 and enhanced E-cadherin expression in PDAC. Lineage tracing by determining the amount of yellow fluorescent protein-tagged CTCs in the control *versus* SNAIL or TWIST-deletion groups showed that tumor-forming potential and metastatic capacity were not affected. These results indicate that suppression of EMT-TF in PDAC

mouse models did not impede tumor invasion, metastasis or dissemination when tumor cells exhibit an epithelial phenotype (Zheng *et al.*, 2015).

The aforementioned studies challenge the classical EMT model in metastasis and tumor dissemination, suggesting that EMT does not correlate with tumor dissemination and metastasis and that tumor cells with epithelial phenotypes expressing high level of E-cadherin can undergo metastasis and form secondary tumors. Although these studies use one or two core EMT related genes or EMT-TF and possibly simplify EMT processes, the findings support an incomplete, partial or hybrid EMT model to explain metastasis without losing epithelial properties and the formation of secondary tumor without interconvertible epithelial to mesenchymal transitions.

Hybrid E/M and Clinical Relevance

EMT is currently characterized according to the upregulated mesenchymal and repressed epithelial markers in combination with functional tests for tumor cell migration and dissemination. It is assumed that cells undergoing EMT completely switch from the epithelial to the mesenchymal phenotypes. Increasing experimental evidence, however, suggests that this switch is not a single binary decision, but rather proceeds along a spectrum, allowing for cells to express partial epithelial and mesenchymal (E/M) phenotypes and possess both E/M functionality (Christiansen and Rajasekaran, 2006; Jolly *et al.*, 2015a; Rhim *et al.*, 2012).

Indeed, hybrid E/M states (i.e. exhibiting both epithelial and mesenchymal characteristics) have been observed in breast, brain, lung, renal, prostate and pancreatic cancers (Andriani *et al.*, 2016; Grosse-Wilde *et al.*, 2015; Jeevan *et al.*, 2016; Rhim *et al.*, 2012; Ruscetti *et al.*, 2015; Sampson *et al.*, 2014). Moreover, the hybrid E/M tumor cells display elevated CSC properties and patients show poor survival in comparison to EMT or MET phenotypes, possibly through synergy

between adhesion, proliferation and migration in the E/M state (Jolly *et al.*, 2015a). In breast, prostate and lung cancer patients, CTCs with E/M markers were found to migrate into blood as clusters (Danila *et al.*, 2007; Jansson *et al.*, 2016; Yoon *et al.*, 2011; Zhang *et al.*, 2013a). This collective migration would reduce anoikis and increase the chances of successful migration to a suitable secondary tumor location (Fu *et al.*, 2016). These attributes may explain why clustered CTCs exhibit a 50-fold increase in metastatic potential (Aceto *et al.*, 2014). Hence, a better understanding of E/M properties may be key to development of an effective therapeutic strategy to control metastasis and disease relapse (Figure 1.0B).

Literature, however, has put the stability of the hybrid E/M tumor phenotype into question. Are these E/M tumor cells stable or is hybrid E/M tumor phenotype a fluctuating transition? Previously, E/M tumor cells were considered metastable and incapable of maintaining their E/M properties. The hybrid phenotype was thought merely a placeholder along the pathway of complete EMT or MET conversion. Recently, studies using prostate, lung and breast cancer have illustrated that this duel E/M phenotype, mediated through OVOL (OVO-like proteins) transcription, can be maintained for the extended periods of time (Jia *et al.*, 2015; Jolly *et al.*, 2016). OVOL are a series of transcription factors (originally found through mathematical models) which play a critical role in maintaining the E/M prostate CTCs through regulation of miR-200/ZEB and miR-34/SNAIL pathways. OVOL expression led to decreased EMT signalling induced by factors such as TGF-β, and promoted a stable shift towards the epithelial and hybrid E/M phenotype (Jia *et al.*, 2015).

Additional mathematical modeling has identified that GRHL2 and miR-145 can also stabilize the hybrid E/M phenotype (Jolly *et al.*, 2016). Hybrid E/M lung cancer cells were able to be maintained through GRHL2, OVOL2 and miR-145 expression that act as stabilizing factors to inhibit themselves and the ZEB/miR-200 network. Knocking down miR-145 or GRHL2 led to

destabilization of the E/M phenotype, driving the cells towards complete EMT induced by SNAIL (Jolly *et al.*, 2016).

Other reports have also emphasized the importance of the miR-34/SNAIL and the miR-200/ZEB regulatory networks (Lu *et al.*, 2013a). Mechanistic modeling has shown that SNAIL is able to inhibit miR-200 while ZEB is able to inhibit miR-34. As such, miR-34/SNAIL activation drives ZEB expression while inhibiting miR-200 leads to three states: high miR-200/low ZEB, low miR-200/high ZEB or medium miR-200/medium ZEB (Lu *et al.*, 2013a). These states are associated with epithelial, mesenchymal or hybrid phenotypes, respectively. E/M stabilizing factors OVOL, GRHL2 and miR-145 couple with this network, prevent ZEB signalling and promote miR-200, which inhibits complete EMT while pushing cells towards an epithelial and hybrid E/M phenotype (Jia *et al.*, 2015; Jolly *et al.*, 2016; Lu *et al.*, 2013a).

Signalling pathways also affect the balance of miR-200/ZEB. For instance, NF-κB drives the LIN28/let-7 axis (Jolly *et al.*, 2015b) and LIN28 inhibits let-7 which in turn inhibits ZEB (Jolly *et al.*, 2015b), whereas Let-7 and miR-200 inhibit LIN-28 and bridge two networks (Jolly *et al.*, 2015b). It has been found that low LIN-28 and high let-7 correlated with an epithelial phenotype while high LIN-28 mediated Let-7 inhibition and pushed cells towards a mesenchymal phenotype (Jolly *et al.*, 2015b). The hybrid E/M phenotype displayed intermediate expression of LIN28 and let-7 (Jolly *et al.*, 2015b). Additionally, the LIN-28/let-7 axis regulates stemness through OCT4 expression (Jolly *et al.*, 2014). An outline of hybrid E/M signalling and stemness acquisition is depicted in Figure 1.1.

Further studies have shown that the acquisition of stemness can be modulated in mesenchymal, epithelial and hybrid E/M. For instance, OVOL enhanced hybrid E/M stemness while reducing mesenchymal stemness (Jolly *et al.*, 2015b). On the contrary, OVOL repression

exerted an opposite effect, enhancing mesenchymal while diminishing epithelial and hybrid E/M stemness (Jolly *et al.*, 2014; Jolly *et al.*, 2015b). It would be interesting to determine whether or not the Wnt, Akt, YAP, and/or other signaling pathways, known in EMT/MET regulation and stemness, are involved in the miR-200/ZEB and/or LIN28/let-7 axis and associated with hybrid E/M formation, and/or involved in acquisition of stemness properties.

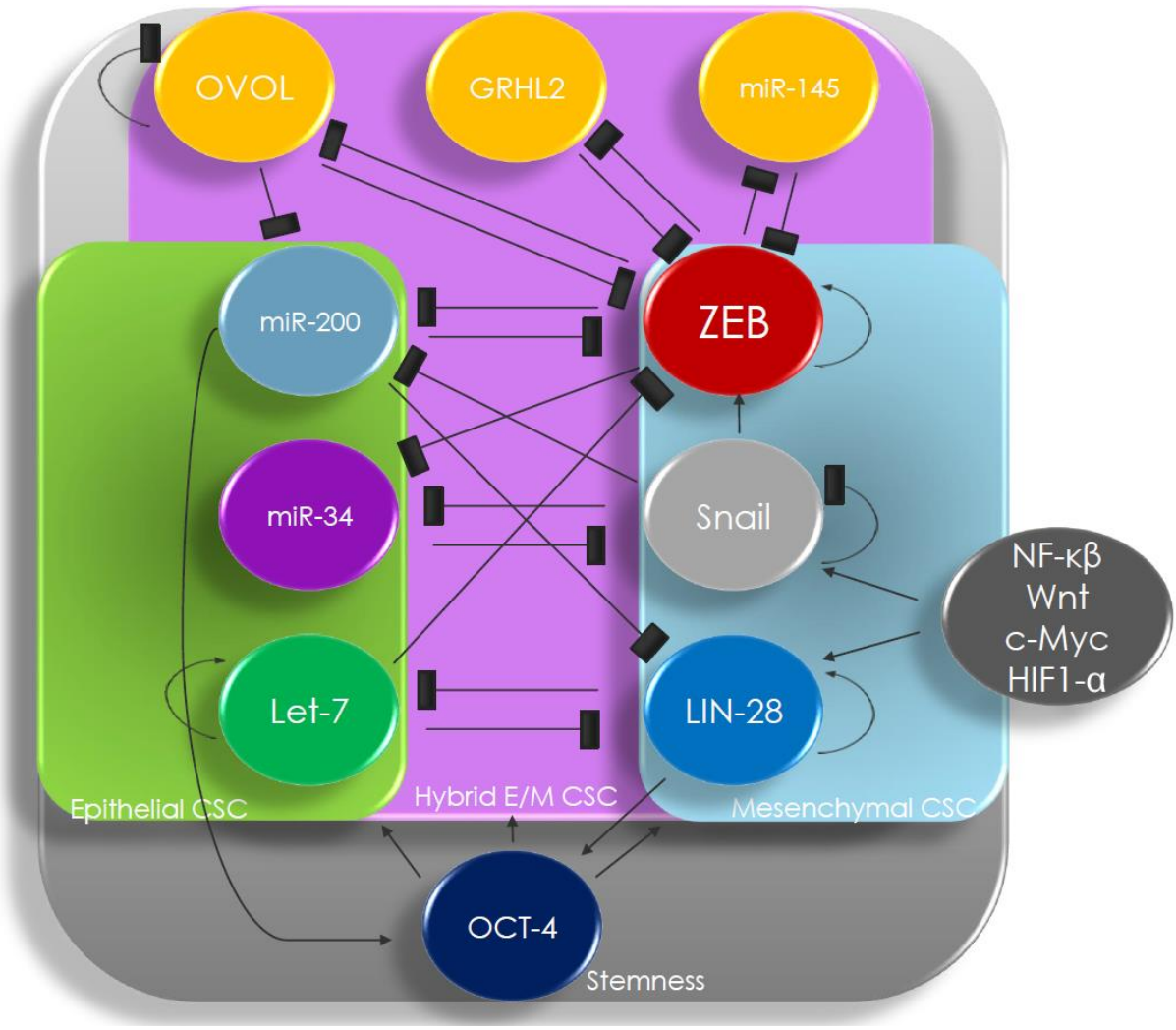

Figure 1.1: A schematic diagram of Hybrid E/M signalling and stemness acquisition. The acquisition of mesenchymal traits is associated with increased ZEB signalling. ZEB feed-forwarding signalling inhibits miR-200 and leads to the expression of mesenchymal markers such as N-cadherin and vimentin while repressing epithelial associated markers such as E-cadherin. Snail upregulates ZEB while inhibiting miR-34. In addition, Snail is stimulated by many signal pathways including NF-κβ, Wnt, c-Myc and HIF1-α. LIN-28 is also associated with the acquisition of mesenchymal traits. LIN-28 inhibits Let-7, increasing ZEB expression while also promoting OCT-4 and enhancing stemness. The acquisition of epithelial traits is associated with high levels of miR-200 and miR-34 which repress ZEB and Snail respectively. MiR-200 also represses LIN-28 signalling, promoting Let-7 expression to further repress ZEB and promote OCT-4 and other stemness feature. Additionally, miR-200 inhibits LIN-28 to increase Let-7 expression, ultimately repressing mesenchymal while promoting epithelial phenotypes. The hybrid E/M phenotype is associated with intermediate signalling between miR-200/ZEB, miR-34/Snail and Let-7/LIN28 axes, which is associated with intermediate OCT-4 expression and the greatest stemness potential. OVOL, GRHL2, and miR-145 are hybrid E/M modulators, stabilizing the hybrid E/M phenotype, inhibiting ZEB signalling and complete EMT. These stabilizers also promote hybrid E/M stemness.

Investigation of Hybrid E/M with Improved Methodologies

Studying hybrid E/M cancer cells proves to be challenging since these cells possess both epithelial and mesenchymal markers and functions. *In vitro* cell culture may produce inconsistent results due to artificial selection of monoculture from thriving cell sublines. Moreover, lack of microenvironment, extracellular matrix and three dimensions add to the discrepancy between *in vitro* and *in vivo* results. However, advances in the development of *in vitro* 3D cell culture systems have led to new discoveries in regards to cancer cell plasticity between epithelial, mesenchymal, and hybrid E/M states.

Recently, co-culture of mammary EpH4 epithelial cells with a bio-engineered 3D matrix composed of solid alginate hydrogel with adhesive RGD (Arg-Gly-Asp) peptides replicated a 3D microenvironment, leading to normal epithelial morphogenesis and producing acini-like structures, native to mammary tissue (Bidarra *et al*., 2015). TGFβ1 was then used to promote EMT where mesenchymal cells were generated, but upon removal of TGFβ1, the cells switched to the hybrid E/M phenotype instead of an epithelial state. Notably, these hybrid cells displayed increased proliferative and tumorigenic capabilities and an aggressive phenotype (Bidarra *et al.*, 2015).

The usage of microfluidic co-culture systems for tumor microenvironment emulation has also been demonstrated to be an effective methodology for analysis of epithelial/mesenchymal/hybrid traits (Aref *et al.*, 2013; Kim *et al.*, 2016; Soon *et al.*; Wang, 2016). This platform can analyze cancer cells in an extracellular matrix and assess proliferation, dissemination and migration in real time. Activators/repressors can be introduced into the co-culture system to stimulate epithelial or mesenchymal phenotypes, and thus enable cellular communication to mimic *in vivo* processes. With further innovation, this system may be invaluable

for further investigation of epithelial/mesenchymal and hybrid E/M characters in real time using lineage tracing with promoter-induced fluorescent proteins as described above.

Marker analysis may also be a useful tool for hybrid E/M research. Besides the dual epithelial and mesenchymal gene and protein expression, P-cadherin has been gaining traction as a hybrid E/M marker (Jolly *et al.*, 2016; Plutoni *et al.*, 2016a; Plutoni *et al.*, 2016b). P-cadherin is associated with poor prognosis in breast, oral squamous, bladder, pancreatic and ovarian cancers (Ko and Naora, 2014; Li *et al.*, 2016; Sakamoto *et al.*, 2015; Vieira *et al.*, 2012; Wang *et al.*, 2014). It interferes with epithelial adhesion and promotes migration and metastasis through MMP upregulation, cell polarization, cdc42 (cell division control protein 42 homolog) activation, and its own cleavage (Mar *et al.*, 2014; Plutoni *et al.*, 2016a; Plutoni *et al.*, 2016b; Ribeiro and Paredes, 2015). Importantly, P-cadherin-promoted migration is through collective but not individual cell movement in both epithelial and mesenchymal cancer cells, mimicking the hybrid E/M phenotype (Jolly *et al.*, 2016; Plutoni *et al.*, 2016a; Plutoni *et al.*, 2016b).

$CD44^{high}/CD24^{low}/ALDH^{high}$ markers may also be employed for the identification of hybrid E/M CSCs. $CD44^{high}/CD24^{low}$ subpopulation are commonly enriched in mesenchymal-like cancer cells while $ALDH^{high}$ is enriched in epithelial-like cancer cells (Mi and Xing, 2015; Paholak *et al.*, 2016). It has been shown *in vivo* in breast cancer that the $ALDH^{high}$ subpopulation resides internally while the $CD44^{high}/CD24^{low}$ tumor population lies at the tumor edge and is prone for tumor dissemination and metastasis (Liu *et al.*, 2014a). The $CD44^{high}/CD24^{low}/ALDH^{high}$ subpopulation in multiple breast cancer cell lines exhibited the enhanced proliferative, tumorigenic, migration, adhesive and metastatic potentials both *in vitro* and *in vivo* (Croker *et al.*, 2009; Ginestier *et al.*, 2007; Liu *et al.*, 2014a; Zhang and Rosen, 2015). Moreover, the $CD44^{high}/CD24^{low}/ALDH^{high}$ subpopulation is able to generate tumors with as few as 20 cells

(Ginestier *et al.*, 2007). This is consistent with the clinical data where $ALDH^{high}$/ $CD44^{high}$ is frequently found in patients with breast cancer and associated with increased tumor growth, disease progression, metastasis, and worsened prognosis despite radiotherapy, endocrine therapy, or chemotherapy (Croker and Allan, 2012; Ginestier *et al.*, 2007; Qiu *et al.*, 2016). From the current literature, it seems that the $CD44^{high}/CD24^{low}/ALDH^{high}$ may be used for the detection of hybrid E/M CSCs.

In conclusion, while much progress has been made, targeting either epithelial or mesenchymal cancer cells seems insufficient due to cancer cell plasticity and the existence of hybrid E/M phenotype. Targeting both bulk and CSC subpopulations of epithelial, mesenchymal and hybrid E/M may be crucial for the development of clinically viable treatments to reduce resistance, relapse and metastasis.

-End of Review Article-

1.8 Chemotherapies and CSC Enrichment

For the treatment of TNBC, due to the lack of specific therapies, chemotherapeutic and radiotherapeutic approaches are commonly prescribed. While radiotherapy and chemotherapy may be effective against the bulk TNBC tumor population; there has been contrasting evidence regarding their efficacy on CSCs.

It has been found that breast cancer $CD44^{+}/CD24^{-}$ CSCs are resistant to radiotherapy compared to the bulk tumor population (Han and Crowe, 2009; Phillips *et al.*, 2006). Additionally, radiation exposure increased the phosphorylation of H2AX (H2A histone family member X) and Notch-1 expression which promoted an increased in CSC enrichment following treatment (Phillips *et al.*, 2006).

Additionally, it has been reported that Paclitaxel, Doxorubicin and 5-Florouracil, (commonly prescribed chemotherapeutic agents for the treatment of TNBC) promote cytokine (IL-6, IL-8 and MCP-1) secretion within the tumor microenvironment which activates the inflammatory STAT3, Wnt/β-catenin, and NF-kB signalling pathways (Jia *et al.*, 2017; Jia *et al.*, 2016). This creates a feed-forward loop leading to further cytokine secretion (TNF-α, IL-17, CSF2, CCL2, IFN-γ, IL-1β, etc) which stimulates additional inflammation and promotes immunosuppression, alters the epigenetics of the tumor cells, stimulates tumor proliferation, increases metastatic potential, promotes hypoxia, promotes survival amongst the tumor population and enriches for the CSC population following treatment (D'Ignazio *et al.*, 2017; Finger and Giaccia, 2010; Jia *et al.*, 2017; Zhang *et al.*, 2017).

Jia *et al* assessed tumorigencity following short-term Paclitaxel treatment using a serial dilution assay. In this assay, following short-term treatment, the original tumor was extracted, dissociated into single cell suspension, cancer cells were counted and subsequently re-implanted

into a new mouse at serially diluted numbers. The ability of the treated versus untreated tumors to form novel tumors at serially diluted concentrations were then assessed. It was demonstrated using 100,000 MDA MB-231 TNBC cells following treatment, that control (DMSO treated) cells were not able to generate any tumors (0/3, three representing the total amount of attempts to form a tumor) (Jia *et al*, 2017). In contrast, MDA MB-231 tumors previously treated with paclitaxel formed tumors 3/3 times (100%) upon injection of 100,000 cells into the mammary fat pad of athymic mice (Jia *et al*, 2017). When Paclitaxel treatment was combined with an agent to inhibit Paclitaxel-induced NF-kβ signalling (Reparixin) the tumorigenicity was reduced to a frequency of 1/3 times (33%) (Jia *et al.*, 2017). This paper highlighted the potency of paclitaxel, a frontline chemotherapeutic agent for the treatment of TNBC, to stimulate CSC enrichment and induce chemoresistance and tumorigenicity following treatment. However, this paper also demonstrated the potency of specific signal pathway inhibition to alleviate paclitaxel-mediated effects (Jia *et al.*, 2017).

Other papers have reported similar findings on $CD44^+/CD24^-$ and $ALDH^+$ CSC enrichment and tumorigenicity following chemotherapeutic treatment (Reynolds *et al.*, 2017; Thakur and Ray, 2017; Yin *et al.*, 2017; Zhou *et al.*, 2018; Zhuang *et al.*, 2012). This issue of chemotherapeutic CSC enrichment is present in other cancer models as well. Abubaker *et al* demonstrated in ovarian cancer that while short term chemotherapeutic treatment effetely targeted bulk tumor cells, due to the enrichment of CSCs following treatment, when the chemotherapy treated HEY ovarian cancer tumors were isolated and implanted into new mice, these mice displayed increased tumor burden compared to mice implanted with vehicle treated cells (Abubaker *et al*, 2013). Additionally, these chemotherapy-treated cells possessed increased proliferative, stem-like and metastatic properties (Abubaker *et al.*, 2013). These findings highlight the failure of chemotherapy to target the CSC

populations in different cancer models and highlights the detrimental effect chemotherapeutic exposure has in regards to CSC enrichment.

These reports demonstrate chemotherapeutic effectiveness at shrinking the initial breast cancer tumor; however, a consequence of these treatments is the promotion of an inflammatory, stressful, hypoxic microenvironment which in turn, promotes CSC enrichment. This may explain the high rates of relapse, metastasis and overall poor prognosis in TNBC following interventional treatment. It has been demonstrated in a meta analysis on 898 breast cancer patients that CD44+/CD24$^-$ and ALDH$^+$ breast cancers are associated with poorer overall patient survival (Zhou *et al.*, 2010). As such, chemotherapy induced CSC enrichment presents a negative consequence and barrier against long-term patient survival.

1.9 Epithelial/Mesenchymal States of Breast Cancer CSCs

Accumulating evidence suggests that breast CSCs are a major barrier preventing patient disease free survival (Al-Hajj *et al.*, 2003; Gupta *et al.*, 2009a; Hemmati *et al.*, 2003; Kreso and Dick, 2014; Lapidot *et al.*, 1994; Valent *et al.*, 2012; Visvader and Lindeman, 2012). Conventional interventions, such as radiation and chemotherapy, may eliminate the bulk of the tumor but are ineffective against breast CSCs which have an exceptional capacity to survive, self-renew, and advance the malignancy (Al-Hajj *et al.*, 2003; Gupta *et al.*, 2009a; Hemmati *et al.*, 2003; Kreso and Dick, 2014; Lapidot *et al.*, 1994; Valent *et al.*, 2012; Visvader and Lindeman, 2012). However, there exists two states of breast CSCs, demarcated by E-cadherin expression; mesenchymal CD44$^+$/CD24$^-$ and epithelial ALDH$^+$ CSCs (Beerling *et al.*, 2016; Liu *et al.*, 2014; Tsuji *et al.*, 2008).

The mesenchymal-like state is associated with expression of mesenchymal markers (e.g. vimentin, N-cadherin), loss of epithelial markers (e.g. E-cadherin) quiescence, and an enhanced invasive capacity. Conversely, the epithelial-like state is associated with the expression of epithelial markers, establishment of cell polarity, and extensive self-renewal and proliferation (Liu *et al.*, 2014). In addition, CSCs also display a cellular plasticity that enables them to transition between epithelial-like and mesenchymal-like states (Beerling *et al.*, 2016; Tam and Weinberg, 2013). While the mesenchymal-like state may be important for cancer cell dissemination, reversal to epithelial-like state seems to be necessary for efficient metastatic colonization (Brabletz, 2012). Consequently, the transition between these two states in breast CSCs have been considered to facilitate breast cancer growth, tumor dissemination and cancer relapse. Due to the differences within these populations, approaches which focus on only one CSC population may spare or enrich the neglected epithelial-like or mesenchymal-like CSC population, promoting resistance, CSC interconversion and relapse.

Current research must focus on targeting both epithelial-like and mesenchymal-like CSC specific signalling and preventing chemotherapeutically induced CSC enrichment in order to improve TNBC treatment efficacy and long-term patient prognosis.

1.10 Wnt and CSCs

In brief, in the absence of Wnt signalling, the destruction complex (consisting of GSK3-β, Axin-2, APC and CK1α) binds to β-Catenin in the cytoplasm, phosphorylates β-Catenin, marks it for ubiquitination by β-TrCP and subsequent destruction (Zhan *et al.*, 2017). Canonical Wnt signalling involves Wnt ligands binding to the LRP5/LRP6/Frizzled co-receptor which promotes the phosphorylation of LRP5/6 via CK1α and GSK3-β (Zhan *et al.*, 2017). Dishevelled is recruited

which in turn binds to Axin-2 and inhibits GSK3-β (Zhan *et al.*, 2017). The inhibition of the destruction complex allows β-Catenin to translocate into the nucleus, where it associates with LEF/TCF transcription factors to stimulate Wnt dependant gene expression (Zhan *et al.*, 2017). Additionally, β-Catenin may associate with p300 or CBP histone modifying proteins to affect the epigenetics of the cell.

Wnt signalling is highly activated in basal-like breast cancers (overexpressed in 50% of patients) and is associated with poorer patient prognosis (Khramtsov *et al.*, 2010; Lin *et al.*, 2000). Wnt signalling is critical for stem cell self-renewal and is associated with CSC development and enrichment. Wnt signaling has also been demonstrated to facilitate the conversion of adult cells to pluripotent stem cells highlighting its importance in stem cell/CSC regulation (Chen *et al.*, 2010; Huang *et al.*, 2015 ; Li *et al.*, 2010; Redmer *et al.*, 2011).

Zeng and Nusse *et al*, demonstrated using the Axin2-lacZ Wnt reporter system in a mouse model, that there was high levels of Wnt activity within the basal membrane of the mammary ducts which were hypothesized to be mammary stem cells (Zeng and Nusse, 2010). The mammary glands were then cleared and $lacZ^{+}/Lin^{-}/CD24^{+}/CD29^{high}$ mammary stem cells were inserted into the cleared ducts. It was found that the inserted mammary stem cells were able to generate mammary glands with only 50 cells at a frequency of 11 times out of 16 attempts. In comparison $lacZ^{-}/Lin^{-}/CD24^{+}/CD29^{high}$ mammary stem cell transplants only reconstituted the mammary gland 5 tines out of 16 attempts (Zeng and Nusse, 2010). Such findings demonstrated the importance of Wnt signalling within the mammary gland and mammary stem cells.

Shackleton *et al*, demonstrated similar findings; however, used a MMTV-*wnt-1* mouse lineage (prone to developing tumors due to high Wnt signalling) and found increased levels of $Lin^{-}/CD24^{+}/CD29^{high}$ mammary stem cells within the mammary glands (Shackleton *et al.*, 2006).

Additionally it was found that when 25 $Lin^{-}/CD24^{+}/CD29^{high}$ MMTV-*wnt-1* mammary stem cells were transplanted into the inguinal glands cleared of endogenous epithelial, there was dramatic hyperplastic outgrowths observed at five weeks post-transplantation (Shackleton *et al.*, 2006). Together this report highlights the importance of Wnt signalling in mammary stem cells, breast CSCs and breast cancer development.

Multiple reports have demonstrated that upon Wnt ablation, CSCs in breast cancer differentiate and are sensitive to apoptosis (El Helou *et al.*, 2017; Li *et al.*, 2018; Petrelli *et al.*, 2015; Xu *et al.*, 2016a). As such, targeting Wnt signalling may be a prime target for the inhibition of TNBC CSCs.

1.11 YAP and CSCs

YAP (Yes Associated Protein) signalling is a part of the Hippo pathway which controls cell growth, organ size, apoptosis and self-renewal (Ehmer and Sage, 2016). When Hippo signalling is active, mediated by a variety of stimuli such as cell contact and adhesional junctions, MST1/2 kinases associate with SAV1 and PDK1 to activate LATS1/2 kinases (Ehmer and Sage, 2016; Fan *et al.*, 2013a). These kinases in turn phosphorylate YAP in the cytoplasm, preventing it from translocating into the nucleus and marking it for protein degradation (Ehmer and Sage, 2016). Upon YAP activation via extracellular signalling, endogenous stimulation and/or mechanotransduction, PDK1 is recruited to the plasma membrane which prevents the activation of the MST1/2/SAV1 complex and subsequent LATS1/2 activation. This prevents YAP phosphorylation and allows for its translocation into the nucleus where it associates with the TEAD1-4 transcription factors which mediate YAP gene expression (Ehmer and Sage, 2016; Fan *et al.*, 2013a).

Aberrant YAP expression has been closely associated with cancer development and progression (Yu *et al.*, 2015; Zhang *et al.*, 2015). In TNBC it has been found that YAP signalling confers resistance to radiotherapy and upon YAP inhibition, TNBC can be sensitized to DNA damage (Andrade *et al.*, 2017). Additionally, YAP signalling has been found to stimulate breast cancer with proliferative, migratory and invasive properties (Lamar *et al.*, 2012). It has been demonstrated that when YAP was transfected into the non-tumorigenic human mammary cell line (MCF-10a), the cells lost cell to cell contact, grew in a scattered patterns, formed invasive spheroids and demonstrated apoptotic resistance (Overholtzer *et al.*, 2006). Additionally, their invasive properties were amplified and their colony forming potential was greatly amplified (Overholtzer *et al.*, 2006).

YAP was found to positively correlate with the expression of *OCT4*, *SOX2* and *NANOG* genes in human pluripotent stem cells (Johnson and Halder, 2014). These pluripotency factors have been closely associated with the regulation of self-renewal versus differentiation in stem cells/progenitors. These factors are also associated with tumorigenesis and mediate breast CSC enrichment (Kim *et al.*, 2015; Beltran *et al.*, 2011; Lu *et al.*, 2013b; Noh *et al.*, 2012; Vazquez-Martin *et al.*, 2013).

Moreover, Kim *et al* found that YAP was highly expressed in TNBC basal-like breast cancers and imparted mammary stem cell signature gene expression and the secretion of IL-6, IL-8 and CXCL1 cytokines (Kim *et al.*, 2015). Moreover, the authors transfected 4T1 (a murine TNBC cell line) cells with a retrovirus to overexpress YAP, and preformed a serial dilution assay where YAP overexpressing cells were implanted into BALB/c mice. It was found that YAP overexpressing 4T1 TNBC cells were capable of forming a tumor with as little at 10 cells (Kim *et al.*, 2015).

Recently, YAP/TAZ signalling through the Hippo pathway has emerged as a potent regulator of Wnt signalling (Azzolin *et al.*, 2014; Beyer *et al.*, 2013; Ohgushi *et al.*, 2015). YAP/TAZ incorporates into the β-catenin destruction complex and is a mediator of β-catenin degradation (Azzolin *et al.*, 2014; Imajo *et al.*, 2012). Conversely, increased E-cadherin, cell density or activated Akt has been shown to suppress YAP/TAZ (Basu *et al.*, 2003; Benham-Pyle *et al.*, 2015; Fan *et al.*, 2013b; Imajo *et al.*, 2012; Kim *et al.*, 2011b; Li *et al.*, 2013). Although YAP is closely associated with cancer (Yu *et al.*, 2015), functional interactions between YAP, epithelial/mesenchymal status, and Wnt in breast cancer cells is still unclear.

1.12 Clinically Translatable Models to Study TNBC

The following review, for which I am the first author, was published in Oncotarget and will discuss pre-clinical models, and the need to adapt patient derived xenograft models (PDX) for clinically translatable findings.

Andrew Sulaiman and Lisheng Wang. Bridging the divide: preclinical research discrepancies between triple-negative breast cancer cell lines and patient tumors. *Oncotarget*, 2017; 8(68): 113269–113281 Published under a Creative Commons Attribution (CC BY) License.

AS wrote the manuscript and created the figures. LW provided feedback, critiques and edited the article.

ABSTRCT

Triple-negative breast cancer (TNBC) is the most refractory subtype of breast cancer and disproportionately accounts for the majority of breast cancer related deaths. Effective treatment of this disease remains an unmet medical need. Over the past several decades, TNBC cell lines have been used as the foundation for drug development and disease modeling. However, ever-mounting research demonstrates striking differences between cell lines and clinical TNBC tumors, disconnecting bench research and actual clinical responses. In this review, we discuss the limitations of cell lines and the importance of using patients' tumors for translational research, and highlight the usage of patient-derived xenograft (PDXs) models that have emerged as a clinically relevant platform for preclinical studies. PDX tumors possess tumor heterogeneity with similar cellular, molecular, genetic and epigenetic properties akin to those found within patients' tumors. Moreover, PDX and clinical tumors possess abnormal vasculature with higher blood vessel permeability, a feature that is not always demonstrated in *in vivo* cell line xenografts. Development of clinically relevant, novel drug-nanoparticles capable of accumulating in PDX tumors through the enhanced permeability and retention effect in tumor vasculature may lead to new and effective TNBC treatments.

INTRODUCTION

Breast cancer remains a leading cause of death in women throughout the world. Triple negative breast cancer (TNBC) accounts for only 15-20% of all breast cancer, but is disproportionally associated with the majority of breast cancer related deaths (Anders and Carey, 2009). Chemotherapy is currently the mainstay of systemic medical treatment for TNBC. However, it is associated with severe off-target tissue toxicity, rapid drug-resistance, and enrichment of cancer stem cells (Gómez-Miragaya *et al.*, 2017; Jia *et al.*, 2016). As such, development of targeted therapies for TNBC is an unmet medical need.

Over past several decades, *in vitro* and *in vivo* preclinical research commonly uses over 27 TNBC cancer cell lines to study cancer pathogenesis, disease advancement, and drug effectiveness. However, a growing disconnection between results generated using TNBC cell lines and clinical trials has been observed. A recent example is the *in vitro* and *in vivo* results of PARP inhibitor veliparib. Veliparib is an oral inhibitor of Poly (ADP-Ribose) Polymerase (PARP) 1 and 2, which enhances the activity of DNA damaging agents in DNA repair to promote apoptosis. *In vitro*, veliparib is capable of suppressing the expression of Snail which promotes epithelial to mesenchymal transition, tumor metastasis and drug resistance. It also sensitizes the MDA-MB-231 TNBC cell line to chemotherapeutic drug doxorubicin, resulting in increased apoptosis (Mariano *et al.*, 2015). *In vivo*, veliparib sensitizes MDA-MB-231 tumor to TMZ (temozolomide , an alkylating agent) in a SCID (severe combined immune deficiency) mouse model (Palma *et al.*, 2009). The effectiveness of other therapeutic combinations with veliparib has also been demonstrated *in vivo* xenograft mouse models using cancer cell lines (Palma *et al.*, 2009; Shelton *et al.*, 2013).

The clinical trials, however, failed to demonstrate the efficacy of veliparib in combination with a DNA damaging agent for the treatment of breast cancer including TNBC. The phase II clinical trial (NCT01506609) recruited 193 metastatic breast cancer patients treated with either the placebo or veliparib in a combination of carboplatin and paclitaxel. Progression-free survival in the control group (chemotherapeutic drugs alone) was 12.3 (9.3–14.5) months compared to the 14.1 (11.5–16.2) months in the combination group, showing statistically insignificant difference (*p* value = 0.231) (Han *et al.*, 2017; Isakoff *et al.*, 2017a). Overall survival in the control was 25.0 (18.1–34.8) months and the combination of veliparib and chemotherapy was 28.5 (22.4– not reported results), which was insignificant (*p* value = 0.148) (Han *et al.*, 2017). Despite these results, veliparib in combination with paclitaxel and carboplatin followed by doxorubicin and cyclophosphamide advanced into phase III clinical trials (NCT02032277) for the treatment of TNBC (Geyer *et al.*, 2017). 634 TNBC patients were involved in the study and treated with veliparib or placebo in combination with paclitaxel and carboplatin followed by doxorubicin and cyclophosphamide. There was no significant difference in the efficacy of treatment (53.2% veliparib + chemotherapy *vs* 57.5% placebo + chemotherapy, $p = 0.36$) (Geyer *et al.*, 2017). This recent failure is by no means a rarity as many similar results have been reported (Flinn *et al.*, 2016; Sinha, 2014; Soria *et al.*, 2015; Taplin *et al.*, 2017; Wakelee *et al.*, 2015). This highlights the disconnection between cell lines *in vitro* and *in vivo* preclinical research and human clinical trials. The translational disparity led to the US National Cancer Institute halting the usage of 60 human cancer cell lines for drug-screening in 2016 and recommending to use patient derived xenograft (PDX) for future research. Appropriate models used in preclinical/translational studies may bridge the divide (Ledford, 2016). In this regard, PDXs have shone as clinically relevant models in

comparison to breast cancer cell lines due to their ability to represent the original tumor's biology and retain the original tumor's architecture and organization (Williams *et al.*, 2013).

THE LIMITATIONS OF CELL LINES IN PRECLINICAL RESEARCH

Breast cancer cell lines used for conventional analysis were originally harvested and generated from patient tumor samples after *in vitro* culture for years or decades. The deviancies observed are thought to arise through selection of specific populations and changes over time to promote adaption to artificial culture environments. Breast cancer cell lines are capable of growing indefinitely and undergoing freezing-thawing cycles for several decades. It has been demonstrated that breast cancer cell lines possess a moderately high mutation frequency in comparison to patient tumors. Over many *in vitro* passages, these mutations can accumulate, possibly making the cells differ dramatically from their starting source (Briske-Anderson *et al.*, 1997; Jiang *et al.*, 2016; Osborne *et al.*, 1987; Wenger *et al.*, 2004). Additionally, these mutations can promote certain traits which provide a survival benefit for *in vitro* growth in a plastic dish. This would promote clonal selection for the fittest subpopulations (Pastrana, 2012). Continuous propagation of cells in a petri dish would also result in accumulating epigenetic alterations (Nestor *et al.*, 2015). It has been demonstrated that human cancer cell lines possess altered methylation patterns after culture (Varley *et al.*, 2013). Altered DNA methylation affects gene and protein expressions, subsequently impacting signal pathways and therapeutic responses. Additional reports have shown that DNA methylation differs dramatically between cancer cell lines in comparison to patient tumors, making epigenetic studies using cell lines discordance with clinical settings (Houshdaran *et al.*, 2010; Poirier *et al.*, 2015).

One example was the expression of ER/PR/HER-2 receptors in two TNBC tumors after culture for 150 passages. Originally, these receptors were all absent in the primary tumors harvested from the TNBC patients (Kamalidehghan *et al.*, 2012). Miller *et al* also recently showed that there were almost no overlaps in gene expression between glioblastoma samples grown in mice and cultured on a dish after 2-3 weeks, suggesting a marked modification of tumor biological features after short-term culture in petri dishes (Miller *et al.,* 2017).

This dramatic deviance is largely associated with the disruption of the original tumor structure and microenvironment which is comprised of a heterogeneous mixture of different subpopulations of tumor cells, macrophages, fibroblasts, endothelial cells, stromal cells, the extracellular matrix, etc. (Balkwill *et al.,* 2012; Binnemars-Postma *et al.*, 2017). Cancer cell lines do not represent these heterogeneous components. Rather, during initial harvesting and culturing, subpopulations adapted better for *in vitro* petri dish environment (e.g. cancer associated fibroblast cells) are commonly selected for, overtaking the other tumor cells and resulting in a relative homogenous population overtime (Nishikata *et al.*, 2013; Speirs *et al.*, 1998; Wang *et al.*, 2001). Culture methodologies which inhibit fibroblastic growth and promote epithelial proliferation, still fall victim to one dominant tumor subpopulation (Janik *et al.*, 2016; Wang *et al.*, 2001). This artificial selection makes the therapies developed highly effective on a particular cell subtype rather than the whole homogenous tumor and its extracellular matrix and tumor microenvironment, which disconnects the bench results from the clinical trials. *In vivo* studies, human breast cancer cell lines are commonly mixed with matrigel and injected into mouse mammary pad to resemble the clinical settings. However, in addition to the aforementioned limitations, this sudden influx of cancerous cells bypasses the early development of a tumor in the patient and skips over the formation of the tumor microenvironment (Mullen *et al.,* 1996; Vargo-Gogola and Rosen, 2007).

This may in part, explain the divergence between the high frequency of bone metastasis for patient with breast cancer (~70% of all breast metastasis) and the very low frequency of spontaneous metastasis of breast cancer cell line implanted in the mammary fat pad (Coleman and Rubens, 1987; Lelekakis *et al.*, 1999; Simmons *et al.*, 2015). As such, to mimic bone metastasis, breast cancer cell lines must be injected either *via* intracardiac, tail vein or intra-osseous, or specialized cell lines must be utilized (Fantozzi and Christofori, 2006; Kang *et al.*, 2003; Lelekakis *et al.*, 1999; Thibaudeau *et al.*, 2014). Additionally, the monocultured breast cancer cell lines do not include factors commonly dysregulated in the tumor such as hypoxia, inflammation, vascularity, stromal cells, immune cell infiltration, and aberrant signalling pathways (Prasetyanti and Medema, 2017). These factors work together to regulate tumor microenvironment, tumor growth and metastasis. As such, translatable research requires a breast cancer model freshly isolated from the patient without disturbing tumor structures to encompass all of these factors and retain tumor heterogeneity and microenvironment (Figure 1.3).

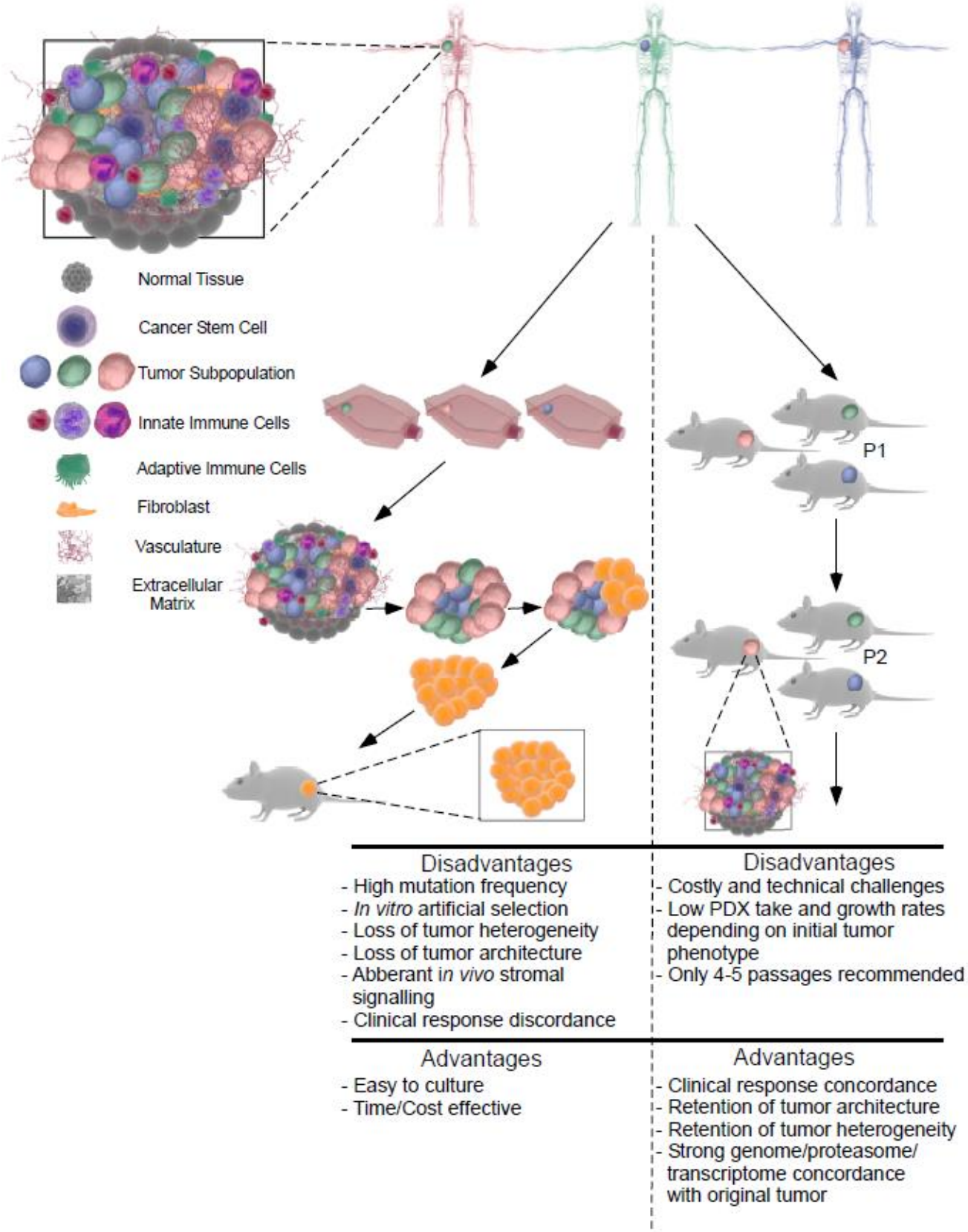
Normal Tissue
Cancer Stem Cell
Tumor Subpopulation
Innate Immune Cells
Adaptive Immune Cells
Fibroblast
Vasculature
Extracellular Matrix
P1
P2
Disadvantages
- High mutation frequency
- *In vitro* artificial selection
- Loss of tumor heterogeneity
- Loss of tumor architecture
- Abberant *in vivo* stromal signalling
- Clinical response discordance
Disadvantages
- Costly and technical challenges
- Low PDX take and growth rates depending on initial tumor phenotype
- Only 4-5 passages recommended
Advantages
- Easy to culture
- Time/Cost effective
Advantages
- Clinical response concordance
- Retention of tumor architecture
- Retention of tumor heterogeneity
- Strong genome/proteasome/ transcriptome concordance with original tumor

Figure 1.3: The main differences between PDX and Cell Line Xenografts for Preclinical Research. *In vitro* culture of patient samples leads to a loss of tumor architecture and heterogeneity. The resultant adherent tumor cells are subject to culture selection and adaptation to artificial conditions, leading to the generation of a subpopulation of cell line from the original patient's tumor containing multiple cell types and subpopulations. Subsequent *in vitro* and *in vivo* experiments preformed using a subpopulation cells may result in discrepancy between breast cell lines and clinical observations and clinical trials. In contrast, implanting breast tumor immediately after harvest from patients into an immune deficient mouse model can preserve tumor heterogeneity, architecture and stromal and extracellular components. After *in vivo* expansion, the PDX tumors retain original tumor properties for up to 4-5passages. In sharp contrast to cancer cell line xenografts, drug responses of PDX models are consistent with patients, making PDX model an invaluable tool for translational research.

THE IMPORTANCE OF USING PATIENTS TUMORS AS MODELS FOR PRECLINCIAL RESEARCH

Considerable observations obtained from patients' tumors cannot be mimicked by using breast cancer cell lines. Acerbi *et al* recently demonstrated that crosstalk between the extracellular matrix and inflammation promotes invasion in 20 breast cancer patient biopsies (Acerbi *et al.*, 2015). Increased amounts of collagen were deposited within invasive breast cancer. Furthermore, the collagen was thicker, underwent a linear reorganization in the stroma of the invasive lesions, associated with increased mechano-signalling and increased stromal stiffness. The invasive edge of the tumors possessed the greatest stromal stiffness illustrating regional stromal heterogeneity. This stiffness at the tumor edge was caused by accumulating activated macrophages and increased TGF-β activity, suggesting a crosstalk between macrophage accumulation, stromal stiffness and tumor invasion. TNBC patient tumors possessed the greatest stromal stiffness, macrophage accumulation, and TGF-β activation at the tumor front compared to the other breast cancer subtypes. Additionally, TNBC exhibited increased YAP (Yes-associated protein) signalling that correlated with stromal stiffness, tumor aggression and invasion. YAP is a mechanically activated signaling pathway that is associated with cancer stem cells (CSCs) and poor patient prognosis (Cordenonsi *et al.*, 2011; Kim *et al.*, 2015a; Xu *et al.*, 2010b). This study highlights the multifaceted interplay between tumor cells, the extra cellular matrix and the immune system, which cannot be modeled by the cultured breast cancer cell lines and their xenografts.

Using patients' tumor samples, Liu *et al*, demonstrated that there exist two pools of CSCs within the breast cancer. A mesenchymal, migratory $CD44^{+}/CD24^{-}$ CSC subpopulation exists at the tumor edge, while an epithelial, proliferative $ALDH^{+}$ CSC subpopulation resides within the tumor core. Moreover, interconversion (plasticity) between the fractionated two CSC

subpopulations was observed, and both epithelial and mesenchymal CSCs were responsible for metastasis and tumor reconstitution at a secondary location. Controversially, *in vivo* xenograft analyses of breast cancer cell lines were unable to demonstrate $ALDH^+$ or $CD44^+/CD24^-$ CSC localization patterns or determine a positive correlation between the frequency of $CD44^+/CD24^-$ CSCs and tumor metastasis as observed in patients with breast cancer (Liu *et al.*, 2014c; Sheridan *et al.*, 2006).

Recent reports demonstrated that a hybrid epithelial/mesenchymal $CD44^+/CD24^-/ALDH^+$ CSC subpopulation is more tumorigenic than its pure counterpart, although its role in metastasis and secondary tumor formation remains to be elaborated (Shao *et al.*, 2016; Shiraishi *et al.*, 2017; Sulaiman *et al.*, 2017a). Using patients' metastatic breast cancer pleural effusions, Shiraishi *et al* demonstrated that $CD44^+/CD24^-/ALDH^+$ CSCs possessed a greater hypoxic response to hypoxia inducible factor (HIF-1α) signalling (Shiraishi *et al.*, 2017). This response in turn promoted an epithelial to mesenchymal transition through the inhibition of E-cadherin and stimulation of Notch-1, Jagged-1, TGF-β, Slug and Snail, which enhanced metastasis and secondary tumor formation *in vivo*. Interestingly, $CD44^+/CD24^-/ALDH^-$ CSCs in contrast, did not undergo EMT upon hypoxia. Instead, hypoxia induced HIF-1α to bind directly to the ALDH1A1 promoter, which converted $CD44^+/CD24^-/ALDH^-$ CSCs into $CD44^+/CD24^- ALDH^+$ CSCs. The newly converted $ALDH^+$ cells expressed angiogenic genes rather than EMT-related genes and were able to generate pulmonary metastasis (Shiraishi *et al.*, 2017). In comparison to patient tumors, breast cancer cell lines differentially expressed ALDH, CD44 and/or CD24, making interpretation of experimental result difficult (Ricardo *et al.*, 2011a). These studies further highlight the importance of using patients' tumor samples over breast cancer cell lines for the studies of inter/intra tumor interactions, CSC localization and plasticity, tumor heterogeneity and metastasis in translational

medicine (Ginestier *et al.*, 2007; Horimoto *et al.*, 2016; Liu *et al.*, 2014c; Velasco-Velázquez *et al.*, 2011).

PATIENT-DERIVED XENOGRAFT MODELS

While fresh patients' tumors are a great model for cancer research, their availability, quantity and quality are limiting factors for widespread usage (Tentler *et al.*, 2012). Patient-derived xenograft (PDX) models become an excellent alternative and are readily available for researchers. The PDX models are generated through the transplantation of patients' tumor tissues into an immunocompromised mouse (Du *et al.*, 2016). The implanted tumors are expanded and serially passaged in mice. PDX procedures exclude tissue dissociation and *in vitro* culture, which prevents cell adaptation to artificial culture system, clonal selection, and homogeneity (Figure 1.3) (Daniel *et al.*, 2009).

Another advantage of the PDX model over cell lines is the preservation of the original tumor architecture and organization such as vasculature and stromal components (Williams *et al.*, 2013). This is thought to represent the original tumor's biology and retain the interactions between the tumor and its microenvironment (Choi *et al.*, 2014; Williams *et al.*, 2013). PDX models also retain intra/inter-tumor heterogeneity, gene expression, single nucleotide polymorphisms, copy number variants and chromosomal architecture of the original tumors (Bertotti *et al.*, 2011; Choi *et al.*, 2014; Daniel *et al.*, 2009; DeRose *et al.*, 2011; Jin *et al.*, 2010; McEvoy *et al.*, 2012; Williams *et al.*, 2013).

The ability of the PDX models to simulate *in vivo* patients' tumors may explain the strong correlation between PDX models and actual patient responses (Berger *et al.*, 1990; Gao *et al.*, 2015; Julien *et al.*, 2012; Owonikoko *et al.*, 2016). Zhang *et al* demonstrated this through

implanting a series of human breast tumor tissues into the mammary fat pad of immunodeficient mice (Zhang *et al.*, 2013b). The tumor growth was correlated with tumor grade and the absence of estrogen (ER)/progesterone (PR) expression. After successful engraftment and growth, it was found that all PDXs retained the primary tumors' histologic phenotypes. PDXs were also evaluated at the transcriptome, proteasome, and genome levels across multiple generations, and all closely resembling the original tumors (Zhang *et al.*, 2013b). Moreover, in a close resemblance to actual breast cancer progression, 48% of PDX tumors exhibited pulmonary metastasis after implantation into mammary fat pad. More importantly, clinical relevance was compared by assessing PDX response to the same treatment regime that had been used in the same patients giving rise to the PDX. Of 13 PDX tumors, 12 (92%) showed the same response as did patients to the chemotherapeutic drugs such as doxorubicin, paclitaxel or dasatinib amongst others, illustrating a high correlation between patients and PDX models (Zhang *et al.*, 2013b).

In another report, Marangoni *et al* implanted 200 breast adenocarcinoma samples into the fat pad of athymic mice and stably generated 22 PDXs. They demonstrated that high breast grade tumors were superior to lower grade counterparts for engraftment and growth. Again, the original patient tumor histology, genomic rearrangements, chromosomal amplifications, and gene expression profiles were preserved in PDXs. Spontaneous metastasis was observed in 10/22 PDXs (45%), which also exhibited similar histology to the original tumors. Similar responses to chemotherapy (e.g. docetaxel/5-flurouracil/trastuzumab) between patients and their PDXs were also demonstrated in five out of seven cases (Marangoni *et al.*, 2007; Whittle *et al.*, 2015).

PDX models also retain the epigenetic patterns of the original patient tumor. Guilhamon *et al* demonstrated that in osteosarcoma and colon cancer, methylation profiles of PDXs were well preserved compared to the primary patient tumor with only 2.7% of CpG sites undergoing a major

methylation shift in PDXs (Guilhamon *et al.*, 2014). The second passage of PDXs showed only 0.07% of alternations in CpG methylation sites in comparison to the first passage (Guilhamon *et al.*, 2014). Tomar *et al* also demonstrated that only 0.66-1.17% of CpGs were significantly altered after 3 passages compared to the original patient tumor in high-grade serious ovarian cancer PDXs (Tomar *et al.*, 2016). While chemotherapy did not alter the DNA methylation pattern, treatment with decitabine (a demethylation agent) significantly demethylated 10.6% CpG sites and inhibited *in vivo* PDX tumor growth. Together, these studies suggest the epigenetic stability of PDX models and their suitability for epigenetic studies in comparison to cancer cells lines (Tomar *et al.*, 2016).

Short-term *ex vivo* cultured PDXs have also been used for pre-clinical high-throughput drug screening. Bruma *et al* showed that all PDX tumor tissues they tested could be successfully cultured *ex vivo* for a short period of time (n=27). These short-term *ex vivo* cultured PDX tissues retained tissue architecture, molecular and genetic features of *in vivo* PDXs. Of 40 *ex vivo* cultured PDX tissues used for drug screening, 33 (82.5%) were verified by *in vivo* PDX models, suggesting that *ex vivo* cultured PDX tissues can be used for high-throughput preclinical drug screening (Bruna *et al.*, 2016).

The predictive power of PDX models has led to the development of co-clinical trials, where patients and mice implanted with PDX tumors developed from the patient will be treated simultaneously or retrospectively. This allows for validation of the PDX results generated, determination of factors affecting drug response/efficacy/resistance, and reduction of side-effects (Hidalgo *et al.*, 2014). These personalized approaches are currently being investigated for various cancer types in multiple ongoing clinical trials (Byrne *et al.*, 2017). One particular ongoing co-clinical trial for the treatment of TNBC is to study the effects of neoadjuvant docetaxel in combination with carboplatin in patients with stage 2-3 TNBC who have not achieved a pathologic

complete response due to chemotherapeutic resistance (NCT02124902) (Ademuyiwa *et al.*, 2016). The PDX models in this study will be developed simultaneously to determine chemotherapeutic response between patients, PDX take rates and to identify signatures of chemotherapy resistance and response (Ademuyiwa *et al.*, 2016). Table 1.1 summarizes current active clinical trials using both PDX models and patients, investigating mechanisms underlying tumor progression, metastasis, and drug response and resistance.

Despite these advantages, PDX models are not perfect (Advantages/Disadvantages being summarized in Figure 1.3). The growth rate of PDX models are very slow compared to cell culture and xenografts generated using cancer cell lines. PDX will take around 4-8 months for the development of a preclinical research specimen (Hidalgo *et al.*, 2014; Paez-Ribes *et al.*, 2016). Low engraftment rate persists as a critical challenge for PDX models. It was reported that TNBC possessed 53.8% of engraftment compared to 15.6% for hormone receptor positive breast cancer (McAuliffe *et al.*, 2015). However, the established PDX samples exhibit over 90% engraftment rate despite low success for the primary PDX. The considerable established PDX samples that have been well characterized are currently available from research institutes or companies. The growth rate in each PDX mouse can also be highly variable depending on the quality and location of the tissues prepared from the same tumor.

Additionally, passaging the PDX samples in mice requires more resources, time and expertise in comparison to cell lines. Long-term passaging of PDX samples also affects PDX characteristics. Pearson *et al* demonstrated that PDXs of human head and neck squamous cell carcinoma increased their growth rate and displayed histopathological features of a higher tumor grade after prolonged *in vivo* passages (Pearson *et al.*, 2016). To avoid deviations, it is recommended to use low passages (less than 5 passages). McAuliffe *et al* showed that high

passages of breast cancer PDX exhibited some aberrations in P13K/mTOR signalling, an abrupt loss of human DNA in the PDX tumor and an increase in murine DNA. This was followed by the spontaneous generation of murine mammary adenocarcinoma (McAuliffe *et al.*, 2015). Additionally, after 3-5 passages, the tumor stroma has been found to be replaced by the host mouse stroma which could influence stromal signalling, tumor rigidity, macrophage infiltration, autocrine and paracrine signalling, possibly deviating PDX from the original patients' tumors (Hidalgo *et al.*, 2014).

Another limitation for current PDX models and for cancer cell line-xenografts is the requirement for the tumor to be implanted into an immunodeficient mouse for tumor engraftment and growth. Due to the lack of immune system, the PDX model is not practical for immunological research. New PDX models have been proposed to address these issues by humanizing the immune deficient mice (e.g. JAX NSG). The human immune system will be generated through early transplantation of human hematopoietic stem cells into immunodeficient mice, followed by PDX implantation. This model will allow for assessment of immuno-tumor interactions in PDX (Simpson-Abelson *et al.*, 2008). This advancement can finally allow for the studies of human chimeric antigen receptor T cell, anti-PDL/PDL-1 and CTLA-4 in a PDX model.

Table 1.1: List of ongoing clinical trials using PDX models.

	Title	Recruitment	Conditions	NCT Number
1	Onco4D(TM) Biodynamic Chemotherapy Selection for Breast Cancer Patients	Recruiting	Breast Cancer	NCT03164863
2	Estrogen Receptor-Positive Breast Cancer Patient-Derived Xenografts	Recruiting	Breast Cancer	NCT02752893
3	Personalized Patient Derived Xenograft (pPDX) Modeling to Test Drug Response in Matching Host	Enrolling by invitation	Colorectal Neoplasms|Colorectal Cancer|Breast Cancer|Breast Neoplasms	NCT02732860
4	Tissue Procurement Protocol for Patients Undergoing Treatment for Early-Stage Breast Cancer	Recruiting	Breast Cancer	NCT02455882
5	Pegylated Liposomal Doxorubicin Hydrochloride and Carboplatin Followed by Surgery and Paclitaxel in Treating Patients With Triple Negative Stage II-III Breast Cancer	Recruiting	Estrogen Receptor-negative Breast Cancer|HER2-negative Breast Cancer|Progesterone Receptor-negative Breast Cancer|Stage IIA Breast Cancer|Stage IIB Breast Cancer|Stage IIIA Breast Cancer|Stage IIIB Breast Cancer|Stage IIIC Breast Cancer|Triple-negative Breast Cancer	NCT02315196
6	Patient-derived Xenograft (PDX) Modeling of Treatment Response for Triple Negative Breast Cancer	Recruiting	Triple Negative Breast Cancer	NCT02247037
7	Neoadjuvant Treatment of Triple Negative Breast Cancer Patients With Docetaxel and Carboplatin to Assess Anti-tumor Activity	Recruiting	Triple Negative Breast Neoplasms	NCT02124902

Different from that in normal vascular system, the presence of endothelial gaps and transcellular holes in tumors increases blood vessel leakiness (Hashizume *et al.*, 2000). It is also found that tumor vasculature lacks vascular hierarchy, and possesses architectural abnormalities (heterogeneous, disorganized, branched/overlapped, and/or loosely connected) that resist blood flow and promote the extravascular erythrocyte accumulation (blood lakes) (Baluk *et al.*, 2005; Hashizume *et al.*, 2000; Hlushchuk *et al.*, 2016; Less *et al.*, 1991). This in turn promotes improper nutrient translocation to the tumor and insufficient metabolite clearance, resulting in ischemia, hypoxia, acidic tumor environment, and necrosis. Increased HIF-1 in tumor further enhances abnormal angiogenesis and tumor growth (Forsythe *et al.*, 1996; Hlushchuk *et al.*, 2016).

PDX models have been demonstrated to be capable of representing human tumor angiogenesis (DeRose *et al.*, 2011). The tumor vasculature comprised of human endothelial cells has been shown to mirror the donor patients' tumor angiogenesis up to 35 days after implantation (Rofstad *et al.*, 2016; Tentler *et al.*, 2012). In contrast, cancer cell line xenografts exhibit different vasculature from patients' tumors, leading to contradictory effectiveness in angiogenic therapy (Drevs *et al.*, 2000; Hecht *et al.*, 2011; Lieu *et al.*, 2013). Since angiogenesis is not only regulated by human tumor cells but also by human stromal cells and extracellular matrix, this might be a possible cause for the discrepancy as cancer cell line xenografts lacking the components of human stromal cells and human extracellular matrix (Garber, 2002; Jain *et al.*, 2006; Montecinos *et al.*, 2012).

Abnormal tumor vasculature plays a key role in nanoparticle-based therapy. Nanotechnology applications in cancer have revolutionized the landscape of cancer drug development by their uniquely appealing features, such as improved blood circulation, higher

tumor accumulation and reduced toxicities leading to higher therapeutic index. Upon systemic administration, therapeutic nanoparticles have been shown to accumulate in tumors as a result of a multitude of biological processes involving mainly leaky tumor vasculature, poor lymphatic drainage and other minor events as well as enhanced permeability, and retention properties of the nanoparticle itself (Bertrand *et al.*, 2014; Guo *et al.*, 2013; McDonald *et al.*, 1999; Miao and Huang, 2015; Min *et al.*, 2012; Shi *et al.*, 2017). As such, considerable nanomedicine based therapies are undergoing clinical trials today (Bobo *et al.*, 2016).

One of challenges for nanoparticle-based therapy is to determine treatment efficacy using a model system that resembles patients' tumor. PDX as a model meets this requirement. It has been demonstrated that PDX TNBC models are highly vascularized in comparison to cell line xenografts, resembling original patients' tumors (Pham *et al.*, 2016). Although this field is advancing rapidly, specificity of nanoparticle-drug accumulation within TNBC PDX tumor as opposed to surrounding tissues and other organs due to enhanced permeability and retention effect has yet to be investigated. Using PDX model to determine the therapeutic efficacy of nanomedicine will provide novel, translatable and tangible approaches for the clinical treatment of TNBC patients.

To conclude, a hierarchy of patient tumors, *in vivo* PDX and short-term *ex vivo* cultured PDX tissues have been depicted with their respective overlapping or distinctive features (Figure 1.3). Since the development of PDX TNBC models is crucial for experimentation, we have included the procedures for the expansion/generation of PDX in NOD-SCID mice (supplemental Information) (DeRose *et al.*, 2013).

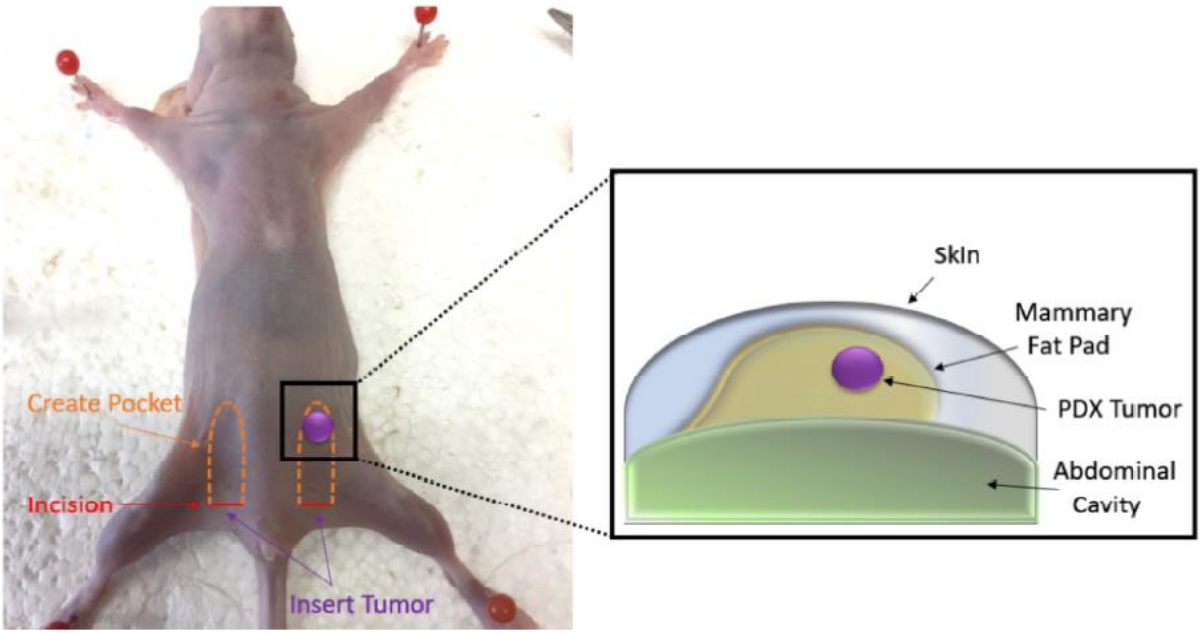

Supplementary Figure 1.0: Schematic of TNBC Tumor Fragment Insertion Procedure in NOD-SCID Mice. An incision below last nipple is made and scissors is placed inside to expand the pocket between the skin and abdominal wall through inverse cutting motions. Once the pocket is large enough and around the above mammary fat pad, the tumor is inserted firmly to the end of the pocket and wound clips close the incision. To the right is an image of the environment the tumor is growing after the procedure.

-End of Review Article-

1.13 Research Rational

The overall goal of my research was to explore novel, clinically translatable therapeutic approaches for the treatment of TNBC and its CSC populations.

1.14 Hypothesis

Combinational suppression of several key targets will effectively target TBNC $CD44^{+}/CD24^{-}$ and $ALDH^{+}$ CSC populations as well as the bulk tumor populations leading to an effective, clinically translatable approach for the treatment.

Chapter 2: Both bulk and CSC subpopulations in TNBC are susceptible to Wnt, HDAC and ERα co-inhibition

Preface

The following chapter consists of a research article for which I am the primary author. The article was published in FEBS Letters.

Sulaiman, A, Sulaiman, B, Khouri, L, McGarry, S, Nessim, C, Arnaout, A, Li, X, Addison, C, Dimitroulakos, J, Wang, L (2016) Both bulk and cancer stem cell subpopulations in triple-negative breast cancer are susceptible to Wnt, HDAC, and ERα coinhibition. *FEBS letters* **590**, 4606-4616.

AS and LW developed the concept and designed experimental outline. AS preformed FACS, clinical sample culture/experiments, transfections/knockdowns, data interpretation and bioinformatics analysis. AS, BS, LK and SM carried out experiments and data acquisition. LW, CA and XL provided conceptual advice. AA, CN, CA, JD were responsible for clinical sample acquisition and experiment design. AS wrote the manuscript and compiled the figures. AS, XL and LW critically revised and edited the manuscript.

Abstract

Development of targeted therapies for triple-negative breast cancer (TNBC, a more aggressive subtype) is an unmet medical need. We analyzed data from 887 patients with invasive breast cancer and observed that increased Wnt and HDAC activities are associated with ESR1 and PGR repression, poor survival and increased relapse. Such a trend was found to be magnified in cancer stem cell (CSC) subpopulation in TNBC cell lines. Co-suppression of Wnt, HDAC and ESR1 using clinically relevant low-dose inhibitors effectively repressed both bulk and CSC subpopulations and converted CSC to non-CSCs in TNBC cells without affecting MCF-10A mammary epithelial cells.

1. Introduction

Breast cancer is one of the leading causes of cancer-related deaths in women throughout the world (Siegel *et al.*, 2016). The triple negative breast cancer (TNBC) subtype, characterised by tumors that that lack expression of estrogen receptor (ER), progesterone receptor (PR), and human epidermal growth factor receptor type 2 (HER2), accounts for only 15-20% of all breast cancers but disproportionately accounts for the majority of breast cancer related deaths. TNBC remains the most difficult subtype of breast cancer to treat. TNBC patients are also prone to recurrence between the first and third years post treatment with majority of deaths within the first five years post therapy (Dent *et al.*, 2007; Rakha *et al.*, 2008).

Development of targeted therapies for TNBC is an unmet medical need. Routinely used chemotherapy regimens have unfortunately been shown to enrich cancer stem cells (CSCs) (Jia *et al.*, 2016; Samanta *et al.*, 2014). These CSCs (commonly identified as $CD44^{high/+}/CD24^{low/-}$ subset)

retain the ability to self-renew and reconstitute the heterogeneous tumor leading to drug resistance, metastasis, and disease relapse (D'Amico *et al.*, 2013; McDermott and Wicha, 2010; Opyrchal *et al.*, 2014; Perrone *et al.*, 2012).

While targeting CSCs has been increasingly considered crucial for successful treatment and improved prognosis (Abdullah and Chow, 2013; Cufi *et al.*, 2011; Luo *et al.*, 2015; Nami *et al.*, 2016), reducing/preventing their conversion from non-CSC subpopulations becomes equally important owing to cancer cell plasticity (Chaffer *et al.*, 2011; Liu *et al.*, 2014). As such, a combinational therapy capable of targeting both bulk and CSC populations and converting CSCs to non-CSCs would be an ideal strategy. Recently, combination pharmacologic therapies have been proposed as one of the most promising strategies in breast cancer studies (Ziauddin *et al.*, 2014). Thus, we evaluated the combination of dual inhibition of Wnt and HDAC to determine its potency at targeting both bulk and CSC TNBC cells.

After analyzing gene expression profiles of 887 patients with invasive breast cancer, we found that Wnt and HDAC overexpression correlated with a significant reduction in ESR1 and PGR protein expression, poor survivability and increased risk of relapse. Through our own experiments we furtherly found that TNBC CSCs exhibit lower *ESR1* and *PGR* expression than non-CSCs. Accordingly, duel inhibitions of Wnt using BC21 (a small molecule repressing TCF4, the downstream effector of the Wnt signaling pathway) and HDAC using valproic acid (VPA, a pan HDAC inhibitor), but neither alone, were able to upregulate gene expression of *ESR1* in TNBC cells. As a result, tamoxifen was included in the combinational treatment and we found that co-suppression of Wnt, HDAC and ESR1 using clinically relevant low-dose inhibitors effectively repressed both bulk and CSC subpopulations. Moreover, the combinational treatment converted CSC to non-CSCs in TNBC cells without affecting the MCF-10A mammary epithelial cells. Part

of these results was verified by using clinical samples from TNBC patients. These findings may lead to a tangible approach to target both bulk and CSC TNBC populations in a clinical setting.

2. Methods and Materials:

2.1 Cell culture and reagents

The breast cancer cell line SUM149-PT was obtained from Asterand (Detroit, MI, USA) and cultured in Hams F-12 medium supplemented with 5 μg/ml insulin, 10 mM HEPES, 1 μg/ml hydrocortisone (Sigma-Aldrich, St. Louis, MO, USA), 1% penicillin/streptomycin, and 5% of fetal bovine serum (FBS, HyClone, Logan, UT, USA). The MDA-MB-231 breast cancer cell line was purchased from the American Type Culture Collection (ATCC, Manassas, VA, USA), maintained in DMEM-F12 media supplemented with 10% FBS and 1% penicillin/streptomycin. Immortalized human breast epithelial cell line MCF-10A was purchased from ATCC and maintained in DMEM-F12 media supplemented with 10% Horse Serum, 20 ng/ml epithelial growth factor (RD Systems, Minneapolis, MN, USA), 0.5 μg/ml hydrocortisone, 10 μg/ml insulin, 100 ng/ml Cholera Toxin (Sigma-Aldrich) and 1% penicillin/streptomycin. Cells were cultured at 37°C in a 5% CO2 incubator. BC21 was purchased from Calbiochem, tamoxifen and valproic acid from Sigma-Aldrich.

2.2 Lentiviral transduction

pLKO.1 puro shRNA β-catenin was a gift from Bob Weinberg (Addgene plasmid # 18803) and scrambled shRNA was a gift from David Sabatini (Addgene plasmid # 1864) (Onder *et al.*, 2008; Sarbassov *et al.*, 2005). Lentiviral production was carried out as described previously (Jia *et al.*, 2016a). Briefly, 10-cm dishes were seeded with 6×10^6 293T cells per dish overnight before

transfection. For two dishes, 8 µg of the shRNA β-catenin or scrambled shRNA vector, 5.4 µg of the psPax2 envelope plasmid, 3.6 µg of the packaging plasmid (pMD2.G) were used. The medium was replaced overnight, and lentiviral supernatant was harvested after 48 hours, filtered through a 0.45 µm PES filter, and concentrated with Lenti-X concentrator (Clontech) according to the manufacturer's instruction. For viral infection, when MDA-MB-231 cells in 6-well plate reached 40-50% confluence, 1 ml of concentrated lentiviral supernatant and 8 µg/ml of polybrene were added for 24h, followed by puromycin (2 µg/ml) selection for 14 days. The stable cell lines were maintained in the presence of 0.5 µg/ml puromycin.

2.3 Flow cytometry analysis

Cells were dissociated with 0.05% of trypsin, filtered through a 0.4mm mesh, and suspended in PBS supplemented with 2% FBS and 2 mM EDTA (FACS buffer). 1 µl of mouse IgG solution (1 mg/ml) was added and incubated for 5 minutes on ice. Appropriate antibodies were then added and incubated for 30 minutes on ice according to the manufacturer's instructions. The cells were washed twice, re-suspended in 1× Binding Buffer (eBioscience, San Diego, CA, USA), and incubated with Annexin-V (eBioscience) for 15 minutes at room-temperature. Finally, the cells were re-suspended in 200 µL FACS buffer in the presence of 1 µl of 7-aminoactinomycin D (7AAD). Antibodies used were anti-CD44-APC, anti-CD24-PE (BD Pharmingen). Appropriate fluorochrome-conjugated isotype matched antibodies were used as negative controls. Flow cytometry was performed on a Cyan-ADP 9 and the BD Fortessa. Data was analyzed with Flowjo software (Ashland, OR, USA).

2.4 Fractionation of CSC and non-CSC subpopulations from breast cancer cells

CSCs and the bulk populations were separated based on $CD44^{high/+}/CD24^{low/-}$ expression in MDA-MB-231 cells. After antibody staining, four sub-populations were analyzed and sorted by

MoFlo Astrios Sorter (Beckman Coulter). Isolation gates, including histogram markers and dot plot quadrants were chosen based on negative controls. Purity (>90%) was determined after sorting.

2.5 Western blotting

Cells were detached and lysed with lysis buffer supplemented with protease inhibitors (Roche). After quantification of the protein concentrations using a Bio-Rad DC protein assay kit (Bio-Rad, Hercules, CA, USA), samples were normalized and de-natured. The samples were separated by 8% SDS-PAGE gel followed by transference to a PVDF membrane. Protein was identified by incubation with primary antibodies followed by horseradish peroxidase-conjugated secondary antibodies and an enhanced chemiluminescence solution (Pierce, Thermo Scientific, USA). Antibodies used in this study include: anti-β-catenin (Clone 14, cat610153, 1:1000) from BD (Mississauga, ON, Canada), anti-active β-catenin (Clone 8E7, cat05665, 1:1000) from Millipore (Billerica, MA, USA), and anti-α-tubulin monoclonal antibody (T9026, 1:500) from Sigma-Aldrich (St. Louis, MO, USA).

2.6 Quantitative real-time PCR (qPCR)

Total RNAs were extracted using RNeasy kit (QIAGEN) and real-time qPCR analysis was performed using the Bio-Rad MyiQ (Bio-Rad, USA). The reaction conditions were: one cycle at 95°C for 20 seconds followed by 45 cycles at 95°C for three seconds and annealing at 60°C for 30 seconds. Results were normalized to the housekeeping gene 18S ribosomal RNA (18S). Relative gene expression was calculated using the $^{2\Delta\Delta}$CT method and compared to the expression of appropriate controls. The primers used are listed in Table 1.

2.7 Cell viability analysis

Cells were seeded into 12 well plates (1.5×10^4 cells/well). After 120 hours of treatment, 10% MTT reagent (tetrazolium, 5mg/ml) was added and incubated for 4 hours. The supernatant was removed, followed by addition of 600 µl DMSO to dissolve formazan crystals. Absorbance was measured at 570 nm.

Alamar blue viability analysis was performed by incubation with 10% alamar blue reagent (Thermo Fisher Scientific) for 4 hours. Florescence was measured at 560 nm excitation and 590 nm emission.

2.8 Clinical database analysis

Using breast cancer datasets from The Cancer Genome Atlas (TCGA, http://cancergenome.nih.gov/), 887 patients with invasive breast cancer were analyzed using cbioportal (http://www.cbioportal.org/index.do) with a z score of ± 2.50. Overexpression was defined as mRNA expression levels greater than 2.5 standard deviations and repression was defined as mRNA expression lesser than 2 standard deviations. Protein or mRNA analysis and Kaplan-Meir survival curves were generated using the same dataset, compiled by August 2016 from the following Database IDs: Wnt overexpression: http://bit.ly/2aztY7w, HDAC overexpression: http://bit.ly/2azrHJU,and Wnt+HDAC overexpression: http://bit.ly/2aLBhMX.

2.9 Primary breast cancer cells

Primary breast cancer tissues/cells were obtained from two TNBC patients with approval of the Ottawa Health Science Network Research Ethics Board and cultured in DMEM-F12 medium supplemented with 10% FBS, 1% penicillin/streptomycin, 1 µg/ml insulin, 0.5 ng/ml hydrocortisol and 3 ng/ml epidermal growth factor. Primary breast cancer cells were treated with

the same concentrations of inhibitors as used in the breast cancer cell lines, followed by a viability assay and flow cytometric analysis.

2.11 Statistical analyses

Data are expressed as mean ± Standard Deviation (SD) unless specified elsewhere. Statistical significance was determined using a Student's *t* test or ANOVA wherever appropriate. Results were considered significant when $p < 0.05$, < 0.01, or < 0.001.

3. Results:

3.1. Upregulated Wnt and HDAC signaling in the patients with invasive breast cancer is associated with decreased expression of ESR1 and PGR proteins and poor survival

Determining overexpressed genes/proteins in breast cancer is a primary step towards the development of novel targeted therapies for TNBC. We analyzed different pathways followed by considerable *in vitro* experiments, eventually focusing on Wnt, HDAC, and ESR1. After analysing 887 patients with invasive breast cancer using TCGA datasets through cBioPortal (Cerami *et al.*, 2012; Gao *et al.*, 2013), we found that Wnt target genes (upregulation of *CTNNB1*, *TCF3*, *TCF4, AXIN2*, *CD44*, *MYC*, *WNT3A*, *SOX2*, *SOX9*, *EGFR*, *HNF1A*, *MMP7* and downregulation of *CDH1* and *GSK3β* (Dandekar *et al.*, 2014; Dey *et al.*, 2013; Hu and Li, 2010; Wu *et al.*, 2012; Yano *et al.*, 2005; Yi *et al.*, 2011)) were inversely correlated with the expression of ESR1, PGR proteins and ERBB2 proteins (Figure 1A). While Wnt upregulation in TNBC is well documented, its involvement in ESR1 repression remains convoluted. As such, we looked at other factors including HDACs that have been shown to mediate Wnt function and also play a role in ESR1 repression (Fortunati *et al.*, 2010; Ng and Littman, 2016). As revealed in Figure 1B, when HDACs (*HDAC*

1, 2, 4, 6, 9 and *11)* were upregulated, ESR1 and PGR but not ERBB2 proteins were repressed. Consistently, *ESR1* gene expression was also found to be inversely correlated with the upregulation of individual HDAC or Wnt gene (supplemental Figure 1A and 1B, respectively).

Furthermore, if both Wnt and HDAC target genes, but neither alone, were upregulated, a decrease in the median month's survival and an increase in the number of relapsed cases were observed (Figure 1C-D). Interestingly, HDAC inhibition has been demonstrated to upregulate Wnt signaling pathway (Debeb *et al.*, 2012), hence it may stimulate Wnt inhibition-induced ESR1 suppression as indicated in Figure 1A. As such, dual inhibition of Wnt and HDAC might be necessary for the upregulation of ESR1 protein expression in TNBC and subsequent sensitization to endocrine therapies (e.g tamoxifen) (Kala and Tollefsbol, 2016).

Since breast CSCs have been attributed to disease recurrence, we further determined the differences between TNBC CSCs and non-CSCs with regards to Wnt signaling and *ESR1* and *PGR* gene expression. We fractionated TNBC MDA-MB-231 CSC ($CD44^{high/+}/CD24^{low/-}$) and non-CSC subpopulations, followed by qPCR analysis. In comparison to bulk populations, CSCs expressed lower levels of *ESR1* and *PGR* genes but higher level of *Axin-2* (an indicator for increased Wnt signalling, Figure 1E), which is in agreement with a previous report (Harrison *et al.*, 2013). Consistently, CSC marker genes were also highly expressed in CSC subpopulation, including *CD44*, *OCT-4*, and *c-MYC* (Figure 1 F). *CD44* has been implicated in treatment resistance (Hiscox *et al.*, 2012) while *OCT-4* and *c-MYC* are associated with enhanced tumor malignancy in breast cancer (Hassiotou *et al.*, 2013; Lavialle *et al.*, 1988). This suggests an inverse correlation between CSC tumorigenicity and *ESR1* and *PGR* expression in TNBC cells. Since antiestrogen is the first-line treatment of choice for ESR1+ patients and has excellent efficacy-to-toxicity ratio, we

reasoned that dual inhibition of Wnt and HDAC might upregulate *ESR1* expression, re-sensitize TNBC cells to antiestrogen treatment, and suppress both bulk and CSC populations.

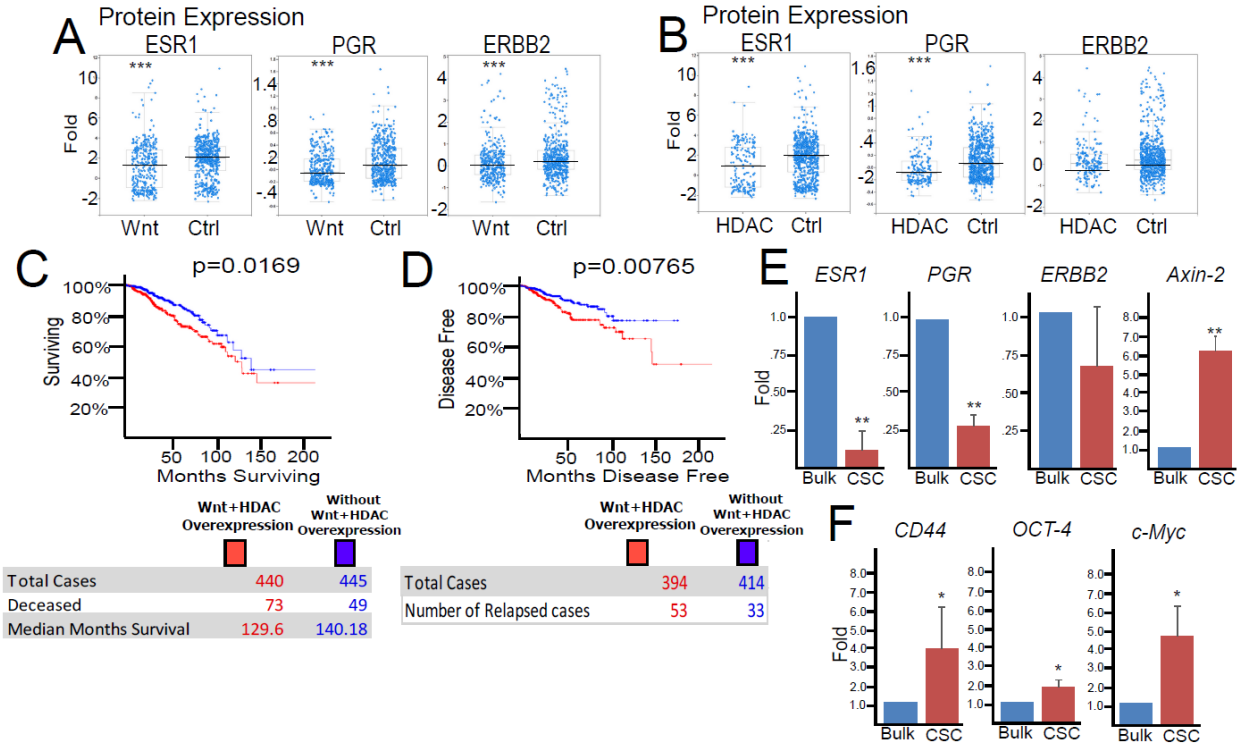

Figure 1. Upregulated Wnt and HDAC signaling in patients with invasive breast cancer is associated with decreased expression of ESR1 and PGR proteins and poor survival. (A) Protein Expression (RRPA) of ESR1, PGR and ERBB in the patients' samples with overexpression of Wnt target genes versus the unaltered counterpart (Ctrl: control, n = 887 patients with invasive breast cancer, ***p < 0.001). **(B)** Protein Expression (RRPA) of ESR1, PGR and ERBB2 in the patients' samples with overexpression of HDAC target genes versus the unaltered counterpart (Ctrl: control, n = 887 patients with invasive breast cancer, ***p < 0.001). **(C)** Kaplan-Meier curve for overall survival of the patients with overexpression of Wnt and HDAC signalling (red curve) in comparison to those without overexpression (blue curve, n =885, p < 0.05, log-rank test). **(D)** Disease Free Survival Kaplan-Meier curve charting the patient relapse rate over time with overexpression of Wnt and HDAC signalling (red curve) in comparison to those without overexpression (blue curve, n = 808, p < 0.05, log-rank test). **(E)** Quantitative real-time PCR analysis of the expression of ESR1, PGR, ERRB2, and the Wnt target gene Axin-2 in the fractionated MDA-MB-231 bulk and CSC (CD44+/CD24-) populations after normalization with housekeeping gene 18S. **(F)** Quantitative real-time PCR analysis of the expression of CSC-associated genes (OCT-4, c-Myc, CD44) in the fractionated MDA MB-231 bulk and CSC (CD44+/CD24-) populations after normalization with 18S. Data represent means ± SD for D and E, n = 3; *p < 0.05, **p < 0.01.

3.2. Combinations of Wnt, HDAC and estrogen inhibitors upregulate *ESR1* expression and effectively repress CSC populations in TNBC cells

To determine whether Wnt, HDAC and estrogen inhibition are effective against CSC populations in TNBC, we suppressed Wnt signaling through shRNA knockdown of β-catenin (Behrens *et al.*, 1996) (Figure 2A) and suppressed HDAC and ESR1 using small molecules. In accordance with the patient data, dual inhibition of Wnt and HDAC (with 250 μM VPA), but neither alone, upregulated *ESR1* gene expression in TNBC cells (Figure 2B), providing a rationale for the combinational use of Wnt, HDAC and ESR1 inhibitors. We therefore included the estrogen receptor modulator tamoxifen (used commonly in the treatment of ESR1+ breast cancer (Jordan, 1997)) in the combination. As expected, shRNA knockdown of β-catenin together with VPA and tamoxifen (1 μM) significantly decreased CSC populations in MDA-MB-231 TNBC cells (Figure 2C and 2D).

For potential clinical application, we replaced shRNA β-catenin with a Wnt inhibitor, BC21 which displayed similar potency to the shRNA β-catenin knockdown in regards to the inhibition of *Axin-2* gene expression (Figure 2E). Consistently, 250 μM VPA and 0.5 μM BC21 treatment in the absence or presence of 1 μM tamoxifen (abbreviated as VB and VBT, respectively) led to *ESR1* upregulation in TNBC cells (Figure 2F). Specifically, VBT, but not other combinations, significantly reduced the living CSC populations by up to 95% in comparison to the control in MDA-MB-231 TNBC cells and elicited similar effect in the SUM149-PT cells (an inflammatory TNBC cell line) (Figure 2G-H and Supplemental Figure 2A). To exclude nonspecific toxicity of the combination treatment, immortalized non-tumorigenic breast epithelial MCF-10A cells were treated with VBT. Significantly, cell viability of MCF10A was not affected by inhibitors individually or in combination (Figure 2I). Notably, tamoxifen and VPA used in our

experiments are clinically relevant and BC21 is approximately 1/6 of the IC_{50} recommended (Daniel *et al.*, 2004). Collectively, these data suggest that the combination of Wnt, HDAC and ESR1 inhibitors can be considered as a new therapeutic approach to upregulate *ESR1* expression and suppress both bulk and CSC populations in TNBC.

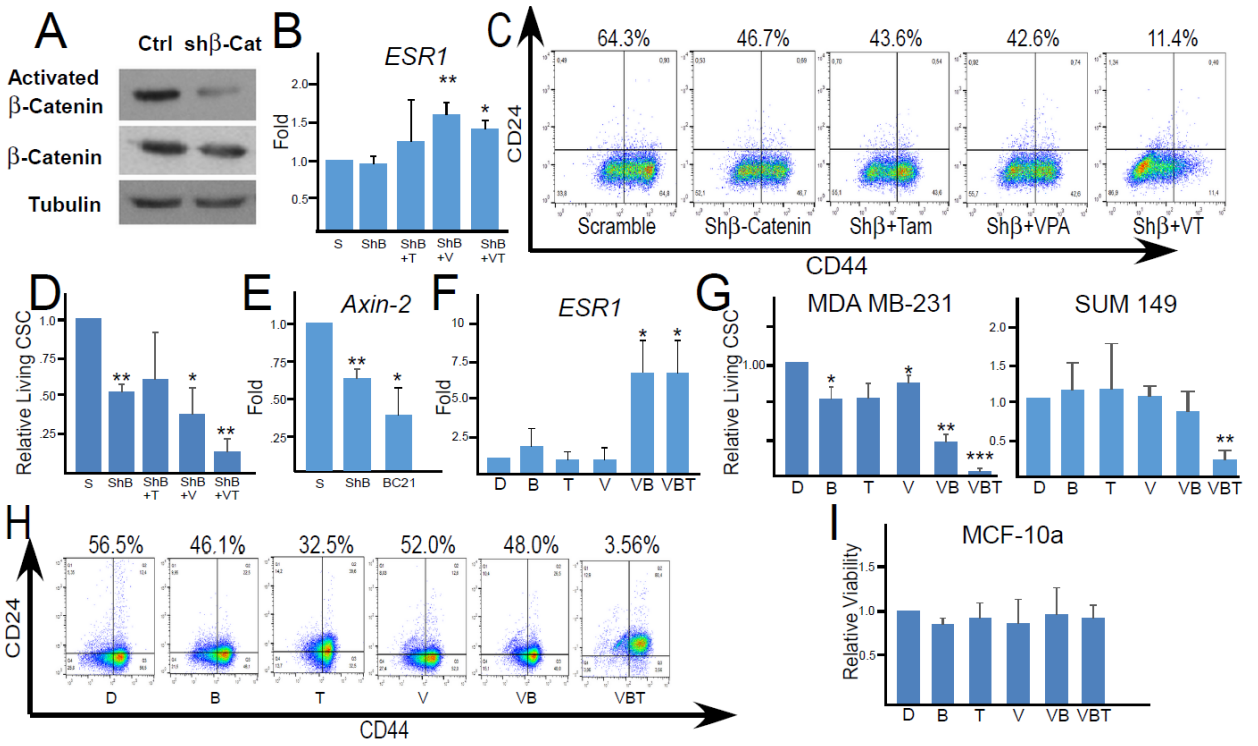

Figure 2. Combinations of Wnt, HDAC and estrogen inhibition upregulate ESR1 expression and effectively repress CSC population in TNBC cells. (A) Representative western blot depicting β-catenin expression in MDA-MB-231 cells after β-catenin shRNA (shβ-Cat) knockdown in comparison to the scrambled shRNA control (Ctrl). **(B)** Quantitative real-time PCR analysis depicting the gene expression of ESR1 in MDA-MB-231 cells 48 hours after exposure to the following treatments: scrambled control (S), Shβ-catenin alone (Shβ), Shβ-catenin + tamoxifen (Shβ+T, 1μM), Shβ-catenin+ VPA (250μM, Shβ+V) or shβ-catenin+ VPA + tamoxifen (Shβ+VT). **(C**) Representative flow cytometric data of the CSC (CD44+/CD24-) subpopulation in MDAMB-231 cells, 48 hours after exposure to the treatments described in B. **(D)** Relative living CSC (CD44+/CD24-/7-AAD-/Annexin-V-) in MDA-MB-231 cells 48 hours after exposure to the treatments as described in B. **(E)** Quantitative real-time PCR analysis depicting the gene expression of Axin-2 in MDA-MB-231 cells 48 hours after treatment as described in B. **(F)** Quantitative real-time PCR analysis depicting the gene expression of ESR1 in MDA-MB-231 cells 48 hours after exposure to DMSO (D, vehicle), Wnt/TCF4 inhibitor BC21 (B, 0.5 μM), tamoxifen (T, 1 μM), VPA (V, 250 μM), VPA+BC21 (VB) or VPA+BC21+tamoxifen (VBT). **(G)** Relative

living CSC (CD44+/CD24-/7-AAD-/Annexin-V-) in TNBC MDA MB-231 and SUM 149-PT cell lines 120 hours after treatments as described in F. **(H)** Representative flow cytometric data of CSC (CD44+/CD24-) subpopulation in MDA-MB-231 cells 120 hours after treatments as described in F. **(I)** Combinations of different inhibitors do not affect MCF-10 viability 120 hours after treatments as described in F. Data represent means ± SD, n = 3 for all figures; *p < 0.05, **p <0.01.

3.3. VBT effectively promotes the conversion of CSCs to non-CSCs while enhancing apoptosis of both bulk and CSC populations in the fractionated TNBC cells

The CSC subset ($CD44^{high/+}/CD24^{low/-}$) in breast cancer has been shown to be able to generate tumors in mice with as few as 100 cells in comparison to other non-CSC subpopulations that required tens of thousands (Al-Hajj *et al.*, 2003). Hence, shifting the population away from CSCs will be an important strategy for effective treatment.

To assess the conversion between non-CSCs to CSCs, we fractionated MDA-MB-231 cells into its CSC ($CD44^{+}/CD24^{-}$) and three non-CSC subpopulations (CD44+/CD24+, CD44-/CD24+ and CD44-/CD24- (Al-Hajj *et al.*, 2003) with >90% purity. In agreement with a previous report (Liu *et al.*, 2014) we found that the fractionated TNBC subpopulations were able to gradually reconstitute the CSC subpopulation after prolonged culture, suggesting that blockade of conversion from non-CSCs to CSCs is crucial in tumor control.

To determine whether VBT treatment is capable of inhibiting the conversion of non-CSCs to CSCs, we exposed the fractionated cells to individual and combinational treatments for 120 hours, after which the total live cells was counted and the reconstituted TNBC population's enrichment of each subpopulations based on CD44 and CD24 expression was determined (illustrated in Figure 3A). Significantly, VBT treatment diminished cell viability in all fractionated sub-populations (Figure 3B and Supplemental Figure 2B). To determine whether apoptosis contributed to the reduced viability, we analyzed the cells by flow cytometry after Annexin-V and

7-AAD staining. Indeed, VBT significantly enhanced apoptosis in all fractionated subpopulations, including the CSC subset of MDA MB-231 cells (Figure 3C and Supplemental Figure 2D) and SUM 149-PT cells (data not shown).

CSC enrichment was then determined through CD44+/CD24- population frequency analysis after VBT exposure for 120 hours in each of the fractionated sub-populations. It was found that within all fractionated sub-populations, after exposure to VBT, the CSC population was drastically diminished (Figure 3D-E and Supplemental Figure 2C and 2E). Furthermore, analyzing the frequency of the other 3 non-CSC sub-populations after exposure to VBT in each fractionated sub-population illustrated that non-CSC populations were enriched in surviving cells, suggesting a halt in CSC conversion (Figure 3F and Supplementary Figure 3A-C).

Collectively, these data suggest that the combinational treatment with VBT is an effective approach to target TNBC via preventing the conversion of non-CSCs to CSCs and promoting apoptosis of both bulk and CSC populations.

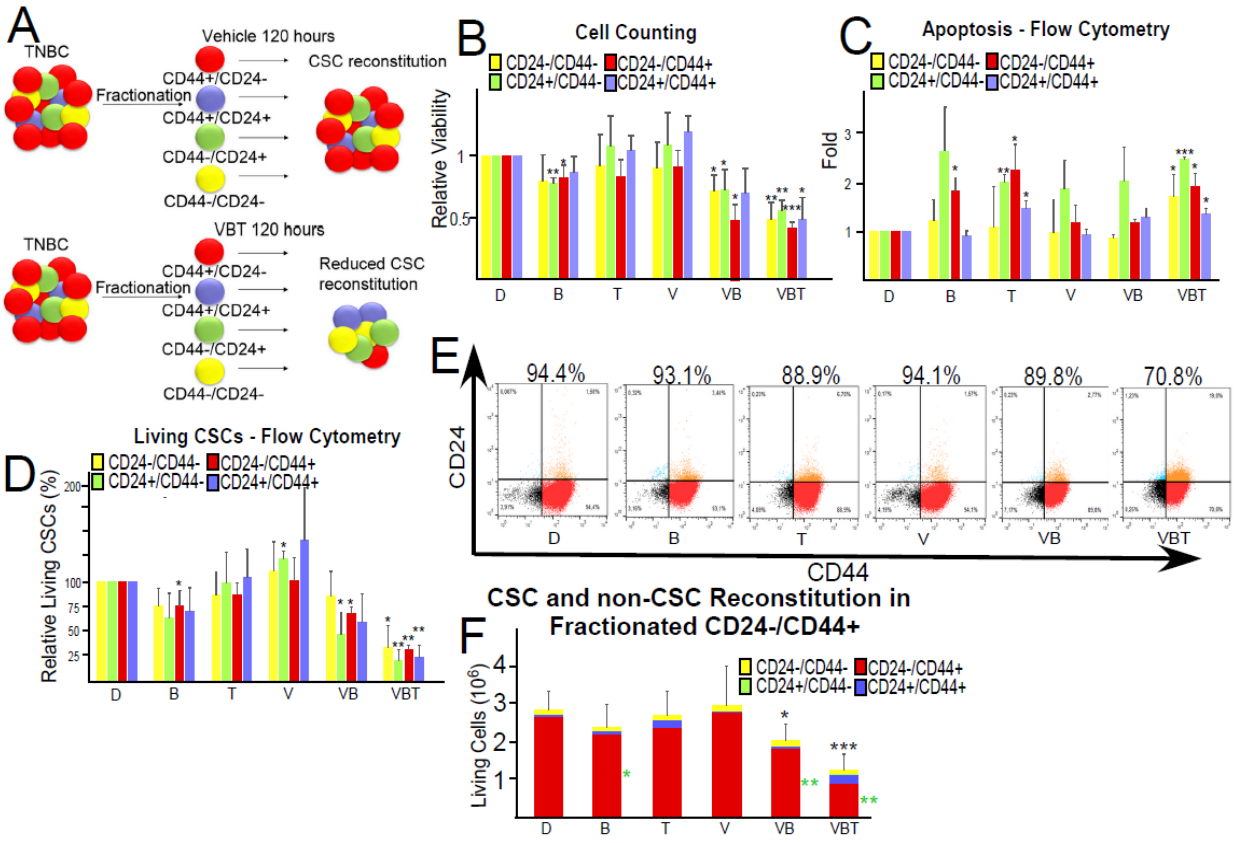

Figure 3. VBT effectively promotes the conversion of CSCs to non-CSCs in the fractionated TNBC cells while enhancing apoptosis of both bulk and CSC populations (A) MDA MB-231 TNBC cells were fractionated into its CSC (CD44+/CD24-) and non-CSC subpopulations based on CD44 and CD24 expression. The fractionated cells were then exposed to the different treatments for 120 hours, followed by flow cytometric reanalysis to determine the reconstitution of CSC and non-CSC subpopulations. **(B)** Fractionated MDA MB-231 subpopulations (based on CD44/CD24 expression) were exposed for 120 hours to the following reagents: DMSO (D, vehicle), BC21 (B, 0.5 μM), tamoxifen (T, 1 μM), VPA (V, 250 μM), VPA+BC21 (VB) and VPA+BC21+tamoxifen (VBT). After treatment, cell viability was assessed by trypan-blue exclusion assay. **(C)** VBT treatment enhances apoptosis of both CSC and non-CSC subpopulations in TNBC cells. Apoptosis (Annexin V+/7AAD+) in each fractionated MDA-MB-231 subpopulations was determined by flow cytometry after 120 hours of treatments as described in B. **(D)** Relative living CSCs (CD44+/CD24-/7-AAD-/Annexin-V-) in each fractionated MDA-MB-231 subpopulation after 120 hours of treatments as described in B (vehicle treatment as controls). **(E)** Representative flow cytometric data of the CSC (CD44+/CD24-) subpopulation in the fractionated MDA-MB-231 cells after 120 hours of treatments as described in B. **(F)** Fractionated MDA-MB-231 subpopulations (based on CD44/CD24 expression) were exposed for 120 hours to different reagents as described in B. After treatment cell viability was assessed by trypan-blue exclusion assay, and the proportion of each subpopulation was determined by flow cytometry based on CD44/CD24 expression. The total number of cells in each subpopulation was calculated by viable cell number × percentage of each subpopulation. Data represent means ± SD and n = 3 for Figure 3A-3F; *p < 0.05, **p < 0.01.

3.4. Combinational VBT treatment effectively inhibits the growth of patients' TNBC cells and reduces the CSC subpopulation

To further verify the above findings, we obtained two clinical samples (named CRDCA and SEM-1) from patients with TNBC. The primary patients' tissues/cells were cultured, followed by treatment with inhibitors individually or in combination for 144 hours. Alamar blue viability analysis depicted the effectiveness of VBT treatment in comparison to other treatments in CRDCA and SEM-1 (Figure 4A). Representative flow cytometric analysis of the CSC population showed that VBT treatment markedly reduced CSCs in CRDCA and SEM-1 (Figure 4B-C). These data indicate the potency of combing the inhibition of Wnt, HDAC and ESR1 in TNBC treatment. It may lead to the development of an effective intervention to reduce metastasis and disease relapse, warranting further studies.

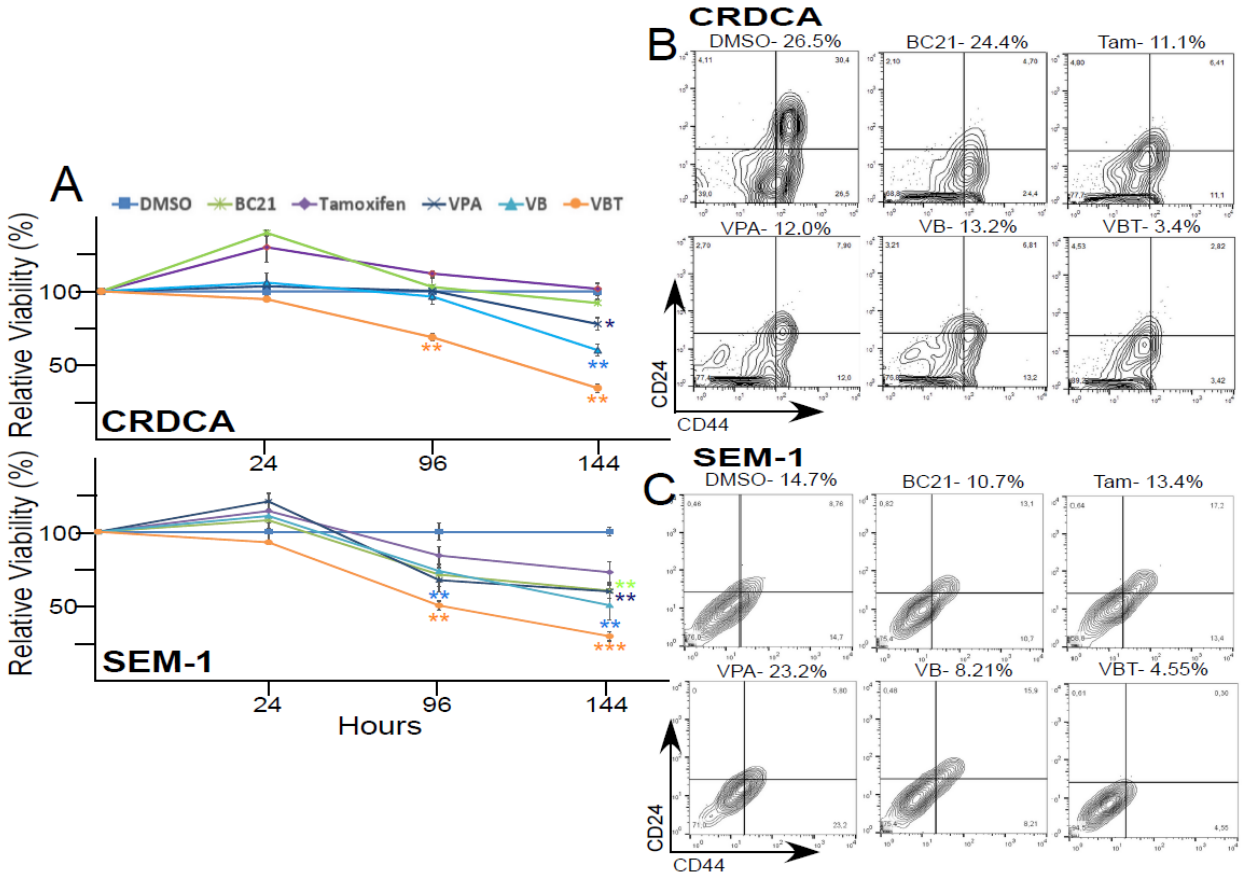

Figure 4. Combinational VBT treatment effectively inhibits the growth of patients' TNBC cells and reduces CSC subpopulation. (A) Alamar blue viability analysis of two primary patients' TNBC cells (CRDCA and SEM-1 samples) after 144 hours of exposure to: DMSO (D, vehicle), BC21 (D, 0.5 μM), tamoxifen (T, 1μM), VPA (V, 250 μM), VPA+BC21 (VB) and VPA+BC21+tamoxifen (VBT). Data represent means ± SD, n = 3 repeats; *p < 0.05, **p < 0.01. **(B)** Representative flow cytometric data showing percentages of CSC (CD44+/CD24-) subpopulation in primary TNBC samples (patient CRDCA samples) after 120 hours of treatments as described in A. **(C)** Representative flow cytometric data showing percentages of CSC (CD44+/CD24-) subpopulation in primary TNBC samples (patient SEM-1 samples) after 120 hours of treatments as described in A.

4. Discussion:

Antiestrogens (e.g. tamoxifen) are safe and effective choices for ESR1+ breast cancer patients. It has been found that epigenetic modifications such as histone deacetylation suppress ESR1 expression and promote breast cancer progression (Kawai *et al.*, 2003; Rhodes *et al.*, 2012). HDACs interact with ESR1 at multiple levels of the ESR1 pathway. HDAC inhibition through trichostatin A has been demonstrated to upregulate *ESR1* gene expression in ESR1-negative breast cancer in response to tamoxifen (Jang *et al.*, 2004). Additionally, the HDAC inhibitor entinostat restores ESR1 expression and enzymatic activity of aromatase in ESR1-negative breast cancer cells in a dose dependant manner, both in *in vitro* and *in vivo* (Sabnis *et al.*, 2011).

However, some inconsistent results do not support the role of HDAC inhibition in the upregulation of ESR1 expression in breast cancer (de Cremoux *et al.*, 2015; Fortunati *et al.*, 2010; Sabnis *et al.*, 2011; Stark *et al.*, 2013; Yang *et al.*, 2000). Our results with primary TNBC samples support this inconsistency with VPA increasing CSC enrichment in SEM-1 but decreasing CSC enrichment in CRDCA when exposed alone. This may be associated with an upregulation of Wnt signalling upon exposure to HDAC inhibitors such as VPA and trichostatin A in certain patient samples. Trichostatin A and VPA have been reported to activate Wnt signalling in HepG2 liver carcinoma and Neuro 2A cells (Phiel *et al.*, 2001; Shi *et al.*, 2014). This is also demonstrated in breast cancer cell lines where HDAC inhibitors have been found to upregulate β-catenin expression leading to increased Wnt signaling (Debeb *et al.*, 2012).

In this report, after analyzing 410 patients with invasive breast cancer, we found that upregulation of either Wnt or HDAC target genes inversely correlates with lower ESR1 protein expression. Since inhibition of HDACs has been shown to upregulate Wnt signaling, inconsistent findings regarding HDAC inhibition and ESR1 upregulation in TNBC may be associated with the

status of Wnt activation. In certain circumstances, HDAC inhibition-induced Wnt activation may result in ESR1 suppression. Indeed, dual inhibition of Wnt (β-catenin shRNA knockdown or using a small molecule) and HDACs, led to an increase in *ESR1* gene expression in TNBC cells (Figures 2B and 2F). This observation is supported by the functional and physical interaction between Wnt and ESR1 as previously reported (Kouzmenko *et al.*, 2004). ESR1 and β-catenin were found to be precipitated within the same immunocomplexes and show genetic interaction *in vitro* and *in vivo* using a transgenic Drosophila model system (Kouzmenko *et al.*, 2004). Taken together, previous reports and this study support the rationale for VBT combination in the treatment of TNBC.

Importantly, VBT used in clinically relevant dosages is capable of inhibiting both bulk and CSC subpopulations (Figures 2 and 3). The presence of tamoxifen, in combination with Wnt and HDAC inhibitors, is significant at effectively suppressing the CSC population in TNBC cells (Figure 2 and 3). This may be mediated by the upregulation of *ESR1* expression after dual inhibition of Wnt and HDAC pathways as tamoxifen alone was ineffective.

In addition, we also revealed that VBT combination facilitated the conversion of CSCs to non-CSC subpopulations (Figure 3). Plasticity between CSCs and non-CSCs has been well recognized (Chaffer *et al.*, 2011; Liu *et al.*, 2014). Thus, blockade of CSC conversion from non-CSCs is equally important for eventual eradication of CSCs to reduce disease recurrence. In this study, we fractionated the TNBC MDA-MB-231 cells into four subpopulations to determine whether VBT treatment is able to prevent CSC development from other fractionated non-CSC subpopulations. The results indicate that VBT combination suppresses CSC enrichment by inhibiting cell growth (MTT and/or Alamar blue assays), promoting apoptosis (flow cytometry analysis), and facilitating conversion of CSCs to non-CSCs. This provides a cellular mechanism

underlying the effectiveness of VBT treatment in TNBC cells. We further verified our findings with two clinical TNBC samples (Figure 4). Since VPA and tamoxifen have been commonly used in clinic and the Wnt inhibitor ICG-001 has recently been approved by the FDA for clinical trial testing, our study may lead to a new avenue in TNBC treatment.

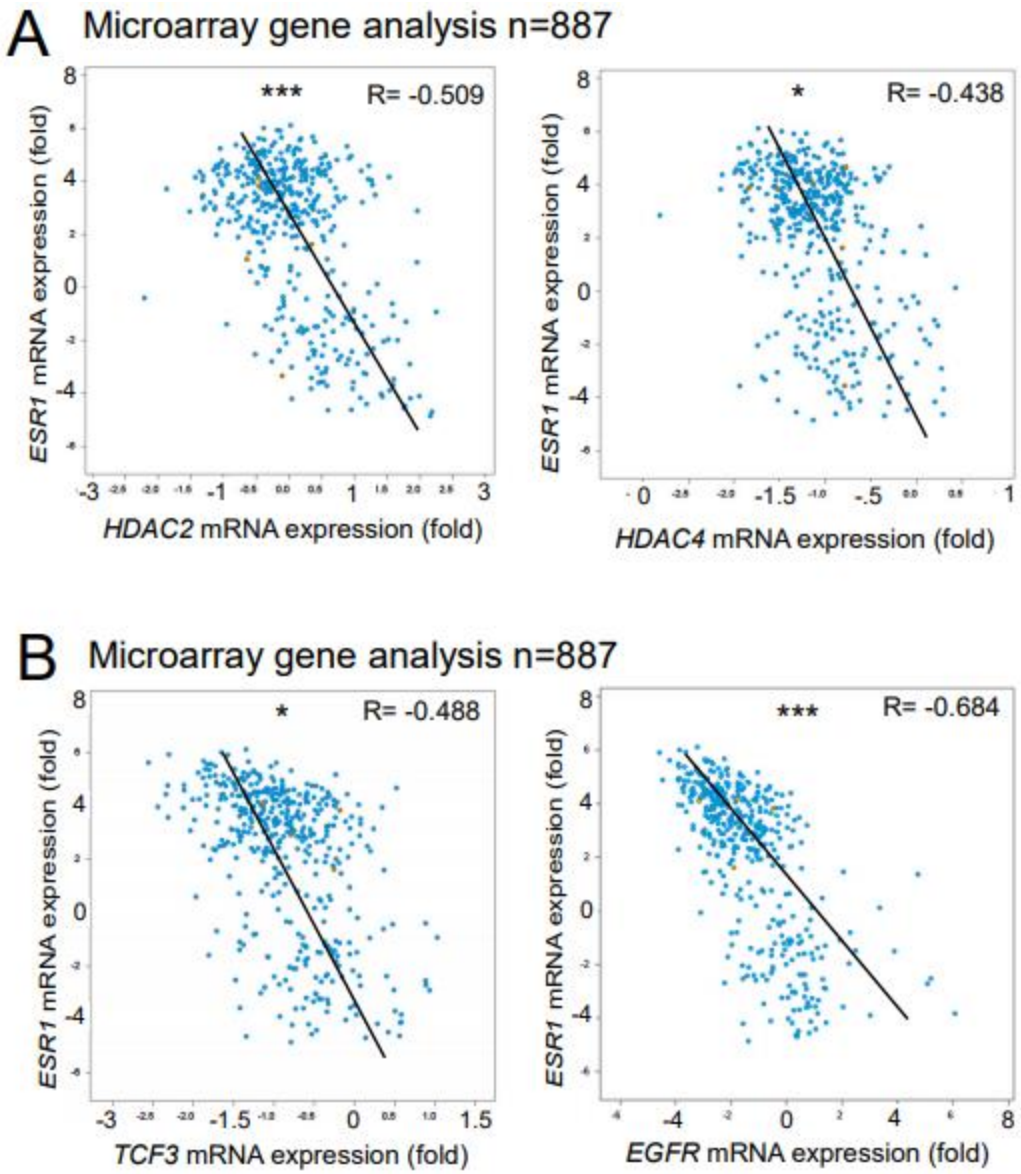

Supplemental Figure 1. Upregulation of HDAC genes and Wnt target genes is inversely correlated with downregulation of ESR1 gene. (A) Inverse correlations between the expression of HDAC genes (x-axis) and ESR1 gene (yaxis). TCGA microarray database, patient with invasive breast cancer, n = 887, *p < 0.05,***p < 0.001. Orange dots indicate mutation, R = Pearson coefficient. **(B)** Inverse correlations between the expression of Wnt target genes (x-axis) and ESR1 gene (yaxis). TCGA microarray database, patient with invasive breast cancer, n = 887, *p < 0.05,***p < 0.001. Orange dots indicate mutation, R = Pearson coefficient.

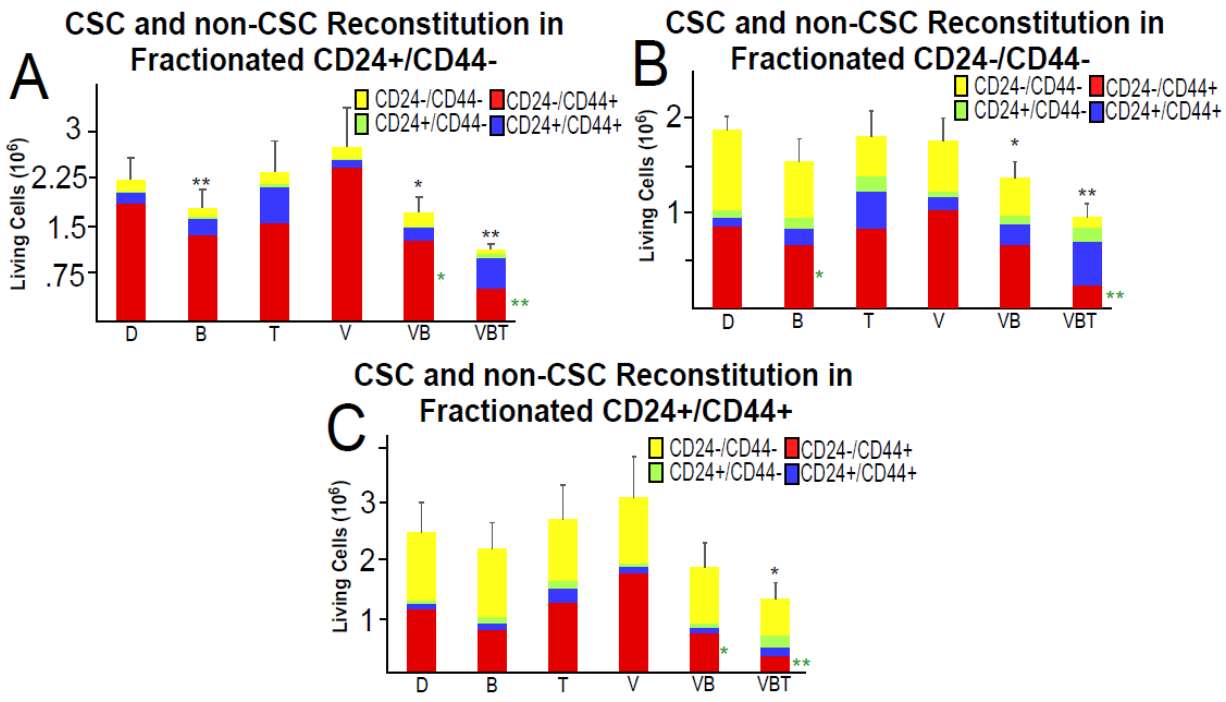

Supplemental Figure 2. VBT effectively prevents the conversion of non-CSCs to CSCs in the fractionated three non-CSC subpopulations (A-C) The fractionated three non-CSC subpopulations from MDA-MB-231 (based on CD44/CD24 expression) were exposed for 120 hours to the reagents as described in Figure 2B. After treatment, cell viability was assessed by trypan-blue exclusion assay, and the CSC and non-CSC subpopulations were determined by flow cytometry. The total number of cells in each subpopulation was calculated by viable cell number × percentage of each subpopulation. Data represent means ± SD, n = 3 for all figures; *$p < 0.05$, **$p < 0.01$.

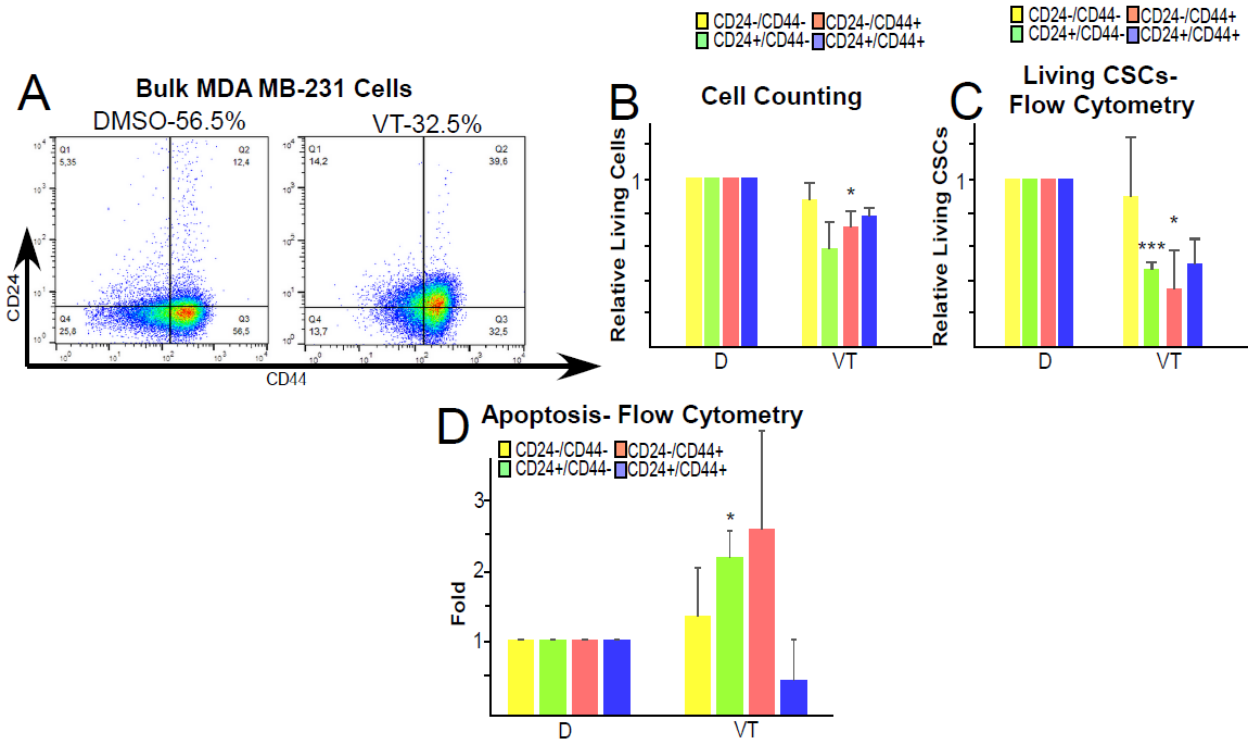

Supplemental Figure 3. Dual valproic acid and tamoxifen treatment exhibits moderate Effects (A) Representative flow cytometric data. MDA-MB-231 cells were treated with valproic acid (250 μM) and tamoxifen (1 μM) (VT) for 120 hours, CSC (CD44+/CD24-) and non-CSC subpopulations were analyzed. **(B)** The fractionated MDA-MB-231 subpopulations (based on CD44/CD24 expression) were treated with vehicle or valproic acid (250 μM) + tamoxifen (1 μM) (VT) for 120 hours, followed by trypan-blue exclusion assay. Data represent means ± SD, n = 3; *p < 0.05. **(C)** Dual valproic acid and tamoxifen treatment moderately inhibits living CSCs in the fractionated CSC and CD24+/CD44- subpopulations. The fractionated MDA-MB-231 cells were treated with vehicle or valproic acid (250 μM) + tamoxifen (1 μM) (VT) for 120 hours, followed by flow cytometric analysis of relative living CSC subpopulations (CD44+/CD24-). Data represent means ± SD, n = 3; *p < 0.05, *** p < 0.001 **(D)** VT moderately enhances apoptosis of CD24+/CD44- subpopulation (non-CSCs). Apoptosis (Annexin V+/7AAD+) of fractionated MDA-MB-231 cells were determined by flow cytometry after 120 hours of treatments as described in B. Data represent means ± SD, n = 3; *p < 0.05.

Chapter 3: Co-inhibition of mTORC1, HDAC and ESR1α Retards the Growth of Triple Negative Breast Cancer and Suppresses Cancer Stem Cells

Preface

The following Chapter consists of a research article for which I am the primary author. The article was published in Cell Death and Disease.

Andrew Sulaiman, Sarah McGarry, Sara El-Sahli, Ka Mien Lam, Jason Chambers, Shelby Kaczmarek, Li Li, Christina Addison, Jim Dimitroulakos, Angel Arnaout, Carolyn Nessim, Zemin Yao, Guang Ji, Haiyan Song, Suresh Gadde, Xuguang Li, Lisheng Wang. Co-inhibition of mTORC1, HDAC and ESR1α Regards the Growth of Triple Negative Breast Cancer and Suppresses Cancer Stem Cells. Cell Death and Disease 2018; 9(8): 815 doi: 10.1038/s41419-018-0811-7).

AS and LW developed the concept and designed experimental outline. AS preformed *in vivo* experiments, serial dilution, FACS, clinical sample culture/experiments, transfections/knockdowns, data interpretation and bioinformatics analysis. AS, SM, SE, KL, JC and SK carried out experiments and data acquisition. LW, LL, CA, ZY, GJ, HS, XL and SG provided conceptual advice. AA, CN, CA, JD were responsible for clinical sample acquisition and experiment design. AS wrote the manuscript and compiled the figures. AS, XL, ZY and LW critically revised and edited the manuscript.

Abstract

Triple negative breast cancer (TNBC) is the most refractory subtype of breast cancer. It causes the majority of breast cancer-related deaths, which has been largely associated with the plasticity of tumor cells and persistence of cancer stem cells (CSCs). Conventional chemotherapeutics enrich CSCs and lead to drug resistance and disease relapse. Development of a strategy capable of inhibiting both bulk and CSC populations is an unmet medical need. Inhibitors against estrogen receptor 1, HDACs or mTOR have been studied in the treatment of TNBC; however, the results are inconsistent. In this work, we found that patient TNBC samples expressed high levels of mTORC1 and HDAC genes in comparison to luminal breast cancer samples. Furthermore, co-inhibition of mTORC1 and HDAC with rapamycin and valproic acid, but neither alone, reproducibly promoted ESR1 expression in TNBC cells. In combination with tamoxifen (inhibiting ESR1), both S6RP phosphorylation and rapamycin-induced 4E-BP1 upregulation in TNBC bulk cells was inhibited. We further showed that fractionated CSCs expressed higher levels of mTORC1 and HDAC than non-CSCs. As a result, co-inhibition of mTORC1, HDAC and ESR1 was capable of reducing both bulk and CSC subpopulations as well as the conversion of fractionated non-CSC to CSCs in TNBC cells. These observations were partially recapitulated with the cultured tumor fragments from TNBC patients. Furthermore, co-administration of rapamycin, valproic acid and tamoxifen retarded tumor growth and reduced $CD44^{high/+}/CD24^{low/-}$ CSCs in a human TNBC xenograft model, and hampered tumorigenesis after secondary transplantation. Since the drugs tested are commonly used in clinic, this study provides a new therapeutic strategy and a strong rationale for clinical evaluation of these combinations for the treatment of patients with TNBC.

1. Introduction

Breast cancer is one of the leading causes of cancer-related deaths in women throughout the world (Siegel *et al.*, 2016). The triple negative breast cancer (TNBC) subtype is characterized as being negative for the estrogen receptor 1 (ESR1), progesterone receptor (PGR), and human epidermal growth factor receptor type 2 (HER2). TNBC patients have high rates of recurrence between the first and third year of treatment, with the majority of deaths occurring within the first five years (Dent *et al.*, 2007; Rakha *et al.*, 2008). It is one of the most difficult subtypes of breast cancer to treat and disproportionately causes the majority of breast cancer related deaths (Liedtke *et al.*, 2008).

Because of the lack of specific targets, chemotherapy regiments are a mainstay for TNBC treatment. Chemotherapeutics, however, have been shown to enrich cancer stem cells (CSCs) in TNBC (Abdullah and Chow, 2013; Jia *et al.*, 2017; Jia *et al.*, 2016). These CSCs (e.g. $CD44^{high/+}/CD24^{low/-}$ subpopulation) have been shown to regenerate the heterogeneous tumor *in vivo*, promoting chemoresistance, and disease relapse (Jia *et al.*, 2017; Sulaiman *et al.*, 2017a). Due to tumor plasticity and the conversion between CSC and non-CSC subpopulations (Liu *et al.*, 2014; Sulaiman *et al.*, 2018b; Sulaiman *et al.*, 2016a; Sulaiman and Wang, 2017), development of a strategy capable of inhibiting both non-CSC and CSC subpopulations is crucial for TNBC therapy (Chaffer *et al.*, 2011).

Given the excellent efficacy-to-toxicity ratio of anti-ESR1 treatment, functional reactivation of ESR1 by inhibition of P13K/Akt/mTORC1 signalling or HDAC to sensitize TNBC to endocrine therapy has been explored, but with inconsistent results and undefined mechanisms (Wang *et al.*, 2016a).

The P13K (phosphoinositide 3 kinase)/Akt/mTORC1 (mammalian target of rapamycin) pathway is commonly activated in breast cancer. For example, PTEN, the negative regulator of P13K, is mutated at a frequency of 44% in luminal and 67% in TNBC (Lee *et al.*, 2015), leading to both endocrine and chemotherapeutic resistance (Cavazzoni *et al.*, 2012; Ramaswamy *et al.*, 2012; Singel *et al.*, 2014). It has been shown that P13K/Akt/mTORC1 activation induces estrogen-independent ESR1 signalling to promote endocrine resistance (Paplomata *et al.*, 2013). P13K/Akt/mTORC1 activation also affects the epigenetic regulation of the chromatin. It modifies histone methylation, acetylation and ubiquitination, resulting in the aberrant silencing/repression of various genes (Huang and Chen, 2005; Spangle *et al.*, 2016; Xu *et al.*, 2012). However, using mTORC1 inhibitors alone failed in the treatment of several types of tumor (Abraham and Gibbons, 2007; LoPiccolo *et al.*, 2008; Wander *et al.*, 2011). This has been attributed to incomplete inhibition of mTORC1. mTORC1 signalling consists of S6RP phosphorylation and 4E-BP1 (eukaryotic translation initiation factor 4E-binding protein 1) phosphorylation that stimulates cap-dependant translation. Rapamycin demonstrates a high affinity of inhibition towards S6K1 phosphorylation but it induces 4EBP1-phosphorylation within 6-hours of treatment, allowing for cap-dependant translation and mTORC1 signalling (Choo *et al.*, 2008). As such, suppressing both S6RP and 4E-BP1 phosphorylation is required for a viable mTORC1 inhibition.

HDACs have been shown to epigenetically suppress ESR1 (Ellison-Zelski *et al.*, 2009; Rasti *et al.*, 2012). As such, HDAC inhibitors have been tested to promote ESR1 re-expression in TNBC. Preclinical studies have shown that various HDAC inhibitors (e.g. PCI-24781, trichostatin A, valproic acid and vorinostat) in combination with tamoxifen (a selective estrogen receptor modulator) lead to endocrine sensitivity and increased cell death of breast cancer. However, these results are controversial with undefined mechanisms (de Cremoux *et al.*, 2015; Jang *et al.*, 2004;

Lyn-Cook *et al.*, 2017; Nilendu *et al.*, 2017; Raha *et al.*, 2015; Thomas *et al.*, 2013).

In this study, we observed that tumor samples from TNBC patients expressed higher levels of mTORC1 and HDAC genes than those from non-TNBC luminal breast cancer. The fractionated TNBC CSC subpopulation expressed higher levels of mTORC1 and HDAC mRNA than non-CSCs. Accordingly, the combination of low dose of rapamycin (repressing mTORC1/S6RP) and valproic acid (a pan HDAC inhibitor) restored ESR1 expression; the combination of rapamycin, valproic acid and tamoxifen suppressed both S6RP and 4E-BP1 phosphorylation, and effectively repressed both bulk and CSC subpopulations in TNBC. Furthermore, in a human xenograft model, three inhibitors in combination effectively attenuated TNBC tumor burden, diminished the $CD44^{high/+}/CD24^{low/-}$ CSC subpopulation and reduced tumorigenesis after secondary transplantation. Combination pharmacologic therapies have been proposed as one of the most promising strategies in breast cancer studies (Ziauddin *et al.*, 2014). These findings suggest that co-inhibition of mTORC1, HDAC and ESR1 can be considered as a tangible approach to target both TNBC bulk and CSC populations in a clinical setting.

2. Materials and methods

2.1 Cell culture and reagents

SUM149-PT breast cancer cells were obtained from Asterand (Detroit, MI, USA) and cultured in Hams F-12 media (Mediatech, Manassas, VA, USA) containing 5% FBS, 5 μg/ml insulin, 1 μg/ml hydrocortisone, 10 mM HEPES and 1% penicillin/streptomycin. MDA-MB-231 breast cancer cells were purchased from the American Type Culture Collection (ATCC, Manassas, VA, USA) and maintained in DMEM-F12 media supplemented with 10% Fetal bovine serum (FBS, HyClone, Logan, UT, USA) and 1% penicillin/streptomycin. Cells were cultured at 37 °C in a 5% CO_2

incubator. Tamoxifen was purchased from CalBiotech (El Cajon, CA, USA), rapamycin from Caymen Chemicals (Ann Arbor, Michigan, USA) and valproic acid from Sigma (Oakville, ON, Canada). Insulin, hydrocortisone, HEPES, and bovine serum albumin were purchased from Sigma-Aldrich (St. Louis, MO, USA).

2.2 Breast cancer tissue and patient-derived xenograft fragments

Tumor tissues from 3 TNBC patients undergoing routine surgical procedures were obtained. The protocol was approved by The Ottawa Hospital Research Ethics Board (Protocol# 20120559-01H). Approximately 2 mm cores were obtained using a sterile biopsy punch that was further sliced with a scalpel to obtain approximately 2 × 1 mm tumor slices (Dayekh *et al.*, 2014; Sulaiman *et al.*, 2018b; Sulaiman *et al.*, 2016). The slices were randomized and three slices were placed into each well of 24-well plate and cultured in DMEM-F12 medium supplemented with 10% FBS, 1% penicillin/streptomycin, 1 µg/ml insulin, 0.5 ng/ml hydrocortisol and 3 ng/ml epidermal growth factor. These primary tissue fragments were treated with the same concentrations of inhibitors as described in the figures, followed by a viability assay and flow cytometric analysis. The TNBC patient-derived xenograft sample HCI-001 was obtained from University of Utah and cultured in the same conditions as the clinical samples.

2.3 Flow cytometry analysis

Dissociated cancer cells were filtered through a 4 µm strainer and suspended in PBS supplemented with 2% FBS and 2 mM EDTA (FACS buffer) as previously described (Sulaiman *et al.*, 2016). 1 µL of mouse IgG (1 mg/mL) was added and incubated at 4 $^{\circ}$C for 10 minutes. The cells were then

re-suspended in 1× binding buffer and anti-CD44 (APC) in combination with anti-CD24 (PE) (BD, Mississauga, ON, Canada) antibodies were added according to the manufacturer's instructions. The cells were washed twice with FACS buffer and 7-aminoactinomycin D (7-AAD, eBioscience, San Diego, CA) and Annexin-V/PE-Cy7 (eBioscience) was added and incubated for 15 minutes at room temperature to assess dead and apoptotic cells. Flow cytometry was performed on a Cyan-ADP 9 and the BD LSRFortessa. Data was analyzed with FlowJo software (Ashland, OR, USA).

2.4 Fractionation of CSC and non-CSC subpopulations from breast cancer cells

CSCs and the bulk populations were separated based on $CD44^{high/+}/CD24^{low/-}$ expression in MDA-MB-231 cells (Sulaiman *et al.*, 2016). After antibody staining, four sub-populations were analyzed and sorted by MoFlo Astrios Sorter (Beckman Coulter). Isolation gates, including histogram markers and dot plot quadrants were chosen based on negative controls. Purity (>90%) was determined after sorting.

2.5 Western blot analysis

Cells were harvested, washed with PBS and lysed with lysis buffer supplemented with protease inhibitors (Roche, Sainte-Agathe-Nord, QC, Canada). Protein concentrations were determined using a Bio-Rad DC protein assay kit (Bio-Rad, Hercules, CA, USA) and samples were then normalized. The samples were loaded into an 8-10% polyacrylamide gel and separated by SDS-PAGE followed by transference to a PVDF membrane. Proteins were identified by incubation with primary antibodies followed by horseradish peroxidase-conjugated secondary antibodies and an enhanced chemiluminescence solution (Pierce, Thermo Scientific, Waltham, MA, USA). Antibodies used in this study include: anti-phosphorylated S6 Ribosomal Protein (1:1000, Cat:

2211S, Cell Signaling, Cambridge, MA, USA), anti-S6 Ribosomal Protein (8E2) monoclonal antibody (1:1000, Cat: 2217S, Cell Signaling), anti-4E-EBP1 (1:1000, Cat: 9452S, Cell Signaling), anti-phosphorylated 4E-BP1 (1:1000, Cat: 2855S, Cell Signaling), anti-acetylated Histone 3 (1:1000, Cat: 4243S, Cell Signaling), anti-Histone 3 1:1000, Cat: 9715S, Cell Signaling), anti-ESR1α (1:1000, Cat: MCA1799T , Bio Rad, CA, USA) and anti-α-tubulin monoclonal antibody (1:500, Cat: T9026, Sigma-Aldrich, St. Louis, MO, USA).

2.6 Quantitative real-time PCR

Total RNAs were extracted using RNeasy kit (QIAGEN) and real-time qPCR (RT-qPCR) analysis was performed using Bio-Rad MyiQ (Bio-Rad, Hercules, CA, USA) as previously described (Sulaiman *et al.*, 2018b; Sulaiman *et al.*, 2016). The conditions for RT-qPCR reactions were: one cycle at 95 °C for 20 seconds followed by 45 cycles at 95 °C for three seconds and annealing at 60 °C for 30 seconds. Results were normalized to the housekeeping gene 18S ribosomal RNA (18S) or GAPDH. Relative expression level of genes from different groups were calculated with the 2ΔΔCT method and compared with the expression level of appropriate control cells. Specific primer sequences for individual genes are listed in Supplemental Table S1.

2.7 siRNA knockdown

siRNAs for S6RP (#AM16708) and the Silencer Select Negative Control #1 siRNA (Scramble, #4390843) were purchased from Thermo Scientific (Waltham, MA,, USA) as SMARTpools. For siRNA transfections, cells were transfected with oligoes using Lipofectamine RNAiMAX reagent (Invitrogen, Carlsbad, CA, USA) according to the manufacturer's instructions. After transfection, efficiency was determined through Western blot or RT-qPCR.

2.8 Cell viability assays

Cells were seeded into 12 well plates (1.5×10^4 cells/well). After 120 hours of treatment, Alamar blue viability analysis was performed by incubation with 10% Alamar blue reagent (Thermo Fisher Scientific) for 4 hours. Florescence was measured at 560 nm excitation and 590 nm emission. Cell viability was also determined through 3-(4,5-dimethylthiazol-2-yl)-2,5-diphenyl tetrazolium bromide (MTT, 5 mg/ml) staining after incubation for 4 hours. Absorbance was measured at 570 nm.

2.9 Xenograft tumor growth

Athymic nude mice were obtained from Charles River Laboratories. The SUM149-PT or MDA-MB-231 breast cancer cells were mixed in 1:1 ratio with Matrigel and injected under aseptic conditions into the mammary fat pads (n = 4 for each group, 2.5×10^6 cells per fat pad). When the tumor reached a mean diameter of ~3 mm, mice were randomly divided into two groups and intraperitoneally injected daily with the vehicle (DMSO), or valproic acid (300 mg/kg/day) + rapamycin (1.5 mg/kg/day) + tamoxifen (0.4 mg/kg/day) for 20 days. At the end of treatment, mice were humanely euthanized and tumors were harvested for further analyses and secondary transplantation.

2.10 Secondary transplantation to assess cancer initiating capacity

Tumors were minced using a scalpel and incubated in antibiotic-free DMEM media containing collagenase/hyaluronidase (STEMCELL Technologies, #07912) at 37 °C. Dissociated single cells were collected every 15 minutes while tumor fragments were digested further to obtain single cells (Sulaiman *et al.*, 2018b). Afterwards, the cells were passed through a 40 µM nylon mesh. The dissociated tumor cells were inoculated into one of the mammary fat pads at a concentration of

10^5, 10^4, 10^3, or 10^2 cells from the original tumors. Tumor growth and size were measured after 6 weeks of growth.

2.11 Clinical database analysis and statistical analysis

Breast cancer datasets from the Cancer Genome Atlas (TCGA, http://cancergenome.nih.gov/) were analyzed with cBioportal (http://www.cbioportal.org/index.do) (Cerami *et al.*, 2012; Gao *et al.*, 2013). High expression of HDAC gene was defined as mRNA expression levels greater than 2.5 standard deviations above the mean. High expression of mTORC1 gene was defined as mRNA levels greater than 2 standard deviations above the mean. Expression data and Kaplan-Meir survival curves were generated using datasets compiled by August 2017 from the following Database IDs (529 patients):mTORC1 and HDAC gene enrichment): http://bit.ly/2wgwyhy, mTORC1 gene enrichment: http://bit.ly/2wh8Mlz and HDAC gene enrichment: http://bit.ly/2whb97U.

Gene Expression Omnibus2R database was used to analyze a dataset (Dataset: GSE65216) to compare TNBC cell lines to 55 TNBC patient samples https://www.ncbi.nlm.nih.gov/geo/geo2r/?acc=GSE65216&platform=GPL570. For all clinical database data, the log rank test was performed to determine whether observed differences between groups were statistically significant. Statistical significance was determined via adjusted P values using Benjamini and Hochberg false discovery rate method by default. Results were considered significant when * $p < 0.05$, ** $p < 0.01$, or *** $p < 0.001$.

3. Results

3.1. Tumor samples from TNBC patients express higher level of mTORC1 and HDAC than those of non-TNBC patients and are associated with decreased ESR1 expression and reduced survival rate.

To determine the correlation between HDAC, mTORC1, and ESR1 in TNBC patients, we analyzed normal mammary tissue, TNBC and luminal breast cancers (ESR1 positive), using samples from 55 TNBC, 59 luminal A/B breast cancer, and 11 normal breast tissues (gene omnibus2R platform, Dataset: GSE65216, Accessed November 1 2017 (Barrett *et al.*, 2012; Edgar *et al.*, 2002; Maire *et al.*, 2013a; Maire *et al.*, 2013b; Maubant *et al.*, 2015). The data was obtained by transcriptome analysis (Affymetrix Human Genome U133 Plus 2.0 Array, GPL570). We found that TNBC samples expressed higher levels of mTORC1 and HDAC mRNAs than normal breast tissue (Figure 1A) and luminal A/B samples (Figure 1B). These results suggest that patients with TNBC might be sensitive to HDAC and mTORC1 inhibition.

We further analysed a TCGA dataset containing 529 patients with invasive breast cancer (cBioportal) (Cerami *et al.*, 2012; Gao *et al.*, 2013), and found that the expression of HDAC protein was inversely correlated with the expression of ESR1 and PGR proteins. In contrast, the expression of HDAC protein was positively correlated with the expression of mTORC1-related S6RP and EIF4EBP1 proteins (Figure 2A and 2B, Dataset ID: http://bit.ly/2whb97U). Also, elevated mTORC1 gene expression negatively associated with low levels of ESR1 and PGR gene expression, while elevated HDAC protein expression positively associated with elevated HDAC gene expression (Figure 2C and 2D, Dataset ID: http://bit.ly/2wh8Mlz). Additionally, patients with low expression levels of both mTORC1 and HDAC mRNAs in their tumor samples exhibited an increased survival rate (Figure 2E, Database ID: http://bit.ly/2wgwyhy, Supplemental Figure 1A).

The trend observed in clinical datasets was also seen in breast cancer cell lines. Both HDAC

and mTORC1 gene expressions were higher in MDA-MB-231 TNBC cells than in luminal ESR1+ MCF-7 breast cancer cells (Figure 2F-G). Accordingly, combination of 250 μM valproic acid (a pan-HDAC inhibitor) and 5 nM rapamycin (mTORC1 inhibitor), but neither alone, increased ESR1 gene expression in TNBC cells (Figure 2H).

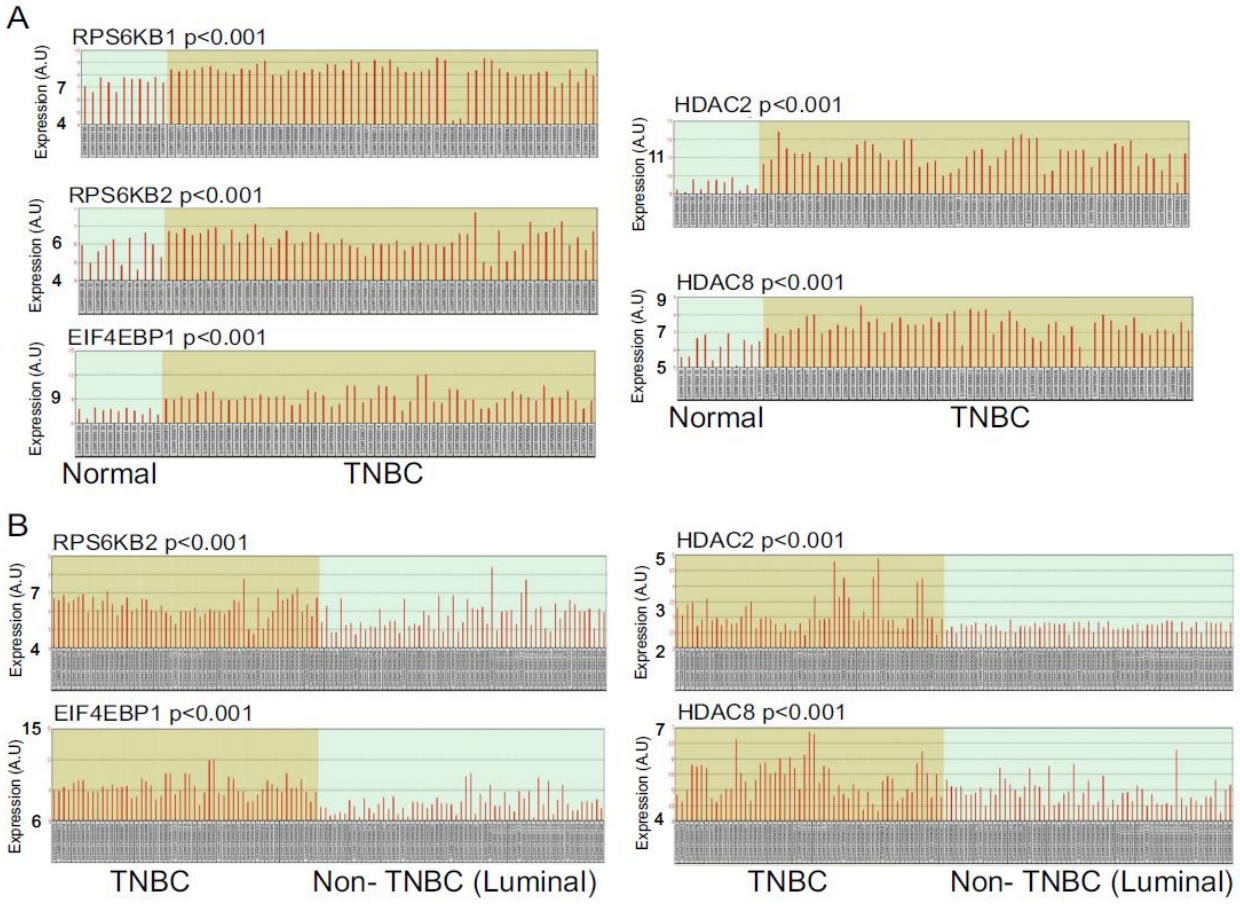

Figure 1. Gene expression levels of mTORC1 and HDAC are higher in TNBC tumor than in normal breast tissues and luminal A/B breast cancer. (A) The relative expression levels (A.U arbitrary unit) of mTORC1 and HDAC genes in 55 TNBC patient tumors and 11 normal breast tissue samples were compared using the NCBI Gene Expression Omnibus (GEO2R). The GSE65216 samples were analyzed with the Affymetrix Human Genome U133 Plus 2.0 Array (GPL570). **(B)** The relative expression levels (A.U: arbitrary unit) of mTORC1 and HDAC genes in 55 TNBC patient tumors and 59 luminal A/B breast cancer samples were compared using the NCBI Gene Expression Omnibus (GEO2R). The GSE65216 samples were analyzed with the Affymetrix Human Genome U133 Plus 2.0 Array (GPL570)

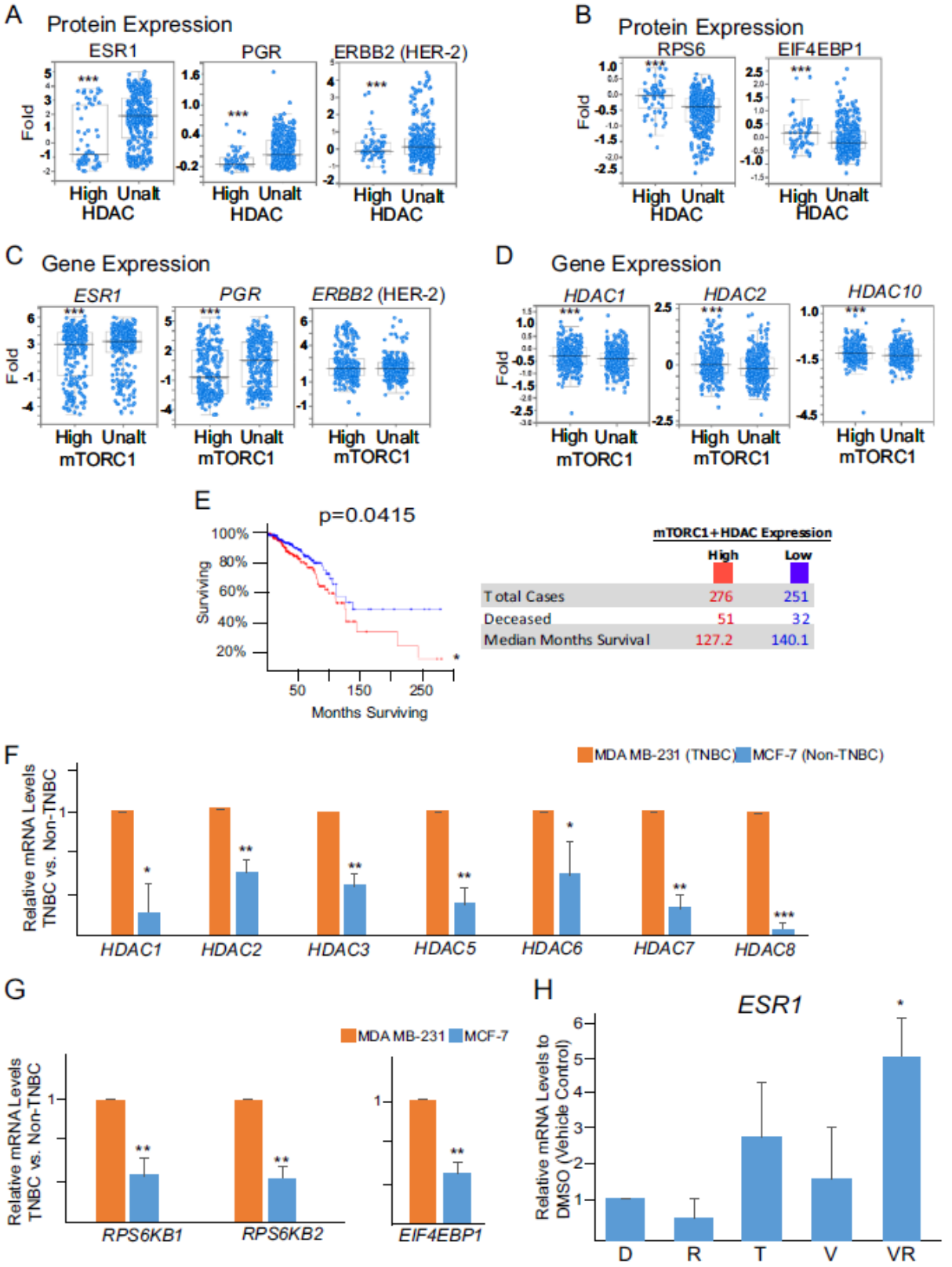
A
Protein Expression
ESR1
PGR
ERBB2 (HER-2)
Fold
High Unalt
HDAC
B
Protein Expression
RPS6
EIF4EBP1
C
Gene Expression
ESR1
PGR
ERBB2 (HER-2)
High Unalt
mTORC1
D
Gene Expression
HDAC1
HDAC2
HDAC10
E
p=0.0415
Surviving
Months Surviving
mTORC1+HDAC Expression
High
Low
Total Cases 276 251
Deceased 51 32
Median Months Survival 127.2 140.1
F
MDA MB-231 (TNBC)
MCF-7 (Non-TNBC)
Relative mRNA Levels TNBC vs. Non-TNBC
HDAC1
HDAC2
HDAC3
HDAC5
HDAC6
HDAC7
HDAC8
G
MDA MB-231
MCF-7
Relative mRNA Levels TNBC vs. Non-TNBC
RPS6KB1
RPS6KB2
EIF4EBP1
H
ESR1
Relative mRNA Levels to DMSO (Vehicle Control)
D
R
T
V
VR

Figure 2. The expression levels of mTORC1 and HDAC are inversely associated with ESR1 and PGR in patients with invasive breast cancer and in TNBC cells. (A) Low expression (RRPA) of ESR1, PGR, and ERBB2 proteins in patients' tumors inversely associated with high expression of HDAC target genes (*HDAC1, HDAC2, HDAC3, HDAC4,* and *HDAC10*) in comparison to their unaltered counterparts (Ctrl: control, n = 892 patients with invasive breast cancer, ***p < 0.001). **(B)** High expression (RRPA) of S6RP and EIF4EBP1 proteins in patients' tumors positively associated with high expression of HDAC target genes (*HDAC1, HDAC2, HDAC3, HDAC4,* and *HDA6*) in comparison to their unaltered counterparts (Ctrl: control, n = 892 patients with invasive breast cancer, ***p < 0.001). **(C)** Low expression (Microarray) of *ESR1, PGR,* and *ERBB2* in patients' tumors inversely associated with high expression of mTORC1 target genes (*MTOR, MYC, CTSD, LDHA, MLST8, SCDP1, ACOX1, CPT1A, LSS, NRF1, TWIST1, SNAI1, TWIST2,* and *S6RPKB2*) in comparison to their unaltered counterparts (Ctrl: control, n = 892 patients with invasive breast cancer, ***p < 0.001). **(D)** High expression (Microarray) of HDAC target genes (*HDAC1, HDAC2,* and *HDAC3*) in patients' tumors positively associated with high expression of mTORC1 target genes (see above) in comparison to their unaltered counterparts (Ctrl: control, n = 825 patients with invasive breast cancer, ***p < 0.001). **(E)** Kaplan–Meier survival curve for overall survival of the patients with high levels of mTORC1 and HDAC gene expression in cancer samples (red curve) in comparison to patients with unaltered expression (blue curve). N = 527, *p < 0.05, log-rank test. **(F-G)** RT-qPCR analysis and comparison of relative mRNA levels of HDAC (*HDAC1, HDAC2, HDAC3, HDAC5, HDAC6, HDAC7,* and *HDAC8*) and mTORC1 (*RPS6KB1, RPS6KB2,* and *EIF4EBP1*) genes between TNBC MDA-MB-231 and non-TNBC luminal breast cancer MCF-7 cell lines. **(H)** RT-qPCR analysis of the expression of *ESR1* gene expression in TNBC MDA-MB-231 cells after treatment with DMSO (D) vehicle control, rapamycin (R, 5 nM), tamoxifen (T, 1 μM), valproic acid (V, 250 μM), or the combination of valproic acid and rapamycin (VR) for 120 h. mRNA levels are relative to the cells treated with DMSO vehicle control.

3.2. Combination of mTORC1, HDAC and ESR1 inhibitors restores ESR1 expression, suppresses rapamycin-induced 4E-BP1 upregulation, and inhibit TNBC cell viability

Rapamycin has been reported to partially inhibit mTORC1 signalling as it ineffectively inhibits 4E-BP1 phosphorylation (Livingstone and Bidinosti, 2012). Indeed, siRNA knockdown of S6RP or 5 nM rapamycin effectively suppressed S6RP phosphorylation but upregulated 4E-BP1 phosphorylation (Figure 3A-B).

It has been shown that 4E-BP1 phosphorylation can be robustly stimulated by 17β-estradiol but inhibited by tamoxifen (Akama and McEwen, 2003; Friedrichs *et al.*, 2004). Suppressing HDACs has also been demonstrated to inhibit 4E-BP1 phosphorylation in a preclinical study

(Miyai *et al.*, 2014). As such, we sought to determine whether HDAC and tamoxifen together could inhibit 4E-BP1 as well as rapamycin-induced 4E-BP1 upregulation when in combination with rapamycin, leading to a complete mTORC1 inhibition. As expected, siRNA knockdown of S6RP in combination with 250 μM valproic acid and 1 μM tamoxifen effectively suppressed both S6RP and 4E-BP1 phosphorylation (Figure 3C). Additionally, we found that the combination of 250 μM valproic acid and 1 μM tamoxifen, but neither alone, reproducibly restored ESR1 protein expression in TNBC cells (Figure 3D).

For potential clinical application, we replaced S6RP siRNA with 5 nM rapamycin that showed a similar potency to siRNA knockdown in reducing S6RP phosphorylation. Consistently, 5 nM rapamycin, 250 μM valproic acid and 1 μM tamoxifen (thereafter as VRT combination) restored ESR1 protein expression and inhibited both phosphorylated S6RP and 4E-BP1 proteins in TNBC cells (Figure 3D and 3E). VRT combination also reduced cell viability of SUM149-PT and MDA-MB-231 TNBC cells (Figure 3G-H). Notably, concentrations of tamoxifen, valproic acid and rapamycin used in these experiments were clinically relevant, suggesting a tangible therapeutic approach to restore ESR1, inhibit mTORC1, and kill TNBC cells.

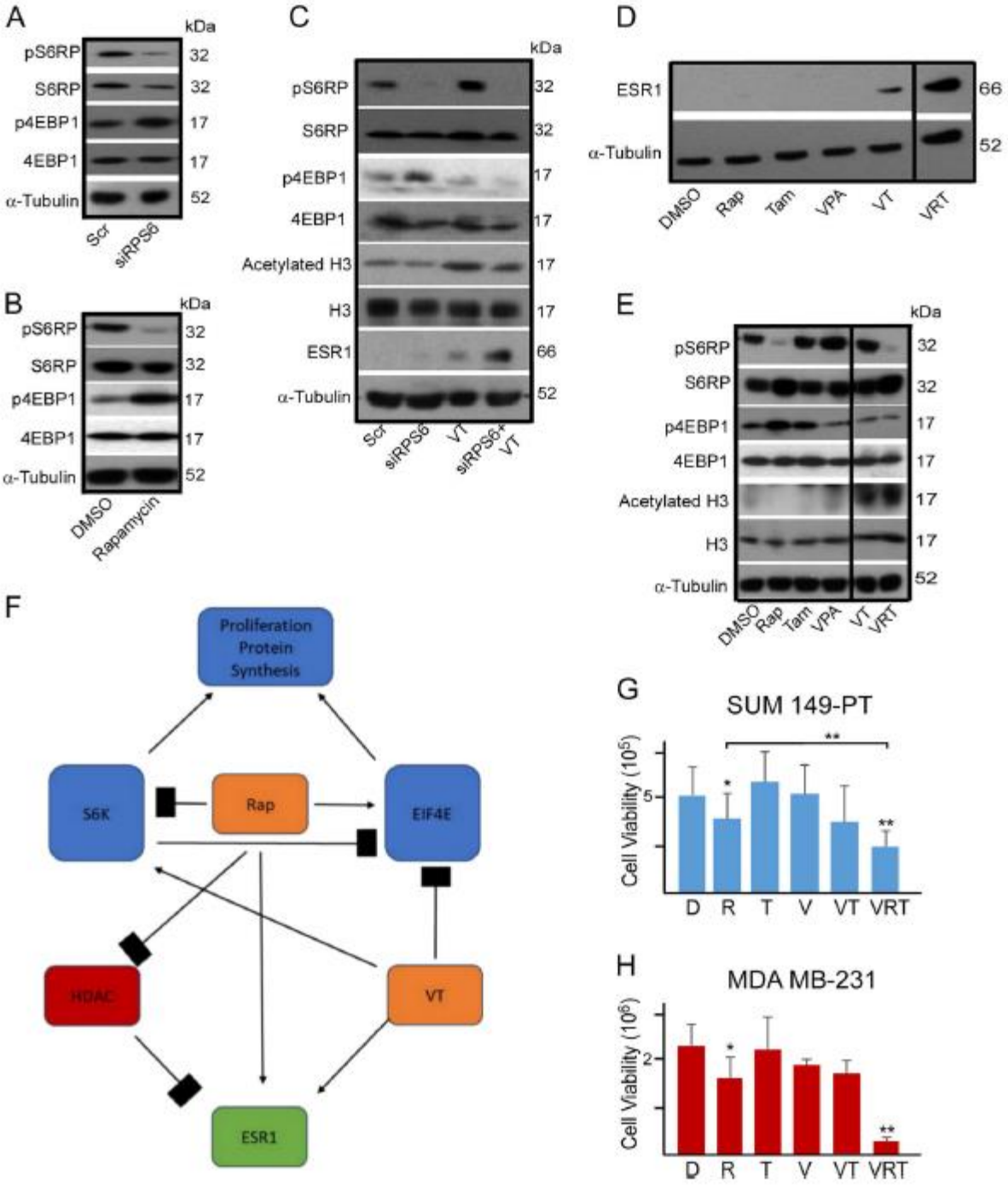
A
kDa
pS6RP
S6RP
p4EBP1
4EBP1
α-Tubulin
32
32
17
17
52
Scr
siRPS6
B
kDa
pS6RP
S6RP
p4EBP1
4EBP1
α-Tubulin
32
32
17
17
52
DMSO
Rapamycin
C
kDa
pS6RP
S6RP
p4EBP1
4EBP1
Acetylated H3
H3
ESR1
α-Tubulin
32
32
17
17
17
17
66
52
Scr
siRPS6
VT
siRPS6+ VT
D
ESR1
α-Tubulin
66
52
DMSO
Rap
Tam
VPA
VT
VRT
E
kDa
pS6RP
S6RP
p4EBP1
4EBP1
Acetylated H3
H3
α-Tubulin
32
32
17
17
17
17
52
DMSO
Rap
Tam
VPA
VT
VRT
F
Proliferation Protein Synthesis
S6K
Rap
EIF4E
HDAC
VT
ESR1
G
SUM 149-PT
Cell Viability (10^5)
5
D
R
T
V
VT
VRT
H
MDA MB-231
Cell Viability (10^6)
2
D
R
T
V
VT
VRT

Figure 3: Co-inhibition of mTORC1, ESR1α and HDACs restores ESR1 expression in TNBC cells and suppresses the expression of pRSP6, p4E-BP1, HDAC and the growth of TNBC cells. (A) Representative western blot depicting S6RP and 4E-BP1 expression in MDA-MB-231 cells after knockdown of S6 ribosomal protein (siS6RP) in comparison to the scramble (Scr) control. **(B)** Representative western blot depicting S6RP and 4E-BP1 expression in MDA-MB-231 cells after rapamycin treatment (5nM) in comparison to the vehicle (DMSO) control. **(C)** Representative western blot depicting S6RP, 4E-BP1, acetylated Histone H3, and ESR1 protein expression in MDA-MB-231 cells after knockdown of S6 ribosomal protein (siS6RP) in combination with valproic acid (VPA, 250 µM), and/or tamoxifen (Tam, 1 µM) for 48 hours. VT: VPA+Tam. **(D)** Representative western blot depicting ESR1 expression in MDA-MB-231 cells after combinational treatment with DMSO (D), rapamycin (R, 5 nM), valproic acid (V, 250 µm), tamoxifen (T, 1 µm), valproic acid and tamoxifen (VT) or valproic acid, rapamycin and tamoxifen (VRT) for 48 hours. **(E)** Representative western blot depicting S6RP, 4E-BP1, Histone H3 and ESR1 protein expression in MDA-MB-231 cells after combinational treatment with DMSO (D), rapamycin (R, 5 nM), valproic acid (V, 250 µm), tamoxifen (T, 1 µm), valproic acid and tamoxifen (VT) or valproic acid, rapamycin and tamoxifen (VRT) for 48 hours. **(F)** Schematic depicting the proposed model for the combinational treatment (VRT). Rapamycin (Rap) effectively inhibits S6RP phosphorylation but upregulates 4E-BP1 phosphorylation, incapable of completely inhibiting mTORC1. Valproic acid inhibits HDAC expression and in combination with tamoxifen (VT) restores ESR1 expression and suppresses 4E-BP1 phosphorylation without affecting S6RP phosphorylation. Combination of VRT promotes ESR1 expression and H3 acetylation (i.e. suppressing HDAC), and suppresses both S6RP and 4E-BP1 (i.e. complete inhibition of mTORC1). **(G-H)** MTT viability analysis of SUM149-PT cells and MDA-MB-231 cells after 120 hours of exposure to vehicle (DMSO, D), rapamycin (R, 5 nM), valproic acid (V, 250 µM), tamoxifen (T, 1 µM), valproic acid and tamoxifen (VT) or valproic acid, rapamycin and tamoxifen (VRT). Data represents means ± SD, n = 3 for Figure 3A-H; * $p < 0.05$, ** $p < 0.01$, *** $p < 0.001$.

3.4. VRT combination inhibits both non-CSC and CSC populations in the fractionated TNBC cells

The CSC subset (characterized by $CD44^{high/+}/CD24^{low/-}$) has been associated with chemoresistance and disease relapse. CSCs were capable of generating new tumors in mice with as few as 100 cells in comparison to non-CSC cells that required tens of thousands of cells (Al-Hajj *et al.*, 2003). In addition, chemotherapeutic drugs enriched CSCs after treatment. Thus, the ability to inhibit both CSCs and non-CSCs and to reduce the conversion of non-CSCs to CSCs is instrumental for an effective treatment.

We fractionated MDA-MB-231 cells into CSC (based on $CD44^{high/+}/CD24^{low/-}$ expression)

and three non-CSC subpopulations ($CD44^{high}/CD24^{high}$, $CD44^{low}/CD24^{high}$ and $CD44^{low}/CD24^{low}$) with >90% purity. RT-qPCR analysis revealed that HDAC and mTORC1 related genes were expressed higher in CSCs than in non-CSCs (Figure 4A-B). Significantly, VRT combination reduced the CSC subpopulation in MDA-MB-231 and SUM149-PT TNBC cells (Figure 4C-D, Supplemental Figure 2A). We further verified these results using siRNA knockdown of S6RP in combination with valproic acid and tamoxifen, showing a similar trend (Supplemental Figure 3A-B).

VRT combination treatment reduced viability of all four fractionated subpopulations (i.e. CSCs and non-CSCs, Figure 4E & 4F). We counted the total cell number and analyzed the percentage of each subpopulation within each fractionated subset based on CD44 and CD24 expression using flow cytometry after 120-hour of treatment with VRT. Significantly, VRT combination treatment not only reduced living CSCs in each fractionated subpopulation but also diminished viability of non-CSCs in each subpopulation (Figure 4G, Supplemental Figure 2B). Furthermore, the remaining cells within each fractionated subpopulation after VRT combination treatment were shifted away from a CSC phenotype to non-CSC subpopulations (e.g. $CD24^{high}/CD44^{low}$, $CD24^{low}/CD44^{low}$ or $CD24^{high}/CD44^{high}$, Figure 4H and Supplemental Figure 4A-C). To estimate the conversion, we normalized the living cells after treatment and graphed the percentage of each subpopulation against total population (taken as 100%). There was an increase in non-CSC subsets than the CSC subset after VRT combination treatment in the fractionated subpopulations based on CD44/CD24 marker expression (Supplemental Figure 5A-D). These data suggest that VRT combination treatment is an effective approach to target TNBC CSC subpopulation.

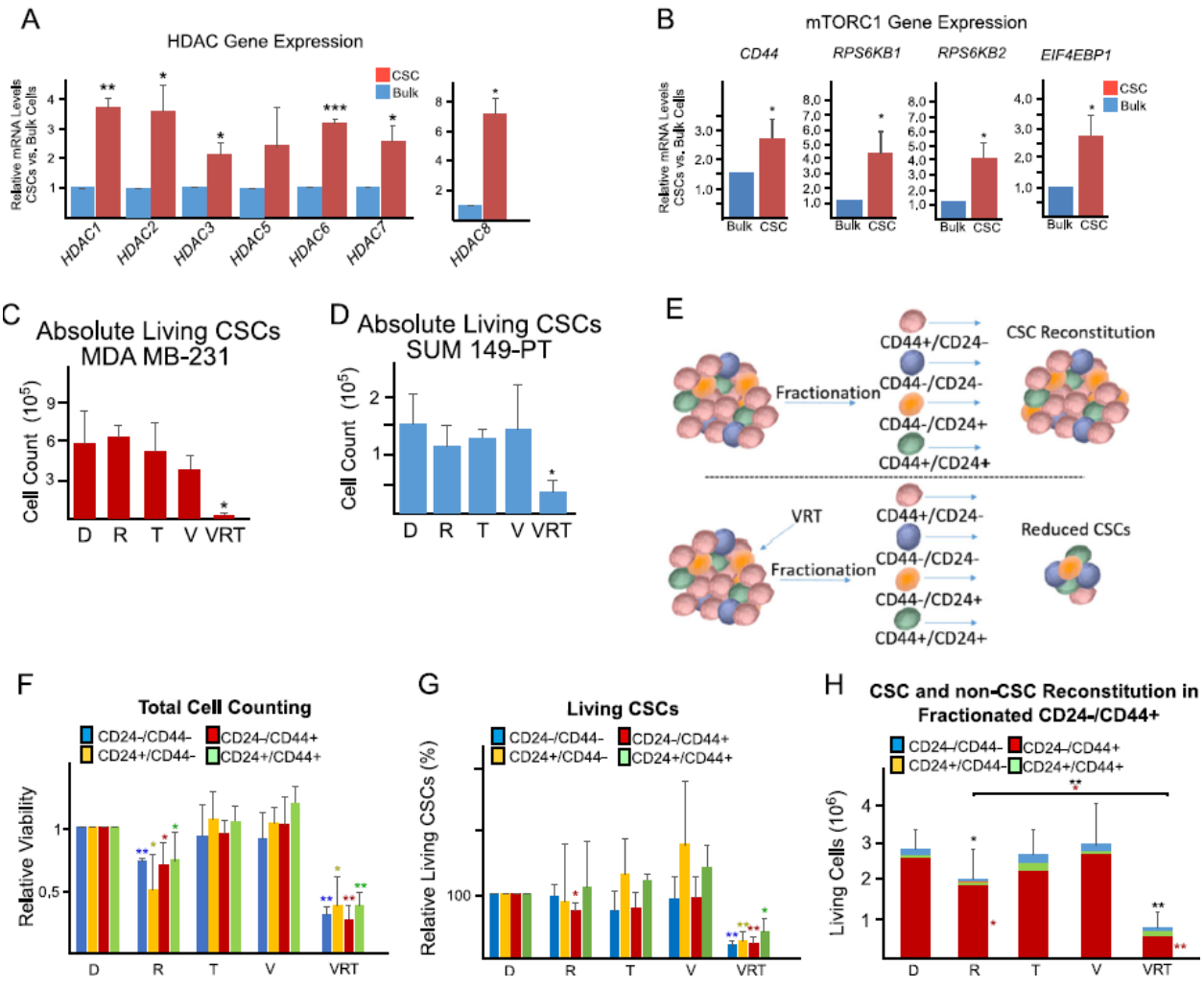

Figure 4: The gene expressions of mTORC1 and HDACs are higher in TNBC CSCs than non-CSCs; co-inhibition of mTORC1, ESR1 and HDACs suppresses the growth of both CSC and non-CSC subpopulations and promotes the conversion of CSCs to non-CSCs. (A-B) RT-qPCR analysis of the expression of HDAC and mTORC1 genes in fractionated MDA-MB-231 CSCs ($CD44^{high/+}/CD24^{low/-}$) and non-CSC populations after normalization with house-keeping gene *18S*. **(C-D)** Flow cytometric analysis of $CD44^{high/+}/CD24^{low/-}$ CSC subpopulation in SUM149-PT and MDA-MB-231 cells after 120 hours of exposure to vehicle (DMSO), rapamycin (R, 5 nM), valproic acid (V, 250 µM), tamoxifen (T, 1 µM) or the combination of rapamycin, valproic acid and tamoxifen (VRT). **(E)** MDA-MB-231 cells were fractionated into CSC ($CD44^{high/+}/CD24^{low/-}$) and non-CSC subpopulations based on CD44 and CD24 expression. Fractionated cells were exposed to vehicle (DMSO), rapamycin (5 nM), valproic acid (250 µM) and tamoxifen (1 µM) for 120 hours. After treatment, fractionated cells were reanalyzed by flow cytometry to determine CSC and non-CSC subpopulations. **(F)** Fractionated MDA-MB-231 CSC and non-CSC subpopulations were treated as described in E. Cell viability was assessed by trypan-blue exclusion assays. **(G)** Relative living CSCs ($CD44^{high/+}/CD24^{low/-}$ and negative for both 7AAD and Annexin-V staining) in each fractionated MDA-MB-231 subpopulation after treatments as described in E. **(H)** Fractionated MDA-MB-231 cells were treated as described in E. After

assessment of cell viability with trypan-blue, the proportion of each subpopulation was determined by flow cytometry based on CD44 and CD24 expression. The total number of cells in each subpopulation was calculated: total viable cell number × the percentage of each subpopulation. Data represents means ± SD and n = 3 for Figure 4A-H; * $p < 0.05$, ** $p < 0.01$, *** $p < 0.001$.

3.5. VRT combination treatment retards tumor growth and inhibits CSC subpopulation and tumorigenesis *in vivo*

We next determined the efficacy of VRT combination treatment *in vivo*. Since the combinations of valproic acid and rapamycin, or valproic acid and tamoxifen showed less *in vitro* potent in inhibition of both CSCs and non-CSCs in comparison to VRT (data not shown), they were not included in the *in vivo* experiments. MDA-MB-231 and SUM149-PT TNBC cells were injected into the mammary fat pad of athymic mice. When tumor reached a mean diameter of 3 mm, mice were randomized into two groups and injected intraperitoneally with either vehicle (DMSO) or combination of valproic acid (300 mg/kg/day), rapamycin (1.5 mg/kg/day) and tamoxifen (0.4 mg/kg/day) for 20 days. As expected, VRT combination reduced tumor burden in both MDA-MB-231 and SUM 149-PT TNBC tumors (Figure 5A-B).

At the end of the VRT combination treatment, we harvested and dissociated the tumors and assessed the $CD44^{high/+}/CD24^{low/-}$ subpopulation using flow cytometry. VRT combination treatment reduced $CD44^{high/+}/CD24^{low/-}$ CSC subpopulations in both MDA-MB-231 and SUM149-PT tumors *in vivo* (Figure 5C-D, Supplemental Figure 6).

To determine if VRT combination inhibits tumor-initiating potential, we performed secondary transplantation. We serially diluted tumor cells containing various percentage of $CD44^{high/+}/CD24^{low/-}$ isolated from the primary tumors, and transplanted them into athymic nude mice for 6 weeks without further treatment. Tumor cells from mice receiving VRT combination

treatment exhibited diminished tumor-initiating capacity in comparison to the vehicle control (Figure 5E and Supplemental Figure 7). Thus, VRT combination reduced tumor burden, suppressed CSCs and tumorigenesis.

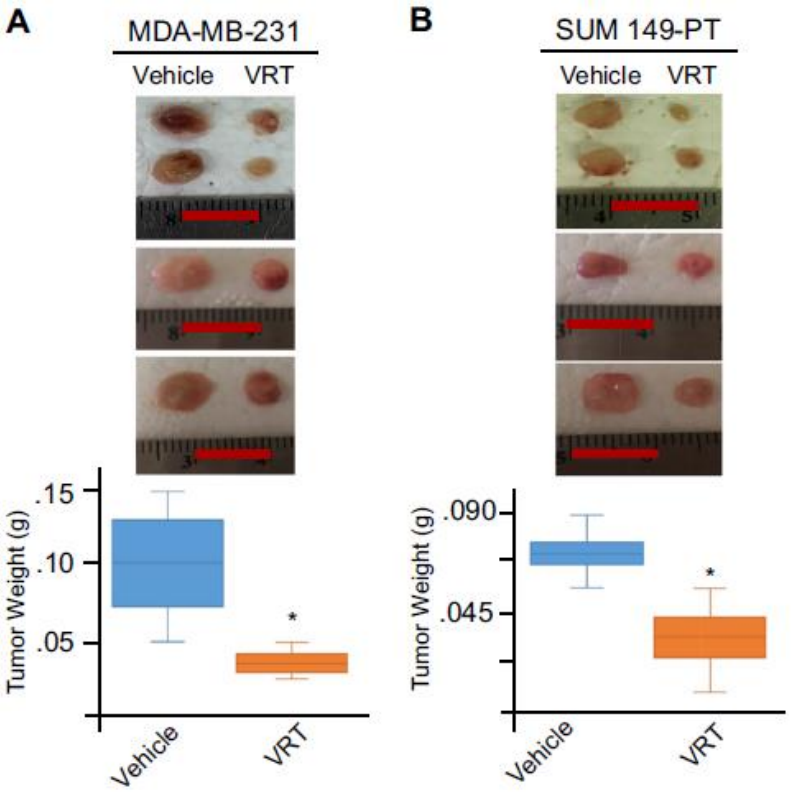

E

MDA-MB-231

	$1x10^5$	$1x10^4$	$1x10^3$	$1x10^2$
Vehicle	3/3	3/3	1/3	0/3
VRT	0/3*	0/3*	0/3	0/3

Figure 5: Co-inhibition of mTORC1, ESR1 and HDACs retards tumor growth and reduces CSCs and tumorigenesis in vivo. (A-B) MDA-MB-231 or SUM149-PT TNBC cells were injected into the mammary fat pads of athymic nude mice (2.5×10^6 cells per fat pad). When the tumors reached a mean diameter of 3mm, mice were randomly divided into two groups and intraperitoneally injected daily with vehicle (DMSO), or VRT combination (valproic acid, 300 mg/kg/day; rapamycin, 1.5 mg/kg/day and tamoxifen, 0.4 mg/kg/day) for 20 days. The tumors were harvested, photographed and weighed. Data represents means ± SD, n = 4, * $p < 0.05$. Scale bar = 0.5 cm. **(C-D)** Flow cytometric analysis of the $CD44^{high/+}/CD24^{low/-}$ CSC subpopulation in SUM149-PT and MDA-MB-231 cells dissociated from tumors after 20 days of treatment with the vehicle (DMSO) or VRT combination as described in A-B. Data represents means ± SD, n = 3, * $p < 0.05$, *** $p < 0.001$. **(E)** MDA-MB-231 tumors from A-B were dissociated into single cell suspension and re-transplanted into the mammary fat pads of new athymic mice in serial dilutions (10^5, 10^4, 10^3, 10^2 cells per mammary pad per injection). Tumor formation was observed for 6 weeks. Data represents means ± SD, n = 3 * $p < 0.05$.

3.6. TNBC patients' tumors express similar levels of mTORC1 and HDAC to TNBC cell lines and VRT combination inhibits the growth of patients' TNBC bulk and CSC populations.

In comparison to TNBC cell lines (10 samples), 55 primary TNBC patient samples expressed similar levels of mTORC1 and HDAC2 and HDAC4 (omnibus2R platform Dataset: GSE65216, Accessed November 1 2017 (Barrett *et al.*, 2012; Edgar *et al.*, 2002; Maire *et al.*, 2013a; Maire *et al.*, 2013b; Maubant *et al.*, 2015), Figures 6A-B). VRT combination treatment suppressed viability of primary TNBC patients' tumor slices (CRDCA, SEM-1 and ARI-1) and a patient-derived xenograft tumor slices (HCI-001) (Figure 6C)(DeRose *et al.*, 2011). Furthermore, VRT combination treatment reduced $CD44^{high/+}/CD24^{low/-}$ CSC subpopulation (Figure 6D-E). Together, these results indicate that co-inhibition of mTORC1, HDAC and ESR1 can be considered as a potential treatment for patients with TNBC.

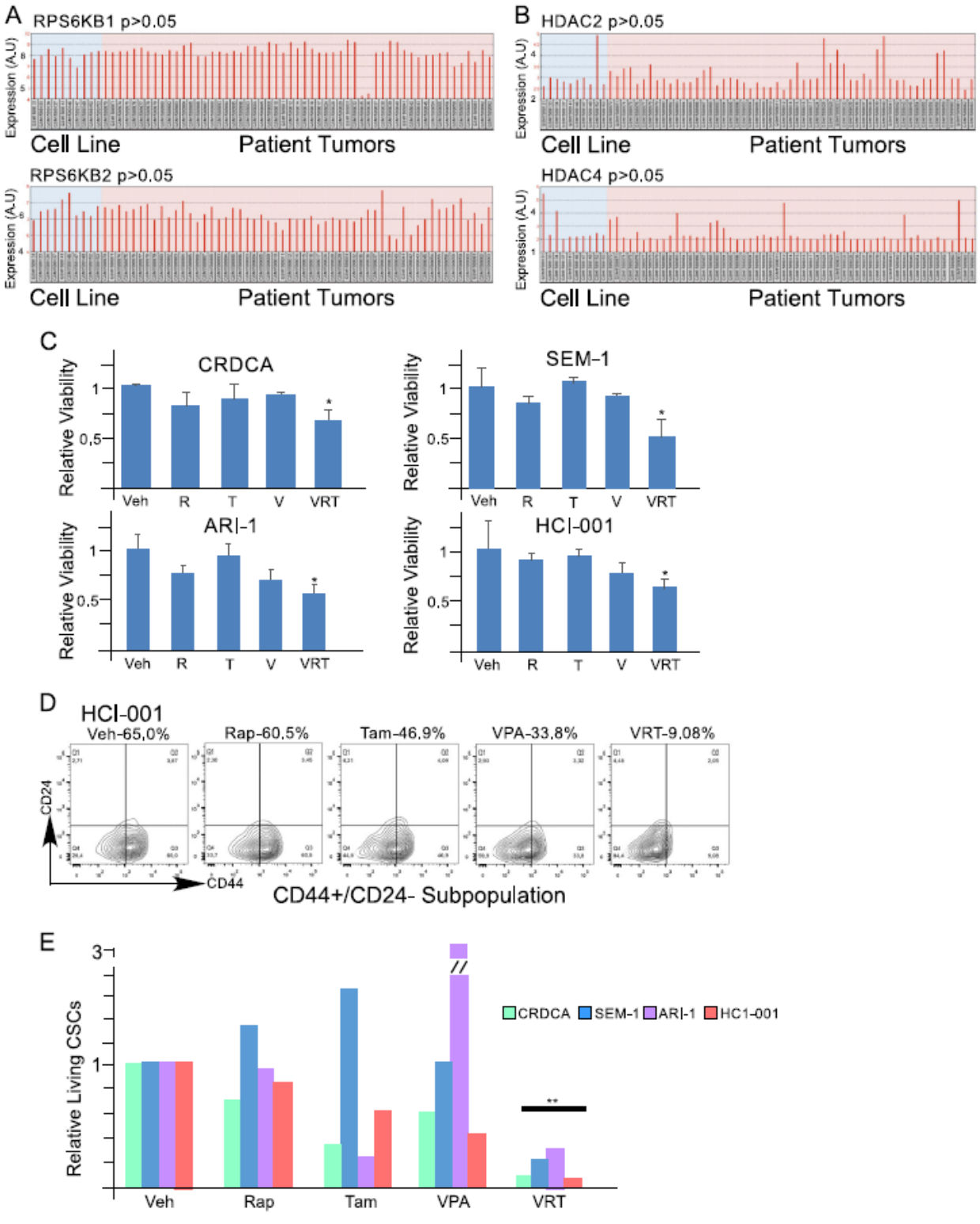
A
RPS6KB1 p>0.05
Expression (A.U)
Cell Line
Patient Tumors
RPS6KB2 p>0.05
Expression (A.U)
Cell Line
Patient Tumors
B
HDAC2 p>0.05
Expression (A.U)
Cell Line
Patient Tumors
HDAC4 p>0.05
Expression (A.U)
Cell Line
Patient Tumors
C
CRDCA
SEM-1
ARI-1
HCI-001
Relative Viability
Veh
R
T
V
VRT
D
HCI-001
Veh-65,0%
Rap-60,5%
Tam-46,9%
VPA-33,8%
VRT-9,08%
CD24
CD44
CD44+/CD24- Subpopulation
E
Relative Living CSCs
CRDCA
SEM-1
ARI-1
HC1-001
Veh
Rap
Tam
VPA
VRT

Figure 6: The expression levels of mTORC1 and HDAC are higher in TNBC cell lines and TNBC patient tumors; Co-inhibition of mTORC1, ESR1α and HDACs reduces the viability of patient tumors' fragments and CSCs. (A-B) The expression of mTORC1 and HDAC genes in 10 TNBC Cell Lines and 55 TNBC patient samples were compared using the NCBI Gene Expression Omnibus (GEO2R). The GSE65216 samples were analyzed with the Affymetrix Human Genome U133 Plus 2.0 Array (GPL570). **(C)** Alamar blue viability analysis of 3 primary TNBC patient fragments (CRDCA, SEM-1 and ARI-1) and 1 patient derived xenograft fragment (HCI-001). TNBC fragments were cultured and treated for 144 hours with vehicle (DMSO, D), rapamycin (5 nM, R), tamoxifen (1 μM, T), valproic acid (250 μM, V), or VRT combination. **(D)** Representative flow cytometric data showing percentages of CSC ($CD44^{high/+}/CD24^{low/-}$) subpopulation in patient-derived xenograft TNBC fragments after treatments as described in C. **(E)** Relative living CSCs ($CD44^{+/high}/CD24^{-/low}$ and also negative for 7AAD and Annexin-V) in TNBC patient tumor fragments after treatment as described in C.

4. Discussion

Anti-estrogen therapies have been used for the treatment of ESR1-postive breast cancers owing to its excellent efficacy-to-toxicity ratio. Since TNBC does not possess targetable markers, functional activation of ESR1 expression, via inhibition of HDACs and mTORC1 to render TNBC sensitive to endocrine treatment, has been an attractive approach (Davies *et al.*, 2013; Petrelli *et al.*, 2013; Wilcken *et al.*, 2003).

HDACs interact with and repress ESR1 at multiple levels along the ESR1 pathway (Ellison-Zelski *et al.*, 2009; Rasti *et al.*, 2012). A HDAC inhibitor Z-ligustilide was shown to restore ESR1 protein expression in ESR1 negative breast cancer lines, re-sensitizing cells to tamoxifen (Ma *et al.*, 2017). Treatment with HDAC inhibitor Trichostatin A was shown to restore ESR1 gene and protein expression in ESR1-negative breast cancer (Yang *et al.*, 2000). The HDAC inhibitor vorinostat was also tested to upregulate ESR1 in TNBC cells (Stark *et al.*, 2013).

However, contrasting results showed that HDAC inhibition does not induce ESR1 gene expression in TNBC and even repress ESR1 in luminal breast cancer under certain conditions (de Cremoux *et al.*, 2015; Noh *et al.*, 2016). We also found that HDACs' inhibitor valproic acid alone was not able to restore ESR1 protein expression in TNBC cells. However, valproic acid in combination with the mTORC1 inhibitor rapamycin reproducibly enhanced ESR1 protein expression in TNBC cells. By analysis of clinical datasets, we found that TNBC expressed high levels of HDAC and mTORC1 in comparison to non-TNBC luminal breast cancers. Additionally, the level of mTORC1 expression is positively correlated with that of HDAC expression in TNBC patients' samples. Thus, repressed ESR1 in TNBC could be partially attributable to dual activation of mTORC1 and HDACs.

HDAC5 has been shown to co-precipitates with regulatory-associated protein of mTOR (Raptor); HDAC5 inhibition promotes raptor acetylation, subsequently inhibiting mTORC1 signalling (Ma *et al.*, 2015b). Conversely, P13K/Akt/mTOR regulates HDAC3 phosphorylation, promoting its activity (Wang *et al.*, 2015). This suggests that mTORC1 facilitates HDAC expression and *vice versa*, providing a rationale for using valproic acid and rapamycin to promote histone H3 acetylation and ESR1 re-expression, as shown in this report.

Previous studies showed that inhibition of P13K/Akt/mTORC1 signalling alone was ineffective in sensitizing ESR1-positive or ESR1-negative breast cancer to endocrine therapy (Wang *et al.*, 2016a). The ineffectiveness of mTORC1 inhibitors in tumor treatment (Abraham and Gibbons, 2007; LoPiccolo *et al.*, 2008; Wander *et al.*, 2011) and in functional reactivation of ESR1 may be related to incomplete inhibition of 4E-BP1 phosphorylation, because rapamycin was known to potently inhibit phosphorylation of S6RP but not that of 4E-BP1(Choo *et al.*, 2008; Ducker *et al.*, 2014; Jiang *et al.*, 2001; Livingstone and Bidinosti, 2012). Thus, inhibition of 4E-BP1 phosphorylation by rapamycin was transient (within 6 hours) and afterwards became resistant to rapamycin treatment (Choo *et al.*, 2008). As a result, cap-dependant translation via mTORC1 signalling can be maintained in the presence of rapamycin. Consistently, retrospective studies of 93 breast cancer patients showed that elevated 4E-BP1 protein was associated with a poor response to endocrine treatment (Karthik *et al.*, 2015, Karlsson *et al.*, 2013).

In this report, we found that the combination of valproic acid and tamoxifen is capable of inhibition of 4E-BP1 phosphorylation, which is associated with functional restoration of ESR1 TNBC. It has been reported that HDAC2 promotes eIF4E/4E-BP1 signalling and cap-dependant translation (Xu *et al.*, 2010a), which can be inhibited by valproic acid. Similarly, tamoxifen has been found to inhibit 4E-BP1 in a MDA-MB-231 tumor xenograft through an ER-independent

mechanism (Scandlyn *et al.*, 2008). Tamoxifen has also been shown to modify histone activity (Liu and Bagchi, 2004; Pasqualini *et al.*, 1983). It is of note that treatment with tamoxifen alone or in combination with rapamycin resulted in enhanced 4E-BP1 phosphorylation in ESR1-positive breast cancer cell lines (Karthik *et al.*, 2015). Mechanisms by which tamoxifen plus valproic acid (HDAC inhibitor), but not tamoxifen plus rapamycin (mTORC1 inhibitor), could effectively prevent 4E-BP1 phosphorylation and restore functional ESR1 expression remain to be further defined.

Cancer cell plasticity (Chaffer *et al.*, 2011; Liu *et al.*, 2014) is a big challenge. For an effective treatment, both CSC and non-CSC subpopulations should be concurrently targeted as bulk cancer cells (i.e. non-CSCs) are capable of converting into CSCs under certain conditions (Liu *et al.*, 2014; Ning *et al.*, 2016). It has been reported that CSCs from patient tumor samples express high levels of S6RP and 4E-BP1 proteins (Karlsson *et al.*, 2013; Karthik *et al.*, 2015). We also observed that the fractionated $CD44^{high/+}/CD24^{low/-}$ CSCs expressed higher levels of S6RP and 4E-BP1 genes than their non-CSC counterparts. It seems that inhibition of both S6RP and 4E-BP1 in breast cancer is required for the suppression of CSCs. VRT combination treatment simultaneously inhibits both S6RP and 4E-BP1 and functionally activates ESR1 expression to re-sensitize TNBC cells for endocrine therapy. This might be one of underlying mechanisms by which VRT combination treatment suppresses the growth of both TNBC CSCs and non-CSCs, thus reducing CSC enrichment from the fractionated non-CSC subpopulations.

In vivo, VRT combination treatment is also able to reduce tumor burden, inhibit CSCs and diminish tumorigenicity after secondary transplantation. As valproic acid, tamoxifen and rapamycin have been commonly used in the clinic, this study may lead to a new, clinically translatable approach for TNBC treatment.

A

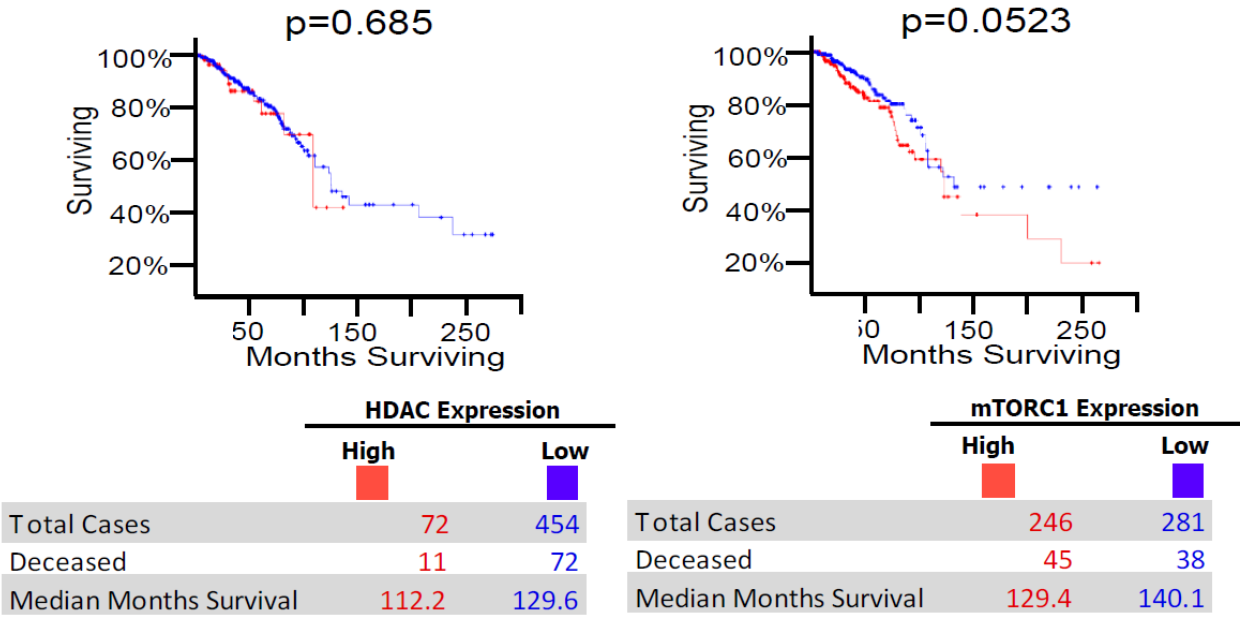

Supplemental Figure 1: Kaplan-Meier survival curve for patients with invasive breast cancer with upregulated mTORC1 or HDAC in tumor samples. (A-B) Kaplan-Meier survival curve for survival of the patients with high level expression of mTORC1 or HDAC genes in cancer samples (red curve) in comparison to the patients with unaltered expression (blue curve). N = 527, * $p < 0.05$, log-rank test.

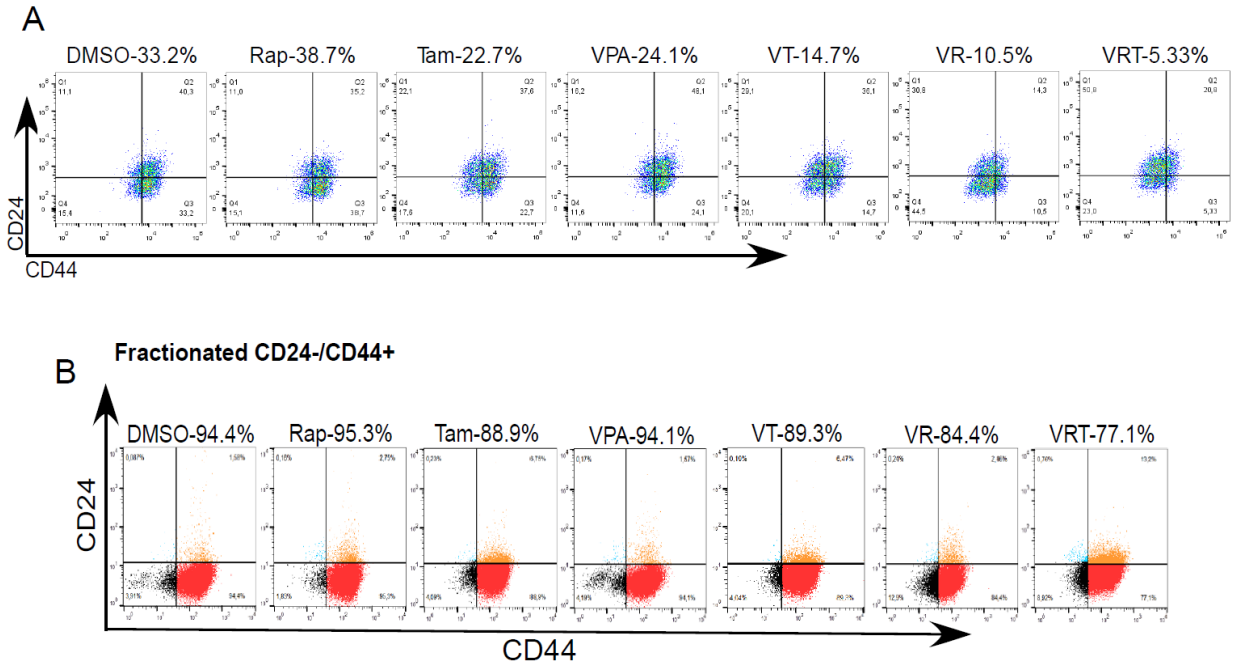

Supplemental Figure 2: Combinational inhibition of mTORC1, ESR1 and HDAC using rapamycin, valproic acid and tamoxifen suppresses CSCs in TNBC cells. (A) Representative flow cytometric data showing percentages of CSC ($CD44^{high/+}/CD24^{low/-}$) subpopulation in MDA-MB-231 cells after 120 hours of treatment with vehicle (DMSO), valproic acid (250 µM, VPA), rapamycin (5 nM, Rap), tamoxifen (1 µM, T) or VT (VPA+T), or VRT (VPA+Rap+T) combination. **(B)** Representative flow cytometric analysis of $CD44^{high/+}/CD24^{low/-}$ CSC subpopulation in the fractionated $CD44^{high/+}/CD24^{low/-}$ MDA-MB-231 cells after 120 hours of treatments as described in A.

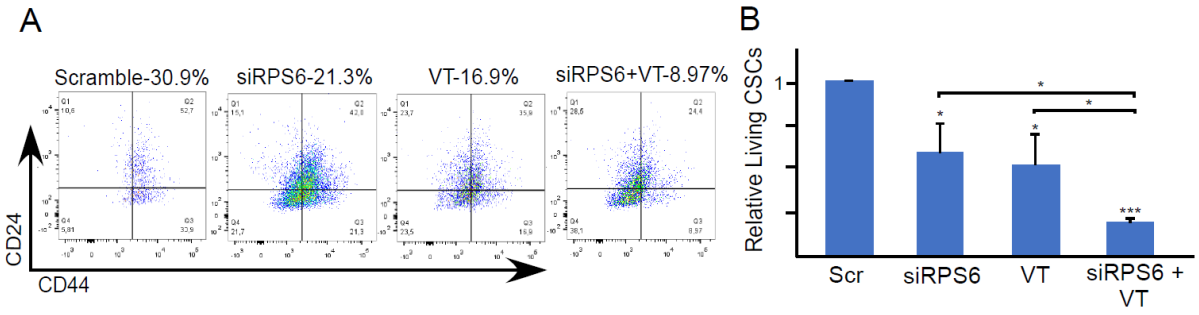

Supplemental Figure 3: S6RP knockdown in combination with valproic acid and tamoxifen inhibits CSCs in TNBC cells. (A-B) Representative and tabulated flow cytometric data showing percentages of CSC ($CD44^{high/+}/CD24^{low/-}$) subpopulation in MDA-MB-231 cells after 72 hours of treatment with scramble control, siRNA knockdown of S6RP in combination with tamoxifen (1 µM, T) and valproic acid (250 µM, VPA).

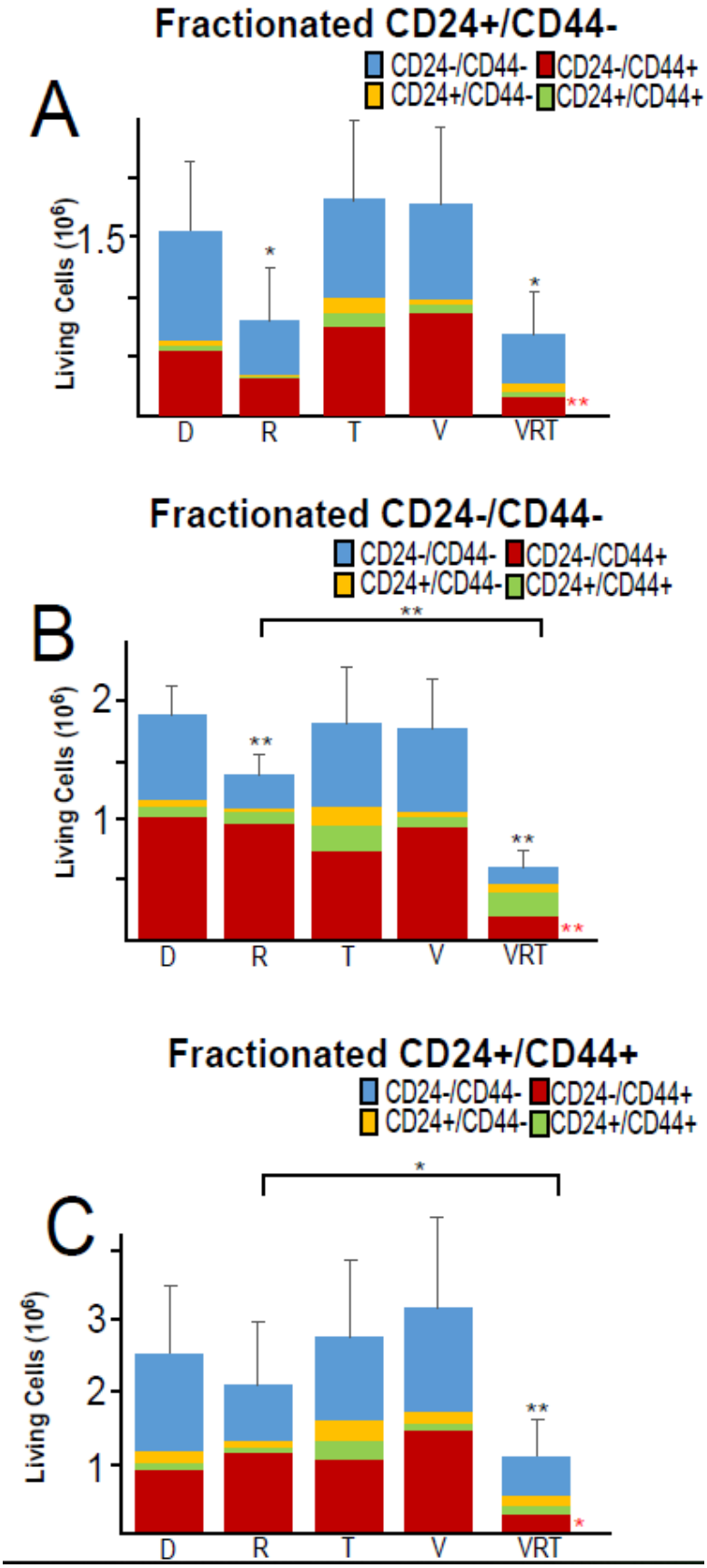
Fractionated CD24+/CD44-
CD24-/CD44-
CD24-/CD44+
CD24+/CD44-
CD24+/CD44+
A
Living Cells (10^6)
1.5
*
*
**
D
R
T
V
VRT
Fractionated CD24-/CD44-
CD24-/CD44-
CD24-/CD44+
CD24+/CD44-
CD24+/CD44+
B
**
Living Cells (10^6)
2
1
**
**
**
D
R
T
V
VRT
Fractionated CD24+/CD44+
CD24-/CD44-
CD24-/CD44+
CD24+/CD44-
CD24+/CD44+
*
C
Living Cells (10^6)
3
2
1
**
*
D
R
T
V
VRT

Supplemental Figure 4: Rapamycin in combination with valproic acid and tamoxifen reduces CSC enrichment in the fractionated non-CSC subpopulations. (A-C) Fractionated MDA-MB-231 non-CSC subpopulations were exposed for 120 hours to vehicle, valproic acid (250 μM, VPA), rapamycin (5 nM, Rap), and tamoxifen (1 μM, T). After treatment, cell viability was determined by trypan-blue exclusion assay and the proportion of each non-CSC and CSC subpopulations was determined by flow cytometry based on CD44 and CD24 expression. The total number of cells in each subpopulation was calculated using total viable cell numbers × percentage of each subpopulation.

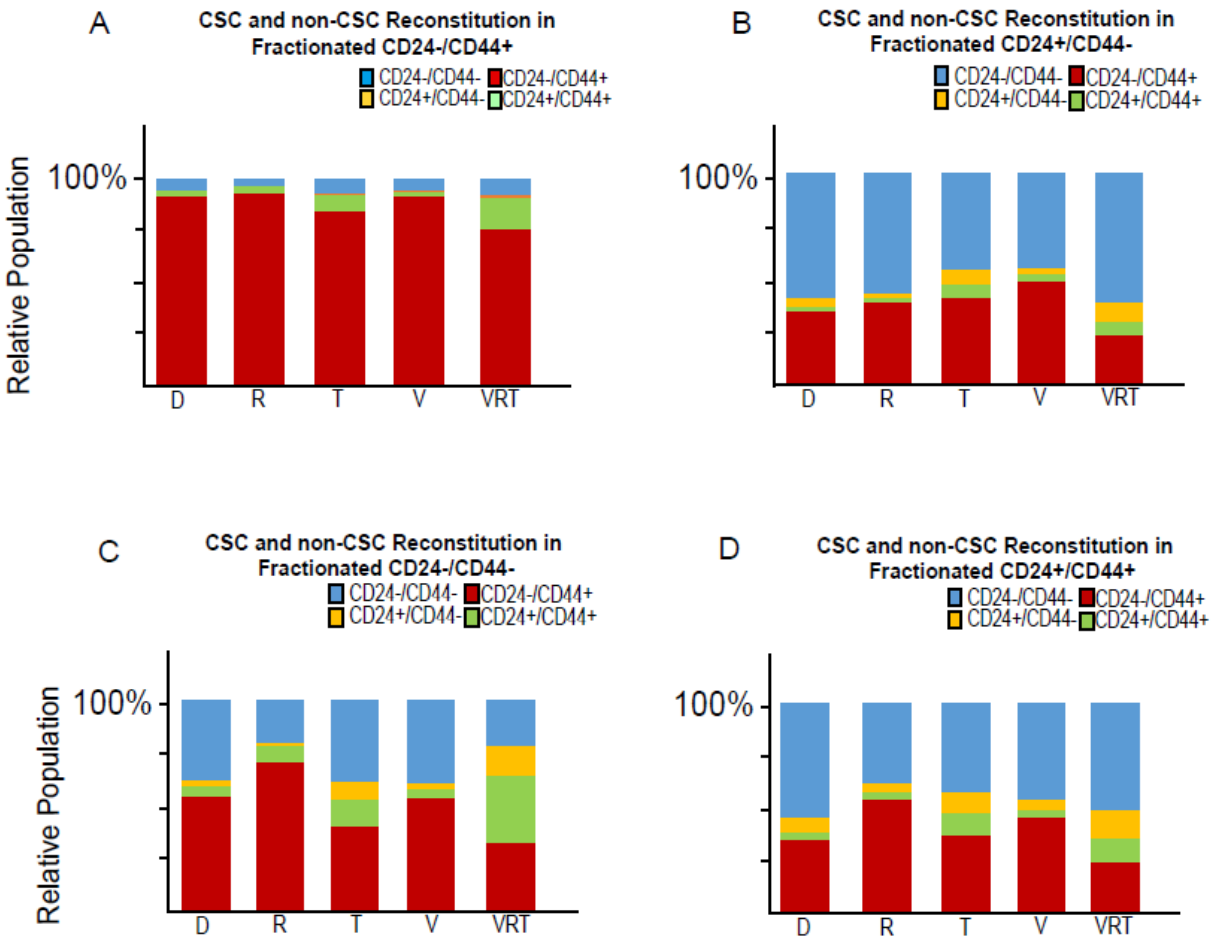

Supplemental Figure 5: Rapamycin in combination with valproic acid and tamoxifen reduces CSC conversion from non-CSC in the fractionated CSCs and non-CSC subpopulations. (A-D) Fractionated MDA-MB-231 CSC and non-CSC subpopulations were exposed for 120 hours to VRT combination as described in Figure 4. After treatment, cell viability was assessed by trypan-blue exclusion assay and the proportion of each CSC and non-CSC subpopulation was determined by flow cytometry based on CD44 and CD24 expression. The total number of cells in each subpopulation was calculated using viable cell number × percentage of each subpopulation. The populations were then normalized to estimate the reconstitution of CSC from each non-CSC subpopulation after VRT combination treatment.

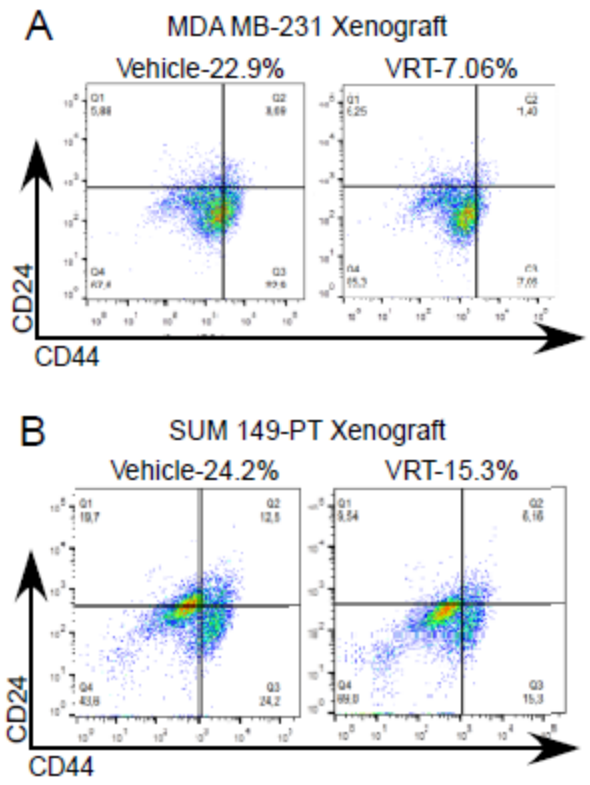

Supplemental Figure 6: Treatment with rapamycin in combination with valproic acid and tamoxifen in vivo reduces CSCs in TNBC tumors in vivo. (A-B) Representative flow cytometric data showing percentages of CSC ($CD44^{high/+}/CD24^{low/-}$) subpopulation in dissociated cells from MDA-MB-231 and SUM 149-PT tumors after 20 days of treatment with the vehicle (DMSO) or VRT combination as described in Figure 5.

A

SUM 149-PT

	$1x10^5$	$1x10^4$	$1x10^3$	$1x10^2$
Vehicle	3/3	2/3	1/3	0/3
VRT	2/3	0/3	0/3	0/3

Supplemental Figure 7: Co-inhibition of mTORC1, ESR1 and HDACs retards tumor tumorigenesis in vivo. (A) SUM 149-PT tumors from Figure 5 were dissociated into single cell suspension and re-transplanted into the mammary fat pads of new athymic mice in serial dilutions (10^5, 10^4, 10^3, 10^2 cells per mammary pad per injection). Tumor formation was observed for 6 weeks.

Chapter 4: Dual inhibition of Wnt and YAP signaling retards the growth of triple negative breast cancer in both mesenchymal and epithelial states

Preface

The following Chapter consists of a research article for which I am the primary author. The article was published in Molecular Oncology.

Andrew Sulaiman, Sarah McGarry, Li Li, Deyong Jia, Sarah Ooi, Christina Addison, Jim Dimitroulakos, Angel Arnaout, Carolyn Nessim, Zemin Yao, Guang Ji, Haiyan Song, Suresh Gadde, Xuguang Li, Lisheng Wang. Dual inhibition of Wnt and YAP signaling retards the growth of both mesenchymal and epithelial TNBC. *Molecular Oncology*, 2018; 12(4):423-440.

AS and LW conceived and designed the study. AS preformed bioninformatics analysis, data analysis, FACS, serial dilution and transfections/knockdowns. AS, SM, LL, DJ, and SO performed the *in vitr*o experiments. SO created the E-cadherin+ MDA MB-231 cell line. AS and SM performed the *in vivo* experiments. AS, SM, and SO analyzed the data. AS drafted the manuscript and created the figures. LW, CA, JD, SG, and ZY edited the manuscript. AA and CN provided clinical samples for the study. CA, JD, ZY, GJ, HS, YS, SG, and XL provided valuable suggestions and assisted in troubleshooting the experiments. AS, LW, XL, ZY, GJ, HS, CA, YS, and SG conceived or designed the experiments. All authors approved the final version of the manuscript.

Abstract

Triple negative breast cancer (TNBC), the most refractory subtype of breast cancer to current treatments, accounts disproportionately for the majority of breast cancer related deaths. This is largely due to cancer plasticity and the development of cancer stem cells (CSCs). Recently, distinct yet interconvertible mesenchymal-like and epithelial-like states have been revealed in breast CSCs. Thus, strategies capable of simultaneously inhibiting bulk and CSC populations in both mesenchymal and epithelial states have yet to be developed. Wnt/β-catenin and Hippo/YAP pathways are crucial in tumorigenesis, but importantly also possess tumor suppressor functions in certain contexts. One possibility is that TNBC cells in epithelial or mesenchymal state may differently affect Wnt/β-catenin and Hippo/YAP signaling and CSC phenotypes. In this report, we found that YAP signaling and $CD44^{high}/CD24^{-/low}$ *CSCs* were upregulated while Wnt/β-catenin signaling and ALDH+ CSCs were downregulated in mesenchymal-like TNBC cells, and vice-versa in their epithelial-like counterparts. Dual knockdown of YAP and Wnt/β-catenin, but neither alone, was required for effective suppression of both $CD44^{high}/CD24^{-/low}$ and ALDH+ CSC populations in mesenchymal and epithelial TNBC cells. These observations were confirmed with cultured tumor fragments prepared from TNBC patients after treatment with Wnt inhibitor ICG-001 and YAP inhibitor simvastatin. In addition, a clinical database showed that decreased gene expression of Wnt and YAP was positively correlated with decreased ALDH and CD44 expression in patients' samples while increased patient survival. Furthermore, tumor growth of TNBC cells in either epithelial or mesenchymal state was retarded, and both $CD44^{high}/CD24^{-/low}$ and ALDH+ CSC subpopulations were diminished in a human xenograft model after dual administration of ICG-001 and simvastatin. Tumorigenicity was also hampered after secondary transplantation. These data suggest a new therapeutic strategy for TNBC *via* dual Wnt and YAP inhibition**.**

1. Introduction

Breast cancer remains a leading cause of death in women worldwide (Siegel *et al.*, 2016). Triple negative breast cancer (TNBC) accounts for 15-20% of all breast cancer, but is disproportionally associated with the majority of breast cancer related deaths (Anders and Carey, 2009; Bauer *et al*., 2007). Chemotherapy is currently the mainstay of systemic medical treatment for TNBC, and is associated with severe normal tissue toxicity, rapid drug-resistance, cancer stem cell (CSC) enrichment, and disease relapse (Jia *et al.*, 2016). Hence, development of effective treatments for TNBC is an important unmet medical need.

Tumor plasticity is thought to drive metastasis and tumor relapse (Beerling *et al*., 2016). E-cadherin is an epithelial marker and an indicator for epithelial to mesenchymal transition (EMT) and its reverse process, MET (Liu *et al*., 2014). Epithelial breast *CSCs* are capable of converting into the mesenchymal CSC subpopulations through EMT and vice versa through MET, which drives metastasis and tumor relapse (Liu *et al*., 2014). Tumor cells in vivo may be able to transiently and reversibly switch between mesenchymal and epithelial states, a process that has been mentioned as epithelial-mesenchymal plasticity (Beerling *et al*., 2016). As such, inhibiting one CSC subpopulation may lead to tumor reconstitution by the other CSC subpopulation. While targeting bulk and both CSC subpopulations is clearly desirable for effective TNBC treatment, mechanistic insights and therapeutic approaches remain elusive (Angeloni *et al*., 2015).

Wnt/β-catenin signaling has been demonstrated to contribute to breast tumorigenesis and CSC plasticity (Anastas and Moon, 2013; Green *et al.*, 2013; Thorpe *et al.*, 2015). β-catenin stabilization and nuclear translocation is essential for Wnt signaling. β-catenin also acts as an adaptor that links to the cytoplasmic tail of E-cadherin to mediate cell-cell adhesion (Nelson and Nusse, 2004). The E-cadherin/β-catenin complex has been demonstrated to maintain epithelial

properties and facilitates self-renewal of human embryonic stem cells (Chen *et al.*, 2010; Huang *et al.*, 2015 ; Li *et al.*, 2010; Redmer *et al.*, 2011; Tian *et al.*, 2011). The intracellular domain of E-cadherin sequesters β-catenin to suppress Wnt signaling. Loss of E-cadherin-mediated cell-cell contact during epithelial-mesenchymal transition promotes Wnt signaling (Jeanes *et al.*, 2008; Serrano-Gomez *et al.*, 2016). However, roles of Wnt signaling in breast cancer remain incompletely understood as it has been shown to either fuel or repress cancer depending on yet to be determined molecular mechanisms (Rodriguez *et al.*, 2012; Tell *et al.*, 2006).

Over the past few years, Yes-associated protein (YAP), a downstream effector/transducer of the Hippo pathway, has emerged as a promising anticancer target although it also exhibits a tumor suppressor function in certain diseases (Moroishi *et al.*, 2015). YAP has recently been shown to incorporate into the β-catenin destruction complex to orchestrate Wnt signaling (Azzolin *et al.*, 2014). YAP drives cell cycle entry in an E-cadherin and β-catenin-dependent manner (Benham-Pyle *et al.*, 2015) and functions as a mediator of organogenesis and tumorigenesis by stimulating cell proliferation (Yu *et al.*, 2015; Zhang *et al.*, 2015). Importantly, YAP is also regulated by E-cadherin (Benham-Pyle *et al.*, 2015). In TNBC cells, E-cadherin homophillic binding at cell surface impedes the nuclear localization of YAP that is important for the biological activities of YAP (Kim *et al.*, 2011a). Additionally, α-catenin, a common binding partner of E-cadherin which strengthens cellular adhesion has been demonstrated to bind and sequester YAP in the cytoplasm (Schlegelmilch *et al.*, 2011). However, it is unknown whether epithelial-mesenchymal plasticity in cancer affects Wnt and YAP signaling and CSC phenotypes. A strategy for therapeutic blockage of Wnt and YAP to treat TNBC in both epithelial and mesenchymal states remains largely unexploited.

In this study, we demonstrated that YAP signaling was upregulated in mesenchymal-like TNBC with enriched *CD44^{high}/CD24$^{-/low}$* CSC subpopulation while Wnt/β-catenin was upregulated in epithelial-like TNBC with enriched ALDH+ CSC subpopulation. Importantly, the mesenchymal and epithelial TNBC exhibited disparate responses to Wnt and YAP inhibition and only dual inhibition is capable of effectively suppressing both *CD44^{high}/CD24$^{-/low}$ and ALDH+ CSC populations*. These findings were corroborated by using patient tumor samples and clinical databases. Furthermore, in a human xenograft model, dual inhibition of Wnt with ICG-001 and YAP with simvastatin effectively attenuated both mesenchymal and epithelial TNBC tumor burden, diminished both *CD44^{high}/CD24$^{-/low}$* and ALDH+ CSC subpopulations, and reduced tumorigenicity after secondary transplantation. These results suggest that Wnt and YAP signaling are dynamically changed during EMT/MET interconversion and dual inhibition using FDA-approved drugs can be a viable approach for the treatment of TNBC.

2. Materials and methods

2.1 Cell culture and reagents

MDA-MB-231 breast cancer cells were purchased from the American Type Culture Collection (ATCC, Manassas, VA, USA) and maintained in DMEM-F12 media supplemented with 10% Fetal bovine serum (FBS, HyClone, Logan, UT, USA) and 1% penicillin/streptomycin. SUM149 breast cancer cells were obtained from Asterand (Detroit, MI, USA) and cultured in Hams F-12 media (Mediatech, Manassas, VA, USA) containing 5% FBS, 5 μg/ml insulin, 1 μg/ml hydrocortisone, 10 mM HEPES and 1% penicillin/streptomycin. Cells were cultured at 37°C in a 5% CO2 incubator. ICG-001 was purchased from CalBiotech (El Cajon, CA, USA), simvastatin from

Caymen Chemicals (Ann Arbor, Michigan, USA). Insulin, hydrocortisone, HEPES, and bovine serum albumin were purchased from Sigma-Aldrich (St. Louis, MO, USA).

2.2 Tet-ON inducible gene expression of E-cadherin

MDA-MB-231 E-cadherin^{high} cells (epithelial-like, Epi) were generated using a lentiviral vector (pLVX-Tight-Puro, Clontech) containing an E-cadherin gene insert, and control MDA-MB-231 E-cadherin$^{-/low}$ cells (mesenchymal-like, Mes) were generated using an empty lentiviral vector of pLVX-Tight-Puro. Stable clones were selected after 3 days using G418 (Clontech) and puromycin dihydrochloride (Thermo Fisher) at a concentration of 1000 µg/mL and 1 µg/mL respectively for 14 days. For maintenance, 250 µg/mL of G418 and 0.25 µg/mL of puromycin were added in the culture medium. E-cadherin expression was activated by adding 1 µg/mL doxycycline hydrochloride (Thermo Fisher) to the cell culture every 2-3 days. E-cadherin levels were examined following RNA extraction by RT-qPCR and protein levels by western blotting.

2.3 Primary normal mammary and breast cancer tissue fragments

Surgical tissues from 3 TNBC patients undergoing routine surgical procedures were obtained and used in the experiments. The protocol was approved by The Ottawa Hospital Research Ethics Board (Protocol# 20120559-01H). Normal mammary tissues or areas containing tumor were identified by gross pathologic examinations. Approximately 2-mm cores were obtained using a sterile biopsy punch that was further sliced with a scalpel to obtain approximately 2 × 1-mm tumor slices (Dayekh *et al.*, 2014; Sulaiman *et al.*, 2016). The slices were randomized and three slices were placed into each well of 24-well plate and cultured in DMEM-F12 medium supplemented with 10% FBS, 1% penicillin/streptomycin, 1 µg/ml insulin, 0.5 ng/ml hydrocortisol and 3 ng/ml

epidermal growth factor. These primary tissue fragments were treated with the same concentrations of inhibitors as used in the breast cancer cell lines, followed by a viability assay and flow cytometric analysis. The patient-derived xenograft sample HCI-001 was obtained from University of Utah and cultured in the same conditions as clinical samples.

2.4 Flow cytometry analysis

Dissociated cancer cells were filtered through a 4µm strainer and suspended in PBS supplemented with 2% FBS and 2mM EDTA. 1uL of mouse IgG (1mg/mL) was added and incubated at 4º for 10 minutes. Afterwards, the cells were resuspended in 1x binding buffer (eBioscience, San Diego, CA, USA) and incubated with Annexin-V (eBioscience) for 15 minutes at room temperature. Antibodies were added according to the manufacturer's instructions. Apoptosis was determined using Annexin-V-PE-Cy7 Apoptosis Detection Kit (eBioscience). ALDH activity was determined using ALDEFLUOR (Stem-cell Technologies, Vancouver) with a DEAB control. Anti-CD44 (APC) and anti-CD24 (PE) (BD Pharmingen) antibodies were used. Lastly, the cells were washed twice with additional ALDEFLUOR assay buffer and 7-aminoactinomycin D (7-AAD, eBioscience, San Diego, CA) was added to exclude dead cells. Flow cytometry was performed on a Cyan-ADP 9 and the BD LSRFortessa. Data was analyzed with FlowJo software (Ashland, OR, USA).

2.5 Soft agar colony formation

In a 12-well plate, the base layer consisted of 0.6% agarose gel containing DMEM/F12 media. The cell layer consisted of 0.35% agarose gel containing DMEM/F12 media and $5x10^3$ MDA- MB-231 cells. Plates were incubated at 37°C in 5% CO_2 for 21 days. Cell viability was then determined

through 3-(4,5-dimethylthiazol-2-yl)-2,5-diphenyl tetrazolium bromide (MTT, 1 mg/ml) staining. Colonies were then counted (>100 μm in diameter). All experiments were performed in triplicate, and data are presented as means ± SD.

2.6 Western blot analysis

Cells were harvested, washed with PBS and lysed with lysis buffer supplemented with protease inhibitors (Roche). After the protein concentrations were determined using a Bio-Rad DC protein assay kit (Bio-Rad, Hercules, CA, USA), samples were then normalized and de-natured. The samples were then loaded into an 8% polyacrylamide gel and separated by SDS-PAGE followed by transference to a PVDF membrane. Proteins were identified by incubation with primary antibodies followed by horseradish peroxidase-conjugated secondary antibodies and an enhanced chemiluminescence solution (Pierce, Thermo Scientific, USA). Antibodies used in this study include: anti-YAP1(1:1000, Cat: 4912, Cell Signaling, Cambridge, USA), anti-CD44 (8E2) monoclonal antibody (1:1000, Cat: 5640, Cell Signaling), anti-ALDH1A1 (1:1000, Cat: ab105920, Abcam, Toronto, ON, Canada), anti-Klf4 (1:1000, Cat: ab72543, Abcam), anti-β-catenin (1:1000, Cat: 610153, Clone 14, BD, Mississauga, ON, Canada), anti-active β-catenin (1:500, Cat: 05665, Clone 8E7, Millipore, Billerica, MA, USA), and anti-α-tubulin monoclonal antibody (1:500, Cat: T9026, Sigma-Aldrich, St. Louis, MO, USA).

2.7 Quantitative real-time PCR

Total RNAs were extracted using RNeasy kit (QIAGEN) and real-time qPCR (RT-qPCR) analysis was performed using Bio-Rad MyiQ (Bio-Rad, USA) as previously described (Sulaiman *et al.*, 2016). The conditions for RT-qPCR reactions were: one cycle at 95°C for 20 seconds followed by

45 cycles at 95°C for three seconds and annealing at 60°C for 30 seconds. Results were normalized to the housekeeping gene 18S ribosomal RNA (18S) or GAPDH. Relative expression level of genes from different groups were calculated with the $^{2\Delta\Delta}$CT method and compared with the expression level of appropriate control cells. Specific primer sequences for individual genes are listed in Supplemental Table S1.

2.8 siRNA knockdown

siRNAs for E-cadherin (#4392420), β-catenin and the Silencer Select Negative Control #1 siRNA (Scramble, #4390843) were purchased from Thermo Scientific (Dharmacon, USA) as SMARTpools. YAP1 silencer® select siRNA was also purchased from Thermo Scientific (ID: s20368). For siRNA transfections, cells were transfected with these oligoes using Lipofectamine RNAiMAX reagent (Invitrogen) according to the manufacturer's instructions. After transfection, efficiency was determined through Western blot or RT-qPCR.

2.9 Lentiviral transduction of short hairpin RNA, generation of transgenic Wnt Reporter 7xTCF-eGFP cell lines and β-catenin/TCF-eGFP reporter assays

pLKO.1 puro shRNA β-catenin was a gift from Bob Weinberg (Addgene plasmid # 18803), shYAP1 was a was a gift from William Hahn (Addgene plasmid # 42540), and scrambled shRNA was a gift from David Sabatini (Addgene plasmid 1864) (Onder *et al.*, 2008; Rosenbluh *et al.*, 2012; Sarbassov *et al.*, 2005). β-catenin/TCF/LEF dependent reporter plasmid (7xTcf-eGFP//SV40-PuroR, 7TGP) containing seven Tcf/Lef-binding sites and a puromycin resistance gene was a gift from Dr. Nusse (Addgene plasmid 24305). Lentiviral production was carried out as previously described (Jia *et al.*, 2016; Sulaiman *et al.*, 2016). 10-cm dishes were seeded with

6×10^6 293T cells overnight. Afterwards, 8 µg of lentivirus vector, 5.4 µg of the psPax2 envelope plasmid, 3.6 µg of the packaging plasmid (pMD2.G) were used. The medium was replaced overnight, and after 48 hours, the lentiviral supernatant was harvested, filtered through a 0.45 µm PES filter, and concentrated with Lenti-X concentrator (Clontech) according to the manufacturer's instruction. When SUM 149-PT cells or Mes- or Epi-MDA-MB-231 cells in 6-well plates reached 40-50% confluence, 1 ml of concentrated lentiviral supernatant and 8 µg/ml of polybrene were added for 24h, followed by puromycin selection. The expression levels of TCF-eGFP were determined by flow cytometry.

2.10 Cell viability assays

Cells were seeded into 12 well plates (1.5×10^4 cells/well). After 120 hours of treatment, Alamar blue viability analysis was performed by incubation with 10% Alamar blue reagent (Thermo Fisher Scientific) for 4 hours. Florescence was measured at 560 nm excitation and 590 nm emission. Cell viability was also determined through 3-(4,5-dimethylthiazol-2-yl)-2,5-diphenyl tetrazolium bromide (MTT, 1 mg/ml) staining after incubation for 4 hours. Absorbance was measured at 570nm.

2.11 ICG-001 and simvastatin concentrations selected for the *in vitro* experiments according to the pharmacological studies reported previously

The inhibitor concentrations used in this study for *in vitro* experiments were selected according to the published pharmacological studies. In a phase I clinical trial, 18 patients were given a continuous infusion of the ICG-001/PRI-724 for 7 days with dose escalations from 40 to 1280 mg/m^2/day (El-Khoueiry *et al.*, 2013). One patient developed dose limiting toxicity of

hyperbilirubinemia. The recommended phase 2 dose for ICG-001/PRI-724 was 905 mg/m^2 based on the incidence of adverse events at 1280 mg/m^2 and the plateau in pharmaceutical kinetic parameters (El-Khoueiry *et al.*, 2013). The median Cmax and AUC 0-t for C-82 at 905 mg/m2/day were 887 ng/mL and 262787 h*ng/mL. Median elimination T ½ was 7.35 h (El-Khoueiry *et al.*, 2013). In another clinical study, up to 160 mg/m^2/day of ICG-001/PRI-724 was used for a continuous intravenous infusion over six cycles of 1 week followed by 1 week off. No adverse effects were observed for 40 mg/m^2/day group (with a maximum blood concentration of 692 ± 418 ng/mL) (Kimura *et al.*, 2017). Accordingly, 2.5 μM ICG-001 (= 1372 ng/ml, molecular weight of ICG-001/PRI-724: 568.683) was chosen for *in vitro* experiments in this study, which is close to the recommended maximum blood concentration.

Simvastatin is a FDA-approved drug that has been widely used for the treatment of Hypercholesterolemia with up to 80 mg of an oral dosage per day. When taking 20 mg of simvastatin, patient's blood concentration could achieve 28 ng/mL with a half-life of 5.5 hours (Tao *et al.*, 2016). Oral intake of 40 mg simvastatin was used in another study, resulting in a maximum blood concentration of 34 ng/mL (Bellosta *et al.*, 2004). Accordingly, 100 nM (= 41.86 ng/mL) of simvastatin (molecular weight = 418.566) was chosen for our *in vitro* experiments.

2.12 Xenograft tumor growth

Athymic nude mice were obtained from Charles River Laboratories. The MDA-MB-231 breast cancer cells were mixed 1:1 with Matrigel and injected under aseptic conditions into the mammary fat pads (n = 4 for each group, 2 × 10^6 cells per fat pad). When the tumor reached a mean diameter of ~3 mm, mice were intraperitoneally injected daily with the vehicle, ICG-001 (100 mg/kg/day), simvastatin (5 mg/kg/day), or both for 15 days. At the end of drug treatment, mice were humanely

euthanized and tumors were harvested for further analyses and secondary transplantation.

2.13 Secondary transplantation of nude mouse model

Tumors were minced using a scalpel and incubated in DMEM media containing collagenase/hyaluronidase (STEMCELL Technologies, #07912) at 37 °C for 60 minutes. Afterwards the solution was passed through a 40-µM nylon mesh for the creation of a single cell solution. The treated tumors were inoculated into one of the mammary fat pads at a concentration of 10^5, 10^4, 10^3, or 10^2 cells from the original tumors. Tumor growth and size were measured after 6 weeks of growth.

2.14 Clinical database analysis and statistical analysis

Breast cancer datasets from the Cancer Genome Atlas (TCGA, http://cancergenome.nih.gov/), Nature Communications 2016 (Pereira *et al.*, 2016), Nature 2012 (Network, 2012) and METABRIC (http://molonc.bccrc.ca/aparicio-lab/research/metabric/) were used and analyzed with cBioportal (http://www.cbioportal.org/index.do). *CTNNB1* and *YAP1* gene repression was defined as mRNA expression levels less than 3 standard deviations below the mean and protein repression was defined as being below the mean. Expression data and Kaplan-Meir survival curves were generated using the datasets compiled by May 2017 from the following Database IDs: *CTNNB1* and *YAP1* gene repression (2509 patients): http://bit.ly/2hTTYOW, CTNNB1 and YAP1 protein repression (887 patients): http://bit.ly/2jNmIgE. CTNNB1, YAP1 and CDH1 protein analysis (410 patients): http://bit.ly/2pHz5xx. Additionally, the Gene Expression Omnibus2R database was used to analyze a dataset (Dataset: GSE45827) to compare the MDA-MB-231 cell line to 41 TNBC patient samples https://www.ncbi.nlm.nih.gov/geo/geo2r/?acc=GSE45827. For

all clinical database data, the log rank test was performed to determine whether observed differences between groups were statistically significant. Data are expressed as means ± Standard Deviation (SD) or Standard Error (SE). Statistical significance was determined using ANOVA or Student's *t* test. Results were considered significant when * $p < 0.05$, ** $p < 0.01$, or *** $p < 0.001$.

3. Results

3.1 Epithelial TNBC cells exhibit reduced YAP but increased Wnt/β-catenin signaling.

E-cadherin has been used routinely to demarcate epithelial or mesenchymal states (Beerling *et al.*, 2016; Liu *et al.*, 2014; Tsuji *et al.*, 2008). Re-expression of E-cadherin in E-cadherin negative mesenchymal-like MDA-MB-231 TNBC cells resulted in an epithelial-like phenotype (Figure 1A and Figure S1: downregulation of a set of mesenchymal genes *N-CADHERIN,, SNAIL, SLUG, ZEB1*, and *ZEB2* and upregulation of a set of epithelial genes *E-CADHERIN, KERATIN 13, KERATIN 15 and DSP).* Notably, Wnt target genes (*TCF4*, *LEF1* and *AXIN2*, Figure 1B) were upregulated in E-cad+ MDA MB-231 cells while YAP target genes (*CTFG, ANKRD1*, and *CYR61*, Figure 1C) were downregulated. This was corroborated by increased active β-catenin and diminished YAP1 protein expression (Figure 1D). Increased Wnt activity in epithelial-like TNBC cells was also confirmed using a 7×TCF-eGFP Wnt reporter that contains seven TCF/LEF consensus binding sites upstream of a promoter expressing GFP (Figure 1E) (Fuerer and Nusse, 2010). Consistently, siRNA knockdown of E-cadherin in epithelial-like SUM 149 cells (an E-cadherin^{high} inflammatory TNBC line) led to a mesenchymal-like morphology (Figure 1F), an increase in YAP expression and a decrease in active β-catenin protein corroborated by the

diminished 7xTCF-eGFP Wnt reporter activity (Figure 1G and Figure S2). Thus, an epithelial phenotype inhibits YAP while promoting Wnt signaling in TNBC.

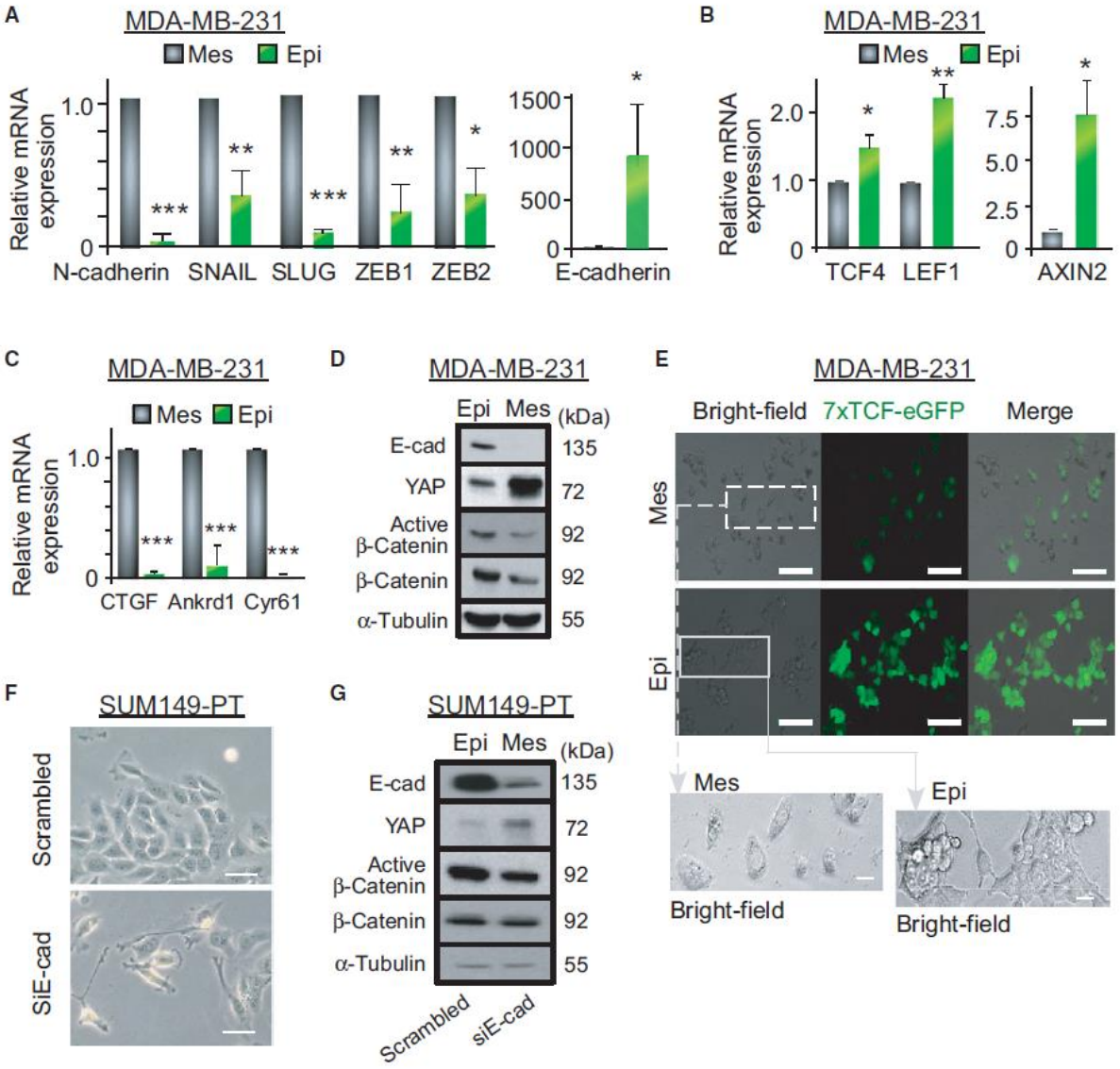

Figure 1. Epithelial-like, not mesenchymal-like TNBC cells, exhibit upregulated Wnt and downregulated YAP signaling. (A) RT-qPCR analysis of mesenchymal associated genes *N-CADHERIN, SNAIL, SLUG, ZEB1, and ZEB2* as well as *E-CADHERIN (CDH1)* in epithelial-like MDA-MB-231 cells (Epi, generated by overexpression of E-cadherin) and in mesenchymal-like control MDA-MB-231 cells (Mes). **(B)** RT-qPCR analysis of Wnt target genes *TCF4, LEF1, and AXIN2* in mesenchymal-like (Mes) and epithelial-like (Epi) MDA-MB-231 cells. **(C)** RT-qPCR

analysis of YAP target genes *CTGF, ANKRD1, and CYR61* in mesenchymal-like (Mes) and epithelial-like (Epi) MDA-MB-231 cells. **(D**) Representative western blot of E-cadherin, YAP1 and β-catenin expression in mesenchymal-like (Mes) and epithelial-like (Epi) MDA-MB-231 cells. **(E)** Bright-field and fluorescence images of mesenchymal-like (Mes) and epithelial-like (Epi) MDA-MB-231 cells after transfection of the 7xTCF-eGFP reporter, scale bar = 100 µm. White squares on bright-field images are enlarged in the bottom panels. The brightness and contrast are adjusted for seeing the shape of the cells, scale bar = 20 µm. **(F)** Representative phase contrast images of epithelial TNBC SUM 149-PT cells 48 hours after siRNA knockdown of E-cadherin, scale bar = 50 µm. **(G)** Representative western blot depicting E-cadherin, YAP1 and β-catenin (total β-catenin and non-phosphorylated at Ser33/37/Thr41 for active β-catenin) expression in epithelial-like (Epi) and mesenchymal–like (Mes) SUM 149-PT cells 48 hours after siRNA E-cadherin knockdown (siE-cad). Data represent means ± SE, n = 3 for all figures; * $p < 0.05$, ** $p < 0.01$, *** $p<0.001$.

3.2 Epithelial and mesenchymal TNBC cells associate with distinct CSC properties.

The existence of interconvertible mesenchymal and epithelial populations and CSCs in breast cancer has been associated with drug resistance, metastasis and diminished survival (Charafe-Jauffret *et al.*, 2010; Li *et al.*, 2008; Liu *et al.*, 2014; Ricardo *et al.*, 2011; Tiran *et al.*, 2017; Yan *et al.*, 2016). We therefore asked whether conversion between mesenchymal and epithelial phenotypes in TNBC also displayed different CSC phenotypes. Indeed, mesenchymal MDA-MB-231 cells contained substantial $CD44^{high}/CD24^{-/low}$ but almost undetectable $ALDH^{+}$ CSCs. After conversion to an epithelial phenotype, E-cad+ MDA-MB-231 cells possessed abundant $ALDH^{+}$ CSCs with diminished $CD44^{high}/CD24^{-/low}$ CSCs (Figure 2A-B, flow cytometry). Consistently, western blot showed increased ALDH and diminished CD44 and pluripotency marker Klf4 after MET (Figure 2C). High expression of Klf4 in breast mesenchymal cells has been associated with metastasis, CSC self-renewal, and tumorigenicity (Okuda *et al.*, 2013; Yu *et al.*, 2011). A similar trend was also seen after partial knockdown of E-cadherin in epithelial SUM149 TNBC cell line (Figure 2D-F). Epithelial CSCs have been associated with enhanced proliferative properties (Liu *et al.*, 2014a). Indeed, more colonies were observed in epithelial TNBC cells in comparison to mesenchymal counterparts as determined by an *in vitro* colony forming assay (Figure 2G). It seems

that epithelial and mesenchymal TNBC cells associate with distinct CSC properties.

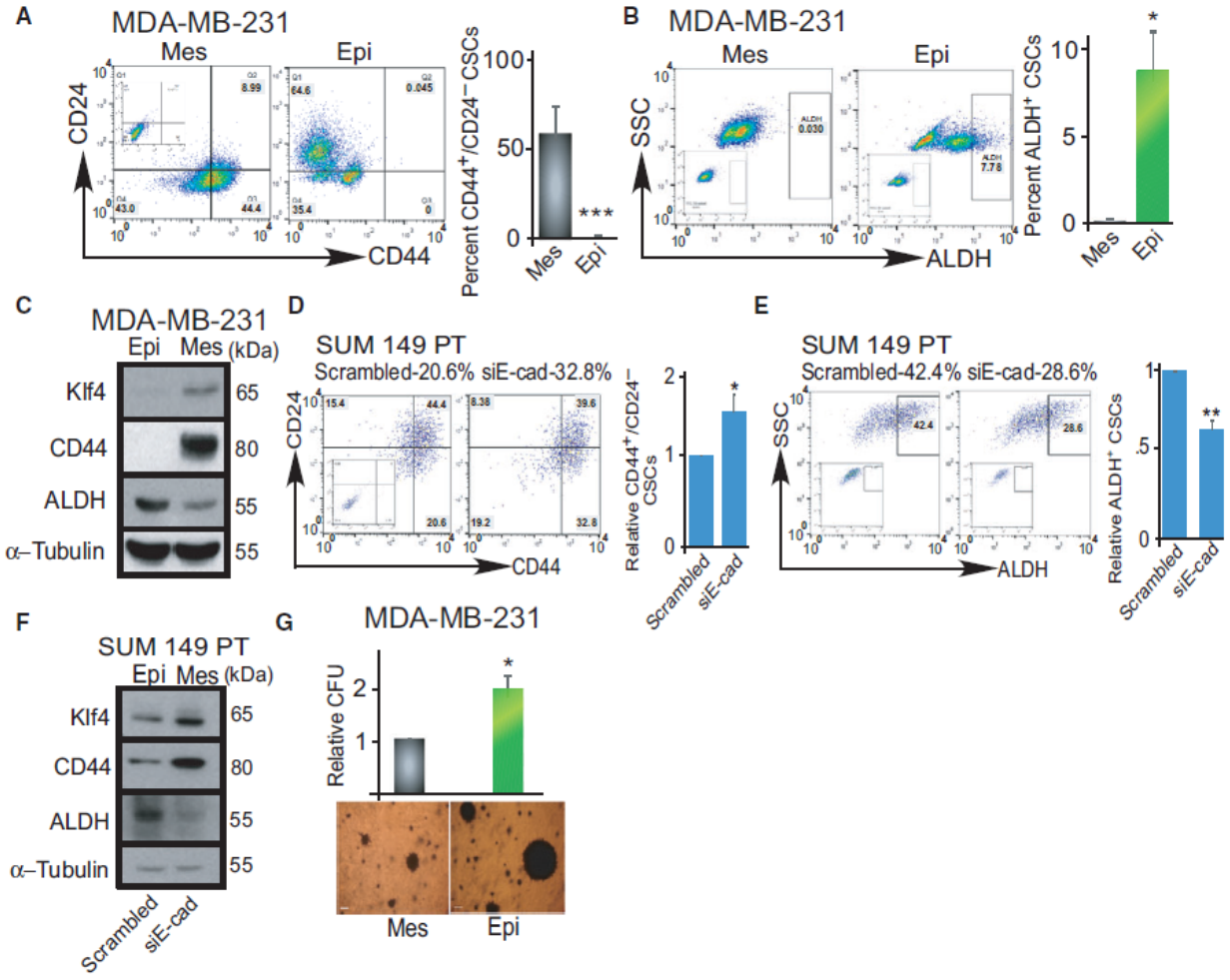

Figure 2. Epithelial-like and Mesenchymal-like TNBC cells display distinct CSC properties. **(A-B)** Flow cytometric analysis of $CD44^{high}/CD24^{low}$ and ALDH+ CSC subpopulations in mesenchymal-like (Mes) and epithelial-like (Epi) MDA-MB-231cells (generated by overexpression of E-cadherin in mesenchymal-like MDA-MB-231 cells). Insets within flow cytometric plots depict isotype controls for CD44/CD24 (A), or DEAB control (B) for ALDH. **(C)** Representative western blot depicting pluripotency related proteins: Klf4, CD44 and ALDH in mesenchymal-like (Mes) and epithelial-like (Epi) MDA-MB-231 cells. **(D-E)** Flow cytometric analysis of $CD44^{high}/CD24^{low}$ and ALDH+ CSC subpopulations in the epithelial-like SUM 149-PT cells (Epi, Scrambled) and mesenchymal-like (Mes, 48 hours after knockdown with siE-cadherin, siE-cad). Insets within flow cytometric plots depict isotype controls for CD44/CD24 (A), or DEAB control (B) for ALDH. **(F)** Representative western blot depicting pluripotency related proteins: Klf4, CD44 and ALDH in epithelial-like SUM 149-PT cells (Epi, Scrambled, transfected with scrambled oligoes) and mesenchymal-like (Mes, 48 hours after transfection with siRNA E-cadherin, siE-cad). **(G)** Soft agar colony formation assay to evaluate colony forming potential of mesenchymal-like (Mes) and epithelial-like (Epi, overexpression of E-cadherin) MDA-MB-231 cells (5000 cells/well). Cells were seeded in soft agar and cultured for 21 days and colonies were counted after staining with MTT for viability. Scale bar = 100 μm. Data represent means ± SD, n = 3 for all figures; * $p < 0.05$, ** $p < 0.01$, *** $p<0.001$.

3.3 Dual knockdown of Wnt and YAP inhibits mesenchymal and epithelial bulk and CSC subpopulations.

We then investigated whether dual knockdown of Wnt and YAP leads to inhibition of both epithelial and mesenchymal bulk and CSC subpopulations. In epithelial TNBC, Wnt reporter assays showed that β-catenin knockdown (i.e. Wnt inhibition), but not YAP knockdown, effectively repressed Wnt signaling, equivalent to dual knockdown (Figure 3A). In mesenchymal TNBC cells, however, knockdown of either β-catenin or YAP only moderately suppressed Wnt signaling, whereas dual knockdown exhibited higher efficacy (Figure 3A). Interestingly, β-catenin knockdown (Figure S3 showing knockdown efficiency) inhibited the expression of YAP target genes in epithelial TNBC cells but upregulated the expression of YAP target genes in their mesenchymal counterparts (Figure 3B). Unexpectedly, while siRNA knockdown of YAP1 effectively inhibited $CD44^{high}/CD24^{-/low}$ CSC subpopulation in mesenchymal TNBC, it increased

$ALDH^+$ CSCs in epithelial TNBC cells. In contrast, siRNA knockdown of β-catenin was more effective in inhibiting ALDH+ CSCs in an epithelial state but less effective in suppressing $CD44^{high}/CD24^{-/low}$ CSCs in a mesenchymal state. These data suggest that Wnt and YAP inhibition alone exhibits differential effects on mesenchymal and epithelial CSCs. As a result, dual knockdown of Wnt and YAP was a more effective approach to inhibit both $CD44^{high}/CD24^{-/low}$ and ALDH+ CSC subpopulations in in both mesenchymal and epithelial states (Figure 3C-D).

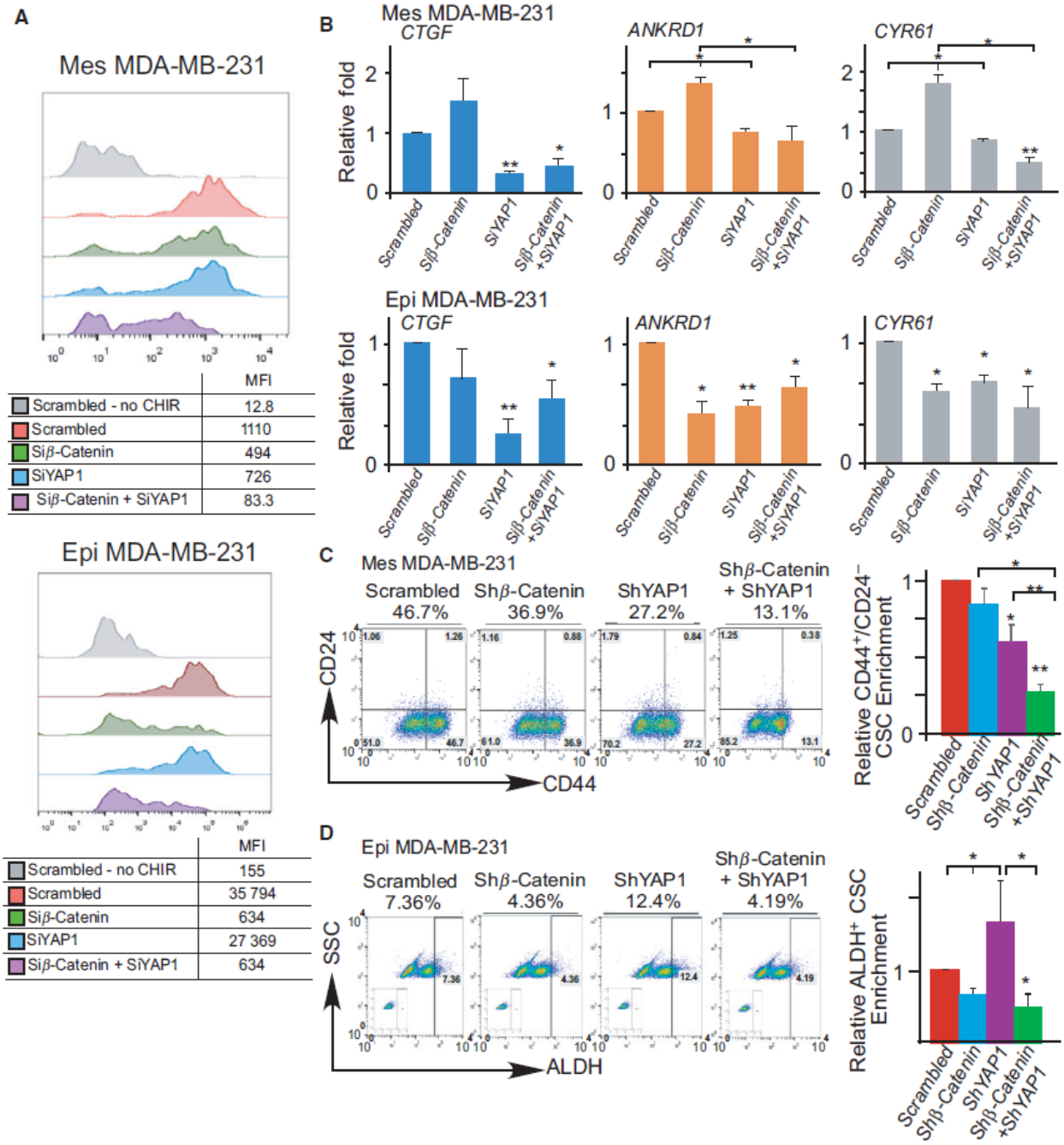

Figure 3. Dual knockdown of Wnt and YAP inhibits mesenchymal and epithelial bulk and CSC subpopulations. (A) Representative flow cytometric analysis of 7xTCF-eGFP Wnt reporter activity (MFI: median fluorescent intensity) in mesenchymal-like (Mes) and epithelial-like (Epi, overexpression of E-cadherin) MDA-MB-231 cells 48 hours after siRNA knockdown of β-catenin and/or YAP1. Cells were exposed to 3μM CHIR99021 (CHIR, a GSK3 inhibitor activating Wnt

signaling) and compared to scrambled + DMSO vehicle and scrambled + CHIR99021 controls. **(B)** RT-qPCR analysis of YAP target genes: *CTGF*, *ANKRD1*, and *CYR61* after β-catenin and/or YAP1 siRNA knockdown in mesenchymal-like (Mes) or epithetical-like (Epi) MDA-MB-231 cells. Data represent means ± SE. **(C-D)** Flow cytometric analysis of the $CD44^{high}/CD24^{low}$ and ALDH+ CSC subpopulations in the mesenchymal-like (Mes) and epithelial-like (Epi) MDA-MB-231 cells after shRNA knockdown of β-catenin and/or YAP1. Insets within flow cytometric plots depict DEAB control for ALDH baseline determination. Data represent means ± SD; n = 3 for all figures; * $p < 0.05$, ** $p < 0.01$, *** $p<0.001$, in comparison to the indicated or scrambled groups.

3.4 Combination of ICG-001 and simvastatin treatment inhibits epithelial and mesenchymal TNBC bulk and CSC populations *in vitro*.

To determine the effect of small molecules on dual inhibition of Wnt and YAP signaling in TNBC cells, we used the FDA-approved ICG-001/PRI-724 (a Wnt inhibitor) and simvastatin (inhibiting YAP signaling revealed in 2014 (Wang *et al.*, 2014) in addition to other targets). Like that observed in β-catenin knockdown experiments, ICG-001 treatment decreased Wnt activity effectively in epithelial TNBC cells (Figure 4A), and upregulated YAP target genes in mesenchymal TNBC cells (Figure 4B). Combination of ICG-001 and simvastatin treatment was able to suppress both Wnt and YAP signaling, reduce cell viability, and promote apoptosis in both mesenchymal and epithelial TNBC cells (Figure 4C-D, Figure S4A and S5A). Flow cytometric analysis showed that the combination treatment also diminished both mesenchymal $CD44^{high}/CD24^{-/low}$ and epithelial $ALDH^{+}$ CSC subpopulations compared to vehicle and single inhibitors (Figure 4F-G, Figure S4B and Figure S5B-S5C), highlighting the necessity of dual Wnt and YAP suppression. Additionally, normal mammary cells from patient breast tissue were not significantly affected by the combination treatment (Figure 4E). Hence, the dual inhibition of Wnt and YAP signaling can be an effective approach to halt the growth of epithelial and mesenchymal TNBC cells *in vitro*.

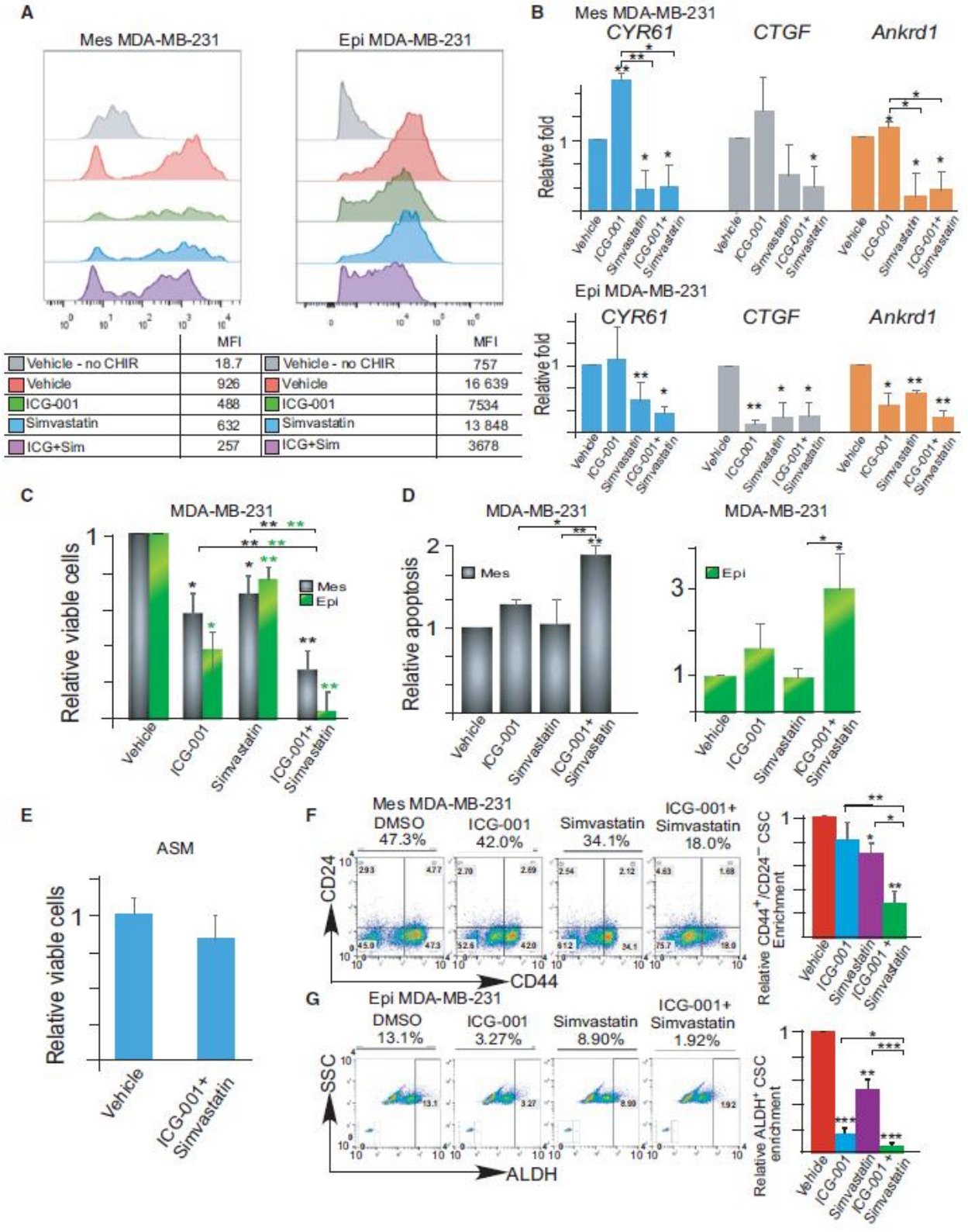
A
Mes MDA-MB-231
Epi MDA-MB-231
MFI
Vehicle - no CHIR 18.7
Vehicle 926
ICG-001 488
Simvastatin 632
ICG+Sim 257
Vehicle - no CHIR 757
Vehicle 16 639
ICG-001 7534
Simvastatin 13 848
ICG+Sim 3678
B
Mes MDA-MB-231
CYR61
CTGF
Ankrd1
Relative fold
Epi MDA-MB-231
Vehicle
ICG-001
Simvastatin
ICG-001+ Simvastatin
C
MDA-MB-231
Relative viable cells
Mes
Epi
D
MDA-MB-231
Relative apoptosis
E
ASM
F
Mes MDA-MB-231
DMSO 47.3%
ICG-001 42.0%
Simvastatin 34.1%
ICG-001+ Simvastatin 18.0%
CD24
CD44
Relative CD44+/CD24− CSC Enrichment
G
Epi MDA-MB-231
DMSO 13.1%
ICG-001 3.27%
Simvastatin 8.90%
ICG-001+ Simvastatin 1.92%
SSC
ALDH
Relative ALDH+ CSC enrichment

Figure 4. Dual inhibition of YAP and Wnt signaling with small molecules suppresses both mesenchymal- and epithelial-like bulk and CSC populations. (A) Representative flow cytometric analysis of 7xTCF-eGFP Wnt reporter activity in mesenchymal-like (Mes) and epithelial-like (Epi, overexpression of E-cadherin) MDA-MB-231 cells after 48 hours of treatment with the vehicle (DMSO), ICG-001 (5 μM) and/or simvastatin (100 nM). Cells were exposed to 2-3μM CHIR99021 (CHIR, a GSK3 inhibitor activating Wnt signaling) and compared to vehicle control +/- CHIR99021. **(B)** RT-qPCR analysis of YAP target genes (*CTGF*, *ANKRD1*, and *CYR61*) 48 hours after treatment with vehicle (DMSO), ICG-001 (2.5 μM) and/or simvastatin (100 nM) in mesenchymal-like (Mes) and epithelial-like (Epi) MDA-MB-231 cells. Data represent means ± SE. **(C)** MTT viability analysis of mesenchymal-like (Mes) and epithelial-like (Epi) MDA-MB-231 cells after 120 hours of exposure to vehicle (DMSO), ICG-001 (2.5 μM) and/or simvastatin (100 nM). **(D)** Flow cytometry analysis of apoptosis (Annexin $V^+/7AAD^+$) of mesenchymal-like (Mes) and epithelial-like (Epi) MDA-MB-231 cells after 120 hours of exposure to vehicle (DMSO), ICG-001 (2.5 μM) and/or simvastatin (100 nM). **(E)** Alamar blue viability assays of normal control mammary tissue (ASM) from patient after 120 hours of exposure to vehicle (DMSO) or ICG-001 (2.5 μM) and/or simvastatin (100 nM). **(F-G)** Flow cytometric analysis of $CD44^{high}/CD24^{low}$ and ALDH+ CSCs after 120 hours of exposure to ICG-001 (2.5 μM) and simvastatin (100 nM) in mesenchymal-like (Mes) and epithelial-like (Epi) MDA-MB-231 cells. Insets within flow cytometric analysis depict DEAB control for ALDH baseline determination. Data represent means ± SD; n = 3 for all figures; * $p < 0.05$, ** $p < 0.01$, *** $p<0.001$, in comparison to the indicated groups or vehicle control.

3.5 Clinical TNBC patients' samples exhibit epithelial-like phenotypes and dual inhibition of Wnt and YAP signaling suppresses both bulk and CSC populations.

In comparison to mesenchymal MDA-MB-231 cell line, almost all 41 primary TNBC tumors (omnibus2R, Dataset:GSE45827, Accessed July 14 2017 (Barrett *et al.*, 2013)) showed increased expression of E-cadherin (*CDH1*) and Wnt target gene *TCF4* but decreased YAP target gene *AXL* (Figure 5A). Likewise, primary TNBC patients' tumor samples (CRDCA, SEM-1 and ARI-1) also showed increased expression of E-cadherin, active β-catenin, and ALDH but decreased expression of YAP and CD44 (Figure 5C, Figure S6). It seems that patients' TNBC samples exhibit a more epithelial-like phenotype in comparison to the mesenchymal-like MDA-MB-231 TNBC cell line. In addition, the E-cadherin protein levels were positively correlated with β-catenin expression in

410 breast cancer patients' tumor samples (Figure 5B, cBioportal) (Network, 2012), consistent with the data obtained from TNBC cell lines in Figure 1.

We then treated three patients' tumor fragments and one patient-derived-xenograft (PDX) fragment (DeRose *et al.*, 2011) with Wnt and/or YAP inhibitors. In all TNBC patients' samples, dual inhibition of Wnt and YAP reduced cell viability (Figure 5D), and inhibited both $CD44^{high}/CD24^{-/low}$ and $ALDH^{+}$ CSC subpopulations than single inhibition alone (Figure E-H).

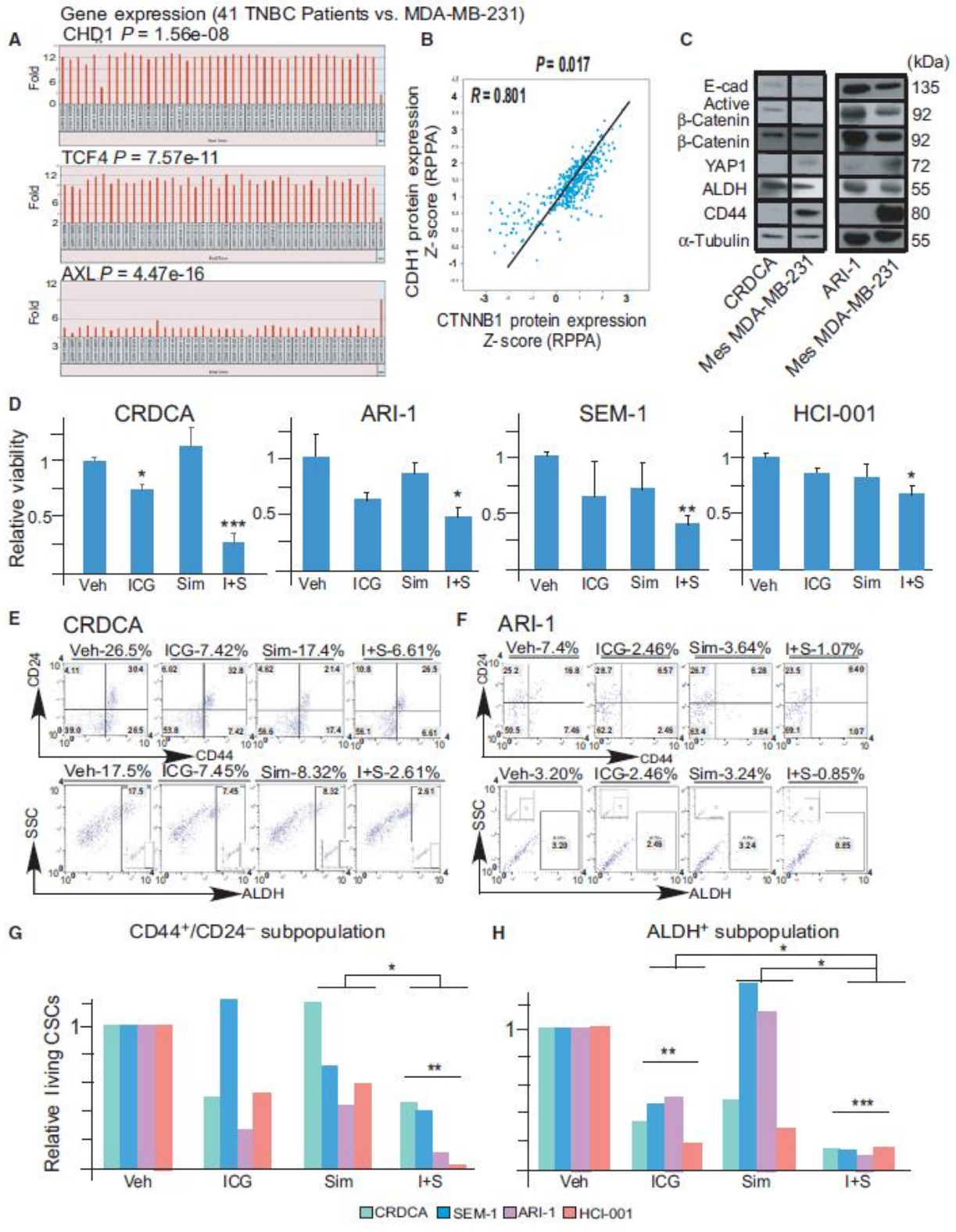
Gene expression (41 TNBC Patients vs. MDA-MB-231)
A
CHD1 P = 1.56e-08
TCF4 P = 7.57e-11
AXL P = 4.47e-16
Fold
B
P= 0.017
R= 0.801
CDH1 protein expression Z-score (RPPA)
CTNNB1 protein expression Z-score (RPPA)
C
(kDa)
E-cad
Active β-Catenin
β-Catenin
YAP1
ALDH
CD44
α-Tubulin
135
92
92
72
55
80
55
CRDCA Mes MDA-MB-231
ARI-1 Mes MDA-MB-231
D
CRDCA
ARI-1
SEM-1
HCI-001
Relative viability
Veh
ICG
Sim
I+S
E
CRDCA
Veh-26.5%
ICG-7.42%
Sim-17.4%
I+S-6.61%
Veh-17.5%
ICG-7.45%
Sim-8.32%
I+S-2.61%
CD24
CD44
SSC
ALDH
F
ARI-1
Veh-7.4%
ICG-2.46%
Sim-3.64%
I+S-1.07%
Veh-3.20%
ICG-2.46%
Sim-3.24%
I+S-0.85%
G
CD44+/CD24− subpopulation
Relative living CSCs
H
ALDH+ subpopulation
CRDCA
SEM-1
ARI-1
HCI-001

Figure 5: Duel inhibition of YAP and Wnt signaling with small molecules effectively inhibits TNBC patients' bulk and CSCs. (A) Wnt and YAP target genes (*TCF4* and *AXL* respectively) and E-cadherin (*CDH1*) was detected in 41 TNBC patient samples and mesenchymal-like MDA-MB-231 cell line using Affymetrix U133 Plus 2.0 transcriptome analysis Chips (n = 41 patients, $*p < 0.05$, $**p < 0.01$, $***p < 0.001$)**. (B)** Positive Pearson correlation between *CDH1* and *CTNNB1* in protein expression (RPPA) in 410 invasive breast cancer patients' samples ($*p < 0.05$). **(C)** Representative western blot depicting β-catenin, YAP, E-cadherin and pluripotency-related proteins (ALDH and CD44) of two patient samples (CRDCA and ARI-1) and mesenchymal-like MDA-MB-231 cell line. See also Figure S6 for additional patient's sample. **(D)** Alamar blue viability analysis of three primary patients' TNBC samples (CRDCA, SEM-1 and ARI-1) and one PDX sample (HCI-001) after 120 hours of exposure to vehicle (DMSO), ICG-001 (2.5 μM) and/or simvastatin (100 nM). **(E-H)** Representative flow cytometric analysis of $CD44^{high}/CD24^{low}$ and ALDH+ CSC subpopulations in patients' sample CRDCA and ARI-1 after 120 hours of exposure to vehicle (DMSO), ICG-001 (2.5 μM) and/or simvastatin (100 nM) (E-F). The relative living $CD44^{high}/CD24^{low}$ and ALDH+ CSCs in all clinical samples are tabulated (G-H). Insets within flow cytometric plots depict DEAB control for ALDH baseline determination. All data in Figure 5 represent means ± SD, n = 3 – 4; $* p < 0.05$, $**p < 0.01$, $*** p<0.001$, in comparison to the indicated groups or vehicle control.

3.6 Dual inhibition of Wnt and YAP signaling is capable of retarding tumor growth and inhibits CSC subpopulations and tumorigenesis *in vivo*.

We next determined the effect of combination treatment *in vivo*. Mesenchymal and epithelial MDA-MB-231 (overexpressing E-cadherin) cells were injected into the mammary fat pad of athymic mice. When tumor reached a mean diameter of 3 mm, mice were randomized into four groups and injected intraperitoneally with vehicle, ICG-001 (100mg/kg/day), simvastatin (5mg/kg/day) or both for 15 days. As expected, the combination treatment reduced tumor burden of both mesenchymal and epithelial TNBC (Figure 6A and 6B). To determine CSC pool *in vivo*, we harvested tumors at the end of the treatment and assessed $CD44^{high}/CD24^{-/low}$ and $ALDH^{+}$ subpopulation using flow cytometry. As shown in Figure 6C and 6D, dual administration of ICG-001 and simvastatin reduced both $CD44^{high}/CD24^{-/low}$ and $ALDH^{+}$ CSC subpopulations in mesenchymal and epithelial-like TNBC respectively, in comparison to vehicle or single drug treatments, suggesting the necessity of dual Wnt and YAP inhibition for suppressing CSC

subpopulations.

To determine whether co-administration of ICG-001 and simvastatin inhibits tumor-initiating potential, we performed secondary transplantation. We serially diluted tumor cells containing various percentage of $CD44^{high}/CD24^{-/low}$ and $ALDH^{+}$ subpopulations isolated from the primary tumors, and transplanted them into athymic nude mice without further treatment for 6 weeks. Tumor cells isolated from mice receiving both ICG-001 and simvastatin exhibited the least tumor-initiating capacity in comparison to single treatments and a vehicle control (Figure 6E). Thus, dual inhibition of Wnt and YAP signaling can reduce tumor burden but more importantly, it suppresses CSCs and attenuates tumorigenesis in mesenchymal and epithelial TNBC after secondary transplantation.

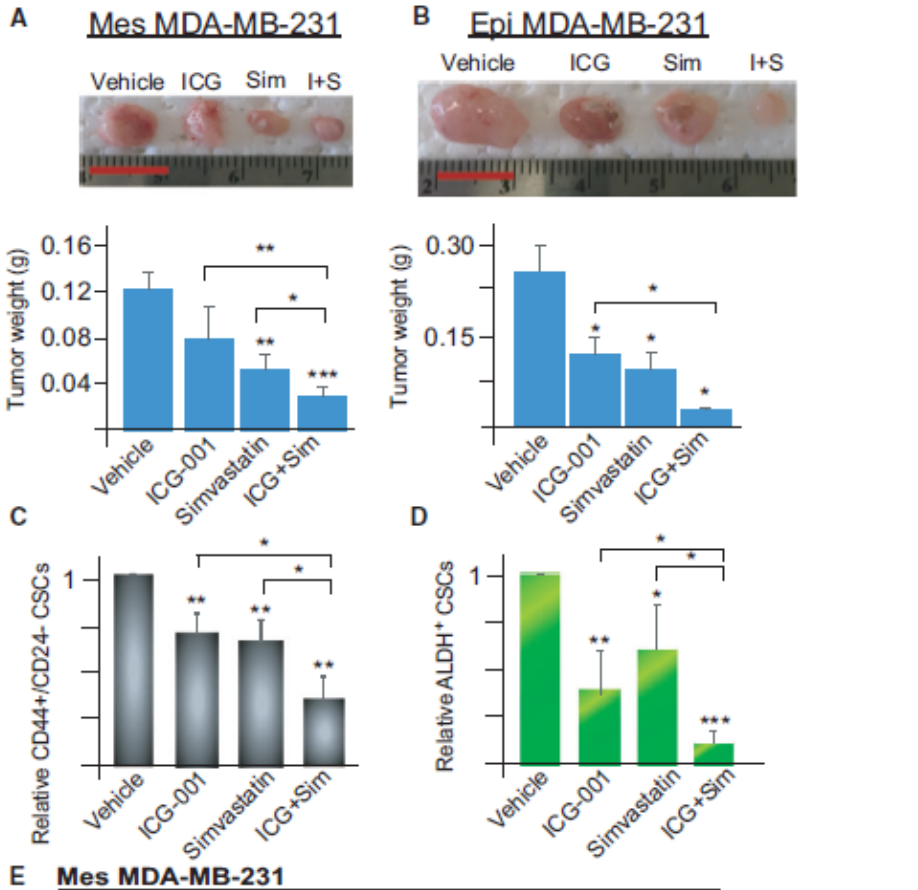

E

Mes MDA-MB-231

	1×10^5	1×10^4	1×10^3	1×10^2
Vehicle	3/3	1/3	1/3	0/3
ICG-001	1/3	0/3	0/3	0/3
Simvastatin	2/3	1/3	1/3	0/3
I+S	0/3*	0/3	0/3	0/3

Epi MDA-MB-231

	1×10^5	1×10^4	1×10^3	1×10^2
Vehicle	3/3	2/3	0/3	0/3
ICG-001	1/3	1/3	0/3	0/3
Simvastatin	2/3	1/3	0/3	0/3
I+S	1/3	0/3	0/3	0/3

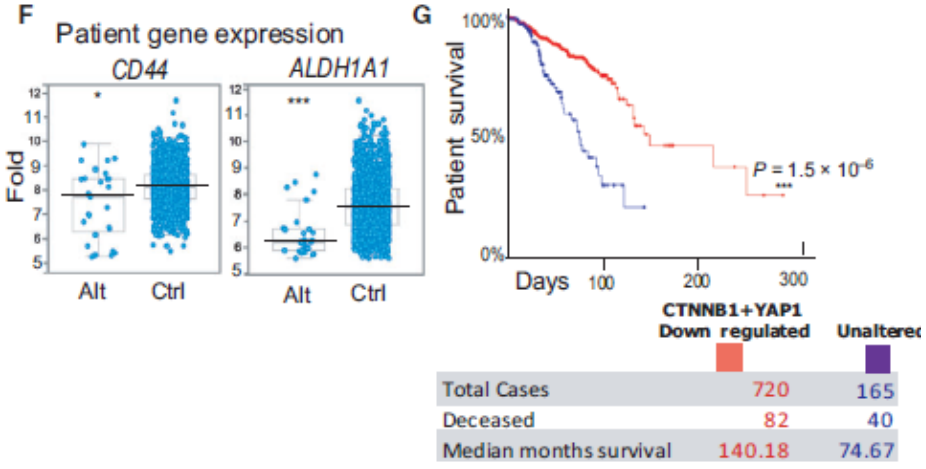

Figure 6. Combination therapy with YAP and Wnt small molecule inhibitors effectively retards tumor growth and reduces CSC enrichment and tumorigenesis in vivo; low expression of CTNNB1 and YAP1 genes correlates with low expression of CD44+ and ALDH1A1+ genes in patients' tumor samples while inversely correlates with improved survival in breast cancer patients. (A-B) Mesenchymal-like (Mes) and epithelial-like (Epi) MDA-MB-231 TNBC cells were injected into the mammary fat pads of athymic nude mice. When the tumors reached a mean diameter of 3mm, mice were separated into 4 groups and intraperitoneally injected daily with the vehicle (DMSO), ICG-001 (100 mg/g/day), simvastatin (5 mg/g/day) and ICG-001 + Simvastatin for 15 days. After conclusion of treatments, tumors were harvested from the mice, photographed and weighed. Data represent means ± SD; n = 4 mice for each group; *$p < 0.05$, **$p < 0.01$. Scale bar = 1 cm. **(C-D)** Flow cytometric analysis of the living $CD44^{high}/CD24^{low}$ and ALDH+ CSC subpopulations of dissociated mesenchymal-like (Mes) and epithelial-like (Epi) tumors after 15 days of treatment with vehicle (DMSO), ICG-001 and/or simvastatin. Insets within flow cytometric plots depict DEAB control for ALDH baseline determination. Data represent means ± SD; n = 4 mice for each group; *$p < 0.05$, **$p < 0.01$, in comparison to the indicated groups or vehicle control. **(E)** Mesenchymal-like (Mes) and epithelial-like (Epi) MDA-MB-231 xenografts were dissociated into single cell suspension and re-transplanted into the mammary fat pads of new nude mice in serial limiting dilutions (10^5, 10^4, 10^3, or 10^2 cells per injection). Tumor formation was observed for 6 weeks. **(F)** Low levels of *CTNNB1* (a pivotal effector of the canonical Wnt signaling pathway) and *YAP1* (YAP signaling) gene expression in breast cancer patients' samples (Alt) correlates with low levels of *CD44* and *ALDH1A1* gene expression in comparison to those patients' samples without showing the reduced expression of *CTNNB1* and *YAP1* genes (Ctrl). N = 2509 patients with invasive breast cancer, *$p < 0.05$, ***$p < 0.001$. **(G)** Kaplan-Meier curves for overall survival of the patients with low levels of CTNNB1 (Wnt) and YAP1 (YAP) protein expression in cancer samples (red curve) in comparison to those patients with unaltered expression (blue curve). N = 887, ***$p < 0.001$, log-rank test.

3.7 Low expression of *CTNNB1* and *YAP1* genes correlate with low expression of CD44+ and ALDH1A1+ genes and improved survival in breast cancer patients.

Analysis of a database containing gene expression of 2509 breast cancer patients using cBioportal (Cerami *et al.*, 2012; Gao *et al.*, 2013; Pereira *et al.*, 2016) showed that, in breast tumor samples, decreased gene expressions of *CTNNB1* (a pivotal effector of the canonical Wnt signaling pathway) and *YAP1* (YAP) were accompanied with reduced gene expressions of *CD44* and *ALDH1A1* that are associated with mesenchymal and epithelial CSC phenotypes (Figure 6F). In addition, analysis of a dataset of 887 patients with invasive breast carcinoma showed that co-reduction of CTNNB1 (Wnt) and YAP1 (YAP) protein expression, was correlated with improved

patients' survival (Figure 6G, median survival of 140.18 months *versus* 74.67 months in the unaltered control). Those with either reduced expression of CTNNB1 or YAP1 protein alone showed only a moderate increase in survival (32.66 months by CTNNB1 and 9.53 months by YAP1) in comparison to the unaltered control (Figure S7).

4. Discussion

Epithelial-mesenchymal plasticity and CSCs are key challenges for effective cancer treatment. In this study, we observed that dynamic changes in Wnt and YAP signaling and CSC phenotypes are dependent on epithelial or mesenchymal states. YAP is upregulated in mesenchymal TNBC cells while Wnt upregulated in epithelial TNBC cells. These observations are clearly supported within the TNBC literature. The intracellular domain of E-cadherin has been shown to mediate YAP nuclear exclusion and β-catenin activity (Benham-Pyle *et al.*, 2015). Additionally, α-catenin and 14-3-3 proteins are known to associate with YAP and prevent its de-phosphorylation via PP2A under the upstream control of E-cadherin (Schlegelmilch *et al.*, 2011).

Importantly, we found that mesenchymal and epithelial TNBC cells exhibited different responses to Wnt and YAP inhibition. Knockdown of Wnt/β-catenin upregulated YAP target genes in mesenchymal-like TNBC cells, which is consistent with a recent report showing that inhibition of Wnt/β-catenin signaling facilitates YAP/TAZ-overexpression induced liver growth and tumor initiation (Kim *et al.*, 2017). We also found Wnt/β-catenin knockdown was more effective in suppressing ALDH+ CSCs in an epithelial state than in suppressing $CD44^{high}/CD24^{-/low}$ CSCs in a mesenchymal state. In contrast, YAP knockdown enriched ALDH+ CSCs in epithelial-like TNBC cells although it potently inhibited $CD44^{high}/CD24^{-/low}$ in mesenchymal-like TNBC cells. These observations suggest that inconsistent results reported in breast cancer cells in response to Wnt or YAP inhibition (Anastas and Moon, 2013; Green *et al.*, 2013; Maugeri-Saccà and De Maria, 2016)

may be associated with ineffective CSC targeting due to epithelial and/or mesenchymal states, TNBC EMT/MET plasticity, and YAP and Wnt feedbacks. Dual inhibition of YAP and Wnt signaling on the other hand, can suppress both epithelial- and mesenchymal-like bulk and CSC populations without significantly affecting cultured normal mammary tissue fragments *in vitro* and mice *in vivo*, suggesting a favorable approach for this combination therapy. This was supported by the alternations of $CD44^{high}/CD24^{-/low}$ and ALDH+ CSC subpopulations in both MDA-MB-231 and SUM149-PT cell lines, although the changes in SUM149-PT cells after siRNA knockdown of E-cadherin (which induces a mesenchymal-like phenotype) were not as robust as seen in mesenchymal MDA-MB-231 cells. This may be associated with incomplete siRNA silence, recovery of E-cadherin after knockdown and/or experimental timing.

We also observed that knockdown of YAP or usage of simvastatin suppressed Wnt signaling. The suppressed Wnt signaling may be associated with the formation of YAP, β-catenin and TBX5 complex that is essential for transformation and survival of β-catenin-driven cancers (Rosenbluh *et al.*, 2012). At present, it is unclear why such an effect is significant in mesenchymal but less in epithelial TNBC cells, warranting further investigations. Nevertheless, since epithelial and mesenchymal cancer cells are interconvertible, simultaneously targeting YAP and Wnt signaling should be taken into consideration in future TNBC treatment.

Administration of ICG-001 and simvastatin was clinically relevant; both are FDA-approved drugs for clinical applications with defined pharmacological dynamics/kinetics, and have the potential to be readily repurposed in this clinical indication. ICG-001/PRI-724 is a fairly specific Wnt inhibitor and is used for the treatment of acute and chronic myeloid leukemia (NCT01606579). Simvastatin is an inhibitor of HMG-CoA reductase and widely employed as a cholesterol-lowering drug. In addition, simvastatin has been reported to affect wide plethora of

targets including YAP, RhoA, Ras, Akt, mTOR, and JAK2/STAT3 (Wang *et al.*, 2016b; Wu and Liu, 2008; Zhang *et al.*, 2013c). We have observed that ICG-001 inhibits TNBC Wnt signaling, and simvastatin suppresses YAP signaling although other off-target effects coexist. Since ICG-001 and simvastatin exhibited effects resembling YAP1 and β-catenin knockdown in TNBC cells, it is likely that the biological changes observed in this study are associated with Wnt and YAP inhibitions. This study identifies different expressions of CSC phenotypes and cellular responses to YAP and Wnt targeting associated with mesenchymal or epithelial state. Through dual inhibition of Wnt and YAP signaling, both epithelial and mesenchymal CSC subpopulations can be inhibited and tumorigenesis can be halted after secondary transplantation, which may reduce TNBC recurrence. Since simvastatin is commonly prescribed and ICG-001/PRI-724 has been approved by FDA for clinical trial evaluation, further investigation of this combination and other Wnt and YAP inhibitors may lead to an effective therapy with reduced toxicity and attenuated CSC enrichment as compared to conventional chemotherapy.

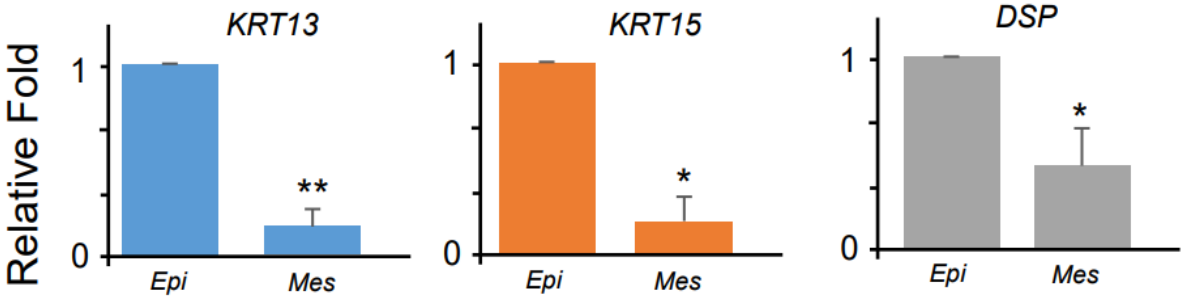

Supplemental Figure 1: Overexpression of E-cadherin in mesenchymal-like MDA-MB-231 TNBC cells resulted in an epithelial-like phenotype. RT-qPCR analysis of epithelial genes *KRT13* (Keratin 13), *KRT15* (Keratin 15) and *DSP* (Desmoplakin) in epithelial-like (Epi) MDA-MB-231 and mesenchymal-like (Mes) cells. Data represent means ± SE, n = 3 for all figures; * $p < 0.05$, ** $p < 0.01$.

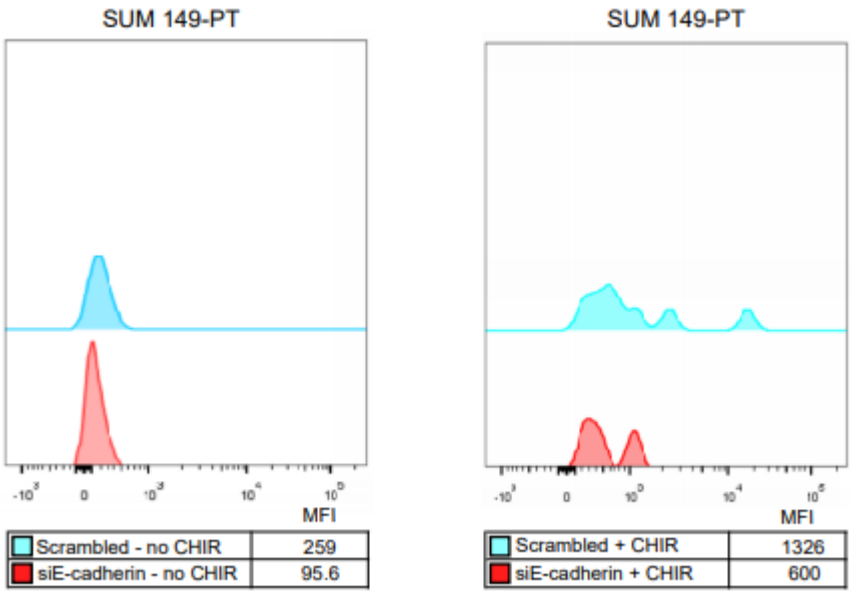

Supplemental Figure 2: 7xTCF-eGFP Wnt reporter activity upon E-cadherin knockdown in SUM 149-PT cells. Representative flow cytometric analysis of 7xTCF-eGFP Wnt reporter activity (MFI: median fluorescent intensity) in SUM 149-PT cells 48 hours after siRNA knockdown of E-cadherin. Cells were exposed to vehicle (left panel) or 3µM CHIR99021 (a GSK3 inhibitor activating Wnt signaling, right panel).

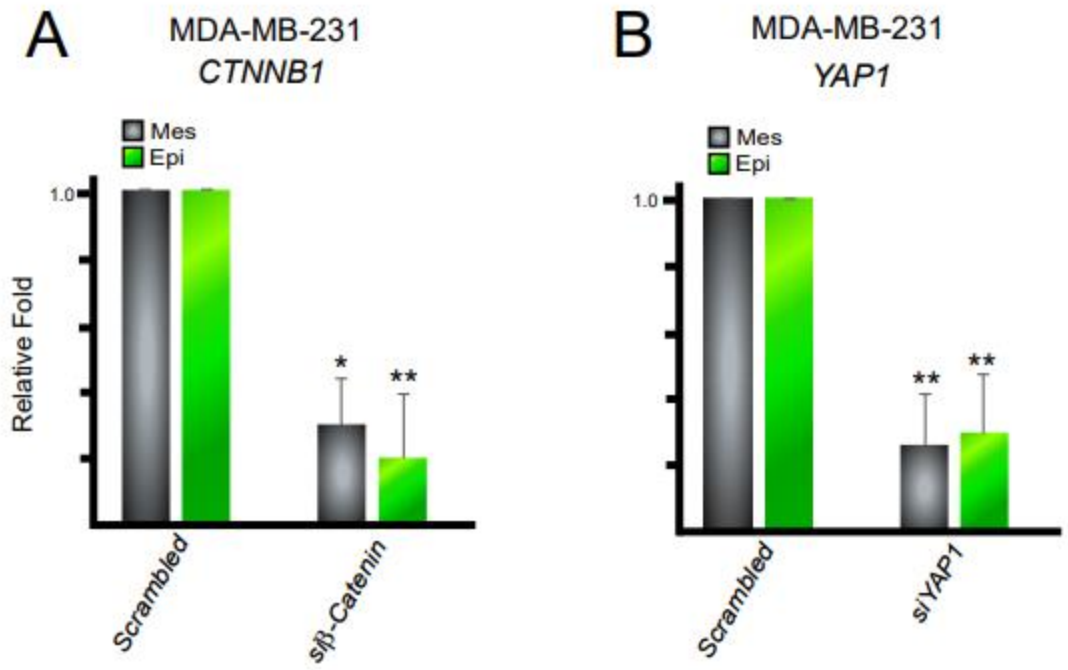

Supplemental Figure 3: CTNNB1 and YAP1 knockdown efficacy in mesenchymal-like (Ctrl) and epithelial-like (E-cad+) MDA-MB-231 TNBC cells.(A-B) RT-qPCR analysis of *CTNNB1* and *YAP1* 48 hours after siRNA knockdown of β-catenin and YAP1 in mesenchymal-like (Mes) or epithetical-like (Epi) MDA-MB-231 cells. Data represent means ± SE, n = 3 for all figures; * $p < 0.05$, ** $p < 0.01$.

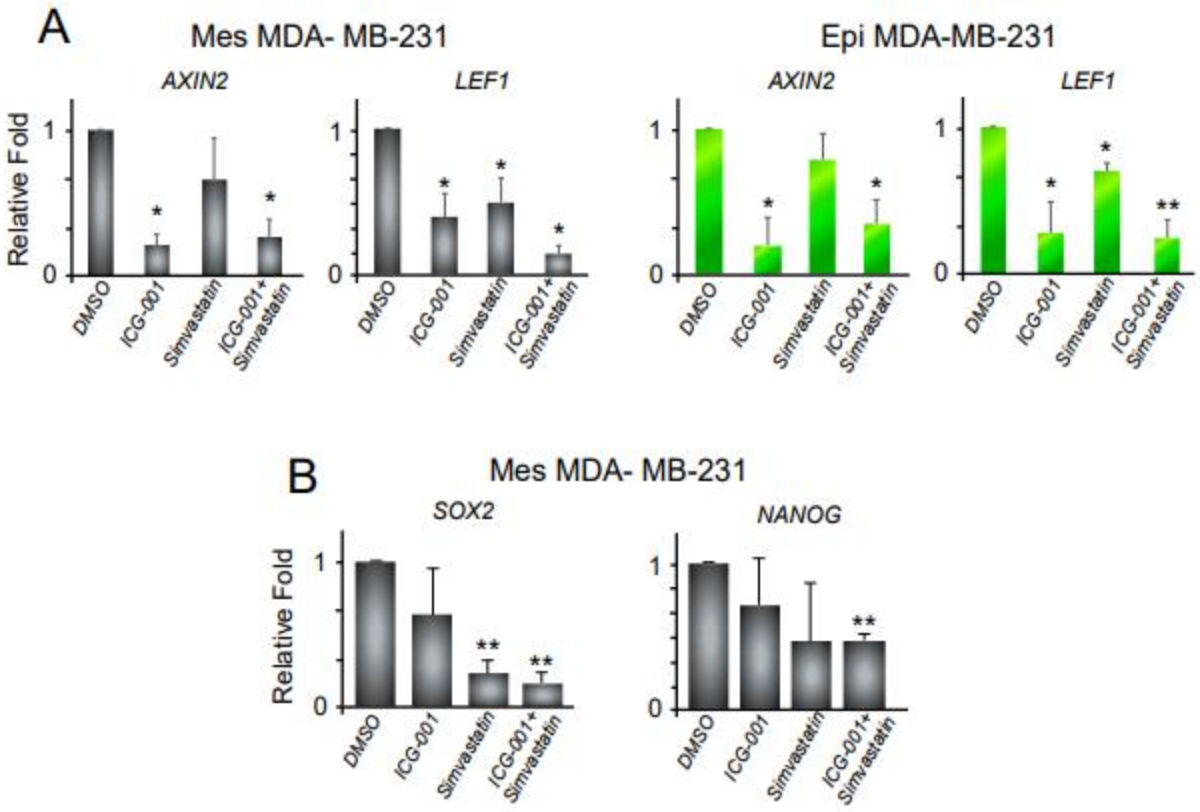

Supplemental Figure 4: Suppression of Wnt and pluripotency-related genes after treatment with ICG-001 and simvastatin in mesenchymal-like (Mes) and epithelial-like (Epi) MDA-MB-231 TNBC cells. (A) RT-qPCR analysis of Wnt genes *AXIN2* and *LEF1* 48 hours after treatment with vehicle (DMSO), ICG-001 (2.5 µM) and/or simvastatin (100 nM) in mesenchymal-like (Mes) and epithelial-like (Epi) MDA-MB-231 cells. **(B)** RT-qPCR analysis of pluripotent genes *SOX2* and *NANOG*, 48 hours after treatment with vehicle (DMSO), ICG-001 (2.5 µM) and/or simvastatin (100 nM) in mesenchymal-like (Mes) and epithelial-like (Epi) MDA-MB-231 cells. Data represent means ± SE, n = 3 for all figures; * $p < 0.05$, ** $p < 0.01$.

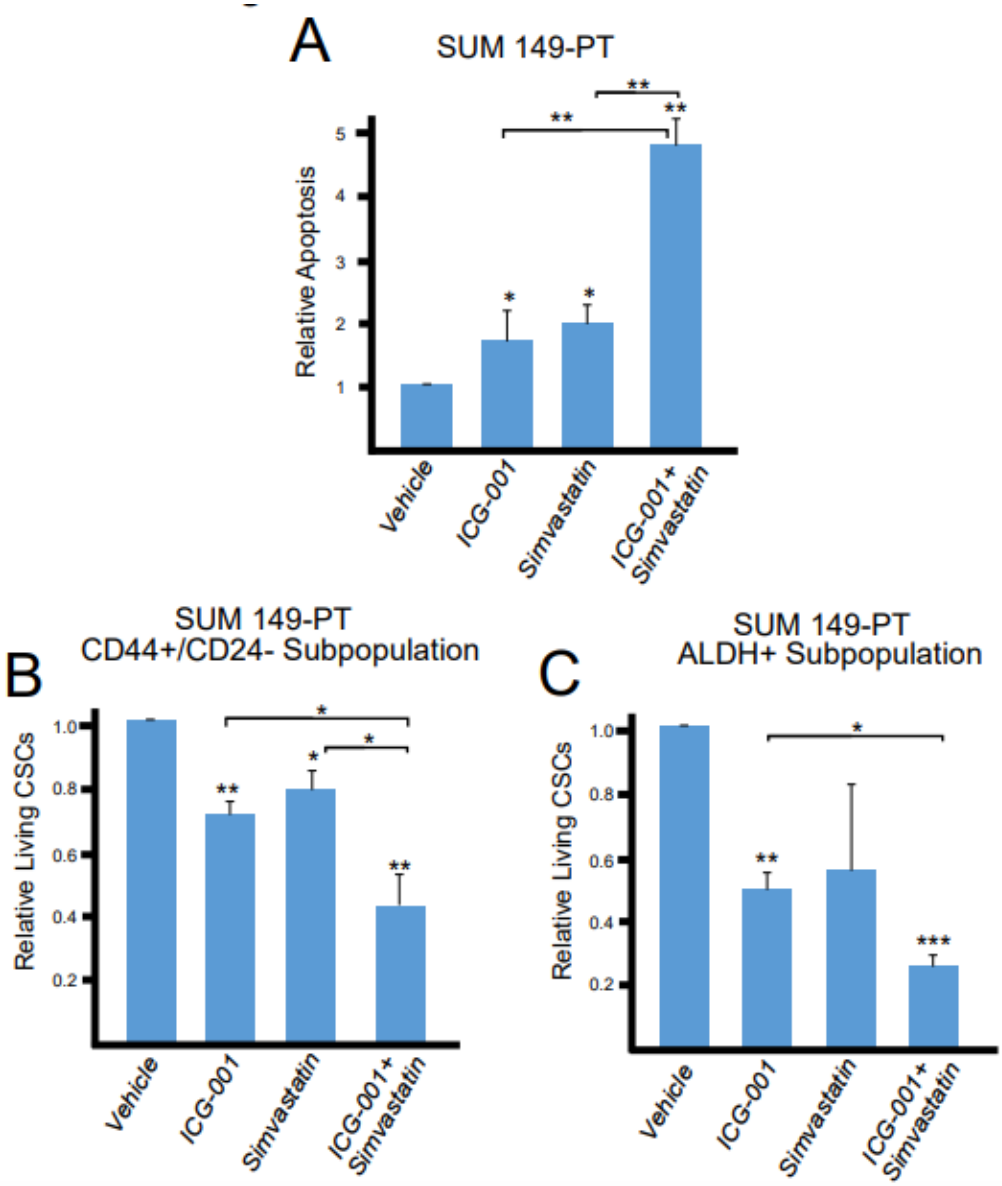

Supplemental Figure 5: Dual inhibition of YAP and Wnt signaling suppresses both mesenchymal and epithelial-like bulk and CSC populations in epithelial-like SUM149-PT TNBC cells. (A) Flow cytometry analysis of apoptosis (Annexin V+/7AAD+) of SUM149-PT cells after 120 hours of exposure to vehicle (DMSO), ICG-001 (2.5 µM) and/or simvastatin (100 nM). **(B-C)** Flow cytometric analysis of $CD44^{high}/CD24^{low}$ and ALDH+ CSCs after 120 hours of exposure to ICG-001 (2.5 µM) and simvastatin (100 nM) in SUM149-PT cells. Data represent means ± SD, n = 3 for all figures; * $p < 0.05$, ** $p < 0.01$, *** $p<0.001$.

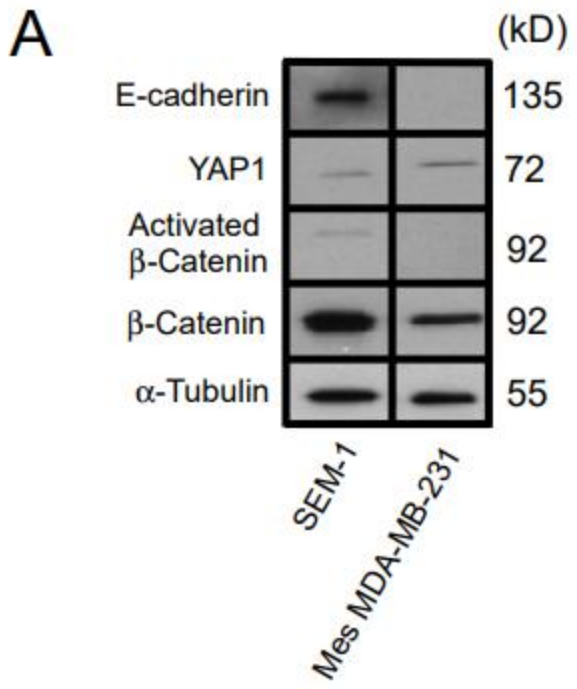

Supplemental Figure 6: Western blot analysis of patient TNBC tumor fragment in comparison to MDA-MB-231 cell line (A) Representative western blot depicting β-catenin, YAP and E-cadherin expression in patient tumor samples (SEM-1) and the mesenchymal-like MDA MB-231 cell line.

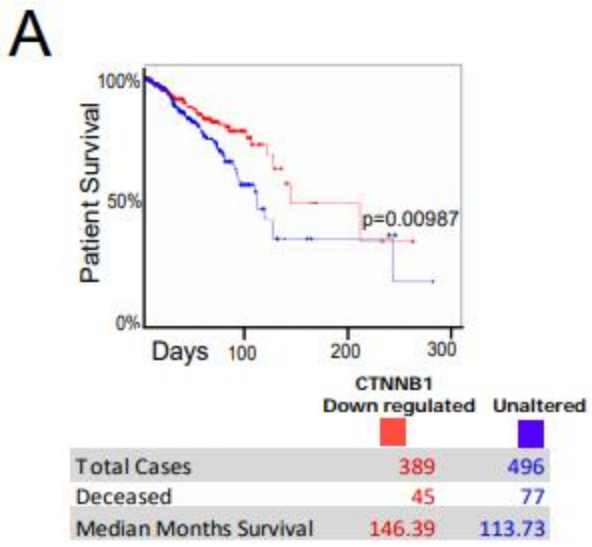

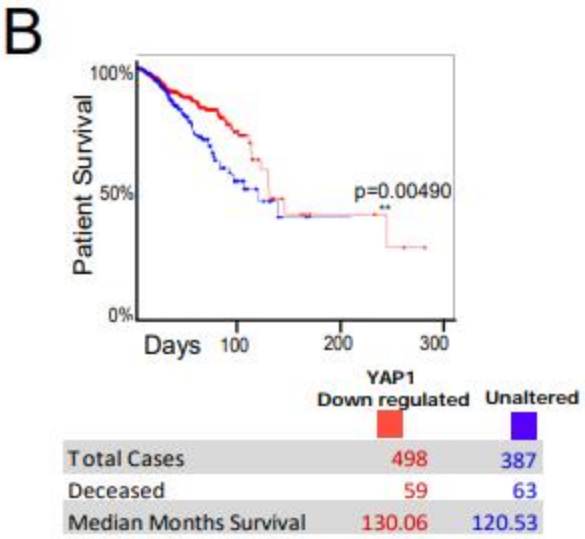

Supplemental Figure 7: Kaplan-Meier curves for overall survival of the patients with low levels of Wnt (CTNNB1) or YAP (YAP1) protein expression in cancer samples (A-B) Kaplan-Meier curves for overall survival of the patients with low levels of CTNNB1 (Wnt) or YAP1 (YAP) protein expression in cancer samples (red curve) in comparison to those patients with unaltered expression (blue curve, n = 885, $^{**}p < 0.01$, log-rank test).

Chapter 5: Co-Targeting Bulk Tumor and CSCs in Clinically Translatable TNBC Patient-Derived Xenografts via Combination Nanotherapy

Preface

The following Chapter consists of a research article for which I am the primary author. The article was submitted to Molecular Cancer Therapeutics.

Andrew Sulaiman, Sarah McGarry, Sara El-Sahli, Li Li, Jason Chambers, Alexandra Phan, Marceline Côté, Greg O. Cron, Tommy Alain, Yevgeniya Le, Seung-Hwan Lee, Sheng Liu, Daniel Figeys, Suresh Gadde and Lisheng Wang. Co-Targeting Bulk Tumor and CSCs in Clinically Translatable TNBC Patient-Derived Xenografts via Combination Nanotherapy. *Molecular Cancer Therapeutics* (2018, Submitted)

AS, LW and SG conceived and designed the study. AS preformed data analysis and FACS. AS, SM, SE, LL, JC and AP performed the *in vitro* experiments. AS and SM performed the *in vivo* experiments. AS preformed *in vivo* serial dilution, MRI analysis (with GC), IVIS, Quantum Dot experiments. AS analyzed the data. AS drafted the manuscript and created the figures. SG and AP prepared reagents and nanoparticles. LW, AS, SM and SG edited the manuscript. MC, GC, TA, YL, S-HL, SL, DF and SG provided valuable suggestions and assisted in troubleshooting the experiments. SL provided supplemental figures 1-3. All authors approved the final version of the manuscript.

Abstract

Triple negative breast cancer (TNBC) accounts disproportionally for the majority of breast cancer related deaths throughout the world. This is largely attributed to lack of a specific therapy capable of targeting both bulk tumor mass and cancer stem cells (CSC) as well as appropriate animal models to accurately evaluate treatment efficacy for clinical translation. Thus, development of effective and clinically translatable targeted therapies for TNBC is an unmet medical need. We developed a hybrid nanoparticles-based co-delivery platform containing both paclitaxel and verteporfin (PV-NPs) to target TNBC patient-derived xenograft (PDX) tumor and CSCs. MRI and IVIS imaging were performed on mice containing PDX tumors to assess tumor vascularity and accumulation of NPs. NF-kB, Wnt and YAP activities were measured by reporter assays. Mice bearing TNBC PDX tumor were treated with PV-NPs and controls, and tumors progression and CSC subpopulations were analyzed. MRI imaging indicated high vascularization of PDX tumors. IVIS imaging showed accumulation of NPs in PDX tumors. In comparison to control-NPs and free-drug combination, PV-NPs significantly retarded tumor growth of TNBC PDX. PV-NPs simultaneously repressed NF-kB, Wnt and YAP signaling, each of which have been shown to be crucial for cancer growth, CSC development and tumorigenesis. In conclusion, NPs containing two clinically used drugs concurrently inhibited NF-kB, Wnt and YAP pathways and exhibited synergic effects on killing TNBC bulk tumor and CSCs. This combination nanotherapy evaluated with a PDX model may lead to an effective treatment of TNBC patients.

1.0 Introduction

Breast cancer remains a leading cause of death in women worldwide (Siegel *et al.*, 2016). Amongst the various breast cancer sub-types, triple negative breast cancer (TNBC, a highly

heterogeneous disease) accounts for only one fifth of all breast cancers, but disproportionally accounts for the majority of breast cancer-related deaths. Relapse has been closely associated with CSCs and is a major challenge in TNBC wherein approximately one third of patients will experience a distant recurrence within 2.6 years (Dent *et al.*, 2007). In contrast to other breast cancer sub-types, due to lack of specific targets, conventional chemotherapy is still the clinical standard treatment for TNBC. However, chemotherapy has been shown to promote CSC enrichment after treatment (Jia *et al.*, 2017).

In TNBC, CSCs have been found to coexist in two distinct but interconvertible subtypes: epithelial ALDH+ and mesenchymal CD44+/CD24- subpopulations that are closely associated with chemoresistance, tumor regrowth, and disease relapse (Liu *et al.*, 2014; Sulaiman *et al.*, 2016; Sulaiman *et al.*, 2017b). A recent study revealed that YAP signaling was highly activated in mesenchymal CSCs while Wnt signaling in epithelial CSCs (Sulaiman *et al.*, 2018b). In addition, it has been found that NF-kB (nuclear factor-κB), an essential mediator of the inflammatory response, is a potent signaling modulator in tumor cells and tumor microenvironment. NF-kB stimulates Wnt and other signaling pathways and facilitates the survival of both bulk and CSC populations (Taniguchi and Karin, 2018; Wang *et al.*, 2018). As such, repression of NF-kB signaling has been considered as one of the most effective approaches in cancer treatment (Taniguchi and Karin, 2018; Wang *et al.*, 2018). We thus hypothesize that therapeutic strategies capable of effectively delivering drugs into tumor to co-inhibit NF-kB, Wnt and YAP signals and evaluating therapeutic efficacy with a clinically translatable model may lead to the effective treatment of TNBC.

Cancer nanomedicines overcome the intrinsic limits of drug delivery and conventional cancer therapies through their uniquely appealing features, such as improved blood circulation,

increased tumor accumulation, reduced off-target toxicities, leading to a higher therapeutic index (Gadde, 2015; Shi *et al.*, 2017). However, in preclinical cancer research, the therapeutic efficacy of drugs and formulated in NPs is assessed by using cancer cell line-based animal models that do not represent the heterogeneity and complexity of patients' primary tumors. Even though cell lines originate from patient's tumors, due to artificial tissue culture conditions, they have adapted for adherence/growth in a monoculture, leading to uniformity in cells and loss of heterogeneity. Most of the cancer cell lines used in preclinical research are genetically and epigenetically divergent from their starting source and real tumors (Miller *et al.*, 2017; Sulaiman and Wang, 2017). This agglomeration may culminate with artifact discoveries and clinical trial failures for the therapeutic agents including cancer nanomedicines (Miller *et al.*, 2017; Sulaiman and Wang, 2017). In contrast, PDX (Patient Derived Xenograft) tumors are obtained from patient and engrafted directly into immunocompromised mice, bypassing extensively *in vitro* selection. As such, PDX tumors retain the original patient's tumor heterogeneity, three-dimensional architecture and microenvironment representing the tumors biology, and resulting in a 92% concordance with patient tumors (Lum *et al.*, 2012).

In this report, we developed a co-delivery NPs containing the conventional chemotherapeutic agent paclitaxel in combination with an FDA-approved porphyrinic photosensitizer, verteporfin (PV-NPs). Paclitaxel is a routinely prescribed chemotherapeutic for the treatment of TNBC. It inhibits the mitotic spindle apparatus, preventing cancer cell division. However, resistance to paclitaxel is common in the clinic. Although the mechanism behind this phenomenon is still under investigation, paclitaxel-induced CSC enrichment has been demonstrated to be one of key players for drug resistance and disease relapse (Jia *et al.*, 2016b; Yu *et al.*, 2007). Verteporfin is a FDA-approved photosensitizer for photodynamic therapy to

eliminate the abnormal blood vessels in the eye such as macular degeneration (Arnold *et al.*, 2001). Verteporfin has been reported to possess potent anti-cancerous activity in pancreatic and breast cancer patients (Huggett *et al.*, 2014; Isakoff *et al.*, 2017b), and is currently in a clinical trial for the treatment of breast cancer (NCT02939274). However, paclitaxel resistance, CSC enrichment, and drug delivery to tumors remain challenges in cancer treatment. Here, we provided the first demonstration that PV-NPs accumulate within TNBC PDX tumors and potently inhibit both bulk tumor mass and CSC populations. Furthermore, we showed that PV-NPs suppressed NF-kB, Wnt and YAP pathways that are crucial for cancer growth, CSC development and tumorigenesis. These findings suggest that development of nanoparticle platforms encapsulated with specific drugs to promote synergetic inhibition of bulk tumor and CSCs is an effective and translatable approach for TNBC treatment.

2.0 Materials and Methods

2.1 Cell culture and reagents

MDA-MB-231 breast cancer cells were purchased from the American Type Culture Collection (ATCC, Manassas, VA, USA) and maintained in DMEM-F12 media supplemented with 10% Fetal bovine serum (FBS, HyClone, Logan, UT, USA) and 1% penicillin/streptomycin. Cells were cultured at 37°C in a 5% CO2 incubator. Verteporfin was purchased from CalBiotech (El Cajon, CA, USA), and paclitaxel from Cedarlane (Burlinton, ON, Canada). PLGA was purchased from LACTEL polymers, Lecithin from Alfa Aesar, and DSPE-PEG_{2K} from Avanti Lipids. Alexa Fluor 750 and Qdot800 were purchased from Thermo Fisher. ACN, dry DMF, and acetone were purchased from Fisher Chemicals.

Synthesis and Characterization of NPs

Lipid-polymer hybrid NPs were synthesized via previously reported nanoprecipitation method (Zhang *et al.*, 2008). Briefly, lecithin and DSPE-PEG_{2K} in molar ratio of 6.5:1 were dissolved in 4% ethanol aqueous solution (0.02% w/v) and heated for 2-4 mins at 68 ^{o}C under gentle stirring. After heating, PLGA (poly lactic co-glycolic acid) and appropriate drugs (10: 1 w/w ratio) in either acetonitrile (ACN) or acetone (1-2 mg/ml) were added dropwise at 0.6ml/min rate and stirred at room temp to form self-assembly of hybrid NPs. NPs were concentrated, and purified by centrifugal filters and analyzed by ZetaView, Malvern Zetasizer (DLS) and TEM. Stability of NPs in biologically relevant conditions were tested according to literature procedure (Marrache and Dhar, 2012). The amount of paclitaxel encapsulated in NPs is analyzed using HPLC at 204 nm, with H_2O:ACN mobile phase with 5-90% ACN gradient. The amount of verteporfin encapsulated in NPs is quantified by Nanodrop at 430nm absorbance. Drug release profiles were performed using published procedures (Abouelmagd *et al.*, 2015).

PLGA-Qdot800 conjugate was synthesized according to previously reported literature procedure (Marrache and Dhar, 2012). PLGA-Alexa750 conjugate was synthesized via ester coupling by reacting amine end group of PLGA with Alexa Fluor 750 NHS ester.

2.2 DAPI staining and fluorescence microscopy

MDA-MB-231 cells cultured on glass coverslips were treated with nanoparticle-Bodipy FL for 3 hours. After being fixed with 4% paraformaldehyde and stained with 100 ng/ml of DNA-specific fluorophore DAPI for one hour at room temperature, the coverslips were mounted on a glass slide for fluorescence microscopy. Fluorescence images were obtained by using a Leica

AF6000 deconvolution microscope system equipped with a fully automated microscope (DMI6000B) and a DFC350 FX digital camera (Leica Microsystems, Heidelberg, Germany). Fluorescence images were acquired under the identical exposure time and instrument settings among different groups, and analyzed using Leica LAS AF6000 software.

2.3 Flow cytometry analysis

Cancer cells or PDX tumor cells were dissociated and filtered through a 40 μm strainer and suspended in PBS supplemented with 2% FBS and 2mM EDTA. 1μL of mouse IgG (1mg/mL) was then added and incubated at 4^{o} C for 10 minutes. Afterwards, the cells were resuspended in 1× binding buffer (eBioscience, San Diego, CA, USA) and cell apoptosis was determined using Annexin-V-V450 Apoptosis Detection Kit (BD Bioscience). Afterwards, cells were incubated with the different reagents as described below at 4^{o} C for 30 minutes in ALDEFLUOR™ Assay Buffer. Anti-CD44 (APC) and anti-CD24 (PE) (BD Pharmingen) antibodies were added according to the manufacturer's instructions as previously described (Sulaiman *et al.,* 2016). ALDH activity was determined using ALDEFLUOR (Stem-cell Technologies, Vancouver) with a DEAB control according to the manufacturer's instructions. Lastly, cells were washed twice and 7-aminoactinomycin D (7-AAD, eBioscience, San Diego, CA) was added to exclude dead cells. Flow cytometry was performed on the BD LSRFortessa. Data was analyzed with FlowJo software (Ashland, OR, USA). To analyze cell uptake of nanoparticle in different organs *versus* TNBC PDX tumors, mice were injected Qdot800 conjugated lipid-hybrid nanoparticles 3 hours before euthanization. Different organs and TNBC PDX tumors were harvested, dissociated into single cell suspensions, and washed three times with PBS before analysis with the BD LSRFortessa. FlowJo software was used for data analysis.

2.4 Cell viability assays

Cells were seeded into 12 well plates (1.5×10^4 cells/well). After 120 hours of treatment, viability analysis was performed by incubation with 3-(4,5-dimethylthiazol-2-yl)-2,5-diphenyl tetrazolium bromide (MTT, 1 mg/ml) for 4 hours. Absorbance was measured at 570nm.

HCI-002 PDX TNBC tumor fragments were incubated in 24 well plates (i.e. organotypic slice culture). After 120 hours of treatment, alamar blue viability assay was preformed via incubation with 10% alamar blue solution (Thermo Fisher Scientific) for 4 hours, followed by measurement of florescence at 560nm excitation and 590nm emission as previously performed (Sulaiman *et al.*, 2018a).

2.5 Luciferase Assay

MDA-MB-231 TNBC cells were seeded into 12-well plates and transfected with 1000 ng of a NF-kB reporter p1242 3x-KB-L (Addgene Plasmid #26699, a gift from Dr. Bill Sugden) (Mitchell and Sugden, 1995), or YAP reporter 8xGTIIC-luciferase (Addgene Plasmid #34615, a gift from Dr. Stefano Piccolo) (Dupont *et al.*, 2011) or Wnt reporter M50 Super 8x TOPFlash (Addgene Plasmid #12456, a gift from Dr. Randall Moon) (Veeman *et al.*, 2003) constructs in conjunction with 1000 ng Renilla pRL-SV40P (Addgene Plasmid #27163, a gift from Dr. Ron Prywes) (Chen and Prywes, 1999) construct using Lipofectamine 2000 (Invitrogen) according to the manufacturer's instructions. After 18 hours, cells were treated with either empty (vehicle) lipid-hybrid nanoparticles or lipid hybrid nanoparticles with paclitaxel (10nM), verteporfin (500nM) or both for 24 hours, after which cells were lysed and both Firefly and Renilla luciferase activity was quantified using a Dual-Luciferase® Reporter Assay System (Promega) following the manufacturer's instructions.

2.6 Xenograft tumor growth

All protocols described throughout this manuscript regarding animal studies were performed in strict pathogen free conditions and in accordance with ethical guidelines as approved by The Ottawa Hospital Research Ethics Board (Protocol# 20120559-01H). TNBC PDX HCI-002 tumor chunks (2mm × 4 mm) were transplanted into the mammary fat pad of athmyic nude mice (purchased from Charles River). After the tumors reached a mean diameter of 3 mm, drug treatment was initiated. Mice were randomly divided into three groups and treated with either vehicle (empty) lipid-polymer hybrid nanoparticles, free drugs (1mg/kg of paclitaxel and 9 mg/kg of verteporfin), or PV-NPs loaded with 0.5mg/kg of paclitaxel and 3.2mg/kg of verteporfin every other day for 20 days (n=5 mice for each group). Tumor growth was monitored every other day using a caliper and tumor volume was determined using the formula: V=1/2(Tumor Length x Tumor Width^2). After the completion of the treatment, mice were humanly euthanized and tumors were weighed and photographed. For flow cytometry analysis, tumors were mechanically minced and then enzymatically digested into single cell suspension using 1x Collagenase/Hyaluronidase in DMEM (Stemcell Technologies).

2.7 IVIS Analysis

Athymic mice were injected via tail vein with lipid-polymer hybrid nanoparticles conjugated with Alexa fluor750. The fluorescence of Alexa fluor750 was measured at 3, 6 and 24 hours using the Perkin Elmer IVIS Spectrum In Vivo Imaging System.

2.8 MRI Analysis

To determine TNBC PDX vascularity for potential nanoparticle delivery, whole body T1-

weighted MRI was conducted using a small-animal MRI machine (7T GE/Agilent MR901). After the first scanning, athymic mice were retrieved and injected with Gadovist via tail vein at a concentration of 0.1 mmol/kg (Bayer). Immediately after injection, the mice were re-scanned using the 7T GE/Agilent MR901.

3.0 Results

3.1 Dual-drug delivery PV-NP platforms

In TNBC therapy, conventional paclitaxel treatment has been shown to upregulate NF-kB, YAP and Wnt pathways, thereby enriching CSCs that are detrimental for long-term disease-free prognosis in patients (Fillmore and Kuperwasser, 2008; Fu *et al.*, 2015; Pan *et al.*, 2016; Yu *et al.*, 2007). We sought to define an agent capable of co-inhibiting these pathways to prevent subsequent CSC enrichment. After reviewing literature and performing initial *in vitro* experiments, we found that verteporfin inhibited Wnt, YAP and NF-kB signaling, thus we theorized that it may be a suitable agent to abolish paclitaxel-induced CSC enrichment as illustrated in the schematic (Fig 1), and developed a co-delivery nanoplatform for its delivery. Co-delivered paclitaxel and verteporfin loaded PV-NPs (1:7.5 molar ratios), paclitaxel loaded P-NPs, and verteporfin encapsulated V-NPs were synthesized via self-assembly using a modified nanoprecipitation method. As expected, there was a small increase in hydrodynamic size of dual-drug containing PV-NPs in comparison to single drug loaded P-NPs and V-NPs, due to the accommodation of both drugs in single NP (Fig 2A, SI Fig1) (Valencia *et al.*, 2013). However, all NPs have slightly negative surface charge without significant difference (~2-3 mV, Fig 2A). Transmission electron microscopy (TEM) imaging showed the spherical structures for all NPs, with size range of 80-100 nm and matched with hydrodynamic radius measured with DLS (Fig. 2B, SI Fig 2). Drug

encapsulation and loading efficiencies for single and dual drug loaded NPs were within acceptable range. Encapsulation efficiency of verteporfin from V-NPs to PV-NPs decreased from ~73% to 67%, whereas paclitaxel encapsulation improved from P-NPs to PV-NPs (60% to 75% EE). This might be due to the presence of verteporfin inside the NPs increased overall hydrophobicity of NP core or π–π interactions between phenyl groups of paclitaxel and π conjugate system in verteporfin. Drug loading efficiencies for paclitaxel in P-NP and PV-NPs are 2.8% and 0.56% whereas for verteporfin in V-NPs and PV-NPs are 4% and 3.4% respectively. *In vitro* serum stability studies for all NPs showed no significant changes in hydrodynamic size and poly dispersity, highlighting the excellent stability of NPs under biologically relevant conditions (SI Fig 1). Drug release profiles of PV-NPs have typical initial burst release followed by slow release for both drugs (SI Fig. 3). Additionally, *in vitro* microscopy studies showed efficient up-take of NPs by MDA-MB-231 TNBC cells after 3 hours of incubation (Fig 2C).

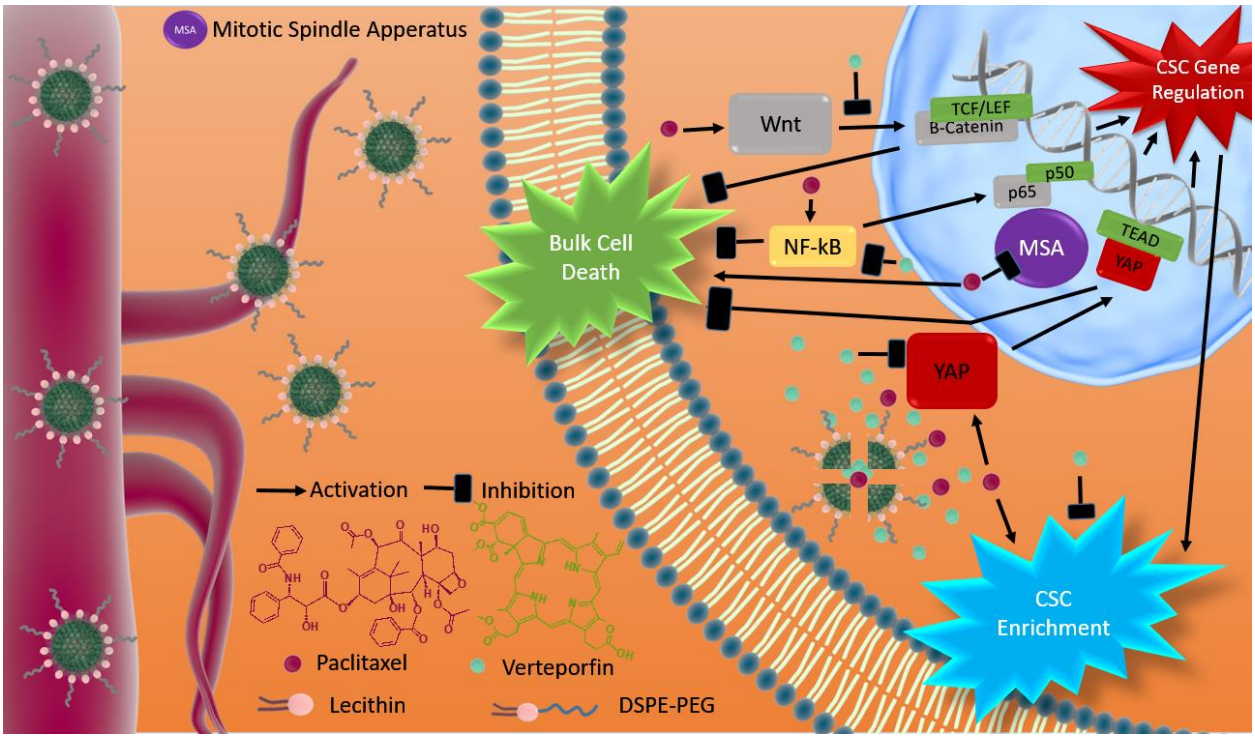

Figure 1. A schematic representation of PV-NPs' effects on TNBC PDX tumors. Upon systemic administration, NPs accumulate and release drugs in PDX tumors *via* the EPR (enhanced permeability and retention) effect. Paclitaxel promotes bulk cell death *via* inhibition of the mitotic spindle apparatus; however, paclitaxel also promotes CSC enrichment due to upregulation of NF-kB, Wnt and YAP signals. Whereas verteporfin co-inhibits NF-kB, Wnt and YAP signals, preventing CSC enrichment and increasing the overall efficacy of combination nanotherapy although it does not potently induce bulk tumour cell death. MSA: mitotic spindle apparatus.

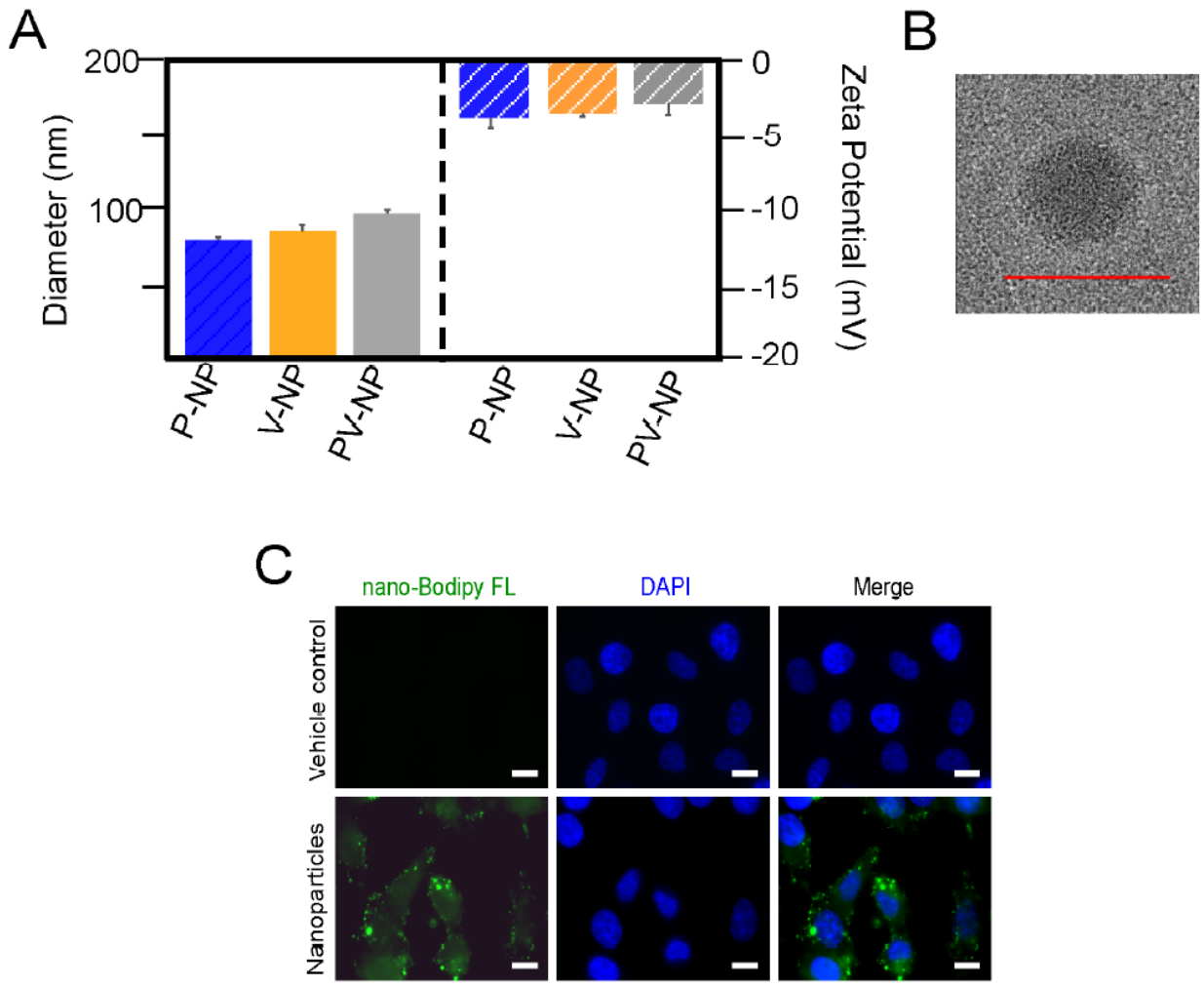

Figure 2. NP characterization and in vitro uptake. (A) Size distribution of PV-NPs. **(B)** Size and surface charge potential of single and dual-drug NPs. **(C)** Fluorescence microscopy of MDA-MB-231 TNBC cells after 3 hours of incubation with BODIPY tagged NPs. Data represent means +/- SD; n = 3 for all figures; there are no statistical differences between the indicated groups or vehicle control. **(D)** Transmission electron microscopy image of PV-NP spherical structure (scale bar, 100nm).

3.2 PV-NPs are capable of simultaneously inhibiting NF-kB, YAP and Wnt signaling activities and concurrently suppressing both mesenchymal and epithelial CSCs in TNBC

Next, we sought to elucidate the effects of P-NPs, V-NPs and PV-NPs on NF-kB, YAP and Wnt pathways which have been shown to be essential for tumor regrowth and CSC development. We transfected MDA-MB-231 cells with pRL-CMV together with the p1242 3x-KB-L luciferase NF-kB reporter, the M50 Super 8x TOPFlash-luciferase Wnt reporter, or the 8xGTIIC-luciferase YAP reporter (Dupont *et al.*, 2011; Mitchell and Sugden, 1995; Veeman *et al.*, 2003). After 24 hours, the cells were exposed to P-NPs, V-NPs or combinations of both for an additional 24 hours and luciferase activity was determined using the Dual-Glo® Luciferase Assay System. It was found that V-NPs simultaneously inhibited NF-kB, Wnt and YAP, and abrogated P-NPs-induced upregulations of NF-kB, Wnt and YAP signaling (Fig. 3A-C). Additionally, combination treatment with P-NPs and V-NPs elicited a reduction in TNBC cell viability (Fig. 3D, SI Fig. 4). For effective drug delivery *in vivo*, we co-encapsulated both P and V in single lipid-hybrid nanoparticles (PV-NPs), which exhibited the same efficacy as combination treatment with individually encapsulated P-NPs plus V-NPs in killing TNBC cells (SI Fig. 4). Significantly, CD44+/CD24- mesenchymal CSCs and ALDH+ epithelial CSCs were enriched after exposure to P-NPs but were diminished after exposure to PV-NPs (Fig. 3E).

Organotypic slice culture of PDX has been shown to faithfully represent PDX tumors and primary patient tumors in drug screening experiments.(Skvortsova, 2018) We plated PDX organotypic slices and treated them over 120 hours with PV-NPs and free drugs. We observed similar results to those of TNBC cell line. In comparison to other treatment groups, P-NPs+V-NPs and PV-NPs effectively decreased viability (SI Fig. 5) and paclitaxel-induced CSC enrichment (SI Fig. 6) whilst promoting apoptosis (SI Fig. 7) in cultured PDX organotypic slices. Together, these

data indicate that the encapsulation of drugs within PV-NPs maintains drug function, *in vitro* efficacy, is capable of co-inhibiting both subtypes of CSCs, and concurrently suppresses NF-kB, Wnt, and YAP signaling crucial for CSC development. In addition, while verteporfin is frequently used as a photosensitizer (Pogue *et al.*, 2003), it showed no photochemical effects on cellular functions at our experimental conditions.

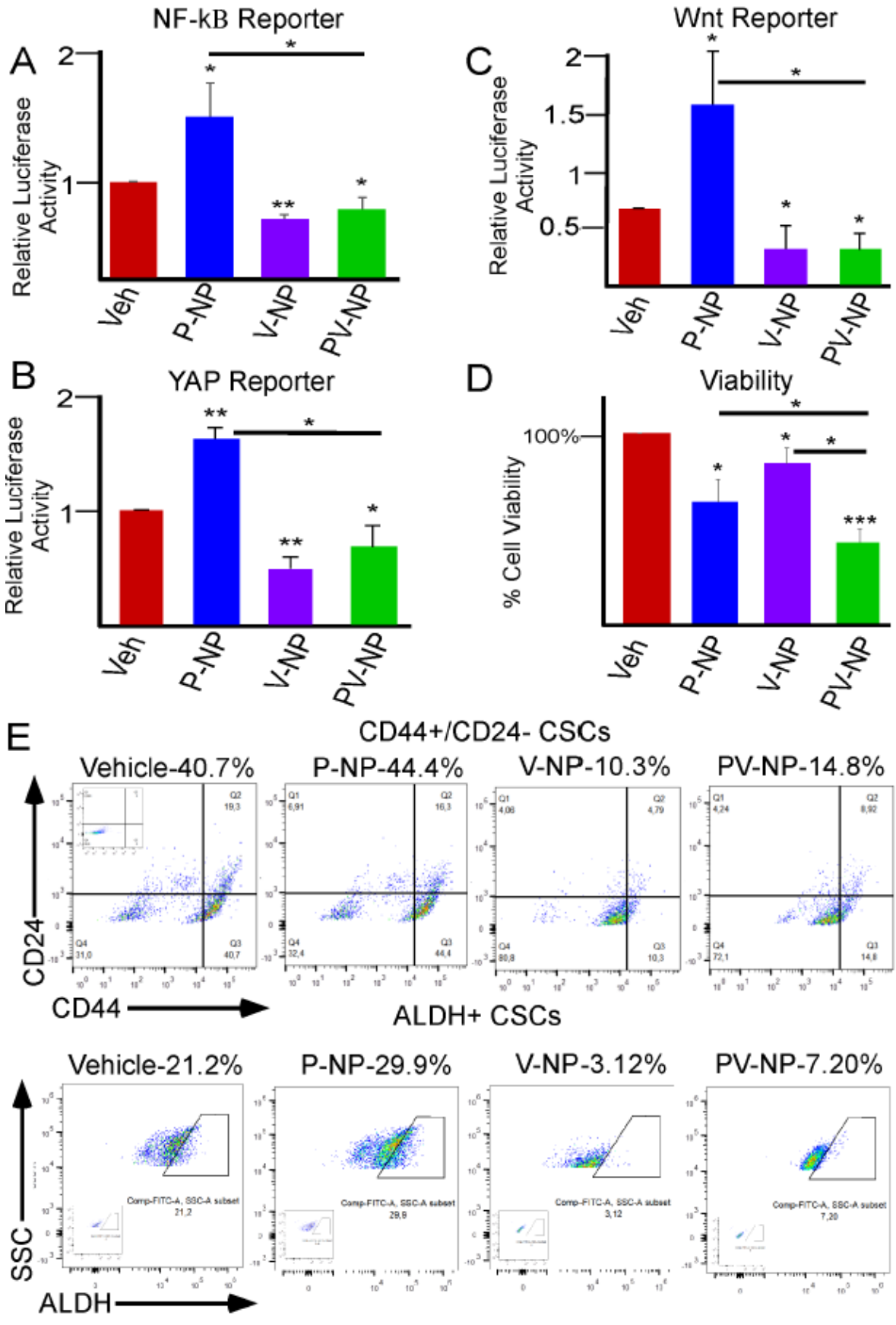
A
NF-kB Reporter
Relative Luciferase Activity
Veh
P-NP
V-NP
PV-NP
B
YAP Reporter
C
Wnt Reporter
D
Viability
% Cell Viability
100%
E
CD44+/CD24- CSCs
Vehicle-40.7%
P-NP-44.4%
V-NP-10.3%
PV-NP-14.8%
CD24
CD44
ALDH+ CSCs
Vehicle-21.2%
P-NP-29.9%
V-NP-3.12%
PV-NP-7.20%
SSC
ALDH

Figure 3. NP-encapsulated verteporfin is capable of simultaneously suppressing NF-kB, Wnt and YAP as well as concurrently inhibiting both mesenchymal and epithelial CSC subpopulations in vitro. (A-C) Luciferase reporter activity of NF-kB, YAP and Wnt activities in MDA MB-231 cells treated with Veh (vehicle-NP), P-NP (containing 25 nM paclitaxel), V-NP (containing 500nM verteporfin) or both (PV-NP). **(D)** Viability analysis after 120 hours of incubation with Vehicle (vehicle-NP), P-NP (5nM), V-NP (100nM) or PV-NP. **(E)** Flow cytometric analysis of CD44+/CD24- CSCs and ALDH+ CSCs after 120 hours of treatments. Data represent means +/- SD; n = 3 for all figures; * $p < 0.05$, ** $p < 0.01$, *** $p<0.001$, in comparison to the indicated groups or vehicle-NP control.

3.3 TNBC PDX vasculature is EPR-active and PDX tumors accumulate NPs.

Following *in vitro* studies, we explored if our results would be translated in the highly clinically relevant TNBC PDX animal model. A simplified interpretation of EPR effect is based on an assumption that macromolecules such as NPs accumulate more in solid tumors due to leaky vasculature and poor lymphatic drainage. EPR driven NPs accumulation in tumors is a complex multistep biological process influenced by several factors including angiogenesis, such as vascular permeability, heterogeneities in genetic profile and tumor microenvironments, tumor tissue penetration, tumor cell internalization, and NPs physicochemical properties.

Unlike tumors generated from cancer cell lines, PDX tumors retain the original patient's tumor heterogeneity, microenvironment, intratumoral vasculature and three-dimensional architecture. Currently, EPR driven nanomedicines accumulation within PDX tumor models has not been fully described. In order to determine if PDX tumors are EPR active, we first preformed MRI and IVIS experiments to study vascularity and NPs accumulation in the tumors (Bertrand *et al.*, 2014; Miller *et al.*, 2015; Prabhakar *et al.*, 2013; Rosenblum *et al.*, 2018). To this end, we surgically engrafted athymic mice with the TNBC PDX tumor fragments within the mammary fat pad. To allow blood vessel growth to detectable size, we waited until tumors reached 100 mm^3. We then performed T1-weighted MRI before and 8 minutes after tail-vein injection of Gadovist

(0.1mM/kg, a clinically used contrast agent in angiography). MRI showed marked contrast enhancement, indicating abundant vascularity within PDX tumors (Fig. 4A). To confirm if this tumor vasculature exhibits EPR effects, fluorescently labeled NPs (Alexa 750) were administrated *via* tail vein and IVIS imaging was performed at 0, 3, 6 and 24 hours to determine NP accumulation inside the tumors. IVIS analysis showed high levels of NP accumulation within the PDX tumor area and upper abdomen area for 6 hours (Fig. 4B).

To accurately quantify NP uptake by tumor cells in comparison with other organ cells, we injected the mice with Qdot 800-labeled NPs. Three hours post-injection, we euthanized the mice, harvested organs and tumors, dissociated them into a single cell suspension and analyzed them using flow cytometry. As shown in Fig 4C, our data support a note that NPs were preferentially located within PDX TNBC tumors in comparison to heart, liver and kidney although NPs were also highly accumulated in non-vital spleen cells (Fig. 4C). Taken together, our data suggests that TNBC PDX vasculature is EPR-active, and NPs accumulate within PDX tumors.

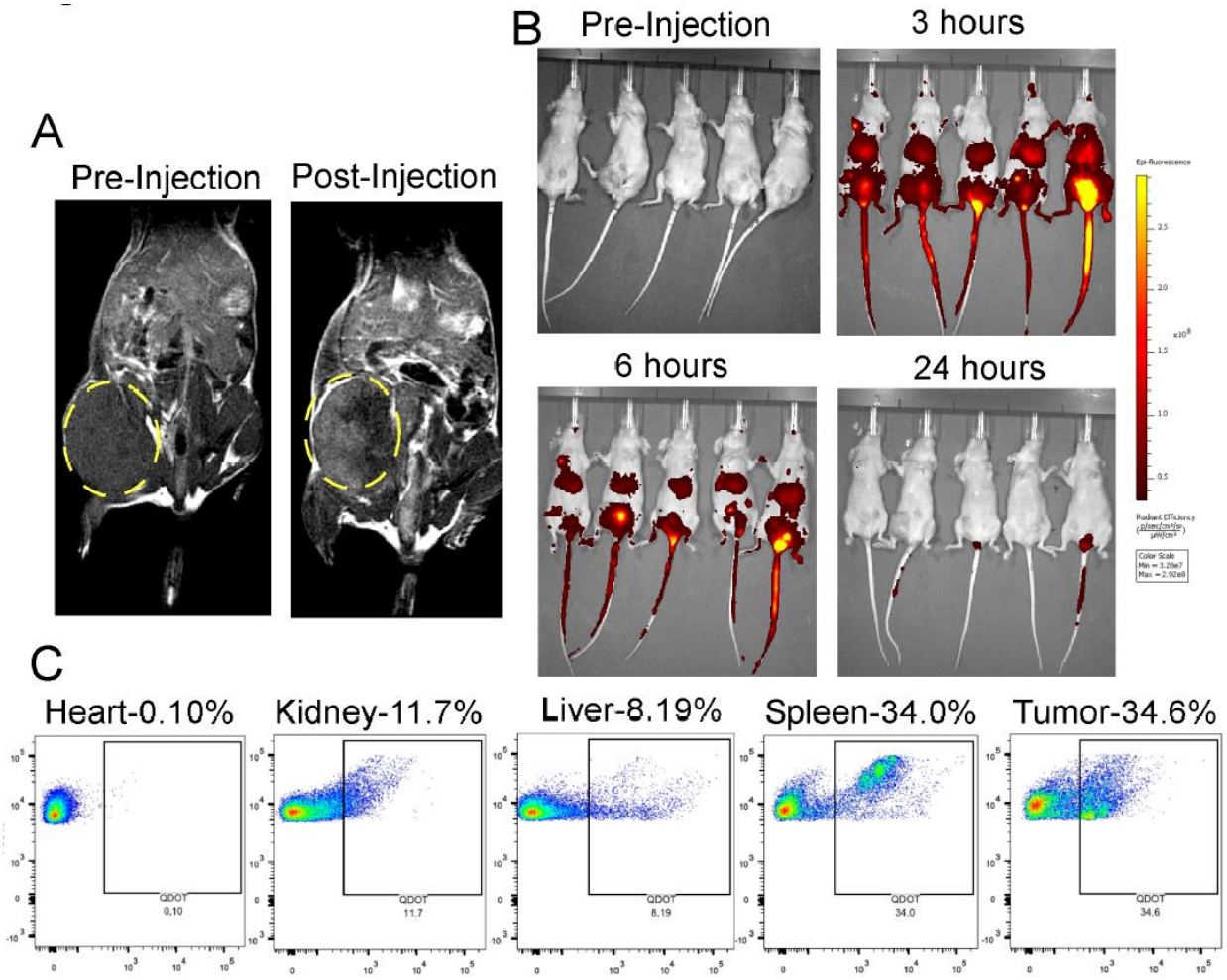

Figure 4: In vivo NP bio-distribution and accumulation within TNBC PDX tumors. (A) T1-weighted MRI of PDX tumors before and 8 minutes after injection of Gadovist in the same mouse. **(B)** IVIS analyses of PDX tumors (low abdomen area) before and after injection of NPs labelled with Alexa750 at indicated time periods using excitation laser of 745 nm and emission filter of 800. **(C)** Flow cytometric analyses of cell uptake of NPs labelled with Qdot 800 in the dissociated organs *vs* PDX tumors 3 hours after tail vein injection. Flow cytometry analysis was performed using a 405 nm excitation laser and a 780/60nm filter to determine cellular uptake.

3.4 PV-NPs retard TNBC PDX tumor growth and suppress CSC populations

Finally, we determined whether co-encapsulated PV-NPs could inhibit the growth of TNBC tumors and abrogate the enrichment of CSCs in a highly clinically relevant PDX mouse model. We again surgically engrafted TNBC PDX tumors into athymic mice. When the tumors reached a mean diameter of 3 mm, mice were randomized and treated with vehicle-NPs (empty NPs), free drug combination (1 mg/kg of paclitaxel and 9 mg/kg verteporfin), or PV-NPs (NPs containing 0.5 mg/kg of paclitaxel and 3.2 mg/kg verteporfin) every other day for 20 days via tail-vein injection (n = 5 for each group). Based on our *in vitro* results using TNBC PDX organotypic slice culture, we did not include P-NPs, V-NPs, and P-NPs+V-NPs treatments in our *in vivo* study.

Given the heterogeneity, composition and variability in each engrafted PDX tumor fragment, it is expected to see differential growth rate for PDX tumors. Indeed, we observed variable tumor growth rate in Vehicle-NPs and free-drug treated groups. However, despite this variability, PV-NPs treatment (even containing low dose of drugs than free-drug control, only 50% paclitaxel and 32% verteporfin) significantly retarded PDX tumor growth in comparison to the free drug and vehicle-NP control groups (Fig. 5A), highlighting the efficacy of PV-NPs treatment. Consistently, mice treated with PV-NPs showed significantly reduced tumor size and tumor weight (Fig. 5B). While PV-NPs treatment effectively diminished TNBC PDX tumor growth, mice body weight remained constant throughout treatment (SI Fig. 8), suggesting the specificity and tolerability of the PV-NP treatment. In contrast to PV-NPs, free-drug did not show statistical difference in comparison to Vehicle-NP control. This is likely due to inadequate tumor accumulation and/or retention of free-drug, highlighting the necessity for NP delivery . Furthermore, in agreement with *in vitro* cell line results, PV-NPs reduced both mesenchymal CD44+/CD24- CSCs and epithelial ALDH+ CSCs in PDX tumors after treatment while the free-

drug combination was unable to significantly suppress CD44+/CD24- CSC subpopulation when compared to Vehicle-NP control (Fig. 5C-D, SI Fig. 9).

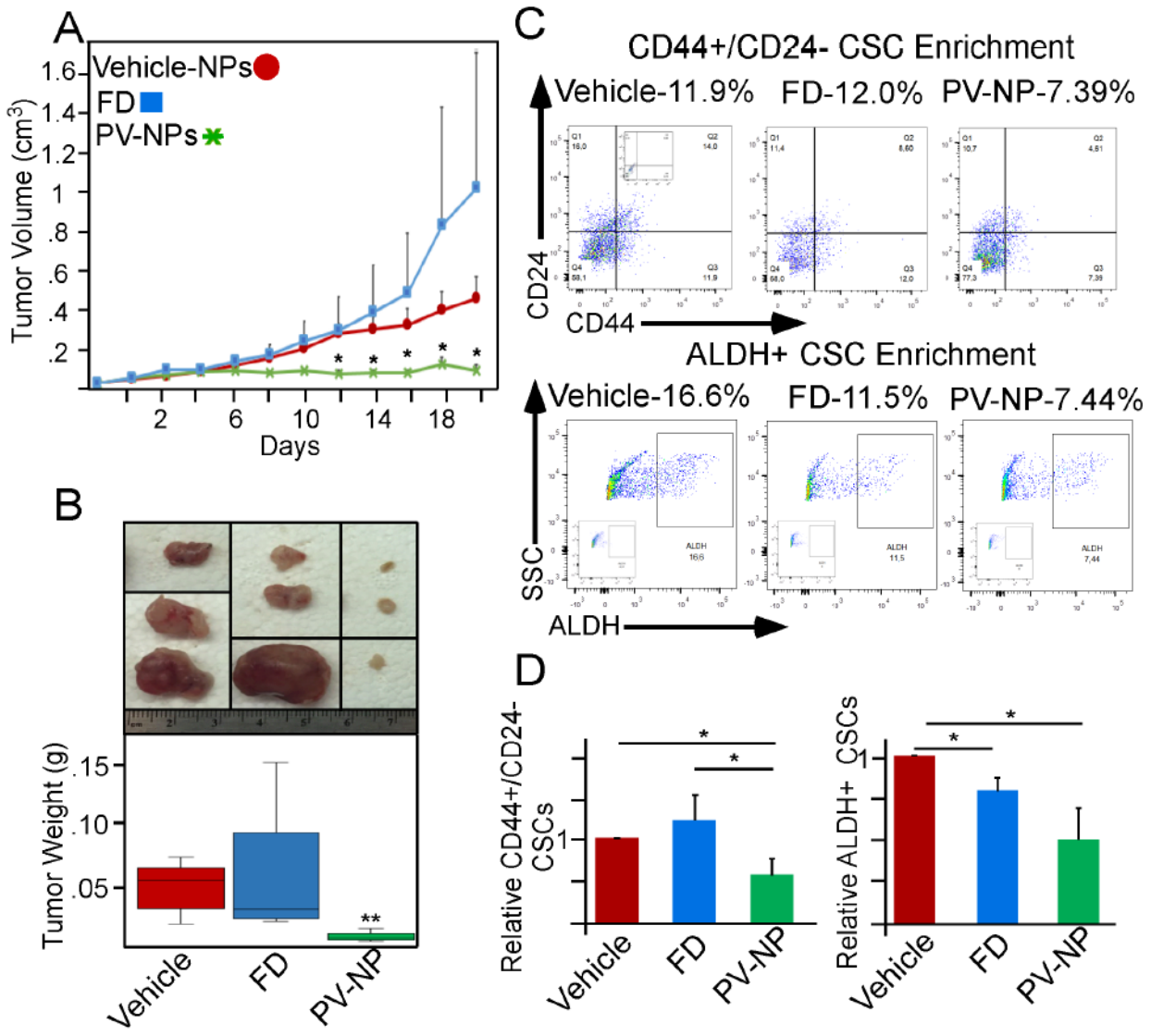

Figure 5: Efficacy of paclitaxel and verteporfin co-loaded NPs in the treatment of TNBC PDX tumors. (A) TNBC PDX tumors were surgically engrafted into the mammary fat pads of athymic nude mice and treated with Vehicle-NPs (empty NPs), free drugs (FD, 1 mg/kg of paclitaxel and 9 mg/kg V), or PV-NP (0.5 mg/kg of paclitaxel and 3.2 mg/kg verteporfin co-loaded NPs) every other day for 20 days. Tumor volumes were determined every 2-day. **(B)** Representative tumor photos after treatments with means of tumor weights shown below. **(C, D)** Flow cytometric analysis of CD44+/CD24- CSCs and ALDH+ CSCs within TNBC PDX tumor after completion of *in vivo* treatment. Data represent means +/- SD; n = 5 for mice/group and n = 3 for flow cytometric analysis; * $p < 0.05$, **$p < 0.01$.

4.0 Discussion:

There is limited data showing EPR effects in patients due to several limitations. One of the main challenges to overcome is achieving meaningful bio-distribution data in patients. A indirect method to analyze EPR effects in treatments is to compare treatment responses within patient groups. However, patients' tumors are heterogeneous and their tumor's biology, microenvironment, vasculature, drug efflux and drug response rates vary significantly. Additionally, tumor heterogeneity leads to dissimilar NP accumulation within tumors and dissimilar treatment responses. This might be one of the reasons for the poor results in Phase II clinical trials of BIND014 and CAALA01. Recent reports showed the benefit of companion imaging of NPs to quantify the EPR effect, in order to stratify patients for better nanomedicine therapeutic response (Miller *et al.*, 2015). Multiple clinical studies demonstrated positive results in identifying patients with positive nanomedicine effect *via* companion imaging (Lee *et al.*, 2017; Ramanathan *et al.*, 2017).

Of note, the majority of preclinical experiments studying NP uptake *via* EPR have employed syngeneic mouse or human cell line xenograft tumors, which develop over days, are comprised of a homogeneous cellular population, and possess immature vasculature in addition to a malformed tumor microenvironment (Damia and D'Incalci, 2009; Prabhakar *et al.*, 2013). In contrast, PDX tumors develop over longer periods of time, are comprised of multiple cellular populations, primary tumor microenvironment, architecture and more mature vasculature, similar to primary patients' tumors (Choi *et al.*, 2014; Whittle *et al.*, 2015). These similarities translate into the success of PDX emulation of patient tumor response upon exposure to chemotherapies. Hence, the increasing mouse-clinical trials are using PDX tumors for drug development,

identification and clinical translation (Bruna *et al.*, 2016; Gao *et al.*, 2015; Migliardi *et al.*, 2012; Yu *et al.*, 2017).

In this study, we have developed a NP platform for the delivery of our combination therapy to TNBC PDX tumors. TNBC PDX tumors were highly vascularized as indicated by the MRI imaging with Gadovist and showed EPR related nanoparticle accumulation as determined by IVIS imaging (Fig 4A-B). Flow cytometry analysis demonstrated tumor cell uptake of fluorophore-NPs, supporting NP tumor delivery of the payload (Fig 4C). We also observed NP accumulation in the spleen. It is likely due to macrophage uptake and spleen red pulp (Franken *et al.*, 2015). In spleen red pulp, red blood cells are sieved by splenic sinuses before re-entering circulation. Nanoparticles 100-200nm in size have been shown to have difficulty traversing through the red pulp, resulting in accumulation within the red pulp as well as uptake by macrophages (Cataldi *et al.*, 2017).

In vivo TNBC PDX studies demonstrated that the efficacy of NP-delivered paclitaxel and verteporfin for inhibiting PDX tumor growth and preventing CD44+/CD24- and ALDH+ CSCs enrichment (Fig 5). To our best knowledge, this is the first report showing the treatment efficacy of drug-NPs using a highly clinically relevant TNBC PDX mouse model. It is also the first demonstration of verteporfin's capability of simultaneously inhibiting NF-κB, Wnt and YAP signaling (Fig 3A-C) as well as repressing both mesenchymal CD44+/CD24- and epithelial ALDH+ TNBC CSC subpopulations (Fig 3E). Recent reports have demonstrated that paclitaxel-mediated CSC enrichment is due to co-upregulation of NF-kB and Wnt pathways and the important role of YAP signaling in CSC development (Jia *et al.*, 2017; Sulaiman *et al.*, 2018b; Yu *et al.*, 2007). Thus, concurrent inhibition of these three signals might be an important mechanism underlying the effective treatment of PV-NPs. Given that two drugs are commonly used in clinic and their synergic effects on inhibiting TNBC bulk and CSCs, such a combination nanotherapy

may lead to an effective treatment of TNBC patients.

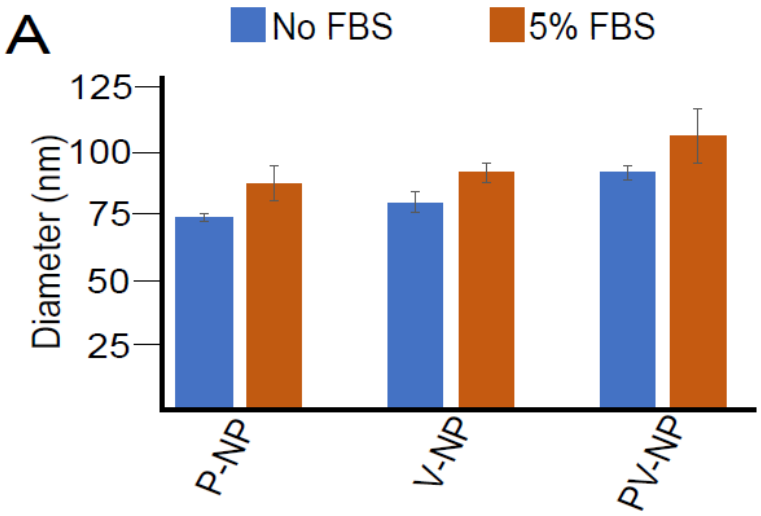

Supplemental Figure S1: The hydrodynamic size of co-encapsulated **V**-NP, **P**-NPs or **PV**-NPs in FBS *versus* water.

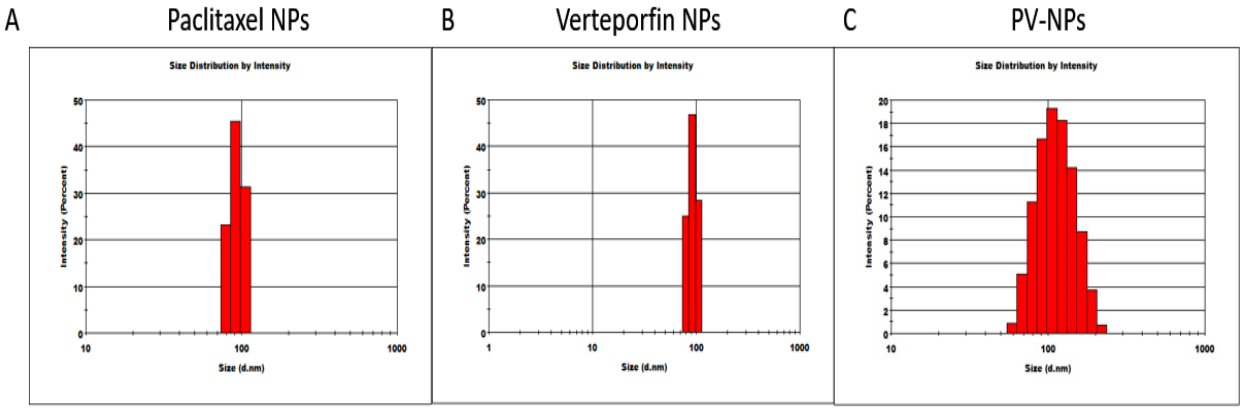

Supplemental Figure S2: The DLS size distribution of P-NPs, V-NPs and PV-NPs

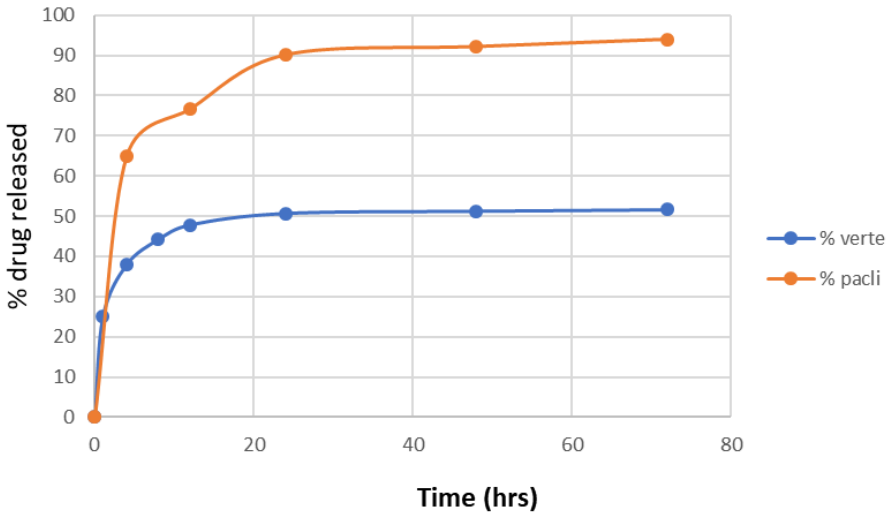

Supplemental Figure S3: The release profile for Verteporfin and Paclitaxel over a time course. Each time point is expressed as total % of drug released.

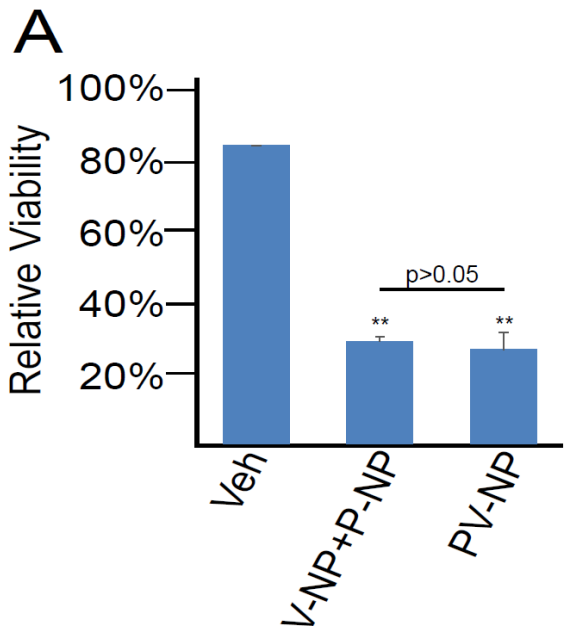

Supplemental Figure S4: The efficacy of co-encapsulated **PV**-NPs in comparison with single drug encapsulated **P**-NP+**V**-NP treatment. MDA-MB231 cells were treated with Vehicle (Veh), and different NPs loaded with drugs as well as free drugs.

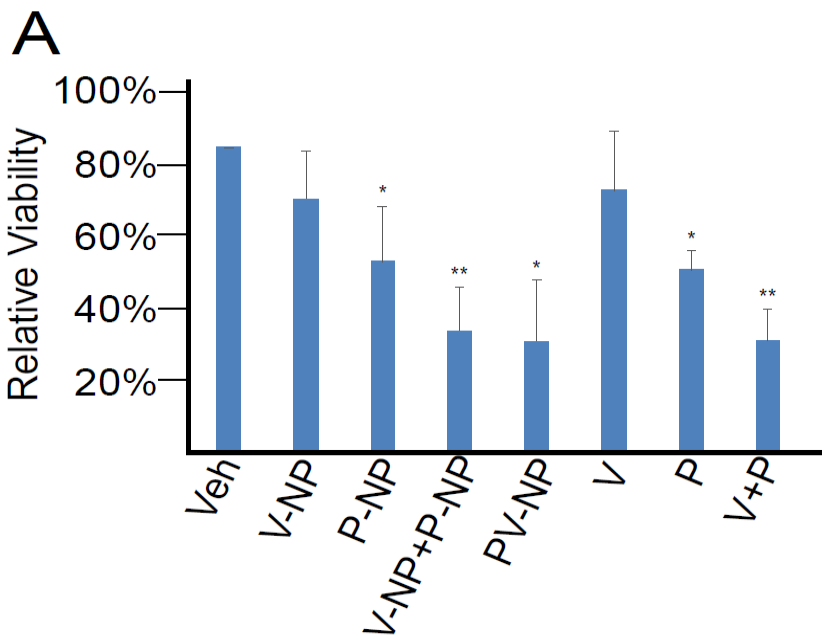

Supplemental Figure S5: Alamar Blue viability analysis of PDX TNBC tumors after treatment with co-encapsulated **PV**-NPs in comparison with single encapsulated **P**-NP+**V**-NP treatment and free drug treatments. HCI-002 PDX TNBC tumor fragments were isolated, plated into 24 well plates and treated with Vehicle (Veh), V-NPs (100nM), P-NPs (5nM) and different NPs loaded with drugs as well as free drugs at the same concentration every day for 120 hours.

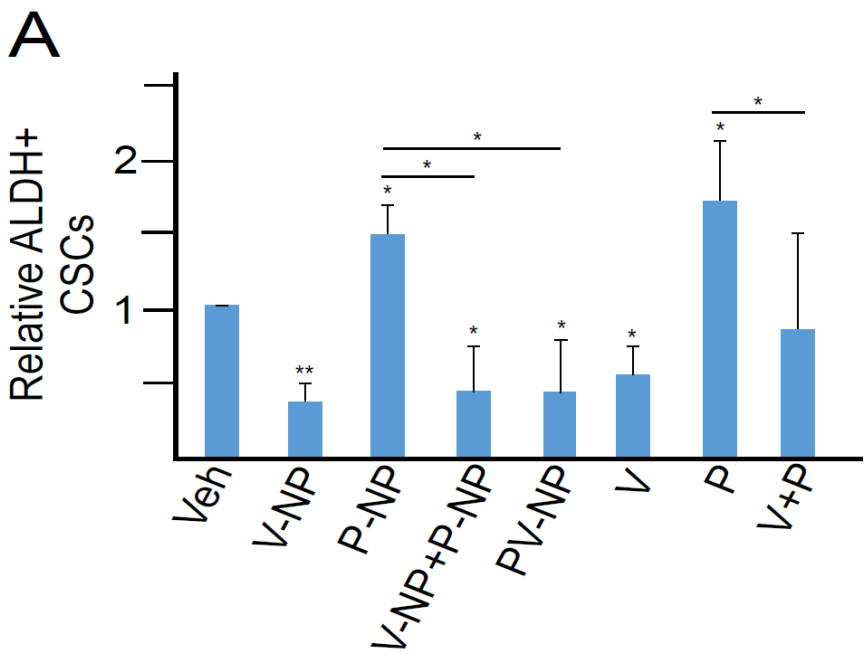

Supplemental Figure S6: Tabulated flow cytometry analysis of ALDH+ CSCs in TNBC PDX HCI-002 tumor fragments after 120 hours of Vehicle (Veh), V-NPs (100nM), P-NPs (5nM) and different NPs loaded with drugs or free drugs at the same concentration.

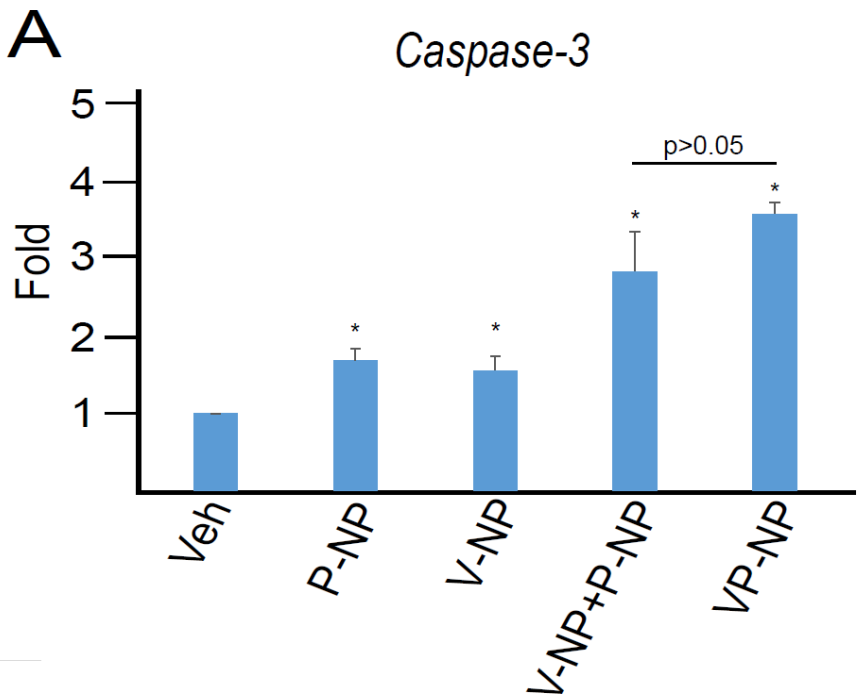

Supplemental Figure S7: RT-qPCR analysis and comparison of relative mRNA levels of Caspase-3 (CASP3) genes between HCI-002 PDX TNBC tumor fragments after treatment for 120 hours with Vehicle (Veh), V-NPs (100nM), P-NPs (5nM) and different NPs loaded with drugs or free drugs at the same concentration.

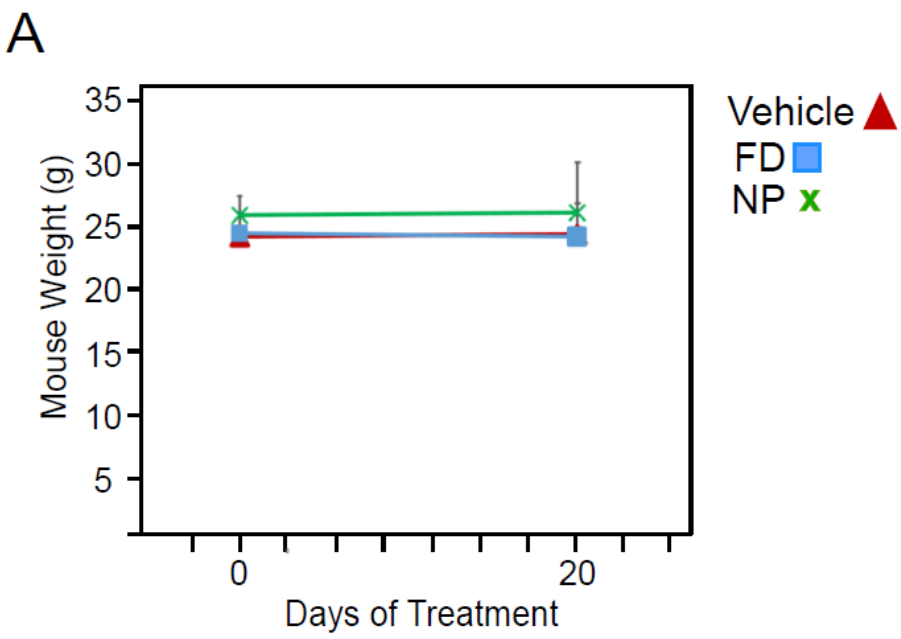

Supplemental Figure S8: The body weights of mice treated with vehicle-nanoparticles (Vehicle-NPs), free drugs (paclitaxel + verteporfin) or **PV**-NPs before the initial treatments and following the last treatment after 20 days. No significant differences of body weight were observed amongst three groups.

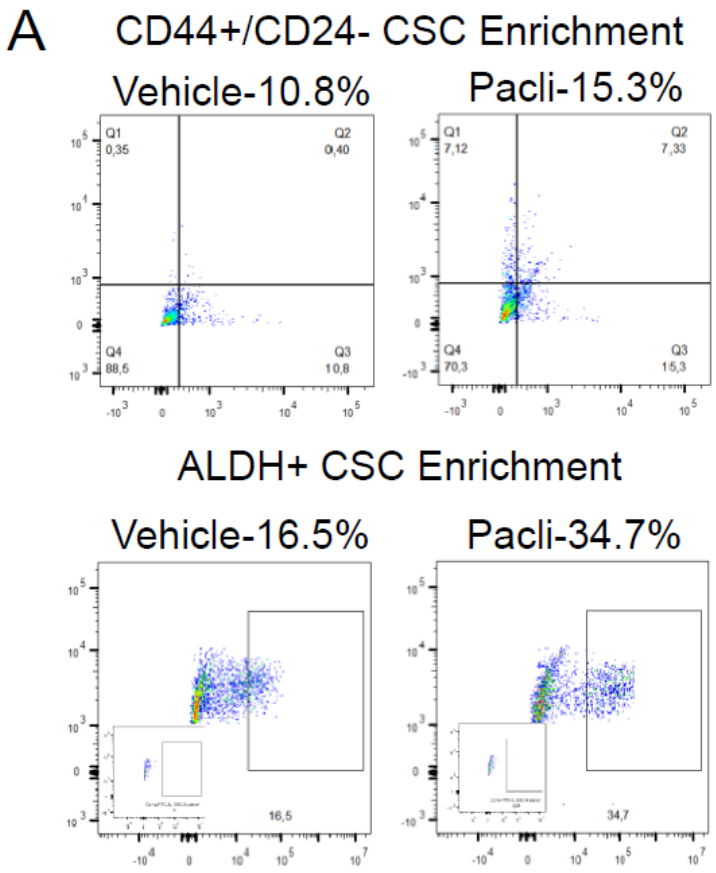

Supplemental Figure S9: Flow cytometry analysis of CD44+/CD24- and ALDH+ CSCs in TNBC PDX HCI-002 tumor after *in vivo* Paclitaxel-NP treatment (Pacli) compared to the Vehicle-lipid-polymer hybrid nanoparticle control (Vehicle).

Chapter 6: Summary

The lack of specific therapies for the treatment of TNBC is a currently unmet medical need. In Chapter 2, it was found that Wnt and HDAC expression was associated with a TNBC phenotype and reduced patient prognosis. Upon Wnt inhibition (via BC21 or shβ-catenin), $CD44^+/CD24^-$ CSCs were diminished, an effect which was further magnified upon HDAC inhibition. *ESR1* re-expression was observed following duel inhibition of Wnt and HDAC. To target the estrogen receptor, the anti-estrogen inhibitor tamoxifen was employed which magnified efficacy of the treatment.

MDA MB-231 cells were fractionated into four sub-populations based on CD44/CD24 expression. It was found that while the CSC population retained majority $CD44^+/CD24^-$ status, the non-CSC populations were able to reconstitute the $CD44^+/CD24^-$ CSC population over time. Due to the plasticity of non-CSC and CSCs, blocking CSC conversion from non-CSCs is important for eradication of CSCs to reduce disease recurrence. The VBT (valproic acid, BC21 and tamoxifen) combination was found to suppress CSC enrichment, and prevent non-CSC to CSC conversion in addition to its inhibition of proliferation and promotion of apoptosis. These results were reproduced in two TNBC patient tumor samples obtained from The Ottawa General Hospital.

While findings generated from this report were positive and demonstrated effective targeting of $CD44^+/CD24^-$ CSCs *in vitro*, BC21, testing has not been approved by the FDA. We thus decided to pursue another avenue as our goal was clinical translation.

In the subsequent study (Chapter 3), it was found that mTORC1 and HDAC were highly expressed in TNBC patients in comparison to normal breast tissue and Luminal ER+ breast cancer patients. Gene expression analysis of TNBC and ER+ breast cancer cell lines replicated these findings. Inhibition of mTORC1, HDAC and ESR1 via VRT (valproic acid, rapamycin and tamoxifen) led to effective inhibition of cell growth and potent ERα protein expression. Using the

same fractionation approach based on CD44/CD24 markers (as described in Chapter 2), it was found that TNBC CSCs expressed higher levels of HDAC and mTORC1 genes compared to non-CSCs. As such, combinational inhibition of mTORC1, HDAC and ESR1 was effective at suppressing CSC enrichment and preventing the non-CSC to CSC conversion.

As rapaymcin, valproic acid and tamoxifen (the inhibitors used for mTORC1, HDAC and ESR1 inhibition respectively) are all well characterized in the clinic with acceptable toxicity profiles (individually), this study was progressed to an *in vivo* TNBC cell line xenograft platform to assess efficacy, tolerability and CSC targeting in a living model.

MDA MB-231 and SUM 149-PT TNBC cell lines were injected into the fat pad of athymic mice after which the mice were treated with a DMSO control or the VRT combination via intraperitoneal injections every day for a period of 20 days. The VRT combination was able to reduce tumor burden, inhibit CSCs, and diminish tumorigenicity after secondary transplantation in both TNBC cell lines following treatment.

The previous research (Chapter 2-3) focused on targeting solely the $CD44^+/CD24^-$ CSC population in TNBC. Due to the plasticity of CSCs, it has been demonstrated that epithelial ($ALDH^+$) and mesenchymal ($CD44^+/CD24^-$) CSCs are interconvertible (Liu *et al*., 2014). As such, I was keen to develop a therapy which could effectively target both CSC populations.

In the subsequent study (Chapter 4), it was found that YAP signalling and $CD44^+/CD24^-$ CSCs were upregulated in mesenchymal-like TNBC cells while Wnt/β-catenin signalling and $ALDH^+$ CSCs were downregulated in mesenchymal-like TNBC cells. In contrast, in epithelial-like possessed *vice-versa* signalling and CSC enrichment patterns. Co-inhibition of Wnt and YAP using FDA approved ICG-001/PRI-724 and simvastatin respectively was able to potently target

and inhibit both $ALDH^+$ and $CD44^+/CD24^-$ CSCs in epithelial and mesenchymal states of MDA MB-231 and SUM 149-PT cells. These findings were corroborated using three patient tumor samples (CRDCA, ARI-1 and SEM-1) and 1 PDX tumor sample (HCI-001) *in vitro*.

Using a human xenograft model, dual inhibition of Wnt via ICG-001/PRI-724 and YAP/mevalonate via simvastatin effectively attenuated both mesenchymal and epithelial TNBC tumor burdens, diminished both $CD44^+/CD24^-$ and $ALDH^+$ CSC subpopulations, and reduced tumorigenicity after secondary transplantation. Together, this study demonstrated differential signal pathway expression within the E/M phenotypes and CSC populations in TNBC. This study also identified a viable strategy for the effective treatment of both epithelial and mesenchymal TNBC and their respective CSC populations via Wnt and YAP/mevalonate co-inhibition. Simvastatin is a widely used to reduce patient cholesterol. ICG-001/PRI-724 is a Wnt inhibitor in clinical trials which has demonstrated tolerability and efficacy for the treatment of a wide variety of cancers (Chan *et al.*, 2015; El-Khoueiry *et al.*, 2013; Ko *et al.*, 2016).

In the last study (Chapter 5), building off the success of Wnt and YAP inhibition as a method to target TNBC and E/M CSC populations, the goal was to translate these findings using a clinically translatable patient derived xenograft (PDX) mouse model. We used a potent Wnt and YAP co-inhibitor, verteporfin (a FDA-approved drug as a photosensitizer for photodynamic therapy to eliminate the abnormal blood vessels, such as macular degeneration). Due to the irregular vasculature reported within patient tumors, we assessed whether adequate blood flow reached the tumors via Gadovist MRI analysis of mice implanted with PDX tumors. Upon determining sufficient levels of blood flow, we tested a nanoparticle drug-delivery system and found high levels of specific localization over 3-6 hours via IVIS analysis within the TNBC PDX tumor. Verteporfin was then encapsulated within the nanoparticles in combination with paclitaxel,

and the PDX tumors were treated with nanoparticle-encapsulated drugs. It was found that tumor burden was substantially inhibited and both $CD44^{+}/CD24^{-}$ and $ALDH^{+}$ CSC populations were reduced following combinational treatment.

In summary, Chapters 2-5 demonstrated novel therapeutic approaches for the treatment of TNBC by targeting not only the bulk tumor population but also the CSC populations. Importantly, it was found that mesenchymal-like TNBC were enriched for $CD44^{+}/CD24^{-}$ CSCs while epithelial-like TNBC were enriched for $ALDH^{+}$ CSCs. CSC plasticity highlights that both epithelial and mesenchymal CSC populations need to be co-targeted. Wnt and YAP/mevalonate pathway inhibitors in combination were identified to inhibit both $ALDH^{+}$ and $CD44^{+}/CD24^{-}$ CSC populations and prevent chemotherapy-induced CSC enrichment and tumorigenesis in TNBC cell lines and PDX models. Further studies should use humanized mouse models engrafted with PDX tumors to assess overall treatment efficacy of drug combinations which may generate tangible therapeutic approaches for future clinical trials.

Rights and Permissions

The following Section contains licensing/referencing/permissive materials obtained directly form the source of the journal in question/government website as well as the link to which this information could be found.

For Andrew Sulaiman, Zemin Yao and Lisheng Wang. Re-evaluating the role of epithelial-mesenchymal-transition in cancer progression. Journal of Biomedical Research, 2017; 31(0): 1–10, please see Appendix 1.

For Andrew Sulaiman and Lisheng Wang. Bridging the divide: preclinical research discrepancies between triple-negative breast cancer cell lines and patient tumors. Oncotarget, 2017; 8(68): 113269–113281:

"COPYRIGHT AND LICENSE POLICIES

Open-Access License No Permission Required

"Oncotarget applies the **Creative Commons Attribution 3.0 License** (CC BY 3.0) to all works we publish (read the **human-readable summary** or the **full license legal code**). Under the CC BY, authors retain ownership of the copyright for their article, but authors allow anyone to download, reuse, reprint, modify, distribute, and/or copy articles in *Oncotarget*, so long as the original authors and source are cited.

No permission is required from the authors or the publishers.

In most cases, appropriate attribution can be provided by simply citing the original article. If the item you plan to reuse is not part of a published article (e.g., a featured issue image), then please indicate the originator of the work, and the volume, issue, and date of the journal in which the item appeared. For any reuse or redistribution of a work, you must also make clear the license terms under which the work was published. This broad license was developed to facilitate open access to, and free use of, original works of all types. Applying this standard license to your own work will ensure your right to make your work freely and openly available.

For queries about the license, please contact us at forms@oncotarget.com"

Attained from: http://www.oncotarget.com/index.php?journal=oncotarget&page=about

For Andrew Sulaiman, Brandon Sulaiman, Lara Khouri, Sarah McGarry, Carolyn Nessim, Angel Arnaout, Sean Xuguang Li, Christina Addison, Jim Dimitroulakos, and Lisheng

Wang. Both bulk and CSC subpopulations in TNBC are susceptible to Wnt, HDAC and ERα co-inhibition. *FEBS Letters*, 2017;590(24):4606-4616, please see Appendix 2:

"AUTHORS - If you wish to reuse your own article (or an amended version of it) in a new publication of which you are the author, editor or co-editor, prior permission is not required (with the usual acknowledgements). However, a formal grant of license can be downloaded free of charge from RightsLink by selecting "Author of this Wiley article" as your requestor type."

Attained from:
https://onlinelibrary.wiley.com/page/journal/18759114/homepage/permissions.html

For Andrew Sulaiman, Sarah McGarry, Sara El-Sahli, Ka Mien Lam, Jason Chambers, Shelby Kaczmarek, Li Li, Christina Addison, Jim Dimitroulakos, Angel Arnaout, Carolyn Nessim, Zemin Yao, Guang Ji, Haiyan Song, Suresh Gadde, Xuguang Li, Lisheng Wang. Co-inhibition of mTORC1, HDAC and ESR1α Regards the Growth of Triple Negative Breast Cancer and Suppresses Cancer Stem Cells. Cell Death and Disease 2018; 9(8): 815 doi: 10.1038/s41419-018-0811-7). Published under CC BY 4.0 International License: https://creativecommons.org/licenses/by/4.0/deed.ast

"Cell Death & Disease articles are published under a CC BY license (Creative Commons Attribution 4.0 International License) by default. This license is preferred by many funding bodies and allows for maximum dissemination and re-use of published materials. Learn more about Creative Commons licenses and the license options available in *Cell Death & Disease* here."

Attained from: https://www.nature.com/cddis/authors-and-referees/authors

"Open access articles in Springer Nature journals are published under Creative Commons licences. These provide an industry-standard framework to support easy re-use of open access material. Under Creative Commons, authors retain copyright of their work. Authors publishing via the open access route in journals on the nature.com platform additionally assign Springer Nature a non-exclusive licence to publish (LTP).

All Springer Nature-owned journals with open access options offer the CC BY licence (Creative Commons Attribution v4.0 International Licence), and this is the default licence for all Springer Nature-owned fully open access journals and for OA content in all journals in the Palgrave Macmillan hybrid portfolio, and in the majority of hybrid academic titles on the nature.com platform. The CC BY licence is the most open licence available and considered the industry 'gold standard' for open access; it is also preferred by many funders. This licence allows readers to copy and redistribute the material in any medium or format, and to alter, transform, or build upon the material, including for commercial use, providing the original author is credited. Other Creative

Commons licences are available for some titles: please see the individual journals for details on other Creative Commons licences offered.

All Springer Nature-owned journals offer intergovernmental organisation (IGO) versions of Creative Commons licences on request, where required by the author's employer.

Where journals offer a range of Creative Commons licences, authors are advised to check their funder's requirements before selecting a licence, to ensure compliance."

Attained from: https://www.nature.com/openresearch/about-open-access/policies-journals/

For Andrew Sulaiman, Sarah McGarry, Li Li, Deyong Jia, Sarah Ooi, Christina Addison, Jim Dimitroulakos, Angel Arnaout, Carolyn Nessim, Zemin Yao, Guang Ji, Haiyan Song, Suresh Gadde, Xuguang Li, Lisheng Wang. Dual inhibition of Wnt and YAP signaling retards the growth of both mesenchymal and epithelial TNBC. *Molecular Oncology*, 2018; 12(4):423-440. Published under CC BY 4.0 International License: https://creativecommons.org/licenses/by/4.0/deed.ast

"All *Molecular Oncology* articles are published under the terms of the Creative Commons Attribution License (CC BY) which allows users to copy, distribute and transmit an article, adapt the article and make commercial use of the article. The CC BY license permits commercial and non-commercial re-use of an open access article, as long as the author is properly attributed.

Use of the article, in whole or part, in any medium requires attribution suitable in form and content as follows: **[Title of Article/Author/Journal Title and Volume/Issue]. Published under a Creative Commons Attribution (CC BY) License**. Links to the final article on Wiley's website are encouraged where applicable."

"Further Details Related to Re-Use of Articles:

Copyright on any research article published by a Wiley Open Access journal is retained by the author(s).

Authors grant Wiley a license to publish the article and identify itself as the original publisher. Authors also grant any third party the right to use the article freely as long as its original authors, citation details and publisher are identified.

The Creative Commons Attribution License does not affect the moral rights of authors, including without limitation the right not to have their work subjected to derogatory treatment. It also does not affect any other rights held by authors or third parties in the article, including trademark or patent rights, or the rights of privacy and publicity. Use of the article must not assert or imply, whether implicitly or explicitly, any connection with, endorsement or sponsorship of such use by the author, publisher or any other party associated with the article.

For any reuse or distribution, users must include the copyright notice and make clear to others that the article is made available under a Creative Commons Attribution license, linking to the relevant Creative Commons web page. Users may impose no restrictions on use of the article other than those imposed by the Creative Commons Attribution license.

To the fullest extent permitted by applicable law, the article is made available as is and without representation or warranties of any kind whether express, implied, statutory or otherwise and including, without limitation, warranties of title, merchantability, fitness for a particular purpose, non-infringement, absence of defects, accuracy, or the presence or absence of errors."

Attained from:
https://febs.onlinelibrary.wiley.com/hub/journal/18780261/about/permissions

For Andrew Sulaiman, Sarah McGarry, Sara El-Sahli, Li Li, Jason Chambers, Alexandra Phan, Marceline Côté, Greg O. Cron, Tommy Alain, Yevgeniya Le, Seung-Hwan Lee, Sheng Liu, Daniel Figeys, Suresh Gadde and Lisheng Wang. Co-Targeting Bulk Tumor and CSCs in Clinically Translatable TNBC Patient-Derived Xenografts via Combination Nanotherapy. ***Molecular Cancer Therapeutics*** **(2018, Submitted):**

"Article Reuse by Authors
Authors of articles published in AACR journals are permitted to use their article or parts of their article in the following ways without requesting permission from the AACR. All such uses must include appropriate attribution to the original AACR publication. Authors may do the following as applicable:

1. Reproduce parts of their article, including figures and tables, in books, reviews, or subsequent research articles they write;
2. Use parts of their article in presentations, including figures downloaded into PowerPoint, which can be done directly from the journal's website;
3. Post the accepted version of their article (after revisions resulting from peer review, but before editing and formatting) on their institutional website, if this is required by their institution. The version on the institutional repository must contain a link to the final, published version of the article on the AACR journal website so that any subsequent corrections to the published record will continue to be available to the broadest readership. The posted version may be released publicly (made open to anyone) 12 months after its publication in the journal;
4. Submit a copy of the article to a doctoral candidate's university in support of a doctoral thesis or dissertation.

Article Reuse by Others
Third parties or individuals who are seeking permission to copy, reproduce, or republish content from an AACR journal and who are not the author of that content may use the Copyright Clearance Center's Rightslink® service to request permission to reuse identified content. Please see **Third Party Permission and Reprints** for detailed instructions on how to submit a request."

Attained from: http://aacrjournals.org/content/authors/copyright-permissions-and-access

For Appendix 3, Statistics Canada. Table 13-10-0394-01 Leading causes of death, total population, by age group. https://www150.statcan.gc.ca/t1/tbl1/en/cv.action?pid=1310039401; the table was published under the Statistics Canada Open Licence.

"Statistics Canada hereby grants you the permission to use, reproduce, publish, freely distribute or sell information covered by the Statistics Canada Open Licence. In any use of this information, you must adhere to the conditions of the Statistics Canada Open Licence. If you do not agree to these terms, you may not use the information."

Attained from https://www.statcan.gc.ca/eng/reference/licence

Curriculum Vitae

PUBLICATIONS

1. **Andrew Sulaiman**, Sarah McGarry, Sara El-Sahli, Li Li, Jason Chambers, Alexandra Phan, Emil Al-Kadi, Zaina Kahiel, Eliya Farah1, Guang Ji, Seung-Hwan Lee, Krishna K Inampudi, Tommy Alain, Suresh Gadde, Lisheng Wang. Retardation of TNBC PDX Tumors growth and diminution of Tumorigenesis via Nanotherapy. Cell Death and Disease (2019, Submitted). **Impact Factor 5.9**
2. Shrey Sindhwani, Abdullah Muhammad Syed, Jessica Ngai, Benjamin R. Kingston, Laura Maiorino, Jeremy Rothschild, Presley MacMillan, Yuwei Zhang, Netra Unni, Tran Hoang, Stefan Wilhelm, Anton Zilman, Suresh Gadde, **Andrew Sulaiman**, Lisheng Wang, Mikala Egeblad and Warren C. W. Chan. How do nanoparticles enter solid tumours? Nature (2018, Submitted). **Impact Factor 41.57**
3. **Andrew Sulaiman**, Sarah McGarry, Sara El-Sahli, Li Li, Greg Cron, Christina Addison, Jim Dimitroulakos, Zemin Yao, Xuguang Li , Suresh Gadde and Lisheng Wang. Co-Targeting Bulk Tumor and CSCs in Clinically Translatable TNBC Patient-Derived Xenografts via Combination Nanotherapy. Molecular Cancer Therapeutics (2018, Submitted) **Impact Factor 5.3**
4. **Andrew Sulaiman**, Sarah McGarry, Sara El-Sahli, Ka Mien Lam, Jason Chambers, Shelby Kaczmarek, Li Li, Christina Addison, Jim Dimitroulakos, Angel Arnaout, Carolyn Nessim, Zemin Yao, Guang Ji, Haiyan Song, Suresh Gadde, Xuguang Li, Lisheng Wang. Co-inhibition of mTORC1, HDAC and ESR1α Regards the Growth of Triple Negative Breast Cancer and Suppresses Cancer Stem Cells. Cell Death and Disease 2018; 9(8): 815 doi: 10.1038/s41419-018-0811-7). **Impact Factor 5.9**
5. **Andrew Sulaiman**, Sarah McGarry, Li Li, Deyong Jia, Sarah Ooi, Christina Addison, Jim Dimitroulakos, Angel Arnaout, Carolyn Nessim, Zemin Yao, Guang Ji, Haiyan Song, Suresh Gadde, Xuguang Li, Lisheng Wang. Dual inhibition of Wnt and YAP signaling retards the growth of both mesenchymal and epithelial TNBC. *Molecular Oncology*, 2018; 12(4):423-440. **Impact Factor 5.3**
6. **Andrew Sulaiman** and Lisheng Wang. Bridging the divide: preclinical research discrepancies between triple-negative breast cancer cell lines and patient tumors. *Oncotarget*, 2017; 8(68): 113269–113281 **Impact Factor 5.1**
7. Deyong Jia, Li Li, **Andrew Sulaiman**, David Allan, Xuguang Li, Jonathan Lee, Zemin Yao, Danial Figeys, Lisheng Wang. An autocrine inflammatory forward-feedback loop after chemotherapy withdrawal facilitates the repopulation of drug-resistant breast cancer cells. *Cell Death and Disease*, 2017;8(7):e2932 **Impact Factor 5.9**
8. **Andrew Sulaiman**, Zemin Yao and Lisheng Wang. Re-evaluating the role of epithelial-mesenchymal-transition in cancer progression. *Journal of Biomedical Research*, 2017; 31(0): 1–10
9. **Andrew Sulaiman**, Li Li, and Lisheng Wang. E-cadherin adhesion-mediated Wnt activation for mesoderm specification in human embryonic stem cells needs a soft mattress. *Stem Cell Investigations*, 2016; 3: 77
10. **Andrew Sulaiman**, Brandon Sulaiman, Lara Khouri, Sarah McGarry, Carolyn Nessim, Angel Arnaout, Sean Xuguang Li, Christina Addison, Jim Dimitroulakos, and Lisheng Wang. Both bulk and CSC subpopulations in TNBC are susceptible to Wnt, HDAC and ERα co-inhibition. *FEBS Letters*, 2017;590(24):4606-4616. **Impact Factor 3.1**

CONFERENCES/PRESENTATIONS

Oral Presentations

- Sulaiman, Andrew. (May 2018) "Nanoparticle Encapsulated Wnt and YAP Inhibitors for the Treatment of Triple Negative Breast Cancer Using Patient Derived Xenograft Models" *BMI Scientific Symposium,* Ottawa, ON.
- Sulaiman, Andrew. (March 2018) "The Roles of Wnt, and YAP and their Effects on CSC Enrichment in Triple Negative Breast Cancer" *University of Ottawa Faculty of Medicine, Seminar Day*. Ottawa, ON. BMI Seminar Day Winner, 3rd Place Amongst PhD Candidates
- Sulaiman, Andrew. (June 2017) "Investigating Epithelial and Mesenchymal Triple Negative Breast Cancer Plasticity: Identification of Duel Wnt and YAP Susceptibility for Effective Tumor Targeting " *EACR-AACR-SIC 2017: From Cancer Biology to the Clinic*. Florence, Italy.
- Sulaiman, Andrew. (March 2016) "Co-Inhibition of HDAC, mTORC1, and ER Pathways to Target Triple Negative Breast Cancer and CSCs" *University of Ottawa Faculty of Medicine, Seminar Day*. Ottawa, ON.
- Sulaiman, Andrew. (November 2015) "Targeting HDACs, MTORC1 and Endocrine Pathways to Overcome Triple Negative Breast Cancer " *University of Ottawa Faculty of Medicine Work In Progress Seminar*. Ottawa, ON.
- Sulaiman, Andrew. (May 2015) "Targeting HDACs, MTORC1 and the WNT/B-Catenin/TCF4 Pathway to Overcome Anti-Estrogen Resistant Breast Cancer." *Ottawa Institute of Systems Biology Symposium*. Tremblant, QB.

Poster Presentations

- Sulaiman, Andrew. (November 2018) "Combinational Nanotherapy Using Clinically Translatable TNBC PDX Models to Retard Tumor Growth and Tumorigenicity" *Journee Pharee, 2018*. Bromont, Canada.
- Sulaiman, Andrew. (July 2018) **"**Nanoparticle Encapsulated Wnt and YAP Inhibitors for the Treatment of Triple Negative Breast Cancer Using Patient Derived Xenograft Models" *European Association of Cancer Research 25th Biannual Congress***.** Amsterdam, Netherlands.
- Sulaiman, Andrew. (November 2017) "Epithelial and mesenchymal breast cancer stem cell plasticity and the differential regulation of Wnt and YAP in TNBC " *Journee Pharee, 2017*. Bromont, Canada.
- Sulaiman, Andrew. (May 2017) "An autocrine inflammatory loop after chemotherapy withdrawal facilitates the repopulation of drug-resistant breast cancer cells" *60th annual Canadian Society for Molecular Biosciences conference*. Ottawa, ON.
- Sulaiman, Andrew. (May 2017) "Dual inhibition of Wnt and YAP pathways retards the growth of both mesenchymal and epithelial TNBC " *60th annual Canadian Society for Molecular Biosciences conference*. Ottawa, ON.
- Sulaiman, Andrew. (May 2017) "A model for epithelial and mesenchymal breast cancer stem cell conversion and the identification of Wnt and YAP as potent inhibitors of TNBC" *University of Ottawa Faculty of Medicine, BMI Poster Day*. Ottawa, ON.
- Sulaiman, Andrew. (December 2016) "A model for epithelial and mesenchymal breast cancer stem cell conversion in TNBC to identify sensitivities within patient samples" *Journee Phare, 2016*. Bromont, Canada.

- Sulaiman, Andrew. (November 2016) "Modeling epithelial and mesenchymal conversion in TNBC to identify sensitivities within breast cancer stem cell populations " *Ottawa University, Student Recruitment Seminar, 2016*. Ottawa, Canada.
- Sulaiman, Andrew. (November 2016) "*World Life Science Conference 2016*. Beijing, China.
- Sulaiman, Andrew. (May 2015) "Targeting HDACs, MTORC1, and the Wnt/β-Catenin/TCF4 Pathway for Overcoming Anti-Estrogen Resistant Breast Cancer" *University of Ottawa Faculty of Medicine, BMI Poster Day*. Ottawa, ON.

Acknowledgements

- Tyng-Shyan Huang, Li Li, Lilian Moalim-Nour, Deyong Jia, Jian Bai, Zemin Yao, Steffany A. L. Bennett, Daniel Figeys and Lisheng Wang. A Regulatory Network Involving β-Catenin, e-Cadherin, PI3k/Akt, and Slug Balances Self-Renewal and Differentiation of Human Pluripotent Stem Cells In Response to Wnt Signaling. *Stem Cells*, (2015) **33** (5): 1419-1433.
- Sarah E. McGarry. A Tightrope Walk Towards the Easter Rising Centenary in 2016. *The Mirror*, 2015.

HONOURS AND AWARDS

- NSERC CGS –Michael Smith Foreign Study Supplement, 2019 $6,000
- University of Ottawa Excellence Scholarship, 2019 $7,500
- NSERC CGS-D, $70,000
  Alexander Graham Bell Canada Graduate Scholarship-Doctoral, 2018-2020
  Ranked 8th amongst all PhD students in Cellular and Molecular Biology in Canada
- Ontario Graduate Scholarship, 2018 (I declined this award) $15,000
- Canada Research Scholars' Exchange to Shanghai, China, 2019 $7,000
- University of Ottawa- Leadership Award, 2018
- University of Ottawa- Biochemistry Program Award for Excellence, 2018
- Eva Princz Memorial Travel Bursary, 2018 $1,000
- Winner of BMI Seminar Day amongst the PhD Candidates (3rd Place), 2018
- Judith R. Raymond Scholarship in Cancer Research, 2018 $5,000
- University of Ottawa Excellence Scholarship, 2018 $7,500
- Canadian Cancer Society Travel Award Recipient, 2017 $1,750
- Judith R. Raymond Scholarship in Cancer Research, 2017 $10,000
- Ontario Graduate Scholarship, 2017 $15,000
- University of Ottawa Excellence Scholarship, 2017 $7,500
- Abstract Selection to present proffered paper at EACR-AACR-SIC 2017
- Travel Award, World Life Science Conference 2016 $1,000
- University of Ottawa Doctoral Scholarship, 2016-2017 $10,000
- University of Ottawa Master to PhD Transfer Exam, Ottawa University, 2016
- Dean's List, Carleton University, 2014
- Admission Scholarship, Carleton University, 2010 $2,000
- Ontario Scholar, Father Michael McGivney Catholic Academy, 2010
- Honeywell Presidential Scholarship, Honeywell, 2008

Education

- Ph.D. Biochemistry- University of Ottawa
- B.Sc. with Honors in Biochemistry and Biotechnology – Carleton University

References

Abdullah, LN, Chow, EK-H (2013) Mechanisms of chemoresistance in cancer stem cells. *Clinical and translational medicine* **2**, 3.

Abouelmagd, SA, Sun, B, Chang, AC, Ku, YJ, Yeo, Y (2015) Release kinetics study of poorly water-soluble drugs from nanoparticles: are we doing it right? *Molecular pharmaceutics* **12**, 997-1003.

Abraham, RT, Gibbons, JJ (2007) The mammalian target of rapamycin signaling pathway: twists and turns in the road to cancer therapy. *Clinical cancer research* **13**, 3109-3114.

Abubaker, K, Latifi, A, Luwor, R, Nazaretian, S, Zhu, H, Quinn, MA, Thompson, EW, Findlay, JK, Ahmed, N (2013) Short-term single treatment of chemotherapy results in the enrichment of ovarian cancer stem cell-like cells leading to an increased tumor burden. *Molecular cancer* **12**, 24.

Acerbi, I, Cassereau, L, Dean, I, Shi, Q, Au, A, Park, C, Chen, Y, Liphardt, J, Hwang, E, Weaver, V (2015) Human breast cancer invasion and aggression correlates with ECM stiffening and immune cell infiltration. *Integrative Biology* **7**, 1120-1134.

Aceto, N, Bardia, A, Miyamoto, DT, Donaldson, MC, Wittner, BS, Spencer, JA, Yu, M, Pely, A, Engstrom, A, Zhu, H (2014) Circulating tumor cell clusters are oligoclonal precursors of breast cancer metastasis. *Cell* **158**, 1110-1122.

Ademuyiwa, FO, Li, S, Skinner, T, Hoshower, J, Luo, J, Ma, CX, Weilbaecher, KN, Naughton, M, Hernandez-Aya, LF, Mardis, ER(2016) A co-clinical phase II trial of carboplatin and docetaxel as neoadjuvant treatment for triple negative breast cancer with genomic discovery analysis. *Journal of Clinical Oncology* **34**, no. 15 supplementory

Akama, KT, McEwen, BS (2003) Estrogen stimulates postsynaptic density-95 rapid protein synthesis via the Akt/protein kinase B pathway. *Journal of Neuroscience* **23**, 2333-2339.

Al-Hajj, M, Wicha, MS, Benito-Hernandez, A, Morrison, SJ, Clarke, MF (2003a) Prospective identification of tumorigenic breast cancer cells. *Proceedings of the National Academy of Sciences* **100**, 3983-3988.

Anastas, JN, Moon, RT (2013) WNT signalling pathways as therapeutic targets in cancer. *Nature reviews. Cancer* **13**, 11-26.

Anders, CK, Carey, LA (2009) Biology, metastatic patterns, and treatment of patients with triple-negative breast cancer. *Clinical breast cancer* **9**, S73-S81.

Andrade, D, Mehta, M, Griffith, J, Panneerselvam, J, Srivastava, A, Kim, T-D, Janknecht, R, Herman, T, Ramesh, R, Munshi, A (2017) YAP1 inhibition radiosensitizes triple negative breast cancer cells by targeting the DNA damage response and cell survival pathways. *Oncotarget* **8**, 98495.

Andriani, F, Bertolini, G, Facchinetti, F, Baldoli, E, Moro, M, Casalini, P, Caserini, R, Milione, M, Leone, G, Pelosi, G (2016) Conversion to stem-cell state in response to microenvironmental cues is regulated by

balance between epithelial and mesenchymal features in lung cancer cells. *Molecular oncology* **10**, 253-271.

Angeloni, V, Tiberio, P, Appierto, V, Daidone, MG(2015) Implications of stemness-related signaling pathways in breast cancer response to therapy. *Seminars in cancer biology* **31**, 43-51.

Aref, AR, Huang, RY-J, Yu, W, Chua, K-N, Sun, W, Tu, T-Y, Bai, J, Sim, W-J, Zervantonakis, IK, Thiery, JP (2013) Screening therapeutic EMT blocking agents in a three-dimensional microenvironment. *Integrative Biology* **5**, 381-389.

Arnold, J, Barbezetto, I, Birngruber, R, Bressler, N, Bressler, S, Donati, G, Fish, G, Flaxel, C, Gragoudas, E, Harvey, P (2001) Verteporfin therapy of subfoveal choroidal neovascularization in age-related macular degeneration: two-year results of a randomized clinical trial including lesions with occult with no classic choroidal neovascularization-verteporfin in photodynamic therapy report 2. *American journal of ophthalmology* **131**, 541-560.

Azzolin, L, Panciera, T, Soligo, S, Enzo, E, Bicciato, S, Dupont, S, Bresolin, S, Frasson, C, Basso, G, Guzzardo, V, Fassina, A, Cordenonsi, M, Piccolo, S (2014) YAP/TAZ incorporation in the beta-catenin destruction complex orchestrates the Wnt response. *Cell* **158**, 157-170.

Badve, S, Dabbs, DJ, Schnitt, SJ, Baehner, FL, Decker, T, Eusebi, V, Fox, SB, Ichihara, S, Jacquemier, J, Lakhani, SR (2011) Basal-like and triple-negative breast cancers: a critical review with an emphasis on the implications for pathologists and oncologists. *Modern Pathology* **24**, 157.

Balkwill, FR, Capasso, M, Hagemann, T(2012) The tumor microenvironment at a glance. Journal of Cell Science **125**, 5591-5596

Baluk, P, Hashizume, H, McDonald, DM (2005) Cellular abnormalities of blood vessels as targets in cancer. *Current opinion in genetics & development* **15**, 102-111.

Barrett, T, Wilhite, SE, Ledoux, P, Evangelista, C, Kim, IF, Tomashevsky, M, Marshall, KA, Phillippy, KH, Sherman, PM, Holko, M (2012) NCBI GEO: archive for functional genomics data sets—update. *Nucleic acids research* **41**, D991-D995.

Barrett, T, Wilhite, SE, Ledoux, P, Evangelista, C, Kim, IF, Tomashevsky, M, Marshall, KA, Phillippy, KH, Sherman, PM, Holko, M (2013) NCBI GEO: archive for functional genomics data sets—update. *Nucleic acids research* **41**, D991-D995.

Bastid, J (2012) EMT in carcinoma progression and dissemination: facts, unanswered questions, and clinical considerations. *Cancer and Metastasis Reviews* **31**, 277-283.

Basu, S, Totty, NF, Irwin, MS, Sudol, M, Downward, J (2003) Akt phosphorylates the Yes-associated protein, YAP, to induce interaction with 14-3-3 and attenuation of p73-mediated apoptosis. *Mol Cell* **11**, 11-23.

Bauer, KR, Brown, M, Cress, RD, Parise, CA, Caggiano, V (2007) Descriptive analysis of estrogen receptor (ER)-negative, progesterone receptor (PR)-negative, and HER2-negative invasive breast cancer, the so-called triple-negative phenotype. *Cancer* **109**, 1721-1728.

Beerling, E, Seinstra, D, de Wit, E, Kester, L, van der Velden, D, Maynard, C, Schafer, R, van Diest, P, Voest, E, van Oudenaarden, A, Vrisekoop, N, van Rheenen, J (2016) Plasticity between Epithelial and Mesenchymal States Unlinks EMT from Metastasis-Enhancing Stem Cell Capacity. *Cell Rep* **14**, 2281-2288.

Behrens, J, von Kries, JP, Kuhl, M, Bruhn, L, Wedlich, D, Grosschedl, R, Birchmeier, W (1996) Functional interaction of beta-catenin with the transcription factor LEF-1. *Nature* **382**, 638-642.

Bellosta, S, Paoletti, R, Corsini, A (2004) Safety of statins. *Circulation* **109**, III-50-III-57.

Beltran, AS, Rivenbark, AG, Richardson, BT, Yuan, X, Quian, H, Hunt, JP, Zimmerman, E, Graves, LM, Blancafort, P (2011) Generation of tumor-initiating cells by exogenous delivery of OCT4 transcription factor. *Breast cancer research : BCR* **13**, R94.

Benham-Pyle, BW, Pruitt, BL, Nelson, WJ (2015) Cell adhesion. Mechanical strain induces E-cadherin-dependent Yap1 and beta-catenin activation to drive cell cycle entry. *Science* **348**, 1024-1027.

Berger, D, Fiebig, H, Winterhalter, B, Wallbrecher, E, Henss, H (1990) Preclinical phase II study of ifosfamide in human tumour xenografts in vivo. *Cancer chemotherapy and pharmacology* **26**, S7-S11.

Bernhard, EJ, Gruber, SB, Muschel, RJ (1994) Direct evidence linking expression of matrix metalloproteinase 9 (92-kDa gelatinase/collagenase) to the metastatic phenotype in transformed rat embryo cells. *Proceedings of the National Academy of Sciences* **91**, 4293-4297.

Bertotti, A, Migliardi, G, Galimi, F, Sassi, F, Torti, D, Isella, C, Corà, D, Di Nicolantonio, F, Buscarino, M, Petti, C (2011) A molecularly annotated platform of patient-derived xenografts ("xenopatients") identifies HER2 as an effective therapeutic target in cetuximab-resistant colorectal cancer. *Cancer discovery* **1**, 508-523.

Bertrand, N, Wu, J, Xu, X, Kamaly, N, Farokhzad, OC (2014) Cancer nanotechnology: the impact of passive and active targeting in the era of modern cancer biology. *Adv Drug Deliv Rev* **66**, 2-25.

Beyer, TA, Weiss, A, Khomchuk, Y, Huang, K, Ogunjimi, AA, Varelas, X, Wrana, JL (2013) Switch enhancers interpret TGF-beta and Hippo signaling to control cell fate in human embryonic stem cells. *Cell Rep* **5**, 1611-1624.

Bidarra, S, Oliveira, P, Rocha, S, Saraiva, D, Oliveira, C, Barrias, C (2015) A 3D in vitro model to explore the inter-conversion between epithelial and mesenchymal states during EMT and its reversion. *Scientific reports* **6**, 27072-27072.

Binnemars-Postma, K, Storm, G, Prakash, J (2017) Nanomedicine Strategies to Target Tumor-Associated Macrophages. *International journal of molecular sciences* **18**, 979.

Bobo, D, Robinson, KJ, Islam, J, Thurecht, KJ, Corrie, SR (2016) Nanoparticle-based medicines: a review of FDA-approved materials and clinical trials to date. *Pharmaceutical research* **33**, 2373-2387.

Bolós, V, Peinado, H, Pérez-Moreno, MA, Fraga, MF, Esteller, M, Cano, A (2003) The transcription factor Slug represses E-cadherin expression and induces epithelial to mesenchymal transitions: a comparison with Snail and E47 repressors. *Journal of cell science* **116**, 499-511.

Brabletz, T (2012) EMT and MET in metastasis: where are the cancer stem cells? *Cancer cell* **22**, 699-701.

Bray, F, Ferlay, J, Soerjomataram, I, Siegel, RL, Torre, LA, Jemal, A (2018) Global cancer statistics 2018: GLOBOCAN estimates of incidence and mortality worldwide for 36 cancers in 185 countries. *CA: a cancer journal for clinicians* **68**, 394-424.

Briske-Anderson, MJ, Finley, JW, Newman, SM (1997) The influence of culture time and passage number on the morphological and physiological development of Caco-2 cells. *Proceedings of the society for experimental biology and medicine* **214**, 248-257.

Bruna, A, Rueda, OM, Greenwood, W, Batra, AS, Callari, M, Batra, RN, Pogrebniak, K, Sandoval, J, Cassidy, JW, Tufegdzic-Vidakovic, A (2016) A biobank of breast cancer explants with preserved intra-tumor heterogeneity to screen anticancer compounds. *Cell* **167**, 260-274. e222.

Byrne, AT, Alferez, DG, Amant, F, Annibali, D, Arribas, J, Biankin, AV, Bruna, A, Budinska, E, Caldas, C, Chang, DK, Clarke, RB, Clevers, H, Coukos, G, Dangles-Marie, V, Eckhardt, SG, Gonzalez-Suarez, E, Hermans, E, Hidalgo, M, Jarzabek, MA, de Jong, S, Jonkers, J, Kemper, K, Lanfrancone, L, Maelandsmo, GM, Marangoni, E, Marine, J-C, Medico, E, Norum, JH, Palmer, HG, Peeper, DS, Pelicci, PG, Piris-Gimenez, A, Roman-Roman, S, Rueda, OM, Seoane, J, Serra, V, Soucek, L, Vanhecke, D, Villanueva, A, Vinolo, E, Bertotti, A, Trusolino, L (2017) Interrogating open issues in cancer precision medicine with patient-derived xenografts. *Nature reviews. Cancer* **17**, 254-268.

Canadian_Cancer_Statistics_Advisory_Committee. Canadian Cancer Statistics 2018. *Toronto, ON: Canadian Cancer Society; 2018* Available at: cancer.ca/Canadian-Cancer-Statistics-2018-EN (accessed [2001.2009.2019]).

Cano, A, Pérez-Moreno, MA, Rodrigo, I, Locascio, A, Blanco, MJ, del Barrio, MG, Portillo, F, Nieto, MA (2000) The transcription factor snail controls epithelial–mesenchymal transitions by repressing E-cadherin expression. *Nature cell biology* **2**, 76-83.

Cataldi, M, Vigliotti, C, Mosca, T, Cammarota, M, Capone, D (2017) Emerging role of the spleen in the pharmacokinetics of monoclonal antibodies, nanoparticles and exosomes. *International journal of molecular sciences* **18**, 1249.

Cavazzoni, A, Bonelli, MA, Fumarola, C, La Monica, S, Airoud, K, Bertoni, R, Alfieri, RR, Galetti, M, Tramonti, S, Galvani, E (2012) Overcoming acquired resistance to letrozole by targeting the PI3K/AKT/mTOR pathway in breast cancer cell clones. *Cancer letters* **323**, 77-87.

Cerami, E, Gao, J, Dogrusoz, U, Gross, BE, Sumer, SO, Aksoy, BA, Jacobsen, A, Byrne, CJ, Heuer, ML, Larsson, E, Antipin, Y, Reva, B, Goldberg, AP, Sander, C, Schultz, N (2012) The cBio cancer genomics portal: an open platform for exploring multidimensional cancer genomics data. *Cancer Discov* **2**, 401-404.

Chaffer, CL, Brueckmann, I, Scheel, C, Kaestli, AJ, Wiggins, PA, Rodrigues, LO, Brooks, M, Reinhardt, F, Su, Y, Polyak, K (2011) Normal and neoplastic nonstem cells can spontaneously convert to a stem-like state. *Proceedings of the National Academy of Sciences* **108**, 7950-7955.

Chan, KC, Chan, LS, Ip, JCY, Lo, C, Yip, TTC, Ngan, RKC, Wong, RNS, Lo, KW, Ng, WT, Lee, AWM (2015) Therapeutic targeting of CBP/β-catenin signaling reduces cancer stem-like population and synergistically suppresses growth of EBV-positive nasopharyngeal carcinoma cells with cisplatin. *Scientific reports* **5**, 9979.

Charafe-Jauffret, E, Ginestier, C, Iovino, F, Tarpin, C, Diebel, M, Esterni, B, Houvenaeghel, G, Extra, J-M, Bertucci, F, Jacquemier, J (2010) Aldehyde dehydrogenase 1–Positive cancer stem cells mediate metastasis and poor clinical outcome in inflammatory breast cancer. *Clinical cancer research* **16**, 45-55.

Chen, T, Yuan, D, Wei, B, Jiang, J, Kang, J, Ling, K, Gu, Y, Li, J, Xiao, L, Pei, G (2010) E-cadherin-Mediated Cell-Cell Contact is Critical for Induced Pluripotent Stem Cell Generation. *Stem Cells* **28**, Jun 2 [Epub ahead of print] PMID: 20521328

Chen, X, Prywes, R (1999) Serum-induced expression of the cdc25AGene by relief of E2F-mediated repression. *Molecular and Cellular Biology* **19**, 4695-4702.

Choi, SYC, Lin, D, Gout, PW, Collins, CC, Xu, Y, Wang, Y (2014) Lessons from patient-derived xenografts for better in vitro modeling of human cancer. *Advanced drug delivery reviews* **79**, 222-237.

Choo, AY, Yoon, S-O, Kim, SG, Roux, PP, Blenis, J (2008) Rapamycin differentially inhibits S6Ks and 4E-BP1 to mediate cell-type-specific repression of mRNA translation. *Proceedings of the National Academy of Sciences* **105**, 17414-17419.

Christiansen, JJ, Rajasekaran, AK (2006) Reassessing epithelial to mesenchymal transition as a prerequisite for carcinoma invasion and metastasis. *Cancer research* **66**, 8319-8326.

Chui, MH (2013) Insights into cancer metastasis from a clinicopathologic perspective: Epithelial-Mesenchymal Transition is not a necessary step. *Int J Cancer* **132**, 1487-1495.

Coleman, R, Rubens, R (1987) The clinical course of bone metastases from breast cancer. *British journal of cancer* **55**, 61.

Cordenonsi, M, Zanconato, F, Azzolin, L, Forcato, M, Rosato, A, Frasson, C, Inui, M, Montagner, M, Parenti, Anna R, Poletti, A, Daidone, Maria G, Dupont, S, Basso, G, Bicciato, S, Piccolo, S (2011) The Hippo Transducer TAZ Confers Cancer Stem Cell-Related Traits on Breast Cancer Cells. *Cell* **147**, 759-772.

Creighton, CJ, Chang, JC, Rosen, JM (2010) Epithelial-Mesenchymal Transition (EMT) in Tumor-Initiating Cells and Its Clinical Implications in Breast Cancer. *Journal of Mammary Gland Biology and Neoplasia* **15**, 253-260.

Cristofanilli, M, Hayes, DF, Budd, GT, Ellis, MJ, Stopeck, A, Reuben, JM, Doyle, GV, Matera, J, Allard, WJ, Miller, MC (2005) Circulating tumor cells: a novel prognostic factor for newly diagnosed metastatic breast cancer. *Journal of Clinical Oncology* **23**, 1420-1430.

Croker, AK, Allan, AL (2012) Inhibition of aldehyde dehydrogenase (ALDH) activity reduces chemotherapy and radiation resistance of stem-like ALDHhiCD44+ human breast cancer cells. *Breast cancer research and treatment* **133**, 75-87.

Croker, AK, Goodale, D, Chu, J, Postenka, C, Hedley, BD, Hess, DA, Allan, AL (2009) High aldehyde dehydrogenase and expression of cancer stem cell markers selects for breast cancer cells with enhanced malignant and metastatic ability. *Journal of cellular and molecular medicine* **13**, 2236-2252.

Cufi, S, Vazquez-Martin, A, Oliveras-Ferraros, C, Martin-Castillo, B, Vellon, L, Menendez, JA (2011) Autophagy positively regulates the CD44(+) CD24(-/low) breast cancer stem-like phenotype. *Cell Cycle* **10**, 3871-3885.

D'Amico, L, Patane, S, Grange, C, Bussolati, B, Isella, C, Fontani, L, Godio, L, Cilli, M, D'Amelio, P, Isaia, G, Medico, E, Ferracini, R, Roato, I (2013) Primary breast cancer stem-like cells metastasise to bone, switch phenotype and acquire a bone tropism signature. *Br J Cancer* **108**, 2525-2536.

D'Ignazio, L, Batie, M, Rocha, S (2017) Hypoxia and inflammation in cancer, focus on HIF and NF-κB. *Biomedicines* **5**, 21.

Damia, G, D'Incalci, M (2009) Contemporary pre-clinical development of anticancer agents–what are the optimal preclinical models? *European Journal of Cancer* **45**, 2768-2781.

Dandekar, S, Romanos-Sirakis, E, Pais, F, Bhatla, T, Jones, C, Bourgeois, W, Hunger, SP, Raetz, EA, Hermiston, ML, Dasgupta, R, Morrison, DJ, Carroll, WL (2014) Wnt inhibition leads to improved chemosensitivity in paediatric acute lymphoblastic leukaemia. *British journal of haematology* **167**, 87-99.

Daniel, AR, Hagan, CR, Lange, CA (2011) Progesterone receptor action: defining a role in breast cancer. *Expert review of endocrinology & metabolism* **6**, 359-369.

Daniel, KG, Gupta, P, Harbach, RH, Guida, WC, Dou, QP (2004) Organic copper complexes as a new class of proteasome inhibitors and apoptosis inducers in human cancer cells. *Biochemical pharmacology* **67**, 1139-1151.

Daniel, VC, Marchionni, L, Hierman, JS, Rhodes, JT, Devereux, WL, Rudin, CM, Yung, R, Parmigiani, G, Dorsch, M, Peacock, CD (2009) A primary xenograft model of small-cell lung cancer reveals irreversible changes in gene expression imposed by culture in vitro. *Cancer research* **69**, 3364-3373.

Danila, DC, Heller, G, Gignac, GA, Gonzalez-Espinoza, R, Anand, A, Tanaka, E, Lilja, H, Schwartz, L, Larson, S, Fleisher, M (2007) Circulating tumor cell number and prognosis in progressive castration-resistant prostate cancer. *Clinical Cancer Research* **13**, 7053-7058.

Das, T, Safferling, K, Rausch, S, Grabe, N, Boehm, H, Spatz, JP (2015) A molecular mechanotransduction pathway regulates collective migration of epithelial cells. *Nature cell biology* **17**, 276-287.

Davies, C, Pan, H, Godwin, J, Gray, R, Arriagada, R, Raina, V, Abraham, M, Alencar, VHM, Badran, A, Bonfill, X (2013) Long-term effects of continuing adjuvant tamoxifen to 10 years versus stopping at 5 years after diagnosis of oestrogen receptor-positive breast cancer: ATLAS, a randomised trial. *The Lancet* **381**, 805-816.

Davis, FM, Stewart, TA, Thompson, EW, Monteith, GR (2014) Targeting EMT in cancer: opportunities for pharmacological intervention. *Trends in pharmacological sciences* **35**, 479-488.

Dayekh, K, Johnson-Obaseki, S, Corsten, M, Villeneuve, PJ, Sekhon, HS, Weberpals, JI, Dimitroulakos, J (2014) Monensin inhibits epidermal growth factor receptor trafficking and activation: synergistic cytotoxicity in combination with EGFR inhibitors. *Molecular cancer therapeutics* **13**, 2559-2571.

de Cremoux, P, Dalvai, M, N'Doye, O, Moutahir, F, Rolland, G, Chouchane-Mlik, O, Assayag, F, Lehmann-Che, J, Kraus-Berthie, L, Nicolas, A (2015) HDAC inhibition does not induce estrogen receptor in human triple-negative breast cancer cell lines and patient-derived xenografts. *Breast cancer research and treatment* **149**, 81-89.

Dean, M, Fojo, T, Bates, S (2005) Tumour stem cells and drug resistance. *Nature reviews. Cancer* **5**, 275-284.

Debeb, BG, Lacerda, L, Xu, W, Larson, R, Solley, T, Atkinson, R, Sulman, EP, Ueno, NT, Krishnamurthy, S, Reuben, JM, Buchholz, TA, Woodward, WA (2012) Histone deacetylase inhibitors stimulate dedifferentiation of human breast cancer cells through WNT/beta-catenin signaling. *Stem Cells* **30**, 2366-2377.

Dent, R, Trudeau, M, Pritchard, KI, Hanna, WM, Kahn, HK, Sawka, CA, Lickley, LA, Rawlinson, E, Sun, P, Narod, SA (2007) Triple-negative breast cancer: clinical features and patterns of recurrence. *Clinical cancer research* **13**, 4429-4434.

DeRose, YS, Gligorich, KM, Wang, G, Georgelas, A, Bowman, P, Courdy, SJ, Welm, AL, Welm, BE (2013) Patient-Derived Models of Human Breast Cancer: Protocols for In Vitro and In Vivo Applications in Tumor Biology and Translational Medicine. *Current protocols in pharmacology*, 14.23. 11-14.23. 43.

DeRose, YS, Wang, G, Lin, Y-C, Bernard, PS, Buys, SS, Ebbert, MT, Factor, R, Matsen, C, Milash, BA, Nelson, E (2011) Tumor grafts derived from women with breast cancer authentically reflect tumor pathology, growth, metastasis and disease outcomes. *Nature medicine* **17**, 1514-1520.

Dey, N, Young, B, Abramovitz, M, Bouzyk, M, Barwick, B, De, P, Leyland-Jones, B (2013) Differential activation of Wnt-beta-catenin pathway in triple negative breast cancer increases MMP7 in a PTEN dependent manner. *PLoS One* **8**, e77425.

Dias, K, Dvorkin-Gheva, A, Hallett, RM, Wu, Y, Hassell, J, Pond, GR, Levine, M, Whelan, T, Bane, AL (2017) Claudin-low breast cancer; clinical & pathological characteristics. *PloS one* **12**, e0168669.

Diaz, V, Vinas-Castells, R, García de Herreros, A (2014) Regulation of the protein stability of EMT transcription factors. *Cell adhesion & migration* **8**, 418-428.

Dieci, MV, Orvieto, E, Dominici, M, Conte, P, Guarneri, V (2014) Rare breast cancer subtypes: histological, molecular, and clinical peculiarities. *The oncologist* **19**, 805-813.

do Nascimento Gonçalves, N, Colombo, J, Lopes, JR, Gelaleti, GB, Moschetta, MG, Sonehara, NM, Hellmén, E, de Freitas Zanon, C, Oliani, SM, de Campos Zuccari, DAP (2016) Effect of Melatonin in Epithelial Mesenchymal Transition Markers and Invasive Properties of Breast Cancer Stem Cells of Canine and Human Cell Lines. *PloS one* **11**, e0150407.

Drevs, J, Hofmann, I, Hugenschmidt, H, Wittig, C, Madjar, H, Müller, M, Wood, J, Martiny-Baron, G, Unger, C, Marmé, D (2000) Effects of PTK787/ZK 222584, a specific inhibitor of vascular endothelial growth factor

receptor tyrosine kinases, on primary tumor, metastasis, vessel density, and blood flow in a murine renal cell carcinoma model. *Cancer research* **60**, 4819-4824.

Du, L, Li, Y-J, Fakih, M, Wiatrek, RL, Duldulao, M, Chen, Z, Chu, P, Garcia-Aguilar, J, Chen, Y (2016) Role of SUMO activating enzyme in cancer stem cell maintenance and self-renewal. *Nature communications* **7**.

Ducker, GS, Atreya, CE, Simko, JP, Hom, YK, Matli, MR, Benes, CH, Hann, B, Nakakura, EK, Bergsland, EK, Donner, DB (2014) Incomplete inhibition of phosphorylation of 4E-BP1 as a mechanism of primary resistance to ATP-competitive mTOR inhibitors. *Oncogene* **33**, 1590-1600.

Dupont, S, Morsut, L, Aragona, M, Enzo, E, Giulitti, S, Cordenonsi, M, Zanconato, F, Le Digabel, J, Forcato, M, Bicciato, S, Elvassore, N, Piccolo, S (2011b) Role of YAP/TAZ in mechanotransduction. *Nature* **474**, 179-183.

Dutertre, Martin, and Carolyn L. Smith (2000) "Molecular mechanisms of selective estrogen receptor modulator (SERM) action." *Journal of Pharmacology and Experimental Therapeutics* **295**, 431-437.

Economopoulou, P, Kaklamani, VG, Siziopikou, K (2012) The role of cancer stem cells in breast cancer initiation and progression: potential cancer stem cell-directed therapies. *The oncologist* **17**, 1394-1401.

Edgar, R, Domrachev, M, Lash, AE (2002) Gene Expression Omnibus: NCBI gene expression and hybridization array data repository. *Nucleic acids research* **30**, 207-210.

Ehmer, U, Sage, J (2016) Control of proliferation and cancer growth by the Hippo signaling pathway. *Molecular Cancer Research* **14**, 127-140.

El-Khoueiry, A, Ning, Y, Yang, D, Cole, S, Kahn, M, Zoghbi, M, Berg, J, Fujimori, M, Inada, T, Kouji, H (2013) A phase I first-in-human study of PRI-724 in patients (pts) with advanced solid tumors. *Journal of Clinical Oncology* **31 (**15_suppl), 2501-2501.

El-Shenawy, NS, Hamza, RZ (2016) Nephrotoxicity of sodium valproate and protective role of L-cysteine in rats at biochemical and histological levels. *Journal of basic and clinical physiology and pharmacology* **27**, 497-504.

El Helou, R, Pinna, G, Cabaud, O, Wicinski, J, Bhajun, R, Guyon, L, Rioualen, C, Finetti, P, Gros, A, Mari, B (2017) miR-600 acts as a bimodal switch that regulates breast cancer stem cell fate through WNT signaling. *Cell reports* **18**, 2256-2268.

Ellison-Zelski, SJ, Solodin, NM, Alarid, ET (2009) Repression of ESR1 through actions of estrogen receptor alpha and Sin3A at the proximal promoter. *Molecular and cellular biology* **29**, 4949-4958.

Fan, R, Kim, N-G, Gumbiner, BM (2013a) Regulation of Hippo pathway by mitogenic growth factors via phosphoinositide 3-kinase and phosphoinositide-dependent kinase-1. *Proceedings of the National Academy of Sciences* **110**, 2569-2574.

Fan, R, Kim, NG, Gumbiner, BM (2013b) Regulation of Hippo pathway by mitogenic growth factors via phosphoinositide 3-kinase and phosphoinositide-dependent kinase-1. *Proc Natl Acad Sci U S A* **110**, 2569-2574.

Fantozzi, A, Christofori, G (2006) Mouse models of breast cancer metastasis. *Breast Cancer Research* **8**, 212.

Ferlay, J, Soerjomataram, I, Dikshit, R, Eser, S, Mathers, C, Rebelo, M, Parkin, DM, Forman, D, Bray, F (2015) Cancer incidence and mortality worldwide: sources, methods and major patterns in GLOBOCAN 2012. *International journal of cancer* **136**, E359-E386.

Fillmore, CM, Kuperwasser, C (2008) Human breast cancer cell lines contain stem-like cells that self-renew, give rise to phenotypically diverse progeny and survive chemotherapy. *Breast cancer research : BCR* **10**, R25.

Finger, EC, Giaccia, AJ (2010) Hypoxia, inflammation, and the tumor microenvironment in metastatic disease. *Cancer and Metastasis Reviews* **29**, 285-293.

Fischer, KR, Durrans, A, Lee, S, Sheng, J, Li, F, Wong, ST, Choi, H, El Rayes, T, Ryu, S, Troeger, J (2015) Epithelial-to-mesenchymal transition is not required for lung metastasis but contributes to chemoresistance. *Nature* **527**, 472-476.

Flinn, IW, Miller, CB, Ardeshna, KM, Tetreault, S, Assouline, SE, Zinzani, PL, Mayer, J, Merli, M, Lunin, SD, Pettitt, AR(2016) Dynamo: A Phase 2 Study Demonstrating the Clinical Activity of Duvelisib in Patients with Relapsed Refractory Indolent Non-Hodgkin Lymphoma. *Blood* **128** (22), 1218

Forsythe, JA, Jiang, B-H, Iyer, NV, Agani, F, Leung, SW, Koos, RD, Semenza, GL (1996) Activation of vascular endothelial growth factor gene transcription by hypoxia-inducible factor 1. *Molecular and cellular biology* **16**, 4604-4613.

Fortunati, N, Bertino, S, Costantino, L, De Bortoli, M, Compagnone, A, Bandino, A, Catalano, MG, Boccuzzi, G (2010) Valproic acid restores ER alpha and antiestrogen sensitivity to ER alpha-negative breast cancer cells. *Molecular and cellular endocrinology* **314**, 17-22.

Franken, L, Klein, M, Spasova, M, Elsukova, A, Wiedwald, U, Welz, M, Knolle, P, Farle, M, Limmer, A, Kurts, C (2015) Splenic red pulp macrophages are intrinsically superparamagnetic and contaminate magnetic cell isolates. *Scientific reports* **5**, 12940.

Frasor, J, Danes, JM, Komm, B, Chang, KC, Lyttle, CR, Katzenellenbogen, BS (2003) Profiling of estrogen up-and down-regulated gene expression in human breast cancer cells: insights into gene networks and pathways underlying estrogenic control of proliferation and cell phenotype. *Endocrinology* **144**, 4562-4574.

Friedl, P, Wolf, K (2003) Tumour-cell invasion and migration: diversity and escape mechanisms. *Nature reviews. Cancer* **3**, 362-374.

Friedrichs, WE, Russell, DH, Donzis, EJ, Middleton, AK, Silva, JM, Roth, RA, Hidalgo, M (2004) Inhibition of mTOR activity restores tamoxifen response in breast cancer cells with aberrant Akt Activity. *Clinical Cancer Research* **10**, 8059-8067.

Frixen, UH, Behrens, J, Sachs, M, Eberle, G, Voss, B, Warda, A, Löchner, D, Birchmeier, W (1991) E-cadherin-mediated cell-cell adhesion prevents invasiveness of human carcinoma cells. *The Journal of cell biology* **113**, 173-185.

Fu, A, Ma, S, Wei, N, Tan, BXX, Tan, EY, Luo, KQ (2016) High expression of MnSOD promotes survival of circulating breast cancer cells and increases their resistance to doxorubicin. *Oncotarget* **7**, 50257-50275.

Fu, Q, Chen, Z, Gong, X, Cai, Y, Chen, Y, Ma, X, Zhu, R, Jin, J (2015) beta-Catenin expression is regulated by an IRES-dependent mechanism and stimulated by paclitaxel in human ovarian cancer cells. *Biochem Biophys Res Commun* **461**, 21-27.

Fuerer, C, Nusse, R (2010) Lentiviral vectors to probe and manipulate the Wnt signaling pathway. *PloS one* **5**, e9370.

Gadde, S (2015) Multi-drug delivery nanocarriers for combination therapy. *MedChemComm*. **6**(11), 1916-1929

Gao, H, Korn, JM, Ferretti, S, Monahan, JE, Wang, Y, Singh, M, Zhang, C, Schnell, C, Yang, G, Zhang, Y (2015) High-throughput screening using patient-derived tumor xenografts to predict clinical trial drug response. *Nature medicine* **21**, 1318.

Gao, J, Aksoy, BA, Dogrusoz, U, Dresdner, G, Gross, B, Sumer, SO, Sun, Y, Jacobsen, A, Sinha, R, Larsson, E (2013) Integrative analysis of complex cancer genomics and clinical profiles using the cBioPortal. *Science signaling* **6**, pl1.

Garber, K (2002) Angiogenesis inhibitors suffer new setback. *Nature biotechnology* **20**, 1067-1068.

Garg, M (2013) Epithelial-mesenchymal transition - activating transcription factors - multifunctional regulators in cancer. *World journal of stem cells* **5**, 188-195.

Geyer, CE, O'Shaughnessy, J, Untch, M, Sikov, W, Rugo, HS, McKee, MD, Huober, JB, Golshan, M, Giranda, VL, Minckwitz, GV, Maag, D, Sullivan, DM, Wolmark, N, McIntyre, K, Lorenzo, JJP, Filho, OM, Rastogi, P, Symmans, WF, Liu, X, Loibl, S (2017) Phase 3 study evaluating efficacy and safety of veliparib (V) plus carboplatin (Cb) or Cb in combination with standard neoadjuvant chemotherapy (NAC) in patients (pts) with early stage triple-negative breast cancer (TNBC). *Journal of Clinical Oncology* **35**, 520-520.

Ginestier, C, Hur, MH, Charafe-Jauffret, E, Monville, F, Dutcher, J, Brown, M, Jacquemier, J, Viens, P, Kleer, CG, Liu, S (2007) ALDH1 is a marker of normal and malignant human mammary stem cells and a predictor of poor clinical outcome. *Cell stem cell* **1**, 555-567.

Gómez-Miragaya, J, Palafox, M, Paré, L, Yoldi, G, Ferrer, I, Vila, S, Galván, P, Pellegrini, P, Pérez-Montoyo, H, Igea, A (2017) Resistance to Taxanes in Triple-Negative Breast Cancer Associates with the Dynamics of a CD49f+ Tumor-Initiating Population. *Stem cell reports* **8**, 1392-1407.

Gong, C, Yao, H, Liu, Q, Chen, J, Shi, J, Su, F, Song, E (2010) Markers of tumor-initiating cells predict chemoresistance in breast cancer. *PloS one* **5**, e15630.

Green, JL, La, J, Yum, KW, Desai, P, Rodewald, LW, Zhang, X, Leblanc, M, Nusse, R, Lewis, MT, Wahl, GM (2013) Paracrine Wnt signaling both promotes and inhibits human breast tumor growth. *Proc Natl Acad Sci U S A* **110**, 6991-6996.

Gregory, PA, Bracken, CP, Smith, E, Bert, AG, Wright, JA, Roslan, S, Morris, M, Wyatt, L, Farshid, G, Lim, Y-Y (2011) An autocrine TGF-β/ZEB/miR-200 signaling network regulates establishment and maintenance of epithelial-mesenchymal transition. *Molecular biology of the cell* **22**, 1686-1698.

Grosse-Wilde, A, d'Hérouël, AF, McIntosh, E, Ertaylan, G, Skupin, A, Kuestner, RE, del Sol, A, Walters, K-A, Huang, S (2015) Stemness of the hybrid epithelial/mesenchymal state in breast cancer and its association with poor survival. *PLoS One* **10**, e0126522.

Guilhamon, P, Butcher, LM, Presneau, N, Wilson, GA, Feber, A, Paul, DS, Schütte, M, Haybaeck, J, Keilholz, U, Hoffman, J (2014) Assessment of patient-derived tumour xenografts (PDXs) as a discovery tool for cancer epigenomics. *Genome medicine* **6**, 116.

Gunasinghe, NP, Wells, A, Thompson, EW, Hugo, HJ (2012) Mesenchymal-epithelial transition (MET) as a mechanism for metastatic colonisation in breast cancer. *Cancer metastasis reviews* **31**, 469-478.

Guo, S, Wang, Y, Miao, L, Xu, Z, Lin, CM, Zhang, Y, Huang, L (2013) Lipid-coated cisplatin nanoparticles induce neighboring effect and exhibit enhanced anticancer efficacy. *ACS nano* **7**, 9896-9904.

Gupta, GP, Massague, J (2006) Cancer metastasis: building a framework. *Cell* **127**, 679-695.

Gupta, PB, Chaffer, CL, Weinberg, RA (2009a) Cancer stem cells: mirage or reality? *Nat Med* **15**, 1010-1012.

Gupta, PB, Onder, TT, Jiang, G, Tao, K, Kuperwasser, C, Weinberg, RA, Lander, ES (2009b) Identification of selective inhibitors of cancer stem cells by high-throughput screening. *Cell* **138**, 645-659.

Han, H, Diéras, V, Robson, M, Palácová, M, Marcom, P, Jager, A, Bondarenko, I, Citrin, D, Campone, M, Telli, M, Domchek, S, Friedlander, M, Kaufman, B, Ratajczak, C, Coates, A, Bonnet, P, Qin, Q, Qian, J, Giranda, V, Shepherd, S, Isakoff, S, Puhalla, S (2017) Abstract S2-05: Efficacy and tolerability of veliparib (V; ABT-888) in combination with carboplatin (C) and paclitaxel (P) vs placebo (Plc)+C/P in patients (pts) with BRCA1 or BRCA2 mutations and metastatic breast cancer: A randomized, phase 2 study. *Cancer research* **77**, S2-05-S02-05.

Han, JS, Crowe, DL (2009) Tumor initiating cancer stem cells from human breast cancer cell lines. *International journal of oncology* **34**, 1449-1453.

Harrison, H, Simoes, BM, Rogerson, L, Howell, SJ, Landberg, G, Clarke, RB (2013) Oestrogen increases the activity of oestrogen receptor negative breast cancer stem cells through paracrine EGFR and Notch signalling. *Breast cancer research : BCR* **15**, R21.

Hashizume, H, Baluk, P, Morikawa, S, McLean, JW, Thurston, G, Roberge, S, Jain, RK, McDonald, DM (2000) Openings between defective endothelial cells explain tumor vessel leakiness. *The American journal of pathology* **156**, 1363-1380.

Hassiotou, F, Hepworth, AR, Beltran, AS, Mathews, MM, Stuebe, AM, Hartmann, PE, Filgueira, L, Blancafort, P (2013) Expression of the Pluripotency Transcription Factor OCT4 in the Normal and Aberrant Mammary Gland. *Front Oncol* **3**, 79.

Hay, ED (1968) Organization and fine structure of epithelium and mesenchyme in the developing chick embryo. *Epithelial-mesenchymal interactions* **2**, 31-35.

Hebert, SA, Bohan, TP, Erikson, CL, Swinford, RD (2017) Thrombotic microangiopathy associated with Valproic acid toxicity. *BMC nephrology* **18**, 262.

Hecht, JR, Trarbach, T, Hainsworth, JD, Major, P, Jäger, E, Wolff, RA, Lloyd-Salvant, K, Bodoky, G, Pendergrass, K, Berg, W (2011) Randomized, placebo-controlled, phase III study of first-line oxaliplatin-based chemotherapy plus PTK787/ZK 222584, an oral vascular endothelial growth factor receptor inhibitor, in patients with metastatic colorectal adenocarcinoma. *Journal of Clinical Oncology* **29**, 1997-2003.

Hemmati, HD, Nakano, I, Lazareff, JA, Masterman-Smith, M, Geschwind, DH, Bronner-Fraser, M, Kornblum, HI (2003) Cancerous stem cells can arise from pediatric brain tumors. *Proc Natl Acad Sci U S A* **100**, 15178-15183.

Hernandez, RK, Sørensen, HT, Pedersen, L, Jacobsen, J, Lash, TL (2009) Tamoxifen treatment and risk of deep venous thrombosis and pulmonary embolism: a Danish population-based cohort study. *Cancer: Interdisciplinary International Journal of the American Cancer Society* **115**, 4442-4449.

Hidalgo, M, Amant, F, Biankin, AV, Budinská, E, Byrne, AT, Caldas, C, Clarke, RB, de Jong, S, Jonkers, J, Mælandsmo, GM (2014) Patient-derived xenograft models: an emerging platform for translational cancer research. *Cancer discovery* **4**, 998-1013.

Hiscox, S, Baruha, B, Smith, C, Bellerby, R, Goddard, L, Jordan, N, Poghosyan, Z, Nicholson, RI, Barrett-Lee, P, Gee, J (2012) Overexpression of CD44 accompanies acquired tamoxifen resistance in MCF7 cells and augments their sensitivity to the stromal factors, heregulin and hyaluronan. *BMC Cancer* **12**, 458.

Hlushchuk, R, Barré, S, Djonov, V (2016) Morphological Aspects of Tumor Angiogenesis. *Tumor Angiogenesis Assays: Methods and Protocols*, 13-24.

Horimoto, Y, Arakawa, A, Sasahara, N, Tanabe, M, Sai, S, Himuro, T, Saito, M (2016) Combination of Cancer Stem Cell Markers CD44 and CD24 Is Superior to ALDH1 as a Prognostic Indicator in Breast Cancer Patients with Distant Metastases. *PloS one* **11**, e0165253.

Hou, M-F, Lin, S-B, Yuan, S-SF, Tsai, S-M, Wu, S-H, Ou-Yang, F, Hsieh, J-S, Tsai, K-B, Huang, T-J, Tsai, L-Y (2003) The clinical significance between activation of nuclear factor kappa B transcription factor and overexpression of HER-2/neu oncoprotein in Taiwanese patients with breast cancer. *Clinica chimica acta* **334**, 137-144.

Houshdaran, S, Hawley, S, Palmer, C, Campan, M, Olsen, MN, Ventura, AP, Knudsen, BS, Drescher, CW, Urban, ND, Brown, PO (2010) DNA methylation profiles of ovarian epithelial carcinoma tumors and cell lines. *PloS one* **5**, e9359.

Hu, T, Li, C (2010) Convergence between Wnt-beta-catenin and EGFR signaling in cancer. *Mol Cancer* **9**, 236.

Huang, T, Chen, Z, Fang, L (2013) Curcumin inhibits LPS-induced EMT through downregulation of NF-kappaB-Snail signaling in breast cancer cells. *Oncology reports* **29**, 117-124.

Huang, TS, Li, L, Moalim-Nour, L, Jia, D, Bai, J, Yao, Z, Bennett, SA, Figeys, D, Wang, L (2015) A Regulatory Network Involving beta-Catenin, E-Cadherin, PI3K/Akt, and Slug Balances Self-Renewal and Differentiation of Human Pluripotent Stem Cells in Response to Wnt Signaling. *Stem Cells* **33**, 1419-1433.

Huang, W-C, Chen, C-C (2005) Akt phosphorylation of p300 at Ser-1834 is essential for its histone acetyltransferase and transcriptional activity. *Molecular and cellular biology* **25**, 6592-6602.

Huggett, MT, Jermyn, M, Gillams, A, Illing, R, Mosse, S, Novelli, M, Kent, E, Bown, S, Hasan, T, Pogue, B (2014) Phase I/II study of verteporfin photodynamic therapy in locally advanced pancreatic cancer. *British journal of cancer* **110**, 1698.

Imajo, M, Miyatake, K, Iimura, A, Miyamoto, A, Nishida, E (2012) A molecular mechanism that links Hippo signalling to the inhibition of Wnt/beta-catenin signalling. *EMBO J* **31**, 1109-1122.

Inic, Z, Zegarac, M, Inic, M, Markovic, I, Kozomara, Z, Djurisic, I, Inic, I, Pupic, G, Jancic, S (2014) Difference between luminal A and luminal B subtypes according to Ki-67, tumor size, and progesterone receptor negativity providing prognostic information. *Clinical Medicine Insights: Oncology* **8**, CMO. S18006.

Inwald, EC, Koller, M, Klinkhammer-Schalke, M, Zeman, F, Hofstädter, F, Gerstenhauer, M, Brockhoff, G, Ortmann, O (2015) 4-IHC classification of breast cancer subtypes in a large cohort of a clinical cancer registry: use in clinical routine for therapeutic decisions and its effect on survival. *Breast cancer research and treatment* **153**, 647-658.

Isakoff, S. J (2010). Triple negative breast cancer: role of specific chemotherapy agents. *Cancer journal* **16**(1), 53

Isakoff, SJ, Puhalla, S, Domchek, SM, Friedlander, M, Kaufman, B, Robson, M, Telli, ML, Diéras, V, Han, HS, Garber, JE (2017a) A randomized Phase II study of veliparib with temozolomide or carboplatin/paclitaxel versus placebo with carboplatin/paclitaxel in BRCA1/2 metastatic breast cancer: design and rationale. *Future Oncology* **13**, 307-320.

Isakoff, SJ, Rogers, GS, Hill, S, McMullan, P, Habin, KR, Park, H, Bartenstein, DW, Chen, ST, Barry, WT, Overmoyer, B (2017b) An open label, phase II trial of continuous low-irradiance photodynamic therapy (CLIPT) using verteporfin for the treatment of cutaneous breast cancer metastases. *Journal of Clinical Oncology* **35**, TPS1121-TPS1121.

Iwanami, T, Uramoto, H, Nakagawa, M, Shimokawa, H, Yamada, S, Kohno, K, Tanaka, F (2014) Clinical significance of epithelial-mesenchymal transition-associated markers in malignant pleural mesothelioma. *Oncology* **86**, 109-116.

Jain, RK, Duda, DG, Clark, JW, Loeffler, JS (2006) Lessons from phase III clinical trials on anti-VEGF therapy for cancer. *Nature clinical practice Oncology* **3**, 24-40.

Jang, ER, Lim, S-J, Lee, ES, Jeong, G, Kim, T-Y, Bang, Y-J, Lee, J-S (2004) The histone deacetylase inhibitor trichostatin A sensitizes estrogen receptor α-negative breast cancer cells to tamoxifen. *Oncogene* **23**, 1724.

Janik, K, Popeda, M, Peciak, J, Rosiak, K, Smolarz, M, Treda, C, Rieske, P, Stoczynska-Fidelus, E, Ksiazkiewicz, M (2016) Efficient and simple approach to in vitro culture of primary epithelial cancer cells. *Bioscience reports* **36**, e00423.

Jansson, S, Bendahl, P-O, Larsson, A-M, Aaltonen, KE, Rydén, L (2016) Prognostic impact of circulating tumor cell apoptosis and clusters in serial blood samples from patients with metastatic breast cancer in a prospective observational cohort. *BMC cancer* **16**, 1.

Jeanes, A, Gottardi, C, Yap, A (2008) Cadherins and cancer: how does cadherin dysfunction promote tumor progression? *Oncogene* **27**, 6920-6929.

Jeevan, DS, Cooper, JB, Braun, A, Murali, R, Jhanwar-Uniyal, M (2016) Molecular pathways mediating metastases to the brain via epithelial-to-mesenchymal transition: Genes, proteins, and functional analysis. *Anticancer research* **36**, 523-532.

Jia, D, Jolly, MK, Boareto, M, Parsana, P, Mooney, SM, Pienta, KJ, Levine, H, Ben-Jacob, E (2015a) OVOL guides the epithelial-hybrid-mesenchymal transition. *Oncotarget* **6**, 15436-15448.

Jia, D, Li, L, Andrew, S, Allan, D, Li, X, Lee, J, Ji, G, Yao, Z, Gadde, S, Figeys, D (2017) An autocrine inflammatory forward-feedback loop after chemotherapy withdrawal facilitates the repopulation of drug-resistant breast cancer cells. *Cell death & disease* **8**, e2932.

Jia, D, Tan, Y, Liu, H, Ooi, S, Li, L, Wright, K, Bennett, S, Addison, CL, Wang, L (2016) Cardamonin reduces chemotherapy-enriched breast cancer stem-like cells in vitro and in vivo. *Oncotarget* **7**, 771-785.

Jia, D, Yang, W, Li, L, Liu, H, Tan, Y, Ooi, S, Chi, L, Filion, LG, Figeys, D, Wang, L (2015b) beta-Catenin and NF-kappaB co-activation triggered by TLR3 stimulation facilitates stem cell-like phenotypes in breast cancer. *Cell death and differentiation* **22**, 298-310.

Jiang, G, Zhang, S, Yazdanparast, A, Li, M, Pawar, AV, Liu, Y, Inavolu, SM, Cheng, L (2016) Comprehensive comparison of molecular portraits between cell lines and tumors in breast cancer. *BMC genomics* **17**, 525.

Jiang, P, Lan, Y, Luo, J, Ren, Y-L, Liu, D-G, Pang, J-X, Liu, J, Li, J, Wang, C, Cai, J-P (2014) Rapamycin promoted thrombosis and platelet adhesion to endothelial cells by inducing membrane remodeling. *BMC cell biology* **15**, 7.

Jiang, Y-P, Ballou, LM, Lin, RZ (2001) Rapamycin-insensitive regulation of 4e-BP1 in regenerating rat liver. *Journal of Biological Chemistry* **276**, 10943-10951.

Jin, K, Teng, L, Shen, Y, He, K, Xu, Z, Li, G (2010) Patient-derived human tumour tissue xenografts in immunodeficient mice: a systematic review. *Clinical and Translational Oncology* **12**, 473-480.

Johnson, R, Halder, G (2014) The two faces of Hippo: targeting the Hippo pathway for regenerative medicine and cancer treatment. *Nat Rev Drug Discov* **13**, 63-79.

Jolly, MK, Boareto, M, Huang, B, Jia, D, Lu, M, Ben-Jacob, E, Onuchic, JN, Levine, H (2015a) Implications of the hybrid epithelial/mesenchymal phenotype in metastasis. *Frontiers in oncology* **5**, 155

Jolly, MK, Huang, B, Lu, M, Mani, SA, Levine, H, Ben-Jacob, E (2014) Towards elucidating the connection between epithelial–mesenchymal transitions and stemness. *Journal of The Royal Society Interface* **11**, 20140962.

Jolly, MK, Jia, D, Boareto, M, Mani, SA, Pienta, KJ, Ben-Jacob, E, Levine, H (2015b) Coupling the modules of EMT and stemness: A tunable 'stemness window'model. *Oncotarget* **6**, 25161-25174.

Jolly, MK, Tripathi, SC, Jia, D, Mooney, SM, Celiktas, M, Hanash, SM, Mani, SA, Pienta, KJ, Ben-Jacob, E, Levine, H (2016) Stability of the hybrid epithelial/mesenchymal phenotype. *Oncotarget* **7**(19), 27067

Jordan, VC (1997) Tamoxifen treatment for breast cancer: concept to gold standard. *Oncology (Williston Park)* **11**, 7-13.

Joshi, PA, Jackson, HW, Beristain, AG, Di Grappa, MA, Mote, PA, Clarke, CL, Stingl, J, Waterhouse, PD, Khokha, R (2010) Progesterone induces adult mammary stem cell expansion. *Nature* **465**, 803.

Julien, S, Merino-Trigo, A, Lacroix, L, Pocard, M, Goéré, D, Mariani, P, Landron, S, Bigot, L, Nemati, F, Dartigues, P (2012) Characterization of a large panel of patient-derived tumor xenografts representing the clinical heterogeneity of human colorectal cancer. *Clinical Cancer Research* **18**(19), 5314-5328

Kala, R, Tollefsbol, TO (2016) A Novel Combinatorial Epigenetic Therapy Using Resveratrol and Pterostilbene for Restoring Estrogen Receptor-α (ERα) Expression in ERα-Negative Breast Cancer Cells. *PLoS ONE* **11**, e0155057.

Kamalidehghan, B, Houshmand, M, Kamalidehghan, F, Jafarzadeh, N, Azari, S, Akmal, SN, Rosli, R (2012) Establishment and characterization of two human breast carcinoma cell lines by spontaneous immortalization: Discordance between Estrogen, Progesterone and HER2/neu receptors of breast carcinoma tissues with derived cell lines. *Cancer cell international* **12**, 43.

Kang, Y, Siegel, PM, Shu, W, Drobnjak, M, Kakonen, SM, Cordón-Cardo, C, Guise, TA, Massagué, J (2003) A multigenic program mediating breast cancer metastasis to bone. *Cancer cell* **3**, 537-549.

Karlsson, E, Pérez-Tenorio, G, Amin, R, Bostner, J, Skoog, L, Fornander, T, Sgroi, DC, Nordenskjöld, B, Hallbeck, A-L, Stål, O (2013) The mTOR effectors 4EBP1 and S6K2 are frequently coexpressed, and associated with a poor prognosis and endocrine resistance in breast cancer: a retrospective study including patients from the randomised Stockholm tamoxifen trials. *Breast Cancer Research* **15**, R96.

Karthik, G-M, Ma, R, Lövrot, J, Kis, LL, Lindh, C, Blomquist, L, Fredriksson, I, Bergh, J, Hartman, J (2015) mTOR inhibitors counteract tamoxifen-induced activation of breast cancer stem cells. *Cancer letters* **367**, 76-87.

Kastan, MB, Schlaffer, E, Russo, J-E, Colvin, OM, Civin, CI, Hilton, J (1990) Direct demonstration of elevated aldehyde dehydrogenase in human hematopoietic progenitor cells. *Blood* **75**, 1947-1950.

Kawai, H, Li, H, Avraham, S, Jiang, S, Avraham, HK (2003) Overexpression of histone deacetylase HDAC1 modulates breast cancer progression by negative regulation of estrogen receptor alpha. *Int J Cancer* **107**, 353-358.

Khramtsov, AI, Khramtsova, GF, Tretiakova, M, Huo, D, Olopade, OI, Goss, KH (2010) Wnt/β-catenin pathway activation is enriched in basal-like breast cancers and predicts poor outcome. *The American journal of pathology* **176**, 2911-2920.

Kiesslich, T, Pichler, M, Neureiter, D (2013) Epigenetic control of epithelial-mesenchymal-transition in human cancer (Review). *Molecular and clinical oncology* **1**, 3-11.

Kim, N-G, Koh, E, Chen, X, Gumbiner, BM (2011a) E-cadherin mediates contact inhibition of proliferation through Hippo signaling-pathway components. *Proceedings of the National Academy of Sciences* **108**, 11930-11935.

Kim, NG, Koh, E, Chen, X, Gumbiner, BM (2011b) E-cadherin mediates contact inhibition of proliferation through Hippo signaling-pathway components. *Proc Natl Acad Sci U S A* **108**, 11930-11935.

Kim, T, Yang, S-J, Hwang, D, Song, J, Kim, M, Kim, SK, Kang, K, Ahn, J, Lee, D, Kim, M-y (2015) A basal-like breast cancer-specific role for SRF-IL6 in YAP-induced cancer stemness. *Nature communications* **6**, 10186

Kim, TH, Yoon, HJ, Nagrath, S (2016) Identification and characterization of EMT/MET signatures in circulating tumor cells isolated from patients with metastatic breast cancer using graphene oxide nano-chip. *Cancer research* **76**, 1685-1685.

Kim, W, Khan, SK, Gvozdenovic-Jeremic, J, Kim, Y, Dahlman, J, Kim, H, Park, O, Ishitani, T, Jho, EH, Gao, B, Yang, Y (2017) Hippo signaling interactions with Wnt/beta-catenin and Notch signaling repress liver tumorigenesis. *J Clin Invest* **127**, 137-152.

Kimura, K, Ikoma, A, Shibakawa, M, Shimoda, S, Harada, K, Saio, M, Imamura, J, Osawa, Y, Kimura, M, Nishikawa, K (2017) Safety, tolerability, and preliminary efficacy of the anti-fibrotic small molecule PRI-724, a CBP/β-catenin inhibitor, in patients with hepatitis C virus-related cirrhosis: a single-center, open-label, dose escalation phase 1 trial. *EBioMedicine* **23**, 79-87.

Ko, AH, Chiorean, EG, Kwak, EL, Lenz, H-J, Nadler, PI, Wood, DL, Fujimori, M, Inada, T, Kouji, H, McWilliams, RR(2016) Final results of a phase Ib dose-escalation study of PRI-724, a CBP/beta-catenin modulator, plus gemcitabine (GEM) in patients with advanced pancreatic adenocarcinoma (APC) as second-line therapy after FOLFIRINOX or FOLFOX. *Journal of Clinical Oncology* **34**, 15 supplementary, 15721-e15721.

Ko, SY, Naora, H (2014) HOXA9 promotes homotypic and heterotypic cell interactions that facilitate ovarian cancer dissemination via its induction of P-cadherin. *Molecular cancer* **13**, 1.

Kong, L, Guo, S, Liu, C, Zhao, Y, Feng, C, Liu, Y, Wang, T, Li, C (2016) Overexpression of SDF-1 activates the NF-κB pathway to induce epithelial to mesenchymal transition and cancer stem cell-like phenotypes of breast cancer cells. *International journal of oncology* **48**, 1085-1094.

Kouzmenko, AP, Takeyama, K, Ito, S, Furutani, T, Sawatsubashi, S, Maki, A, Suzuki, E, Kawasaki, Y, Akiyama, T, Tabata, T, Kato, S (2004) Wnt/beta-catenin and estrogen signaling converge in vivo. *J Biol Chem* **279**, 40255-40258.

Kreso, A, Dick, JE (2014) Evolution of the cancer stem cell model. *Cell Stem Cell* **14**, 275-291.

Lamar, JM, Stern, P, Liu, H, Schindler, JW, Jiang, Z-G, Hynes, RO (2012) The Hippo pathway target, YAP, promotes metastasis through its TEAD-interaction domain. *Proceedings of the National Academy of Sciences* **109**, E2441-E2450.

Lamouille, S, Xu, J, Derynck, R (2014) Molecular mechanisms of epithelial–mesenchymal transition. *Nature reviews. Molecular cell biology* **15**, 178.

Lapidot, T, Sirard, C, Vormoor, J, Murdoch, B, Hoang, T, Caceres-Cortes, J, Minden, M, Paterson, B, Caligiuri, MA, Dick, JE (1994) A cell initiating human acute myeloid leukaemia after transplantation into SCID mice. *Nature* **367**, 645-648.

Lavialle, C, Modjtahedi, N, Cassingena, R, Brison, O (1988) High c-myc amplification level contributes to the tumorigenic phenotype of the human breast carcinoma cell line SW 613-S. *Oncogene* **3**, 335-339.

Ledford, H (2011) Cancer theory faces doubts. *Nature* **472**, 273-273.

Ledford, H (2016) US cancer institute to overhaul tumour cell lines. *Nature News* **530**, 391.

Lee, H, Shields, AF, Siegel, BA, Miller, KD, Krop, I, Ma, CX, LoRusso, PM, Munster, PN, Campbell, K, Gaddy, DF (2017) 64Cu-MM-302 positron emission tomography quantifies variability of enhanced permeability and retention of nanoparticles in relation to treatment response in patients with metastatic breast cancer. *Clinical Cancer Research*, clincanres. 3193.2016. indolylmethane in human colon cancer cells. *Int J Oncol* **43**, 1992-1998.

Liedtke, C, Mazouni, C, Hess, KR, André, F, Tordai, A, Mejia, JA, Symmans, WF, Gonzalez-Angulo, AM, Hennessy, B, Green, M (2008) Response to neoadjuvant therapy and long-term survival in patients with triple-negative breast cancer. *Journal of clinical oncology* **26**, 1275-1281.

Lieu, CH, Tan, A-C, Leong, S, Diamond, JR, Eckhardt, SG (2013) From bench to bedside: lessons learned in translating preclinical studies in cancer drug development. *Journal of the National Cancer Institute* **105**, 1441-1456.

Lin, S-Y, Xia, W, Wang, JC, Kwong, KY, Spohn, B, Wen, Y, Pestell, RG, Hung, M-C (2000) β-catenin, a novel prognostic marker for breast cancer: its roles in cyclin D1 expression and cancer progression. *Proceedings of the National Academy of Sciences* **97**, 4262-4266.

Liu, S, Cong, Y, Wang, D, Sun, Y, Deng, L, Liu, Y, Martin-Trevino, R, Shang, L, McDermott, SP, Landis, MD, Hong, S, Adams, A, D'Angelo, R, Ginestier, C, Charafe-Jauffret, E, Clouthier, SG, Birnbaum, D, Wong, ST, Zhan, M, Chang, JC, Wicha, MS (2014) Breast cancer stem cells transition between epithelial and mesenchymal states reflective of their normal counterparts. *Stem Cell Reports* **2**, 78-91.

Liu, X-f, Bagchi, MK (2004) Recruitment of distinct chromatin-modifying complexes by tamoxifen-complexed estrogen receptor at natural target gene promoters in vivo. *Journal of Biological Chemistry* **279**, 15050-15058.

Liu, Y, Nenutil, R, Appleyard, M, Murray, K, Boylan, M, Thompson, A, Coates, P (2014c) Lack of correlation of stem cell markers in breast cancer stem cells. *British journal of cancer* **110**, 2063.

Livingstone, M, Bidinosti, M (2012) Rapamycin-insensitive mTORC1 activity controls eIF4E: 4E-BP1 binding. *F1000Research* **1**.

LoPiccolo, J, Blumenthal, GM, Bernstein, WB, Dennis, PA (2008) Targeting the PI3K/Akt/mTOR pathway: effective combinations and clinical considerations. *Drug Resistance Updates* **11**, 32-50.

Lu, M, Jolly, MK, Levine, H, Onuchic, JN, Ben-Jacob, E (2013a) MicroRNA-based regulation of epithelial–hybrid–mesenchymal fate determination. *Proceedings of the National Academy of Sciences* **110**, 18144-18149.

Lu, X, Mazur, SJ, Lin, T, Appella, E, Xu, Y (2013b) The pluripotency factor nanog promotes breast cancer tumorigenesis and metastasis. *Oncogene*, **33**(20), 2655 .

Lum, DH, Matsen, C, Welm, AL, Welm, BE (2012) Overview of human primary tumorgraft models: comparisons with traditional oncology preclinical models and the clinical relevance and utility of primary tumorgrafts in basic and translational oncology research. *Curr Protoc Pharmacol* **Chapter 14**, Unit 14 22.

Luo, M, Brooks, M, Wicha, MS (2015) Epithelial-mesenchymal plasticity of breast cancer stem cells: implications for metastasis and therapeutic resistance. *Current pharmaceutical design* **21**, 1301-1310.

Lyn-Cook, BD, Getz, J, Word, B, Moore, R, Miranda-Carboni, G(2017) Vorinostat reexpressed estrogen receptor (ER) in triple negative breast cancer cell line subtypes and sensitized cells to tamoxifen and indole-3-carbinol in vitro. *Cancer Res* **77**,13 Supplement

Ma, F, Chen, D, Chen, F, Chi, Y, Han, Z, Feng, X, Li, X, Han, Z (2015a) Human Umbilical Cord Mesenchymal Stem Cells Promote Breast Cancer Metastasis by Interleukin-8-and Interleukin-6-Dependent Induction of CD44+/CD24− Cells. *Cell transplantation* **24**, 2585-2599.

Ma, H, Li, L, Dou, G, Wang, C, Li, J, He, H, Wu, M, Qi, H (2017) Z-ligustilide restores tamoxifen sensitivity of ERα negative breast cancer cells by reversing MTA1/IFI16/HDACs complex mediated epigenetic repression of ERα. *Oncotarget* **8**, 29328.

Ma, I, Allan, AL (2011) The role of human aldehyde dehydrogenase in normal and cancer stem cells. *Stem cell reviews and reports* **7**, 292-306.

Ma, L, Tang, H, Yin, Y, Yu, R, Zhao, J, Li, Y, Mulholland, MW, Zhang, W (2015b) HDAC5-mTORC1 Interaction in Differential Regulation of Ghrelin and Nucleobindin 2 (NUCB2)/Nesfatin-1. *Molecular Endocrinology* **29**, 1571-1580.

Ma, M, He, M, Jiang, Q, Yan, Y, Guan, S, Zhang, J, Yu, Z, Chen, Q, Sun, M, Yao, W (2016) MiR-487a Promotes TGF-β1-induced EMT, the Migration and Invasion of Breast Cancer Cells by Directly Targeting MAGI2. *International journal of biological sciences* **12**, 397.

Maire, V, Baldeyron, C, Richardson, M, Tesson, B, Vincent-Salomon, A, Gravier, E, Marty-Prouvost, B, De Koning, L, Rigaill, G, Dumont, A (2013a) TTK/hMPS1 is an attractive therapeutic target for triple-negative breast cancer. *PloS one* **8**, e63712.

Maire, V, Némati, F, Richardson, M, Vincent-Salomon, A, Tesson, B, Rigaill, G, Gravier, E, Marty-Prouvost, B, De Koning, L, Lang, G (2013b) Polo-like kinase 1: a potential therapeutic option in combination with conventional chemotherapy for the management of patients with triple-negative breast cancer. *Cancer research* **73**, 813-823.

Mar, J, Robinson, A, Neville, R, Lysne, D, Lawson, K (2014) P-cadherin modulates signaling of multiple growth factor receptors and cellular aggressiveness in oral carcinoma cells. *Cancer research* **74**, 4409-4409.

Marangoni, E, Vincent-Salomon, A, Auger, N, Degeorges, A, Assayag, F, de Cremoux, P, De Plater, L, Guyader, C, De Pinieux, G, Judde, J-G (2007) A new model of patient tumor-derived breast cancer xenografts for preclinical assays. *Clinical cancer research* **13**, 3989-3998.

Marcato, P, Dean, CA, Giacomantonio, CA, Lee, PW (2011) Aldehyde dehydrogenase: its role as a cancer stem cell marker comes down to the specific isoform. *Cell cycle* **10**, 1378-1384.

Mariano, G, Ricciardi, MR, Trisciuoglio, D, Zampieri, M, Ciccarone, F, Guastafierro, T, Calabrese, R, Valentini, E, Tafuri, A, Del Bufalo, D (2015) PARP inhibitor ABT-888 affects response of MDA-MB-231 cells to doxorubicin treatment, targeting Snail expression. *Oncotarget* **6**, 15008.

Marrache, S, Dhar, S (2012) Engineering of blended nanoparticle platform for delivery of mitochondria-acting therapeutics. *Proceedings of the National Academy of Sciences* **109**, 16288.

Marti, H-P, Frey, FJ (2005) Nephrotoxicity of rapamycin: an emerging problem in clinical medicine. *Nephrology Dialysis Transplantation* **20**, 13-15.

Maubant, S, Tesson, B, Maire, V, Ye, M, Rigaill, G, Gentien, D, Cruzalegui, F, Tucker, GC, Roman-Roman, S, Dubois, T (2015) Transcriptome analysis of Wnt3a-treated triple-negative breast cancer cells. *PloS one* **10**, e0122333.

Maugeri-Saccà, M, De Maria, R (2016) Hippo pathway and breast cancer stem cells. *Critical reviews in oncology/hematology* **99**, 115-122.

McAuliffe, PF, Evans, KW, Akcakanat, A, Chen, K, Zheng, X, Zhao, H, Eterovic, AK, Sangai, T, Holder, AM, Sharma, C (2015) Ability to generate patient-derived breast cancer xenografts is enhanced in chemoresistant disease and predicts poor patient outcomes. *PloS one* **10**, e0136851.

McDermott, SP, Wicha, MS (2010) Targeting breast cancer stem cells. *Mol Oncol* **4**, 404-419.

McDONALD, DM, Thurston, G, Baluk, P (1999) Endothelial gaps as sites for plasma leakage in inflammation. *Microcirculation* **6**, 7-22.

McEvoy, J, Ulyanov, A, Brennan, R, Wu, G, Pounds, S, Zhang, J, Dyer, MA (2012) Analysis of MDM2 and MDM4 single nucleotide polymorphisms, mRNA splicing and protein expression in retinoblastoma. *PloS one* **7**, e42739.

Medici, D, Hay, ED, Olsen, BR (2008) Snail and Slug promote epithelial-mesenchymal transition through beta-catenin-T-cell factor-4-dependent expression of transforming growth factor-beta3. *Molecular biology of the cell* **19**, 4875-4887.

Mi, K, Xing, Z (2015) CD44+/CD24− breast cancer cells exhibit phenotypic reversion in three-dimensional self-assembling peptide RADA16 nanofiber scaffold. *International journal of nanomedicine* **10**, 3043.

Miao, L, Huang, L, 2015. Exploring the tumor microenvironment with nanoparticles. *Nanotechnology-Based Precision Tools for the Detection and Treatment of Cancer*. Springer, pp. 193-226.

Migliardi, G, Sassi, F, Torti, D, Galimi, F, Zanella, ER, Buscarino, M, Ribero, D, Muratore, A, Massucco, P, Pisacane, A (2012) Inhibition of MEK and PI3K/mTOR suppresses tumor growth but does not cause tumor regression in patient-derived xenografts of RAS-mutant colorectal carcinomas. *Clinical Cancer Research* **18**(9), 2515-2525.

Miller, MA, Gadde, S, Pfirschke, C, Engblom, C, Sprachman, MM, Kohler, RH, Yang, KS, Laughney, AM, Wojtkiewicz, G, Kamaly, N (2015a) Predicting therapeutic nanomedicine efficacy using a companion magnetic resonance imaging nanoparticle. *Science Translational Medicine* **7**, 314ra183-314ra183.

Miller, TE, Liau, BB, Wallace, LC, Morton, AR, Xie, Q, Dixit, D, Factor, DC, Kim, LJY, Morrow, JJ, Wu, Q, Mack, SC, Hubert, CG, Gillespie, SM, Flavahan, WA, Hoffmann, T, Thummalapalli, R, Hemann, MT, Paddison, PJ, Horbinski, CM, Zuber, J, Scacheri, PC, Bernstein, BE, Tesar, PJ, Rich, JN (2017) Transcription elongation factors represent in vivo cancer dependencies in glioblastoma. *Nature* **547**, 355-359.

Min, KH, Lee, HJ, Kim, K, Kwon, IC, Jeong, SY, Lee, SC (2012) The tumor accumulation and therapeutic efficacy of doxorubicin carried in calcium phosphate-reinforced polymer nanoparticles. *Biomaterials* **33**, 5788-5797.

Minafra, L, Bravata, V, Forte, GI, Cammarata, FP, Gilardi, MC, Messa, C (2014) Gene expression profiling of epithelial–mesenchymal transition in primary breast cancer cell culture. *Anticancer research* **34**, 2173-2183.

Mitchell, T, Sugden, B (1995) Stimulation of NF-kappa B-mediated transcription by mutant derivatives of the latent membrane protein of Epstein-Barr virus. *Journal of Virology* **69**, 2968-2976.

Miyai, K, Schwartz, MR, Divatia, MK, Anton, RC, Park, YW, Ayala, AG, Ro, JY (2014) Adenoid cystic carcinoma of breast: recent advances. *World Journal of Clinical Cases: WJCC* **2**, 732.

Moasser, MM (2007) The oncogene HER2: its signaling and transforming functions and its role in human cancer pathogenesis. *Oncogene* **26**, 6469.

Montecinos, VP, Godoy, A, Hinklin, J, Vethanayagam, RR, Smith, GJ (2012) Primary xenografts of human prostate tissue as a model to study angiogenesis induced by reactive stroma. *PLoS One* **7**, e29623.

Montserrat, N, Gallardo, A, Escuin, D, Catasus, L, Prat, J, Gutiérrez-Avignó, FJ, Peiró, G, Barnadas, A, Lerma, E (2011) Repression of E-cadherin by SNAIL, ZEB1, and TWIST in invasive ductal carcinomas of the breast: a cooperative effort? *Human pathology* **42**, 103-110.

Morante, Z, Ku, GADlC, Enriquez, D, Saavedra, A, Luján, M, Luque, R, Eyzaguirre, E, Guardamino, D, Valcárcel, B, Araujo, JM, Pinto, J, Fuentes, HA, Neciosup, SP, Gomez, HL (2018) Post-recurrence survival in triple negative breast cancer. *Journal of Clinical Oncology* **36**, e13120-e13120.

Moreno-Bueno, G, Portillo, F, Cano, A (2008) Transcriptional regulation of cell polarity in EMT and cancer. *Oncogene* **27**, 6958-6969.

Moroishi, T, Hansen, CG, Guan, KL (2015) The emerging roles of YAP and TAZ in cancer. *Nature reviews. Cancer* **15**, 73-79.

Morton, J., Bird, G., Keysar, S.B., Astling, D.P., Lyons, T.R., Anderson, R.T., Glogowska, M.J., Estes, P., Eagles, J.R., Le, P.N., Gan, G. (2016) XactMice: humanizing mouse bone marrow enables microenvironment reconstitution in a patient-derived xenograft model of head and neck cancer. *Oncogene* **35**(3), 290.

Mullen, P, Ritchie, A, Langdon, SP, Miller, WR (1996) Effect of Matrigel on the tumorigenicity of human breast and ovarian carcinoma cell lines. *International journal of cancer* **67**, 816-820.

Nabholtz, J-M., T. Pienkowski, D. Nothfelt, W. Eiermann, E. Quan, P. Fumoleau, R. Patel, J. Crown, D. Toppmeyer, and D. Slamon (2001) "Results of two open label multicentre phase II pilot studies with Herceptin in combination with docetaxel and platinum salts (cis or carboplatin)(TCH) as therapy for advanced breast cancer (ABC) in women with tumors over-expressing the HER2-neu proto-oncogene." *European Journal of Cancer* **37**, S190.

Nami, B, Donmez, H, Kocak, N (2016) Tunicamycin-induced endoplasmic reticulum stress reduces in vitro subpopulation and invasion of CD44+/CD24- phenotype breast cancer stem cells. *Experimental and toxicologic pathology : official journal of the Gesellschaft fur Toxikologische Pathologie* **68**, 419-426.

Nelson, WJ, Nusse, R (2004) Convergence of Wnt, beta-catenin, and cadherin pathways. *Science* **303**, 1483-1487.

Nestor, CE, Ottaviano, R, Reinhardt, D, Cruickshanks, HA, Mjoseng, HK, McPherson, RC, Lentini, A, Thomson, JP, Dunican, DS, Pennings, S (2015) Rapid reprogramming of epigenetic and transcriptional profiles in mammalian culture systems. *Genome biology* **16**, 11.

Network, CGA (2012) Comprehensive molecular portraits of human breast tumors. *Nature* **490**, 61-70.

Ng, CP, Littman, DR (2016) Tcf1 and Lef1 pack their own HDAC. *Nature immunology* **17**, 615-616.

Nilendu, P, Kumar, A, Kumar, A, Pal, JK, Sharma, NK (2017) Breast cancer stem cells as last soldiers eluding therapeutic burn: A hard nut to crack. *International journal of cancer* **142**(1), 7-17

Ning, X, Du, Y, Ben, Q, Huang, L, He, X, Gong, Y, Gao, J, Wu, H, Man, X, Jin, J (2016) Bulk pancreatic cancer cells can convert into cancer stem cells (CSCs) in vitro and 2 compounds can target these CSCs. *Cell Cycle* **15**, 403-412.

Nishikata, T, Ishikawa, M, Matsuyama, T, Takamatsu, K, Fukuhara, T, Konishi, Y (2013) Primary culture of breast cancer: A model system for epithelial-mesenchymal transition and cancer stem cells. *Anticancer research* **33**, 2867-2873.

Nishita, M, Hashimoto, MK, Ogata, S, Laurent, MN, Ueno, N, Shibuya, H, Cho, KW (2000) Interaction between Wnt and TGF-β signalling pathways during formation of Spemann's organizer. *Nature* **403**, 781-785.

Noh, H, Park, J, Shim, M, Lee, Y (2016) Trichostatin A enhances estrogen receptor-alpha repression in MCF-7 breast cancer cells under hypoxia. *Biochemical and biophysical research communications* **470**, 748-752.

Noh, KH, Kim, BW, Song, KH, Cho, H, Lee, YH, Kim, JH, Chung, JY, Hewitt, SM, Seong, SY, Mao, CP, Wu, TC, Kim, TW (2012) Nanog signaling in cancer promotes stem-like phenotype and immune evasion. *J Clin Invest* **122**, 4077-4093.

Ohgushi, M, Minaguchi, M, Sasai, Y (2015) Rho-Signaling-Directed YAP/TAZ Activity Underlies the Long-Term Survival and Expansion of Human Embryonic Stem Cells. *Cell Stem Cell* **17**, 448-461.

Okuda, H, Xing, F, Pandey, PR, Sharma, S, Watabe, M, Pai, SK, Mo, Y-Y, Iiizumi-Gairani, M, Hirota, S, Liu, Y (2013) miR-7 suppresses brain metastasis of breast cancer stem-like cells by modulating KLF4. *Cancer research* **73**, 1434-1444.

Onder, TT, Gupta, PB, Mani, SA, Yang, J, Lander, ES, Weinberg, RA (2008) Loss of E-cadherin promotes metastasis via multiple downstream transcriptional pathways. *Cancer research* **68**, 3645-3654.

Opyrchal, M, Salisbury, JL, Iankov, I, Goetz, MP, McCubrey, J, Gambino, MW, Malatino, L, Puccia, G, Ingle, JN, Galanis, E, D'Assoro, AB (2014) Inhibition of Cdk2 kinase activity selectively targets the CD44(+)/CD24(-)/Low stem-like subpopulation and restores chemosensitivity of SUM149PT triple-negative breast cancer cells. *Int J Oncol* **45**, 1193-1199.

Orsulic, S, Huber, O, Aberle, H, Arnold, S, Kemler, R (1999) E-cadherin binding prevents beta-catenin nuclear localization and beta-catenin/LEF-1-mediated transactivation. *Journal of cell science* **112**, 1237-1245.

Osborne, CK, Hobbs, K, Trent, JM (1987) Biological differences among MCF-7 human breast cancer cell lines from different laboratories. *Breast cancer research and treatment* **9**, 111-121.

Overholtzer, M, Zhang, J, Smolen, GA, Muir, B, Li, W, Sgroi, DC, Deng, C-X, Brugge, JS, Haber, DA (2006) Transforming properties of YAP, a candidate oncogene on the chromosome 11q22 amplicon. *Proceedings of the National Academy of Sciences* **103**, 12405-12410.

Owonikoko, TK, Zhang, G, Kim, HS, Stinson, RM, Bechara, R, Zhang, C, Chen, Z, Saba, NF, Pakkala, S, Pillai, R (2016) Patient-derived xenografts faithfully replicated clinical outcome in a phase II co-clinical trial of arsenic trioxide in relapsed small cell lung cancer. *Journal of translational medicine* **14**, 111.

Paez-Ribes, M, Man, S, Xu, P, Kerbel, RS (2016) Development of patient derived xenograft models of overt spontaneous breast cancer metastasis: a cautionary note. *PloS one* **11**, e0158034.

Paholak, HJ, Stevers, NO, Chen, H, Burnett, JP, He, M, Korkaya, H, McDermott, SP, Deol, Y, Clouthier, SG, Luther, T (2016) Elimination of epithelial-like and mesenchymal-like breast cancer stem cells to inhibit metastasis following nanoparticle-mediated photothermal therapy. *Biomaterials* **104**, 145-157.

Palma, JP, Wang, Y-C, Rodriguez, LE, Montgomery, D, Ellis, PA, Bukofzer, G, Niquette, A, Liu, X, Shi, Y, Lasko, L (2009) ABT-888 confers broad in vivo activity in combination with temozolomide in diverse tumors. *Clinical Cancer Research* **15**, 7277-7290.

Pan, W, Wang, Q, Zhang, Y, Zhang, N, Qin, J, Li, W, Wang, J, Wu, F, Cao, L, Xu, G (2016) Verteporfin can Reverse the Paclitaxel Resistance Induced by YAP Over-Expression in HCT-8/T Cells without Photoactivation through Inhibiting YAP Expression. *Cell Physiol Biochem* **39**, 481-490.

Paplomata, E, Zelnak, A, O'Regan, R (2013) Everolimus: side effect profile and management of toxicities in breast cancer. *Breast cancer research and treatment* **140**, 453-462.

Park, C, Kim, T, Kim, H, Kim, Y, Jeoung, M, Lee, W, Go, N, Heo, K, Lee, S (2016) Therapeutic targeting of tetraspanin8 in epithelial ovarian cancer invasion and metastasis. *Oncogene* **35**(34), 4540

Pasqualini, JR, Cosquer-Clavreul, C, Gelly, C (1983) Rapid modulation by progesterone and tamoxifen of estradiol effects on nuclear histone acetylation in the uterus of the fetal guinea pig. *Biochimica et Biophysica Acta (BBA)-Gene Structure and Expression* **739**, 137-140.

Pastrana, E (2012) Stem Cells: The survival of the fittest. *Nat Meth* **9**, 16-16.

Pearson, AT, Finkel, KA, Warner, KA, Nör, F, Tice, D, Martins, MD, Jackson, TL, Nör, JE (2016) Patient-derived xenograft (PDX) tumors increase growth rate with time. *Oncotarget* **7**, 7993.

Pei, D, Weiss, SJ (1996) Transmembrane-deletion mutants of the membrane-type matrix metalloproteinase-1 process progelatinase A and express intrinsic matrix-degrading activity. *Journal of Biological Chemistry* **271**, 9135-9140.

Pereira, B, Chin, S-F, Rueda, OM, Vollan, H-KM, Provenzano, E, Bardwell, HA, Pugh, M, Jones, L, Russell, R, Sammut, S-J (2016) The somatic mutation profiles of 2,433 breast cancers refines their genomic and transcriptomic landscapes. *Nature communications* **7**.

Perou, CM (2011) Molecular stratification of triple-negative breast cancers. *The oncologist* **16**, 61-70.

Perrone, G, Gaeta, LM, Zagami, M, Nasorri, F, Coppola, R, Borzomati, D, Bartolozzi, F, Altomare, V, Trodella, L, Tonini, G, Santini, D, Cavani, A, Muda, AO (2012) In situ identification of CD44+/CD24- cancer cells in primary human breast carcinomas. *PLoS One* **7**, e43110.

Petrelli, A, Carollo, R, Cargnelutti, M, Iovino, F, Callari, M, Cimino, D, Todaro, M, Mangiapane, LR, Giammona, A, Cordova, A (2015) By promoting cell differentiation, miR-100 sensitizes basal-like breast cancer stem cells to hormonal therapy. *Oncotarget* **6**, 2315.

Petrelli, F, Coinu, A, Cabiddu, M, Ghilardi, M, Lonati, V, Barni, S (2013) Five or more years of adjuvant endocrine therapy in breast cancer: a meta-analysis of published randomised trials. *Breast cancer research and treatment* **140**, 233-240.

Pham, E, Yin, M, Peters, CG, Lee, CR, Brown, D, Xu, P, Man, S, Jayaraman, L, Rohde, E, Chow, A (2016) Preclinical Efficacy of Bevacizumab with CRLX101, an Investigational Nanoparticle–Drug Conjugate, in Treatment of Metastatic Triple-Negative Breast Cancer. *Cancer research* **76**, 4493-4503.

Phiel, CJ, Zhang, F, Huang, EY, Guenther, MG, Lazar, MA, Klein, PS (2001) Histone deacetylase is a direct target of valproic acid, a potent anticonvulsant, mood stabilizer, and teratogen. *Journal of Biological Chemistry* **276**, 36734-36741.

Phillips, TM, McBride, WH, Pajonk, F (2006) The response of CD24−/low/CD44+ breast cancer–initiating cells to radiation. *Journal of the National Cancer Institute* **98**, 1777-1785.

Plutoni, C, Bazellières, E, Gauthier-Rouvière, C (2016a) P-cadherin-mediated Rho GTPase regulation during collective cell migration. *Small GTPases **7**(3), 156-163*

Plutoni, C, Bazellieres, E, Le Borgne-Rochet, M, Comunale, F, Brugues, A, Séveno, M, Planchon, D, Thuault, S, Morin, N, Bodin, S (2016b) P-cadherin promotes collective cell migration via a Cdc42-mediated increase in mechanical forces. *The Journal of cell biology* **212**, 199-217.

Pogoda, K, Niwińska, A, Murawska, M, Pieńkowski, T (2013) Analysis of pattern, time and risk factors influencing recurrence in triple-negative breast cancer patients. *Medical Oncology* **30**, 388.

Pogue, BW, O'Hara, JA, Demidenko, E, Wilmot, CM, Goodwin, IA, Chen, B, Swartz, HM, Hasan, T (2003) Photodynamic therapy with verteporfin in the radiation-induced fibrosarcoma-1 tumor causes enhanced radiation sensitivity. *Cancer research* **63**, 1025-1033.

Poirier, JT, Gardner, EE, Connis, N, Moreira, AL, De Stanchina, E, Hann, CL, Rudin, CM (2015) DNA methylation in small cell lung cancer defines distinct disease subtypes and correlates with high expression of EZH2. *Oncogene* **34**, 5869-5878.

Ponti, D, Costa, A, Zaffaroni, N, Pratesi, G, Petrangolini, G, Coradini, D, Pilotti, S, Pierotti, MA, Daidone, MG (2005) Isolation and in vitro propagation of tumorigenic breast cancer cells with stem/progenitor cell properties. *Cancer research* **65**, 5506-5511.

Postigo, AA, Depp, JL, Taylor, JJ, Kroll, KL (2003) Regulation of Smad signaling through a differential recruitment of coactivators and corepressors by ZEB proteins. *The EMBO journal* **22**, 2453-2462.

Prabhakar, U, Maeda, H, Jain, RK, Sevick-Muraca, EM, Zamboni, W, Farokhzad, OC, Barry, ST, Gabizon, A, Grodzinski, P, Blakey, DC(2013) Challenges and key considerations of the enhanced permeability and retention effect for nanomedicine drug delivery in oncology. *Cancer Res* **73**(8); 2412–7

Prasetyanti, PR, Medema, JP (2017) Intra-tumor heterogeneity from a cancer stem cell perspective. *Molecular cancer* **16**, 41.

Prat, A, Adamo, B, Cheang, MC, Anders, CK, Carey, LA, Perou, CM (2013) Molecular characterization of basal-like and non-basal-like triple-negative breast cancer. *The oncologist* **18**, 123-133.

Prat, A, Perou, CM (2011) Deconstructing the molecular portraits of breast cancer. *Molecular oncology* **5**, 5-23.

Prowell, Tatiana M., and Nancy E. Davidson (2004) "What is the role of ovarian ablation in the management of primary and metastatic breast cancer today?" *The oncologist* **9**, no. 5, 507-517.

Qiu, Y, Pu, T, Guo, P, Wei, B, Zhang, Z, Zhang, H, Zhong, X, Zheng, H, Chen, L, Bu, H (2016) ALDH+/CD44+ cells in breast cancer are associated with worse prognosis and poor clinical outcome. *Experimental and molecular pathology* **100**, 145-150.

Raha, P, Thomas, S, Thurn, KT, Park, J, Munster, PN (2015) Combined histone deacetylase inhibition and tamoxifen induces apoptosis in tamoxifen-resistant breast cancer models, by reversing Bcl-2 overexpression. *Breast Cancer Research* **17**, 26.

Rakha, EA, Reis-Filho, JS, Ellis, IO (2008) Basal-like breast cancer: a critical review. *Journal of clinical oncology : official journal of the American Society of Clinical Oncology* **26**, 2568-2581.

Ramanathan, RK, Korn, R, Raghunand, N, Sachdev, JC, Newbold, RG, Jameson, G, Fetterly, GJ, Prey, J, Klinz, SG, Kim, J (2017) Correlation between ferumoxytol uptake in tumor lesions by MRI and response to nanoliposomal irinotecan in patients with advanced solid tumors: a pilot study. *Clinical Cancer Research*, clincanres. 1990.2016.

Ramaswamy, B, Lu, Y, Teng, K-y, Nuovo, G, Li, X, Shapiro, CL, Majumder, S (2012) Hedgehog signaling is a novel therapeutic target in tamoxifen-resistant breast cancer aberrantly activated by PI3K/AKT pathway. *Cancer research* **72**, 5048-5059.

Rasti, M, Arabsolghar, R, Khatooni, Z, Mostafavi-Pour, Z (2012) p53 Binds to estrogen receptor 1 promoter in human breast cancer cells. *Pathology & Oncology Research* **18**, 169-175.

Redmer, T, Diecke, S, Grigoryan, T, Quiroga-Negreira, A, Birchmeier, W, Besser, D (2011) E-cadherin is crucial for embryonic stem cell pluripotency and can replace OCT4 during somatic cell reprogramming. *EMBO Rep* **12**, 720-726.

Reuben, JM, Lee, B-N, Gao, H, Cohen, EN, Mego, M, Giordano, A, Wang, X, Lodhi, A, Krishnamurthy, S, Hortobagyi, GN (2011) Primary breast cancer patients with high risk clinicopathologic features have high percentages of bone marrow epithelial cells with ALDH activity and CD44+ CD24lo cancer stem cell phenotype. *European journal of cancer* **47**, 1527-1536.

Reynolds, DS, Tevis, KM, Blessing, WA, Colson, YL, Zaman, MH, Grinstaff, MW (2017) Breast Cancer Spheroids Reveal a Differential Cancer Stem Cell Response to Chemotherapeutic Treatment. *Scientific reports* **7**, 10382.

Rhim, AD, Mirek, ET, Aiello, NM, Maitra, A, Bailey, JM, McAllister, F, Reichert, M, Beatty, GL, Rustgi, AK, Vonderheide, RH (2012) EMT and dissemination precede pancreatic tumor formation. *Cell* **148**, 349-361.

Rhodes, LV, Nitschke, AM, Segar, HC, Martin, EC, Driver, JL, Elliott, S, Nam, SY, Li, M, Nephew, KP, Burow, ME, Collins-Burow, BM (2012) The histone deacetylase inhibitor trichostatin A alters microRNA expression profiles in apoptosis-resistant breast cancer cells. *Oncology reports* **27**, 10-16.

Ribeiro, AS, Paredes, J (2015) P-cadherin linking breast cancer stem cells and invasion: a promising marker to identify an "intermediate/metastable" EMT state. *Frontiers in oncology* **4**, 371.

Ricardo, S, Vieira, AF, Gerhard, R, Leitão, D, Pinto, R, Cameselle-Teijeiro, JF, Milanezi, F, Schmitt, F, Paredes, J (2011) Breast cancer stem cell markers CD44, CD24 and ALDH1: expression distribution within intrinsic molecular subtype. *Journal of clinical pathology* **64**, 937-946.

Rodriguez, FJ, Lewis-Tuffin, LJ, Anastasiadis, PZ (2012) E-cadherin's dark side: possible role in tumor progression. *Biochimica et Biophysica Acta (BBA)-Reviews on Cancer* **1826**, 23-31.

Rofstad, EK, Huang, R, Galappathi, K, Andersen, L, Wegner, CS, Hauge, A, Gaustad, J-V, Simonsen, TG (2016) Functional intratumoral lymphatics in patient-derived xenograft models of squamous cell carcinoma of the uterine cervix: implications for lymph node metastasis. *Oncotarget* **7**, 56986-56997.

Rosenbluh, J, Nijhawan, D, Cox, AG, Li, X, Neal, JT, Schafer, EJ, Zack, TI, Wang, X, Tsherniak, A, Schinzel, AC (2012) β-Catenin-driven cancers require a YAP1 transcriptional complex for survival and tumorigenesis. *Cell* **151**, 1457-1473.

Rosenblum, D, Joshi, N, Tao, W, Karp, JM, Peer, D (2018) Progress and challenges towards targeted delivery of cancer therapeutics. *Nature communications* **9**, 1410.

Roy, V, Perez, EA (2009) Beyond trastuzumab: small molecule tyrosine kinase inhibitors in HER-2–positive breast cancer. *The oncologist* **14**, 1061-1069.

Rubin, M, Putzi, M, Mucci, N, Smith, D, Wojno, K, Korenchuk, S, Pienta, K (2000) Rapid (" warm") autopsy study for procurement of metastatic prostate cancer. *Clinical cancer research: an official journal of the American Association for Cancer Research* **6**, 1038.

Ruscetti, M, Quach, B, Dadashian, EL, Mulholland, DJ, Wu, H (2015) Tracking and Functional Characterization of Epithelial–Mesenchymal Transition and Mesenchymal Tumor Cells during Prostate Cancer Metastasis. *Cancer research* **75**, 2749-2759.

Sabnis, GJ, Goloubeva, O, Chumsri, S, Nguyen, N, Sukumar, S, Brodie, AM (2011) Functional activation of the estrogen receptor-alpha and aromatase by the HDAC inhibitor entinostat sensitizes ER-negative tumors to letrozole. *Cancer research* **71**, 1893-1903.

Sakamoto, K, Imai, K, Higashi, T, Taki, K, Nakagawa, S, Okabe, H, Nitta, H, Hayashi, H, Chikamoto, A, Ishiko, T (2015) Significance of P-cadherin overexpression and possible mechanism of its regulation in intrahepatic cholangiocarcinoma and pancreatic cancer. *Cancer science* **106**, 1153-1162.

Samanta, D, Gilkes, DM, Chaturvedi, P, Xiang, L, Semenza, GL (2014) Hypoxia-inducible factors are required for chemotherapy resistance of breast cancer stem cells. *Proc Natl Acad Sci U S A* **111**, E5429-5438.

Sampson, VB, David, JM, Puig, I, Patil, PU, de Herreros, AG, Thomas, GV, Rajasekaran, AK (2014) Wilms' tumor protein induces an epithelial-mesenchymal hybrid differentiation state in clear cell renal cell carcinoma. *PloS one* **9**, e102041.

Sarbassov, DD, Guertin, DA, Ali, SM, Sabatini, DM (2005) Phosphorylation and regulation of Akt/PKB by the rictor-mTOR complex. *Science* **307**, 1098-1101.

Scandlyn, M, Stuart, E, Somers-Edgar, T, Menzies, A, Rosengren, R (2008) A new role for tamoxifen in oestrogen receptor-negative breast cancer when it is combined with epigallocatechin gallate. *British Journal of Cancer* **99**, 1056.

Schlegelmilch, K, Mohseni, M, Kirak, O, Pruszak, J, Rodriguez, JR, Zhou, D, Kreger, BT, Vasioukhin, V, Avruch, J, Brummelkamp, TR (2011) Yap1 acts downstream of α-catenin to control epidermal proliferation. *Cell* **144**, 782-795.

Scotton, CJ, Wilson, JL, Milliken, D, Stamp, G, Balkwill, FR (2001) Epithelial cancer cell migration a role for chemokine receptors? *Cancer research* **61**, 4961-4965.

Serrano-Gomez, SJ, Maziveyi, M, Alahari, SK (2016) Regulation of epithelial-mesenchymal transition through epigenetic and post-translational modifications. *Molecular cancer* **15**, 18.

Shackleton, M, Vaillant, F, Simpson, KJ, Stingl, J, Smyth, GK, Asselin-Labat, M-L, Wu, L, Lindeman, GJ, Visvader, JE (2006) Generation of a functional mammary gland from a single stem cell. *Nature* **439**, 84.

Shao, J, Fan, W, Ma, B, Wu, Y (2016) Breast cancer stem cells expressing different stem cell markers exhibit distinct biological characteristics. *Molecular medicine reports* **14**, 4991-4998.

Shelton, JW, Waxweiler, TV, Landry, J, Gao, H, Xu, Y, Wang, L, El-Rayes, B, Shu, H-KG (2013) In vitro and in vivo enhancement of chemoradiation using the oral PARP inhibitor ABT-888 in colorectal cancer cells. *International Journal of Radiation Oncology* Biology* Physics* **86**, 469-476.

Shen, H, Yuan, J, Yuan, S, Yang, Y, Feng, X, Niu, Y (2016) Survival estimates based on molecular subtype and age in patients with early node-negative breast cancer. *INTERNATIONAL JOURNAL OF CLINICAL AND EXPERIMENTAL PATHOLOGY* **9**, 5357-5367.

Sheridan, C, Kishimoto, H, Fuchs, RK, Mehrotra, S, Bhat-Nakshatri, P, Turner, CH, Goulet, R, Badve, S, Nakshatri, H (2006) CD44+/CD24-breast cancer cells exhibit enhanced invasive properties: an early step necessary for metastasis. *Breast Cancer Research* **8**, R59.

Shi, J, Kantoff, PW, Wooster, R, Farokhzad, OC (2017) Cancer nanomedicine: progress, challenges and opportunities. *Nature reviews. Cancer* **17**, 20-37.

Shi, QQ, Zuo, GW, Feng, ZQ, Zhao, LC, Luo, L, You, ZM, Li, DY, Xia, J, Li, J, Chen, DL (2014) Effect of trichostatin A on anti HepG2 liver carcinoma cells: inhibition of HDAC activity and activation of Wnt/beta-Catenin signaling. *Asian Pacific journal of cancer prevention : APJCP* **15**, 7849-7855.

Shiraishi, A, Tachi, K, Essid, N, Tsuboi, I, Nagano, M, Kato, T, Yamashita, T, Bando, H, Hara, H, Ohneda, O (2017) Hypoxia promotes the phenotypic change of aldehyde dehydrogenase activity of breast cancer stem cells. *Cancer science* **108**, 362-372.

Siegel, RL, Miller, KD, Jemal, A (2016) Cancer statistics, 2016. *CA: a cancer journal for clinicians* **66**, 7-30.

Simmons, J, Hildreth III, B, Supsavhad, W, Elshafae, S, Hassan, B, Dirksen, W, Toribio, RE, Rosol, TJ (2015) Animal models of bone metastasis. *Veterinary pathology* **52**, 827-841.

Simpson-Abelson, MR, Sonnenberg, GF, Takita, H, Yokota, SJ, Conway, TF, Kelleher, RJ, Shultz, LD, Barcos, M, Bankert, RB (2008) Long-term engraftment and expansion of tumor-derived memory T cells following the implantation of non-disrupted pieces of human lung tumor into NOD-scid IL2Rγnull mice. *The Journal of Immunology* **180**, 7009-7018.

Singel, SM, Cornelius, C, Zaganjor, E, Batten, K, Sarode, VR, Buckley, DL, Peng, Y, John, GB, Li, HC, Sadeghi, N (2014) KIF14 promotes AKT phosphorylation and contributes to chemoresistance in triple-negative breast cancer. *Neoplasia* **16**, 247-256. e242.

Sinha, G(2014) Downfall of iniparib: a PARP inhibitor that doesn't inhibit PARP after all. *JNCI: Journal of the National Cancer Institute* 106.1

Skvortsova, I(2018) Special Issue "Cancer Stem Cells: Impact on Treatment". *Seminars in Cancer Biology* **53**, iii-iv.

Smith, I, Procter, M, Gelber, RD, Guillaume, S, Feyereislova, A, Dowsett, M, Goldhirsch, A, Untch, M, Mariani, G, Baselga, J (2007) 2-year follow-up of trastuzumab after adjuvant chemotherapy in HER2-positive breast cancer: a randomised controlled trial. *The lancet* **369**, 29-36.

Sokol, JP, Neil, JR, Schiemann, BJ, Schiemann, WP (2005) The use of cystatin C to inhibit epithelial-mesenchymal transition and morphological transformation stimulated by transforming growth factor-beta. *Breast cancer research : BCR* **7**, R844-853.

Song, X, Liu, X, Chi, W, Liu, Y, Wei, L, Wang, X, Yu, J (2006) Hypoxia-induced resistance to cisplatin and doxorubicin in non-small cell lung cancer is inhibited by silencing of HIF-1α gene. *Cancer chemotherapy and pharmacology* **58**, 776-784.

Soon, L, Braet, F, Ratinac, K, Schuliga, M, Chien, H, Stewart, A The benefits of microfluidics for imaging cell migration.

Soria, J-C, Wu, Y-L, Nakagawa, K, Kim, S-W, Yang, J-J, Ahn, M-J, Wang, J, Yang, JC-H, Lu, Y, Atagi, S (2015) Gefitinib plus chemotherapy versus placebo plus chemotherapy in EGFR-mutation-positive non-small-cell lung cancer after progression on first-line gefitinib (IMPRESS): a phase 3 randomised trial. *The Lancet Oncology* **16**, 990-998.

Sørlie, T, Perou, CM, Tibshirani, R, Aas, T, Geisler, S, Johnsen, H, Hastie, T, Eisen, MB, Van De Rijn, M, Jeffrey, SS (2001) Gene expression patterns of breast carcinomas distinguish tumor subclasses with clinical implications. *Proceedings of the National Academy of Sciences* **98**, 10869-10874.

Spangle, JM, Dreijerink, KM, Groner, AC, Cheng, H, Ohlson, CE, Reyes, J, Lin, CY, Bradner, J, Zhao, JJ, Roberts, TM (2016) PI3K/AKT signaling regulates H3K4 methylation in breast cancer. *Cell reports* **15**, 2692-2704.

Speirs, V, Green, A, Walton, D, Kerin, M, Fox, J, Carleton, P, Desai, S, Atkin, S (1998) Short-term primary culture of epithelial cells derived from human breast tumours. *British journal of cancer* **78**, 1421.

Stark, K, Burger, A, Wu, J, Shelton, P, Polin, L, Li, J (2013) Reactivation of estrogen receptor alpha by vorinostat sensitizes mesenchymal-like triple-negative breast cancer to aminoflavone, a ligand of the aryl hydrocarbon receptor. *PLoS One* **8**, e74525.

Statistics-Canada.(2016) Table 13-10-0394-01 Leading causes of death, total population, by age group. https://www150.statcan.gc.ca/t1/tbl1/en/tv.action?pid=1310039401. Accessed 01.09.2019.

Steinestel, K, Eder, S, Schrader, AJ, Steinestel, J (2014) Clinical significance of epithelial-mesenchymal transition. *Clinical and translational medicine* **3**, 17.

Sulaiman, A, McGarry, S, Lam, KM, El-Sahli, S, Chambers, J, Kaczmarek, S, Li, L, Addison, C, Dimitroulakos, J, Arnaout, A (2018a) Co-inhibition of mTORC1, HDAC and ESR1α retards the growth of triple-negative breast cancer and suppresses cancer stem cells. *Cell death & disease* **9**, 815.

Sulaiman, A, McGarry, S, Li, L, Jia, D, Ooi, S, Addison, C, Dimitroulakos, J, Arnaout, A, Nessim, C, Yao, Z, Ji, G, Song, H, Gadde, S, Li, X, Wang, L (2018b) Dual inhibition of Wnt and Yes-associated protein signaling retards the growth of triple-negative breast cancer in both mesenchymal and epithelial states. *Mol Oncol* **12**, 423-440.

Sulaiman, A, Sulaiman, B, Khouri, L, McGarry, S, Nessim, C, Arnaout, A, Li, X, Addison, C, Dimitroulakos, J, Wang, L (2016) Both bulk and cancer stem cell subpopulations in triple-negative breast cancer are susceptible to Wnt, HDAC, and ERalpha coinhibition. *FEBS Lett* **590**, 4606-4616.

Sulaiman, A, Wang, L (2017) Bridging the divide: preclinical research discrepancies between triple-negative breast cancer cell lines and patient tumors. *Oncotarget* **8**, 113269-113281.

Sulaiman, A, Yao, Z, Wang, L (2017a) Re-evaluating the role of epithelial-mesenchymal-transition in cancer progression. *Journal of biomedical research* **32**(2), 81

Tabassum, H, Parvez, S, Rehman, H, Dev Banerjee, B, Siemen, D, Raisuddin, S (2007) Nephrotoxicity and its prevention by taurine in tamoxifen induced oxidative stress in mice. *Human & experimental toxicology* **26**, 509-518.

Tam, WL, Weinberg, RA (2013) The epigenetics of epithelial-mesenchymal plasticity in cancer. *Nat Med* **19**, 1438-1449.

Tan, TZ, Miow, QH, Miki, Y, Noda, T, Mori, S, Huang, RY, Thiery, JP (2014) Epithelial-mesenchymal transition spectrum quantification and its efficacy in deciphering survival and drug responses of cancer patients. *EMBO molecular medicine* **6**, 1279-1293.

Taniguchi, K, Karin, M (2018) NF-kappaB, inflammation, immunity and cancer: coming of age. *Nat Rev Immunol* **18**, 309-324.

Tao, J, Jiang, P, Peng, C, Li, M, Liu, R, Zhang, W (2016) The pharmacokinetic characters of simvastatin after co-administration with Shexiang Baoxin Pill in healthy volunteers' plasma. *Journal of Chromatography B* **1026**, 162-167.

Taplin, M-E, Antonarakis, ES, Ferrante, KJ, Horgan, K, Blumenstein, BA, Saad, F, Luo, J, De Bono, JS(2017) Clinical factors associated with AR-V7 detection in ARMOR3-SV, a randomized trial of galeterone (Gal) vs

enzalutamide (Enz) in men with AR-V7+ metastatic castration-resistant prostate cancer (mCRPC). *Journal of Clinical Oncology* 35, no. 15_suppl

Tarin, D, Thompson, EW, Newgreen, DF (2005) The fallacy of epithelial mesenchymal transition in neoplasia. *Cancer research* **65**, 5996-6000; discussion 6000-5991.

Tell, S, Yi, H, Jockovich, M-E, Murray, TG, Hackam, AS (2006) The Wnt signaling pathway has tumor suppressor properties in retinoblastoma. *Biochemical and biophysical research communications* **349**, 261-269.

Tentler, JJ, Tan, AC, Weekes, CD, Jimeno, A, Leong, S, Pitts, TM, Arcaroli, JJ, Messersmith, WA, Eckhardt, SG (2012) Patient-derived tumour xenografts as models for oncology drug development. *Nature reviews Clinical oncology* **9**, 338-350.

Terao, M, Ishikawa, A, Nakahara, S, Kimura, A, Kato, A, Moriwaki, K, Kamada, Y, Murota, H, Taniguchi, N, Katayama, I, Miyoshi, E (2011) Enhanced epithelial-mesenchymal transition-like phenotype in N-acetylglucosaminyltransferase V transgenic mouse skin promotes wound healing. *J Biol Chem* **286**, 28303-28311.

Thakur, B, Ray, P (2017) Cisplatin triggers cancer stem cell enrichment in platinum-resistant cells through NF-κB-TNFα-PIK3CA loop. *Journal of Experimental & Clinical Cancer Research* **36**, 164.

Thibaudeau, L, Quent, VM, Holzapfel, BM, Taubenberger, AV, Straub, M, Hutmacher, DW (2014) Mimicking breast cancer-induced bone metastasis in vivo: current transplantation models and advanced humanized strategies. *Cancer and Metastasis Reviews* **33**, 721-735.

Thomas, C, Gustafsson, J-Å (2011) The different roles of ER subtypes in cancer biology and therapy. *Nature Reviews Cancer* **11**, 597.

Thomas, S, Thurn, KT, Raha, P, Chen, S, Munster, PN (2013) Efficacy of histone deacetylase and estrogen receptor inhibition in breast cancer cells due to concerted down regulation of Akt. *PloS one* **8**, e68973.

Thorpe, LM, Yuzugullu, H, Zhao, JJ (2015) PI3K in cancer: divergent roles of isoforms, modes of activation and therapeutic targeting. *Nature reviews. Cancer* **15**, 7-24.

Tian, X, Liu, Z, Niu, B, Zhang, J, Tan, TK, Lee, SR, Zhao, Y, Harris, DC, Zheng, G (2011) E-cadherin/β-catenin complex and the epithelial barrier. *BioMed Research International* **2011**.

Tiran, V, Stanzer, S, Heitzer, E, Meilinger, M, Rossmann, C, Lax, S, Tsybrovskyy, O, Dandachi, N, Balic, M (2017) Genetic profiling of putative breast cancer stem cells from malignant pleural effusions. *PloS one* **12**, e0175223.

Tojo, M, Hamashima, Y, Hanyu, A, Kajimoto, T, Saitoh, M, Miyazono, K, Node, M, Imamura, T (2005) The ALK-5 inhibitor A-83-01 inhibits Smad signaling and epithelial-to-mesenchymal transition by transforming growth factor-beta. *Cancer science* **96**, 791-800.

Tomar, T, de Jong, S, Alkema, NG, Hoekman, RL, Meersma, GJ, Klip, HG, Zee, AG, Wisman, GBA (2016) Genome-wide methylation profiling of ovarian cancer patient-derived xenografts treated with the demethylating agent decitabine identifies novel epigenetically regulated genes and pathways. *Genome medicine* **8**, 107.

Trivanović, D, Jauković, A, Krstić, J, Nikolić, S, Okić Djordjević, I, Kukolj, T, Obradović, H, Mojsilović, S, Ilić, V, Santibanez, JF, Bugarski, D (2016) Inflammatory cytokines prime adipose tissue mesenchymal stem cells to enhance malignancy of MCF-7 breast cancer cells via transforming growth factor-β1. *IUBMB Life* **68**, 190-200.

Tsuji, T, Ibaragi, S, Shima, K, Hu, MG, Katsurano, M, Sasaki, A, Hu, GF (2008) Epithelial-mesenchymal transition induced by growth suppressor p12CDK2-AP1 promotes tumor cell local invasion but suppresses distant colony growth. *Cancer research* **68**, 10377-10386.

Valencia, PM, Pridgen, EM, Perea, B, Gadde, S, Sweeney, C, Kantoff, PW, Bander, NH, Lippard, SJ, Langer, R, Karnik, R, Farokhzad, OC (2013) Synergistic cytotoxicity of irinotecan and cisplatin in dual-drug targeted polymeric nanoparticles. *Nanomedicine (Lond)* **8**, 687-698.

Valent, P, Bonnet, D, De Maria, R, Lapidot, T, Copland, M, Melo, JV, Chomienne, C, Ishikawa, F, Schuringa, JJ, Stassi, G, Huntly, B, Herrmann, H, Soulier, J, Roesch, A, Schuurhuis, GJ, Wohrer, S, Arock, M, Zuber, J, Cerny-Reiterer, S, Johnsen, HE, Andreeff, M, Eaves, C (2012) Cancer stem cell definitions and terminology: the devil is in the details. *Nature reviews. Cancer* **12**, 767-775.

Vargo-Gogola, T, Rosen, JM (2007) Modelling breast cancer: one size does not fit all. *Nature reviews. Cancer* **7**, 659.

Varley, KE, Gertz, J, Bowling, KM, Parker, SL, Reddy, TE, Pauli-Behn, F, Cross, MK, Williams, BA, Stamatoyannopoulos, JA, Crawford, GE (2013) Dynamic DNA methylation across diverse human cell lines and tissues. *Genome research* **23**, 555-567.

Vazquez-Martin, A, Cufi, S, Lopez-Bonet, E, Corominas-Faja, B, Cuyas, E, Vellon, L, Iglesias, JM, Leis, O, Martin, AG, Menendez, JA (2013) Reprogramming of non-genomic estrogen signaling by the stemness factor SOX2 enhances the tumor-initiating capacity of breast cancer cells. *Cell Cycle* **12**, 3471-3477.

Vazquez-Martin, A, Oliveras-Ferraros, C, Cufí, S, Del Barco, S, Martin-Castillo, B, Menendez, JA (2010) Metformin regulates breast cancer stem cello ntogeny by transcriptional regulation of the epithelial-mesenchymal transition (EMT) status. *Cell cycle* **9**, 3831-3838.

Veeman, MT, Slusarski, DC, Kaykas, A, Louie, SH, Moon, RT (2003b) Zebrafish prickle, a modulator of noncanonical Wnt/Fz signaling, regulates gastrulation movements. *Current Biology* **13**, 680-685.

Velasco-Velázquez, MA, Popov, VM, Lisanti, MP, Pestell, RG (2011) The role of breast cancer stem cells in metastasis and therapeutic implications. *The American journal of pathology* **179**, 2-11.

Vesuna, F, van Diest, P, Chen, JH, Raman, V (2008) Twist is a transcriptional repressor of E-cadherin gene expression in breast cancer. *Biochemical and biophysical research communications* **367**, 235-241.

Vieira, AF, Ricardo, S, Ablett, MP, Dionísio, MR, Mendes, N, Albergaria, A, Farnie, G, Gerhard, R, Cameselle-Teijeiro, JF, Seruca, R (2012) P-cadherin is coexpressed with CD44 and CD49f and mediates stem cell properties in basal-like breast cancer. *Stem Cells* **30**, 854-864.

Vincent-Salomon, A, Gruel, N, Lucchesi, C, MacGrogan, G, Dendale, R, Sigal-Zafrani, B, Longy, M, Raynal, V, Pierron, G, de Mascarel, I (2007) Identification of typical medullary breast carcinoma as a genomic sub-group of basal-like carcinomas, a heterogeneous new molecular entity. *Breast Cancer Research* **9**, R24.

Visvader, JE, Lindeman, GJ (2012) Cancer stem cells: current status and evolving complexities. *Cell Stem Cell* **10**, 717-728.

Vleminckx, K, Vakaet, L, Mareel, M, Fiers, W, Van Roy, F (1991) Genetic manipulation of E-cadherin expression by epithelial tumor cells reveals an invasion suppressor role. *Cell* **66**, 107-119.

Wakelee, HA, Dahlberg, SE, Keller, SM, Tester, WJ, Gandara, DR, Graziano, SL, Adjei, A, Leighl, N, Aisner, SC, Rothman, JM(2015) Randomized phase III trial of adjuvant chemotherapy with or without bevacizumab in resected non-small cell lung cancer (NSCLC): results of E1505. *JOURNAL OF THORACIC ONCOLOGY* **10**, S796-S796.

Wander, SA, Hennessy, BT, Slingerland, JM (2011) Next-generation mTOR inhibitors in clinical oncology: how pathway complexity informs therapeutic strategy. *The Journal of clinical investigation* **121**, 1231-1241.

Wang, CS, Goulet, F, Tremblay, N, Germain, L, Auger, F, Têtu, B (2001) Selective culture of epithelial cells from primary breast carcinomas using irradiated 3T3 cells as feeder layer. *Pathology-Research and Practice* **197**, 175-181.

Wang, P, Bahreini, A, Gyanchandani, R, Lucas, PC, Hartmaier, RJ, Watters, RJ, Jonnalagadda, AR, Bittar, HET, Berg, A, Hamilton, RL (2016a) Sensitive detection of mono-and polyclonal ESR1 mutations in primary tumors, metastatic lesions, and cell-free DNA of breast cancer patients. *Clinical cancer research* **22**, 1130-1137.

Wang, P, Lin, S, Zhang, L, Li, Z, Liu, Q, Gao, J, Liu, D, Bo, J, Huang, Y (2014) The prognostic value of P-cadherin in non-muscle-invasive bladder cancer. *European Journal of Surgical Oncology (EJSO)* **40**, 255-259.

Wang, Q, Gao, X, Yu, T, Yuan, L, Dai, J, Wang, W, Chen, G, Jiao, C, Zhou, W, Huang, Q, Cui, L, Zhang, P, Moses, RE, Yang, J, Chen, F, Fu, J, Xiao, J, Li, L, Dang, Y, Li, X (2018) REGgamma Controls Hippo Signaling and Reciprocal NF-kappaB-YAP Regulation to Promote Colon Cancer. *Clinical cancer research : an official journal of the American Association for Cancer Research* **24**, 2015-2025.

Wang, S, Jiang, B, Zhang, T, Liu, L, Wang, Y, Wang, Y, Chen, X, Lin, H, Zhou, L, Xia, Y (2015) Insulin and mTOR pathway regulate HDAC3-mediated deacetylation and activation of PGK1. *PLoS biology* **13**, e1002243.

Wang, T, Seah, S, Loh, X, Chan, C-W, Hartman, M, Goh, B-C, Lee, S-C (2016b) Simvastatin-induced breast cancer cell death and deactivation of PI3K/Akt and MAPK/ERK signalling are reversed by metabolic products of the mevalonate pathway. *Oncotarget* **7**, 2532.

Wang, Y (2016a) Mutation and gene expression analysis of circulating tumor cells (CTCs) enriched and retrieved by a sensitive microfluidic device. *Cancer research* **76**, 1688-1688.

Wang, Z, Wu, Y, Wang, H, Zhang, Y, Mei, L, Fang, X, Zhang, X, Zhang, F, Chen, H, Liu, Y, Jiang, Y, Sun, S, Zheng, Y, Li, N, Huang, L (2014b) Interplay of mevalonate and Hippo pathways regulates RHAMM transcription via YAP to modulate breast cancer cell motility. *Proc Natl Acad Sci U S A* **111**, E89-98.

Wenger, SL, Senft, JR, Sargent, LM, Bamezai, R, Bairwa, N, Grant, SG (2004) Comparison of established cell lines at different passages by karyotype and comparative genomic hybridization. *Bioscience reports* **24**, 631-639.

Whittle, JR, Lewis, MT, Lindeman, GJ, Visvader, JE (2015) Patient-derived xenograft models of breast cancer and their predictive power. *Breast cancer research* **17**, 17.

Wilcken, N, Hornbuckle, J, Ghersi, D (2003) Chemotherapy alone versus endocrine therapy alone for metastatic breast cancer. *The Cochrane Library*.

Williams, SA, Anderson, WC, Santaguida, MT, Dylla, SJ (2013) Patient-derived xenografts, the cancer stem cell paradigm, and cancer pathobiology in the 21st century. *Laboratory investigation* **93**, 970.

Wu, Y, Ginther, C, Kim, J, Mosher, N, Chung, S, Slamon, D, Vadgama, JV (2012) Expression of Wnt3 activates Wnt/beta-catenin pathway and promotes EMT-like phenotype in trastuzumab-resistant HER2-overexpressing breast cancer cells. *Molecular cancer research : MCR* **10**, 1597-1606.

Wu, Y, Liu, J (2008) Simvastatin attenuated cardiac hypertrophy via inhibiting JAK-STAT pathways. *Zhonghua xin xue guan bing za zhi* **36**, 738-743.

Xu, K, Wu, ZJ, Groner, AC, He, HH, Cai, C, Lis, RT, Wu, X, Stack, EC, Loda, M, Liu, T (2012) EZH2 oncogenic activity in castration-resistant prostate cancer cells is Polycomb-independent. *Science* **338**, 1465-1469.

Xu, L, Zhang, L, Hu, C, Liang, S, Fei, X, Yan, N, Zhang, Y, Zhang, F (2016a) WNT pathway inhibitor pyrvinium pamoate inhibits the self-renewal and metastasis of breast cancer stem cells. *International journal of oncology* **48**, 1175-1186.

Xu, Q, Deng, F, Qin, Y, Zhao, Z, Wu, Z, Xing, Z, Ji, A, Wang, Q (2016b) Long non-coding RNA regulation of epithelial–mesenchymal transition in cancer metastasis. *Cell Death & Disease* **7**, e2254.

Xu, X, Vatsyayan, J, Gao, C, Bakkenist, CJ, Hu, J (2010a) HDAC2 promotes eIF4E sumoylation and activates mRNA translation gene specifically. *Journal of Biological Chemistry* **285**, 18139-18143.

Xu, Y, Stamenkovic, I, Yu, Q (2010b) CD44 attenuates activation of the hippo signaling pathway and is a prime therapeutic target for glioblastoma. *Cancer research* **70**, 2455-2464.

Yan, Y, Li, Z, Xu, X, Chen, C, Wei, W, Fan, M, Chen, X, Li, JJ, Wang, Y, Huang, J (2016a) All-trans retinoic acids induce differentiation and sensitize a radioresistant breast cancer cells to chemotherapy. *BMC complementary and alternative medicine* **16**, 113.

Yang, M-H, Wu, M-Z, Chiou, S-H, Chen, P-M, Chang, S-Y, Liu, C-J, Teng, S-C, Wu, K-J (2008) Direct regulation of TWIST by HIF-1α promotes metastasis. *Nature cell biology* **10**, 295-305.

Yang, MH, Imrali, A, Heeschen, C (2015) Circulating cancer stem cells: the importance to select. *Chinese journal of cancer research = Chung-kuo yen cheng yen chiu* **27**, 437-449.

Yang, X, Ferguson, AT, Nass, SJ, Phillips, DL, Butash, KA, Wang, SM, Herman, JG, Davidson, NE (2000) Transcriptional activation of estrogen receptor alpha in human breast cancer cells by histone deacetylase inhibition. *Cancer research* **60**, 6890-6894.

Yang, Y, Jiang, Y, Wan, Y, Zhang, L, Qiu, J, Zhou, S, Cheng, W (2016) UCA1 functions as a competing endogenous RNA to suppress epithelial ovarian cancer metastasis. *Tumor Biology*, 1-9.

Yano, F, Kugimiya, F, Ohba, S, Ikeda, T, Chikuda, H, Ogasawara, T, Ogata, N, Takato, T, Nakamura, K, Kawaguchi, H, Chung, UI (2005) The canonical Wnt signaling pathway promotes chondrocyte differentiation in a Sox9-dependent manner. *Biochem Biophys Res Commun* **333**, 1300-1308.

Yao, D, Dai, C, Peng, S (2011) Mechanism of the mesenchymal-epithelial transition and its relationship with metastatic tumor formation. *Molecular cancer research : MCR* **9**, 1608-1620.

Yauch, RL, Januario, T, Eberhard, DA, Cavet, G, Zhu, W, Fu, L, Pham, TQ, Soriano, R, Stinson, J, Seshagiri, S (2005) Epithelial versus mesenchymal phenotype determines in vitro sensitivity and predicts clinical activity of erlotinib in lung cancer patients. *Clinical Cancer Research* **11**, 8686-8698.

Yi, F, Pereira, L, Hoffman, JA, Shy, BR, Yuen, CM, Liu, DR, Merrill, BJ (2011) Opposing effects of Tcf3 and Tcf1 control Wnt stimulation of embryonic stem cell self-renewal. *Nat Cell Biol* **13**, 762-770.

Yin, S, Cheryan, VT, Xu, L, Rishi, AK, Reddy, KB (2017) Myc mediates cancer stem-like cells and EMT changes in triple negative breast cancers cells. *PloS one* **12**, e0183578.

Yoon, SO, Kim, YT, Jung, KC, Jeon, YK, Kim, B-H, Kim, C-W (2011) TTF-1 mRNA-positive circulating tumor cells in the peripheral blood predict poor prognosis in surgically resected non-small cell lung cancer patients. *Lung Cancer* **71**, 209-216.

Yoshida, T, Ozawa, Y, Kimura, T, Sato, Y, Kuznetsov, G, Xu, S, Uesugi, M, Agoulnik, S, Taylor, N, Funahashi, Y, Matsui, J (2014) Eribulin mesilate suppresses experimental metastasis of breast cancer cells by reversing phenotype from epithelial-mesenchymal transition (EMT) to mesenchymal-epithelial transition (MET) states. *Br J Cancer* **110**, 1497-1505.

Yu, F, Li, J, Chen, H, Fu, J, Ray, S, Huang, S, Zheng, H, Ai, W (2011) Kruppel-like factor 4 (KLF4) is required for maintenance of breast cancer stem cells and for cell migration and invasion. *Oncogene* **30**, 2161-2172.

Yu, F, Yao, H, Zhu, P, Zhang, X, Pan, Q, Gong, C, Huang, Y, Hu, X, Su, F, Lieberman, J (2007) let-7 regulates self renewal and tumorigenicity of breast cancer cells. *Cell* **131**, 1109-1123.

Yu, FX, Zhao, B, Guan, KL (2015) Hippo Pathway in Organ Size Control, Tissue Homeostasis, and Cancer. *Cell* **163**, 811-828.

Yu, J, Qin, B, Moyer, AM, Sinnwell, JP, Thompson, KJ, Copland, JA, Marlow, LA, Miller, JL, Yin, P, Gao, B (2017) Establishing and characterizing patient-derived xenografts using pre-chemotherapy percutaneous biopsy and post-chemotherapy surgical samples from a prospective neoadjuvant breast cancer study. *Breast Cancer Research* **19**, 130.

Zeng, YA, Nusse, R (2010) Wnt proteins are self-renewal factors for mammary stem cells and promote their long-term expansion in culture. *Cell stem cell* **6**, 568-577.

Zhan, T, Rindtorff, N, Boutros, M (2017) Wnt signaling in cancer. *Oncogene* **36**, 1461.

Zhang, B-N, Cao, X-C, Chen, J-Y, Chen, J, Fu, L, Hu, X-C, Jiang, Z-F, Li, H-Y, Liao, N, Liu, D-G (2012) Guidelines on the diagnosis and treatment of breast cancer (2011 edition). *Gland surgery* **1**, 39.

Zhang, H, Li, Y, Lai, M (2010) The microRNA network and tumor metastasis. *Oncogene* **29**, 937-948.

Zhang, K, Qi, HX, Hu, ZM, Chang, YN, Shi, ZM, Han, XH, Han, YW, Zhang, RX, Zhang, Z, Chen, T, Hong, W (2015) YAP and TAZ Take Center Stage in Cancer. *Biochemistry* **54**, 6555-6566.

Zhang, L, Chan, JM, Gu, FX, Rhee, JW, Wang, AZ, Radovic-Moreno, AF, Alexis, F, Langer, R, Farokhzad, OC (2008) Self-assembled lipid--polymer hybrid nanoparticles: a robust drug delivery platform. *ACS Nano* **2**, 1696-1702.

Zhang, L, Ridgway, LD, Wetzel, MD, Ngo, J, Yin, W, Kumar, D, Goodman, JC, Groves, MD, Marchetti, D (2013a) The identification and characterization of breast cancer CTCs competent for brain metastasis. *Science translational medicine* **5**, 180ra148-180ra148.

Zhang, M-w, Fujiwara, K, Che, X, Zheng, S, Zheng, L (2017) DNA methylation in the tumor microenvironment. *Journal of Zhejiang University-SCIENCE B* **18**, 365-372.

Zhang, M, Rosen, JM (2015) Developmental Insights into Breast Cancer Intratumoral Heterogeneity. *Trends in cancer* **1**, 242-251.

Zhang, Q, Ding, J, Liu, J, Wang, W, Zhang, F, Wang, J, Li, Y (2016) Helicobacter pylori-infected MSCs acquire a pro-inflammatory phenotype and induce human gastric cancer migration by promoting EMT in gastric cancer cells. *Oncology letters* **11**, 449-457.

Zhang, X, Claerhout, S, Prat, A, Dobrolecki, LE, Petrovic, I, Lai, Q, Landis, MD, Wiechmann, L, Schiff, R, Giuliano, M (2013b) A renewable tissue resource of phenotypically stable, biologically and ethnically diverse, patient-derived human breast cancer xenograft models. *Cancer research* **73**, 4885-4897.

Zhang, X, Lin, SH, Fang, B, Gillin, M, Mohan, R, Chang, JY (2013c) Therapy-resistant cancer stem cells have differing sensitivity to photon versus proton beam radiation. *Journal of Thoracic Oncology* **8**, 1484-1491.

Zheng, X, Carstens, JL, Kim, J, Scheible, M, Kaye, J, Sugimoto, H, Wu, C-C, LeBleu, VS, Kalluri, R (2015) Epithelial-to-mesenchymal transition is dispensable for metastasis but induces chemoresistance in pancreatic cancer. *Nature* **527**(7579), 525

Zhou, B, Jin, Y, Zhang, D, Lin, D (2018) 5-Fluorouracil may enrich cancer stem cells in canine mammary tumor cells in vitro. *Oncology letters* **15**, 7987-7992.

Zhou, L, Jiang, Y, Yan, T, Di, G, Shen, Z, Shao, Z, Lu, J (2010) The prognostic role of cancer stem cells in breast cancer: a meta-analysis of published literatures. *Breast cancer research and treatment* **122**, 795-801.

Zhuang, X, Zhang, W, Chen, Y, Han, X, Li, J, Zhang, Y, Zhang, Y, Zhang, S, Liu, B (2012) Doxorubicin-enriched, ALDH br mouse breast cancer stem cells are treatable to oncolytic herpes simplex virus type 1. *BMC cancer* **12**, 549.

Ziauddin, MF, Hua, D, Tang, S-C (2014) Emerging strategies to overcome resistance to endocrine therapy for breast cancer. *Cancer and Metastasis Reviews* **33**, 791-807.

Zuo, T, Zeng, H, Li, H, Liu, S, Yang, L, Xia, C, Zheng, R, Ma, F, Liu, L, Wang, N (2017) The influence of stage at diagnosis and molecular subtype on breast cancer patient survival: a hospital-based multi-center study. *Chinese journal of cancer* **36**, 84.

Appendix

Appendix 1: Rights and Permissions for re-use of: Sulaiman, A, Yao, Z, Wang, L (2017) Re-evaluating the role of epithelial-mesenchymal-transition in cancer progression. *Journal of biomedical research*. **32**(*2*): 81–90.

Copyright Clearance Center

Note: Copyright.com supplies permissions but not the copyrighted content itself.

1 PAYMENT — 2 REVIEW — 3 CONFIRMATION

Step 3: Order Confirmation

Thank you for your order! A confirmation for your order will be sent to your account email address. If you have questions about your order, you can call us 24 hrs/day, M-F at +1.855.239.3415 Toll Free, or write to us at info@copyright.com. This is not an invoice.

Confirmation Number: 11767576
Order Date: 11/23/2018

If you paid by credit card, your order will be finalized and your card will be charged within 24 hours. If you choose to be invoiced, you can change or cancel your order until the invoice is generated.

Payment Information

Andrew Sulaiman

Payment Method: n/a

Order Details

Journal of biomedical research

Order detail ID:	71673861
Order License Id:	4474581205461
ISSN:	1674-8301
Publication Type:	Journal
Volume:	
Issue:	
Start page:	
Publisher:	Journal of Biomedical Research

Permission Status:	Granted
Permission type:	Republish or display content
Type of use:	Thesis/Dissertation
Requestor type	Author of requested content
Format	Print, Electronic
Portion	chapter/article
Number of pages in chapter/article	1
The requesting person/organization	Andrew Sulaiman
Title or numeric reference of the portion(s)	Full Article- A model for epithelial and mesenchymal conversion in TNBC: Identification of duel Wnt and YAP sensitivity within both breast cancer stem cell populations

Title of the article or chapter the portion is from	A model for epithelial and mesenchymal conversion in TNBC: Identification of duel Wnt and YAP sensitivity within both breast cancer stem cell populations
Editor of portion(s)	N/A
Author of portion(s)	N/A
Volume of serial or monograph	N/A
Page range of portion	100
Publication date of portion	May 2019
Rights for	Main Product, any product related to main product, and other compilations/derivative products
Duration of use	Life of current edition
Creation of copies for the disabled	no
With minor editing privileges	yes
For distribution to	Canada
In the following language(s)	Original language of publication
With incidental promotional use	no
Lifetime unit quantity of new product	Up to 499
Title	Molecular Targets for the Treatment of TNBC in Clinically Translatable Models
Institution name	n/a
Expected presentation date	May 2019

Note: This item will be invoiced or charged separately through CCC's **RightsLink** service. More info **$ 0.00**

Confirmation Number: 11767576

Special Rightsholder Terms & Conditions

The following terms & conditions apply to the specific publication under which they are listed

Journal of biomedical research
Permission type: Republish or display content
Type of use: Thesis/Dissertation

TERMS AND CONDITIONS

The following terms are individual to this publisher:

None

Other Terms and Conditions:

STANDARD TERMS AND CONDITIONS

1. Description of Service; Defined Terms. This Republication License enables the User to obtain licenses for republication of one or more copyrighted works as described in detail on the relevant Order Confirmation (the "Work(s)"). Copyright Clearance Center, Inc. ("CCC") grants licenses through the Service on behalf of the rightsholder identified on the Order Confirmation (the "Rightsholder"). "Republication", as used herein, generally means the inclusion of a Work, in whole or in part, in a new work or works, also as described on the Order Confirmation. "User", as used herein, means the person or entity making such republication.

2. The terms set forth in the relevant Order Confirmation, and any terms set by the Rightsholder with respect to a particular Work, govern the terms of use of Works in connection with the Service. By using the Service, the person transacting for a republication license on behalf of the User represents and warrants that he/she/it (a) has been duly authorized by the User to accept, and hereby does accept, all such terms and conditions on behalf of User, and (b) shall inform User of all such terms and conditions. In the event such person is a "freelancer" or other third party independent of User and CCC, such party shall be deemed jointly a "User" for purposes of these terms and conditions. In any event, User shall be deemed to have accepted and agreed to all such terms and conditions if User republishes the Work in any fashion.

3. Scope of License; Limitations and Obligations.

3.1 All Works and all rights therein, including copyright rights, remain the sole and exclusive property of the Rightsholder. The license created by the exchange of an Order Confirmation (and/or any invoice) and payment by User of the full amount set forth on that document includes only those rights expressly set forth in the Order Confirmation and in these terms and conditions, and conveys no other rights in the Work(s) to User. All rights not expressly granted are hereby reserved.

3.2 General Payment Terms: You may pay by credit card or through an account with us payable at the end of the month. If you and we agree that you may establish a standing account with CCC, then the following terms apply: Remit Payment to: Copyright Clearance Center, 29118 Network Place, Chicago, IL 60673-1291. Payments Due: Invoices are payable upon their delivery to you (or upon our notice to you that they are available to you for downloading). After 30 days, outstanding amounts will be subject to a service charge of 1-1/2% per month or, if less, the maximum rate allowed by applicable law. Unless otherwise specifically set forth in the Order Confirmation or in a separate written agreement signed by CCC, invoices are due and payable on "net 30" terms. While User may exercise the rights licensed immediately upon issuance of the Order Confirmation, the license is automatically revoked and is null and void, as if it had never been issued, if complete payment for the license is not received on a timely basis either from User directly or through a payment agent, such as a credit card company.

3.3 Unless otherwise provided in the Order Confirmation, any grant of rights to User (i) is "one-time" (including the editions and product family specified in the license), (ii) is non-exclusive and non-transferable and (iii) is subject to any and all limitations and restrictions (such as, but not limited to, limitations on duration of use or circulation) included in the Order Confirmation or invoice and/or in these terms and conditions. Upon completion of the licensed use, User shall either secure a new permission for further use of the Work(s) or immediately cease any new use of the Work(s) and shall render inaccessible (such as by deleting or by removing or severing links or other locators) any further copies of the Work (except for copies printed on paper in accordance with this license and still in User's stock at the end of such period).

3.4 In the event that the material for which a republication license is sought includes third party materials (such as photographs, illustrations, graphs, inserts and similar materials) which are identified in such material as having been used by permission, User is responsible for identifying, and seeking separate licenses (under this Service or otherwise) for, any of such third party materials; without a separate license, such third party materials may not be used.

3.5 Use of proper copyright notice for a Work is required as a condition of any license granted under the Service. Unless otherwise provided in the Order Confirmation, a proper copyright notice will read substantially as follows: "Republished with permission of [Rightsholder's name], from [Work's title, author, volume, edition number and year of copyright]; permission conveyed through Copyright Clearance Center, Inc. " Such notice must be provided in a reasonably legible font size and must be placed either immediately adjacent to the Work as used (for example, as part of a by-line or footnote

Confirmation Number: 11767576

Citation Information

Order Detail ID: 71673861

Journal of biomedical research by Journal of Biomedical Research. Reproduced with permission of Journal of Biomedical Research in the format Thesis/Dissertation via Copyright Clearance Center.

Close

Appendix 2: Rights and Permissions for re-use of: Andrew Sulaiman, Brandon Sulaiman, Lara Khouri, Sarah McGarry, Carolyn Nessim, Angel Arnaout, Sean Xuguang Li, Christina Addison, Jim Dimitroulakos, and Lisheng Wang. Both bulk and CSC subpopulations in TNBC are susceptible to Wnt, HDAC and ERα co-inhibition. *FEBS Letters*, 2017;590(24):4606-4616

JOHN WILEY AND SONS LICENSE TERMS AND CONDITIONS

Nov 23, 2018

This Agreement between ("You") and John Wiley and Sons ("John Wiley and Sons") consists of your license details and the terms and conditions provided by John Wiley and Sons and Copyright Clearance Center.

License Number	4474570763253
License date	Nov 23, 2018
Licensed Content Publisher	John Wiley and Sons
Licensed Content Publication	FEBS Letters
Licensed Content Title	Both bulk and cancer stem cell subpopulations in triple-negative breast cancer are susceptible to Wnt, HDAC, and ERα coinhibition
Licensed Content Author	Lisheng Wang, Jim Dimitroulakos, Christina Addison, et al
Licensed Content Date	Dec 9, 2016
Licensed Content Volume	590
Licensed Content Issue	24
Licensed Content Pages	11
Type of use	Dissertation/Thesis
Requestor type	Author of this Wiley article
Format	Print and electronic
Portion	Full article
Will you be translating?	No
Title of your thesis / dissertation	Molecular Targets for the Treatment of TNBC in Clinically Translatable Models
Expected completion date	May 2019
Expected size (number of pages)	300
Requestor Location	

Publisher Tax ID	EU826007151
Total	0.00 USD
Terms and Conditions	

TERMS AND CONDITIONS

This copyrighted material is owned by or exclusively licensed to John Wiley & Sons, Inc. or one of its group companies (each a"Wiley Company") or handled on behalf of a society with which a Wiley Company has exclusive publishing rights in relation to a particular work (collectively "WILEY"). By clicking "accept" in connection with completing this licensing transaction, you agree that the following terms and conditions apply to this transaction (along with the billing and payment terms and conditions established by the Copyright

Clearance Center Inc., ("CCC's Billing and Payment terms and conditions"), at the time that you opened your RightsLink account (these are available at any time at http://myaccount.copyright.com).

Terms and Conditions

- The materials you have requested permission to reproduce or reuse (the "Wiley Materials") are protected by copyright.

- You are hereby granted a personal, non-exclusive, non-sub licensable (on a stand-alone basis), non-transferable, worldwide, limited license to reproduce the Wiley Materials for the purpose specified in the licensing process. This license, **and any CONTENT (PDF or image file) purchased as part of your order,** is for a one-time use only and limited to any maximum distribution number specified in the license. The first instance of republication or reuse granted by this license must be completed within two years of the date of the grant of this license (although copies prepared before the end date may be distributed thereafter). The Wiley Materials shall not be used in any other manner or for any other purpose, beyond what is granted in the license. Permission is granted subject to an appropriate acknowledgement given to the author, title of the material/book/journal and the publisher. You shall also duplicate the copyright notice that appears in the Wiley publication in your use of the Wiley Material. Permission is also granted on the understanding that nowhere in the text is a previously published source acknowledged for all or part of this Wiley Material. Any third party content is expressly excluded from this permission.

- With respect to the Wiley Materials, all rights are reserved. Except as expressly granted by the terms of the license, no part of the Wiley Materials may be copied, modified, adapted (except for minor reformatting required by the new Publication), translated, reproduced, transferred or distributed, in any form or by any means, and no derivative works may be made based on the Wiley Materials without the prior permission of the respective copyright owner.**For STM Signatory Publishers clearing permission under the terms of the STM Permissions Guidelines only, the terms of the license are extended to include subsequent editions and for editions in other languages, provided such editions are for the work as a whole in situ and does not involve the separate exploitation of the permitted figures or extracts,** You may not alter, remove or suppress in any manner any copyright, trademark or other notices displayed by the Wiley Materials. You may not license, rent, sell, loan, lease, pledge, offer as security, transfer or assign the Wiley Materials on a stand-alone basis, or any of the rights granted to you hereunder to any other person.

- The Wiley Materials and all of the intellectual property rights therein shall at all times remain the exclusive property of John Wiley & Sons Inc, the Wiley Companies, or their respective licensors, and your interest therein is only that of having possession of and the right to reproduce the Wiley Materials pursuant to Section 2 herein during the continuance of this Agreement. You agree that you own no right, title or interest in or to the Wiley Materials or any of the intellectual property rights therein. You shall have no rights hereunder other than the license as provided for above in Section 2. No right, license or interest to any trademark, trade name, service mark or other branding ("Marks") of WILEY or its licensors is granted hereunder, and you agree that you shall not assert any such right, license or interest with respect thereto

- NEITHER WILEY NOR ITS LICENSORS MAKES ANY WARRANTY OR REPRESENTATION OF ANY KIND TO YOU OR ANY THIRD PARTY, EXPRESS, IMPLIED OR STATUTORY, WITH RESPECT TO THE MATERIALS

OR THE ACCURACY OF ANY INFORMATION CONTAINED IN THE MATERIALS, INCLUDING, WITHOUT LIMITATION, ANY IMPLIED WARRANTY OF MERCHANTABILITY, ACCURACY, SATISFACTORY QUALITY, FITNESS FOR A PARTICULAR PURPOSE, USABILITY, INTEGRATION OR NON-INFRINGEMENT AND ALL SUCH WARRANTIES ARE HEREBY EXCLUDED BY WILEY AND ITS LICENSORS AND WAIVED BY YOU.

- WILEY shall have the right to terminate this Agreement immediately upon breach of this Agreement by you.
- You shall indemnify, defend and hold harmless WILEY, its Licensors and their respective directors, officers, agents and employees, from and against any actual or threatened claims, demands, causes of action or proceedings arising from any breach of this Agreement by you.
- IN NO EVENT SHALL WILEY OR ITS LICENSORS BE LIABLE TO YOU OR ANY OTHER PARTY OR ANY OTHER PERSON OR ENTITY FOR ANY SPECIAL, CONSEQUENTIAL, INCIDENTAL, INDIRECT, EXEMPLARY OR PUNITIVE DAMAGES, HOWEVER CAUSED, ARISING OUT OF OR IN CONNECTION WITH THE DOWNLOADING, PROVISIONING, VIEWING OR USE OF THE MATERIALS REGARDLESS OF THE FORM OF ACTION, WHETHER FOR BREACH OF CONTRACT, BREACH OF WARRANTY, TORT, NEGLIGENCE, INFRINGEMENT OR OTHERWISE (INCLUDING, WITHOUT LIMITATION, DAMAGES BASED ON LOSS OF PROFITS, DATA, FILES, USE, BUSINESS OPPORTUNITY OR CLAIMS OF THIRD PARTIES), AND WHETHER OR NOT THE PARTY HAS BEEN ADVISED OF THE POSSIBILITY OF SUCH DAMAGES. THIS LIMITATION SHALL APPLY NOTWITHSTANDING ANY FAILURE OF ESSENTIAL PURPOSE OF ANY LIMITED REMEDY PROVIDED HEREIN.
- Should any provision of this Agreement be held by a court of competent jurisdiction to be illegal, invalid, or unenforceable, that provision shall be deemed amended to achieve as nearly as possible the same economic effect as the original provision, and the legality, validity and enforceability of the remaining provisions of this Agreement shall not be affected or impaired thereby.
- The failure of either party to enforce any term or condition of this Agreement shall not constitute a waiver of either party's right to enforce each and every term and condition of this Agreement. No breach under this agreement shall be deemed waived or excused by either party unless such waiver or consent is in writing signed by the party granting such waiver or consent. The waiver by or consent of a party to a breach of any provision of this Agreement shall not operate or be construed as a waiver of or consent to any other or subsequent breach by such other party.
- This Agreement may not be assigned (including by operation of law or otherwise) by you without WILEY's prior written consent.
- Any fee required for this permission shall be non-refundable after thirty (30) days from receipt by the CCC.
- These terms and conditions together with CCC's Billing and Payment terms and conditions (which are incorporated herein) form the entire agreement between you and WILEY concerning this licensing transaction and (in the absence of fraud) supersedes

all prior agreements and representations of the parties, oral or written. This Agreement may not be amended except in writing signed by both parties. This Agreement shall be binding upon and inure to the benefit of the parties' successors, legal representatives, and authorized assigns.

- In the event of any conflict between your obligations established by these terms and conditions and those established by CCC's Billing and Payment terms and conditions, these terms and conditions shall prevail.

- WILEY expressly reserves all rights not specifically granted in the combination of (i) the license details provided by you and accepted in the course of this licensing transaction, (ii) these terms and conditions and (iii) CCC's Billing and Payment terms and conditions.

- This Agreement will be void if the Type of Use, Format, Circulation, or Requestor Type was misrepresented during the licensing process.

- This Agreement shall be governed by and construed in accordance with the laws of the State of New York, USA, without regards to such state's conflict of law rules. Any legal action, suit or proceeding arising out of or relating to these Terms and Conditions or the breach thereof shall be instituted in a court of competent jurisdiction in New York County in the State of New York in the United States of America and each party hereby consents and submits to the personal jurisdiction of such court, waives any objection to venue in such court and consents to service of process by registered or certified mail, return receipt requested, at the last known address of such party.

WILEY OPEN ACCESS TERMS AND CONDITIONS

Wiley Publishes Open Access Articles in fully Open Access Journals and in Subscription journals offering Online Open. Although most of the fully Open Access journals publish open access articles under the terms of the Creative Commons Attribution (CC BY) License only, the subscription journals and a few of the Open Access Journals offer a choice of Creative Commons Licenses. The license type is clearly identified on the article.

The Creative Commons Attribution License

The Creative Commons Attribution License (CC-BY) allows users to copy, distribute and transmit an article, adapt the article and make commercial use of the article. The CC-BY license permits commercial and non-

Creative Commons Attribution Non-Commercial License

The Creative Commons Attribution Non-Commercial (CC-BY-NC)License permits use, distribution and reproduction in any medium, provided the original work is properly cited and is not used for commercial purposes.(see below)

Creative Commons Attribution-Non-Commercial-NoDerivs License

The Creative Commons Attribution Non-Commercial-NoDerivs License (CC-BY-NC-ND) permits use, distribution and reproduction in any medium, provided the original work is properly cited, is not used for commercial purposes and no modifications or adaptations are made. (see below)

Use by commercial "for-profit" organizations

Use of Wiley Open Access articles for commercial, promotional, or marketing purposes requires further explicit permission from Wiley and will be subject to a fee.

Further details can be found on Wiley Online Library

http://olabout.wiley.com/WileyCDA/Section/id-410895.html

Other Terms and Conditions:

v1.10 Last updated September 2015

Questions? customercare@copyright.com or +1-855-239-3415 (toll free in the US) or +1-978-646-2777.

Appendix 3. Table 1.1: The Leading Causes of Deaths by Males and Females from 2012 to 2016.

(Table from Statistics Canada. Table 13-10-0394-01 Leading causes of death, total population, by age group. https://www150.statcan.gc.ca/t1/tbl1/en/cv.action?pid=1310039401. Accessed 01.09.2019. Reproduced with permission under the Statistics Canada Open License. Please see Rights and Permissions for further details)

		Canada, place of residence														
		Age at time of death, all ages														
		Both sexes					Males					Females				
Leading causes of death (ICD-10)	Characteristics	2012	2013	2014	2015	2016	2012	2013	2014	2015	2016	2012	2013	2014	2015	2016
		Number														
Malignant neoplasms [C00-C97]	Rank of leading causes of death	1	1	1	1	1	1	1	1	1	1	1	1	1	1	1
	Number of deaths	74,361	75,112	77,059	77,054	79,084	39,080	39,384	40,721	40,410	41,447	35,281	35,728	36,338	36,644	37,637
Diabetes mellitus [E10-E14]	Rank of leading causes of death	6	6	6	7	6	6	6	6	6	6	7	8	8	8	8
	Number of deaths	6,993	7,045	7,071	7,172	6,838	3,702	3,786	3,818	3,948	3,686	3,291	3,259	3,253	3,224	3,152
Alzheimer's disease [G30]	Rank of leading causes of death	7	8	8	8	7	9	10	10	9	10	6	6	6	6	6
	Number of deaths	6,293	6,345	6,410	6,587	6,521	1,900	1,954	1,901	2,130	2,075	4,393	4,391	4,509	4,457	4,446
Diseases of heart [I00-I09, I11, I13, I20-I51]	Rank of leading causes of death	2	2	2	2	2	2	2	2	2	2	2	2	2	2	2
	Number of deaths	48,681	49,891	51,014	51,534	51,396	25,816	26,454	27,084	27,290	27,486	22,865	23,437	23,930	24,244	23,910
Cerebrovascular diseases [I60-I69]	Rank of leading causes of death	3	3	3	3	3	5	5	5	5	5	3	3	3	3	3
	Number of deaths	13,174	13,400	13,573	13,795	13,551	5,581	5,543	5,660	5,763	5,678	7,593	7,857	7,913	8,032	7,873
Influenza and pneumonia [J09-J18]	Rank of leading causes of death	8	7	7	6	8	8	8	8	7	7	8	7	7	7	7
	Number of deaths	5,694	6,551	6,597	7,630	6,235	2,586	2,992	2,962	3,420	2,955	3,108	3,559	3,635	4,210	3,280
Chronic lower respiratory diseases [J40-J47]	Rank of leading causes of death	5	4	4	4	5	4	4	4	4	4	4	4	4	4	4
	Number of deaths	11,130	11,976	11,876	12,573	12,293	5,683	6,030	5,973	6,230	6,170	5,447	5,946	5,903	6,343	6,123